ANALYSIS OF THE FUNCTION OF MEGF7 DURING DEVELOPMENT

APPROVED BY SUPERVISORY COMMITTEE

_____

_____

_____

_____

_____

DEDICATION

I would like to thank the members of the Herz lab, both past and present, for their assistance. In particular, Jamie Holland, Natalie Kapesser, Christian Tennert, Chris Jones, and Uwe Beffert provided significant technical and intellectual assistance during my thesis work. I would also like to thank my committee for their invaluable advice for this project. I would also like to thank all of the friends that I have met in Dallas including Michael Melkus, Cheryl Vahling, Robert Ratts, Erin Willert, and Jenny Garcia. Their positive support definitely contributed to the productivity of this project.

ANALYSIS OF THE FUNCTION OF MEGF7 DURING DEVELOPMENT

by

ERIC BOYD JOHNSON

DISSERTATION /THESIS

Presented to the Faculty of the Graduate School of Biomedical Sciences

The University of Texas Southwestern Medical Center at Dallas

In Partial Fulfillment of the Requirements

For the Degree of

DOCTOR OF PHILOSOPHY

The University of Texas Southwestern Medical Center at Dallas

Dallas, Texas

ANALYSIS OF THE FUNCTION OF MEGF7 DURING DEVELOPMENT

Publication No. _____

ERIC BOYD JOHNSON, Ph.D.

The University of Texas Southwestern Medical Center at Dallas, 2007

JOACHIM HERZ, M.D.

Lrp4/Megf7, a member of the low-density lipoprotein receptor gene family, is a major regulator of tissue patterning during embryonic development. Prior to this work, the function *Megf7* had largely been unknown. Eight distinct mutations in *Megf7* were introduced into mice in order to facilitate a functional analysis of *Megf7*. The *Megf7*$^{EC\ Stop}$ mutant, which has a premature stop codon inserted upstream of the transmembrane domain, had defects in limb, tooth, and mammary gland development. Subsequent analysis showed that the defects in limb development were caused by the expansion of the limb bud structure called the apical ectodermal ridge. Biochemical analysis suggests that Megf7 acts as an inhibitor of the Wnt signaling pathway both *in vivo* and *in vitro*. The analysis of the tooth defect of the

Megf7$^{EC\ Stop}$ mutant shows that there is an increase in BMP activity, one of the major cellular signals involved in development. This increase in BMP activity leads to a loss of patterning during tooth development. The complete *Megf7* null allele that was generated, in addition to having limbs defects, also failed to form kidneys and was paralyzed at birth. The kidney agenesis is the result of a failure of the ureteric bud to grow and branch during the initial stages of kidney development. The phenotype of the *Megf7*$^{EC\ Stop}$ and *Megf7*^{KO} mutants prompted us to look for natural mutants in other animals. We found that Mulefoot Disease, a form of syndactyly in cows, is caused by a single base change at the exon/intron border of exon 37 of bovine *Megf7*. *In vivo* and *in vitro* data suggests that this mutation leads to altered splicing of the gene and premature truncation of the translated gene product. The other six mutant mouse alleles that were generated had specific mutations introduced into the cytoplasmic domain of *Megf7*. The limb phenotypes of these mice suggest that Megf7 may serve as an endocytic receptor. This work establishes *Megf7* as a major regulator of patterning during development and is involved in a natural form of limb dysgenesis. This work will serve as the groundwork for future analysis of *Megf7*.

TABLE OF CONTENTS

CHAPTER ONE Introduction **1**

THe Low-density lipoprotein receptor gene family *1*
General Overview of the LDLR Gene Family 1
Lrp4/Megf7 9
Wnt Signaling Pathway 14
Vertebrate Limb Development 16
Kidney Development 20

CHAPTER TWO Materials and Methods **28**

Animals *28*
Megf7$^{EC\ Stop}$ Plasmid Construction 28
Allelic Series Generation 29
Megf7 Knockout Generation 30
Targeted ES Cell Generation 30
Genetic Analysis of Mice/ES Cells 36
Body Weight Measurements 44
Alcian Blue/Alizarin Red Staining 45
Whole Mount *In Situ* Protocol 46
Whole Mount TUNEL Staining 53
Mulefoot Gene Analysis 54
Wnt Activity 56
Yeast Two-Hybrid Screen 58
Adult Mouse Tissue RT-PCR 59

CHAPTER THREE Results **60**

Analysis of the Hypomorphic Megf7$^{EC\ Stop}$ *allele* *60*
General Description of the *Megf7*$^{EC\ Stop}$ Mutants 60
Regulation of Tooth Development by *Megf7* 65
Defective Mammary Gland Patterning in the *Megf7*$^{EC\ Stop}$ Mutants 73
Polysyndactyly in the *Megf7*$^{EC\ Stop}$ Mutants 74
Disruption of Wnt Signaling in *Megf7* Mutant Limbs 101

CHAPTER FOUR Results **111**

Functional motifs within the cytoplasmic domain of Megf7 ..... *111*
Megf7 Knockin Alleles 111
Yeast Two-Hybrid 121

CHAPTER FIVE Results **130**

Mulefoot Disease and Megf7 ..... *130*
Introduction to Mulefoot Disease 130
Discovery of a Splice Junction Mutation in *Megf7* in MFD Samples 132

CHAPTER SIX Results **141**

The function of Megf7 during kidney development *141*
Generation of the *Megf7*^{KO} Allele 141

CHAPTER Seven Discussion 165

Clues for the function of Megf7 165
Megf7 in Limb Development 165
Regulation of Signaling Pathways 176

Bibliography 199

Vitae 212

PRIOR PUBLICATIONS

Johnson E.B., Steffen D.J, Lynch K.W., Herz J. Defective splicing of *Megf7/Lrp4*, a regulator of distal limb development, in autosomal recessive mulefoot disease. Genomics 88:600-609 (2006)

Johnson E.B., Hammer R.E., Herz J. Abnormal development of the apical ectodermal ridge and polysyndactyly in *Megf7*-deficient mice. Hu. Mol. Gen. 14(22): 2523-3538 (2005)

LIST OF FIGURES

Figure 1 Diagram of the Low-Density Lipoprotein Receptor Gene Family. 2
Figure 2 *Megf7* Expression in the CNS. 12
Figure 3 Limb Development 17
Figure 4 Kidney Development 21
Figure 5 Design of the *Megf7*$^{EC\ Stop}$ Allele. 61
Figure 6 RT-PCR Analysis of the *Megf7*$^{EC\ Stop}$ Transcript. 63
Figure 7 *Megf7*$^{EC\ Stop}$ Mice have Significantly Lower Body Weights. 64
Figure 8 Defective Patterning of the Incisors and Molars in the *Megf7*$^{EC\ Stop}$ Mouse. 68
Figure 9 *Megf7* Expression in the Developing Tooth. 69
Figure 10 Expression of *Shh* and *Ptc* in the *Megf7*$^{EC\ Stop}$ Mutant. 71
Figure 11 Upregulation of Phospho-SMAD Levels in the *Megf7*$^{EC\ Stop}$ Mutant 72
Figure 12 Disruption of Mammary Gland Patterning in the *Megf7*$^{EC\ Stop}$ Mutant. 74
Figure 13 Polysyndactyly in the *Megf7*$^{EC\ Stop}$ Mutant. 75
Figure 14 Alizarin Red/Alcian Blue Staining of the *Megf7*$^{EC\ Stop}$ Limbs. 76
Figure 15 Alizarin Red/Alcian Blue Staining of P0 *Megf7*$^{EC\ Stop}$ Limbs. 77
Figure 16 Defective Cartilage Patterning in the *Megf7*$^{EC\ Stop}$ Mutant. 78
Figure 17 Expression of *Megf7* During Limb Development. 79
Figure 18 Expression of *Fgf8* in the *Megf7*$^{EC\ Stop}$ Mutant. 81
Figure 19 Expansion of the AER in the *Megf7*$^{EC\ Stop}$ Mutants 83
Figure 20 Expression of *Shh* in the *Megf7*$^{EC\ Stop}$ Mutant Limb 85
Figure 21 *Wnt7a* Expression in the *Megf7*$^{EC\ Stop}$ Limb 87
Figure 22 Expression of *Lmx1b* in the *Megf7*$^{EC\ Stop}$ Limb Bud 89
Figure 23 Cross-Sections of the Autopod of Adult *Megf7*$^{EC\ Stop}$ Mice. 91
Figure 24 Expression of *Bmp4* in the *Megf7*$^{EC\ Stop}$ Limb. 93
Figure 25 Expression of *Msx1* in the *Megf7*$^{EC\ Stop}$ Mutant. 94
Figure 26 Expression of *Bmp2* in the *Megf7*$^{EC\ Stop}$ Mutants. 96
Figure 27 Apoptosis in the *Megf7*$^{EC\ Stop}$ Limb. 98
Figure 28 Expression of *Hoxd12* in the *Megf7*$^{EC\ Stop}$ Limb. 99
Figure 29 Expression of *Gli1* in the *Megf7*$^{EC\ Stop}$ Limb 101
Figure 30 Megf7 Inhibits the Wnt Signaling Pathway in the TOPflash Assay. 104
Figure 31 BAT-gal Expression in the *Megf7* Mutant Limb. 106
Figure 32 Stabilization of β-catenin in the Ectoderm of the *Megf7*^{KO} limb. 108
Figure 33 Megf7 does not Bind to Dkk1 or Dkk3. 110
Figure 34 RT-PCR Analysis of *Megf7* Expression in Adult Tissues. 114
Figure 35 Whole Fore Limbs of the Allelic Series. 117
Figure 36 Whole Hind Limbs of the Allelic Series. 118
Figure 37 Alizarin Red/Alcian Blue Staining of the Allelic Series Mutants 120
Figure 38 PDZ Domain Proteins that Bind to Megf7. 123
Figure 39 PTB Domain Proteins that Bind to Megf7 125
Figure 40 Nuclear Proteins that Bind to Megf7 129
Figure 41 Mulefoot Disease 131
Figure 42 Location of *Megf7* Relative to the MFD Locus. 132

Figure 43 A G-to-A MFD Mutation Disrupts the 5' Splice Site of Intron 37 of *Megf7* in Angus cattle. 134
Figure 44 RT-PCR Analysis of Wild Type and MFD RNA. 136
Figure 45 Minigene Splicing Analysis of the MFD Mutation. 140
Figure 46 Diagram of the *Megf7*^{KO} Allele. 143
Figure 47 Defective Limb Development in *Megf7*^{KO} Embryos. 145
Figure 48 Polysyndactyly in *Megf7* Mutant Mice. 146
Figure 49 Expansion of the AER in *Megf7*^{KO} Embryos. 147
Figure 50 Kidney Agenesis in the *Megf7*^{KO} Mutant. 148
Figure 51 Normal Appearance of the *Megf7*^{KO} Kidney. 149
Figure 52 Expression of *Megf7* in the Developing Kidney. 151
Figure 53 Expression of *Wnt9b* in the *Megf7*^{KO} Embryo. 153
Figure 54 Retarded Ureteric Bud Growth and Branching in the *Megf7*^{KO} embryo. 155
Figure 55 Expression of *c-Ret* in the *Megf7*^{KO} embryo. 156
Figure 56 Expression of *Wnt11* in the *Megf7*^{KO} embryo. 158
Figure 57 Expression of *Pax8* in the *Megf7*^{KO} embryo. 160
Figure 58 Expression of *Pax2* in the *Megf7*^{KO} Embryo. 161
Figure 59 Expression of *Gdnf* in the *Megf7*^{KO} Embryo 163
Figure 60 List of Known *Megf7* Mutations 167
Figure 61 *Megalin* Expression in the Developing Kidney 182
Figure 62 Binding of Megf7 to Rap and Mesd2 184
Figure 63 Common Putative Wnt binding Domains 185
Figure 64 Organ Defects in *Megf7* Knockin Mutants 188
Figure 65 Model of the Mechanism of Patterning by *Megf7* 193

LIST OF DEFINITIONS/ABREVIATIONS

Adaptor protein -2 (AP-2) – One of the three adapter proteins involved in clathrin mediated endocytosis.

Alkaline Phosphatase (AP) – An enzyme that is used to convert chromogenic molecules to detect protein binding in assays such as ELISA or whole mount *in situ* hybridization.

Alzheimer's precursor protein (APP) – A membrane bound protein thought to be directly involved in the progression of Alzheimer's Disease.

Apical ectodermal ridge (AER) – A band of pseudostratified epithelium at the distal edge of the developing limb bud that is responsible for the organization of the limb.

Apolipoprotein E Receptor 2 (ApoEr2) – One of the small members of the LDLR gene family that is required for neural patterning and function.

Arrow – The drosophila homologue of Lrp5/6 that is required for canonical Wnt signaling.

β-catenin – the cytoplasmic protein that mediates the canonical Wnt signal as well as being a component of Adherens junctions.

β-galactosidase – A bacterial gene used as a reporter for gene activity in reporter assays such as the BAT-gal mouse, yeast two-hybrid, and transfection based reporter assays.

Bone morphogenic protein (BMP) – One of the major signaling molecules involved in the patterning of many developing organs.

Calmodulin dependent kinase II (CAMKII) – A protein that is found at the post-synaptic compartment in neurons that is involved in the "molecular memory" of the synapse.

Casein Kinase I (CK1) – One of the proteins that phosphorylates β-catenin to inhibit the canonical Wnt signaling pathway.

Dendrites – The processes of neurons that receive stimuli from other neurons or sensory organs.

Dickkopf (DKK) – A protein that inhibits the Wnt signaling pathway through the endocytosis of Wnt molecules.

Disabled (Dab) – A class of proteins that modulate the function of the members of the LDLR gene family through their PTB domains.

Ectoderm – One of the three cell types in the early embryo that eventually forms the skin and the nervous system.

Embryonic stem cells (ES cells) – Cells that are derived from the inner cell mass of a blastocyst that are thought to be totipotent.

Endosome – The intracellular organelle that is the first compartment for endocytosed material.

Engrailed (En1) – A transcription factor involved in the specification of the ventral identity of the limb.

Epidermal growth factor (EGF) precursor homology domains – One of the classes of protein folds involved in the secondary structure of the members of the LDLR gene family.

Exon – The portion of a gene that codes for the amino acid sequence of the protein product.

Fibroblast growth factor (Fgf8) – One of the major signaling molecules involved in the patterning of many developing organs.

Forward genetics – The strategy of gene discovery that involves the discovery of mutant animals and then deducing the gene that is responsible for the mutant phenotype.

Glomeruli – The structures of the kidney that are responsible for the filtration of the blood and recovery of essential molecules.

Glycogen synthase kinase (GSK3) - One of the proteins that phosphorylates β-catenin to inhibit the canonical Wnt signaling pathway.

Glycosylation – The process of adding carbohydrates to a protein to ensure proper folding and to increase solubility.

Herpes Simplex Virus Thymidine Kinase (HSVTK) – The gene used to ensure proper recombination. This enzyme converts a thymidine analog to a toxic compound.

Hippocampus – A structure of the brain that is involved in acquiring and saving memories.

Hypomorph – a mutant that retains a portion of the wild type activity.

***In situ* hybridization** – The technique used to examine the expression of genes using labeled nucleotide probes that bind to the transcripts in the whole tissue.

Intron – A portion of a gene that does not code for protein sequence and is spliced out of the final transcript.

Kremen – A protein that mediates the endocytosis of DKK proteins to inhibit the Wnt signaling pathway.

Ligand Binding Repeats (LRs) – One of the classes of protein folds involved in the secondary structure of the members of the LDLR gene family.

Long-Term Potentiation (LTP) – The process that enhances the strength of a synapse based on the previous activity of the neuron.

Low-density lipoprotein (LDL) – One of the classes of particles that is responsible for the transport of mainly lipids through the blood stream.

Low-Density Lipoprotein Receptor (LDLR) – The founding member of the LDLR gene family. This is one of the smaller genes of the gene family that is involved in the endocytosis of LDL.

Low-Density Lipoprotein Receptor LDLR related protein 1 (Lrp1) – One of the larger members of the LDLR gene family that is required for multiple processes including atherosclerosis and early development.

Low-Density Lipoprotein Receptor LDLR related protein 1b (Lrp1b) - One of the larger members of the LDLR gene family that is downregulated in many cases of lung cancer.

Luciferase – A gene that is used to measure gene activity in reporter assays such as the TOPflash assay.

Low-Density Lipoprotein Receptor LDLR related protein 5/6 (LRP5/6) – Two homologous genes that are distantly related to the LDLR gene family that regulate the Wnt signaling pathway.

Mesenchyme – Cells that are of mesodermal or neural crest origin that condense to form structures such as cartilage, bone, and teeth.

Mesoderm – One of the three early cell types that form the muscles, bones and cartilage.

Metanephric mesenchyme – The mesodermal tissue that condenses to form the kidney in mammals.

Morphogen – A proteins that establishes patterning by creating gradients of signaling intensity within a developing organism.

Multiple EGF Domain protein 7 (Megf7/Lrp4) – The focus of this thesis. This is an intermediate sized member of the LDLR gene family that is involved in the patterning of multiple organs.

Myc epitope – A small peptide sequence that is added to proteins that aids in the detection of the protein through well-characterized antibodies.

Neomycin resistance cassette – A genetic sequence containing a neomycin resistance gene that is used to select for cells that have incorporated the introduced genetic element.

Northern blot – A procedure used to detect the amount of a specific transcript in an RNA sample using a labeled nucleotide probe.

Oligodontia – A condition characterized by the presence of ectopic or malformed teeth.

Parathyroid hormone (PTH) – A hormone that involved in calcium homeostasis.

Peri-telomeric – Near the telomere, a structure at the ends of a chromosome that regulates the number of times the DNA can be replicated.

Platelet derived growth factor (PDGF) – A hormone that is involved in angiogenesis and atherosclerosis.

Polydactyly – The condition of having extra digits.

Polysyndactyly – The condition of having fusion and duplication of digits.

Postsynaptic density protein (PSD-95) – A PDZ motif-containing protein that is involved in the organization of the post-synaptic compartment of the neuron.

PSD-95, Drosophila discs large protein, and the zona occludens (PDZ) motif – A structural protein motif that typically binds carboxy-terminal sequences that end in hydrophobic amino acids.

Prevesicular – Describing cells in the metanephric mesenchyme that are to condense to form the glomeruli of the kidney.

Receptor Associated Protein (Rap) – A 39kDa protein that is involved in the folding of the members of the LDLR gene family.

Reelin – An matrix protein that activated ApoER2 and Vldlr to provide spatial information for migrating neurons.

Synapse-Associated Protein (SAP97) – A PDZ-containing protein involved in the function of the post-synaptic density of neurons.

Syndactyly – The condition of the fusion of digits.

SMA/MAD related proteins (SMAD) – The cytoplasmic proteins involved in the transduction of BMP and other TGF-related receptors.

Southern blot – A procedure used to detect the amount or changes in structure of DNA samples. This is most often used to detect correct homologous recombination.

Sonic hedgehog (Shh) – A morphogen involved in multiple developmental processes including the anterior/posterior patterning of the developing limb.

Sumoylation – The post-translational addition of SUMO, a protein related to ubiquitin, to change the function of a protein.

Terminal deoxynucleotidyl Transferase Biotin-dUTP Nick End Labeling (TUNEL) – A procedure used to detect the DNA degradation that occurs during apoptosis.

Ubiquitin - A protein that is added post-translationally to other proteins through a series of ligases to affect the activity or degradation of the target protein.

Very Low-Density Lipoprotein Receptor (Vldlr) – One of the smaller members of the LDLR gene family that is involved in the patterning of the developing brain.

Wolffian duct – The mesodermal tube structure that is involved in the development of the pronephros, mesonephros, and metanephros.

Yeast Two-Hybrid – A technique used to detect an interaction between two candidate proteins. This technique involves the fusion of two proteins to either a LexA DNA binding element or transcription activation domain. A binding event leads to the expression of reporter genes.

Zone of Polarizing Activity (ZPA) – The region in the posterior mesoderm of the limb bud that is required for anterior/posterior patterning.

CHAPTER ONE
Introduction

Until recently, the function of *Megf7*, a member of a well-characterized Low-Density Lipoprotein Receptor (LDLR) gene family, has been largely unknown. This thesis will explore the function of *Megf7* during embryonic development and provide clues about its molecular mechanism of action.

THE LOW-DENSITY LIPOPROTEIN RECEPTOR GENE FAMILY

General Overview of the LDLR Gene Family

The Low-Density Lipoprotein Receptor (LDLR) gene family consists of seven closely related single pass type I transmembrane proteins. As shown in Figure 1 these include *Ldlr*, Apolipoprotein E Receptor 2 (*Apoer2*), Very Low-Density Lipoprotein Receptor (*Vldlr*), Multiple EGF Domain protein 7 (*Megf7/Lrp4*), LDLR related protein 1 (*Lrp1*), *Lrp1b*, and *Megalin* (*gp330*). These genes produce proteins ranging in size from 93kD to 512kD and yet share the same basic structural motifs. All genes contain ligand-binding repeats and EGF precursor homology domains in the predicted extracellular region of the protein. In the cytoplasmic domain, all of the gene family members contain one or more NPXY motifs. Some members also contain O-glycosylation sites in the extracellular region or PDZ domain-binding sites in the cytoplasmic region. Two other more distantly related genes in the gene family, *Lrp5* and *Lrp6*, also encode the ligand binding repeats as well as EGF precursor homology domains. But, instead of containing the intracellular NPXY motif,

these receptors contain multiple PPPSP motifs that are required for their particular function in Wnt signaling (Figure 1)(Tamai et al., 2004).

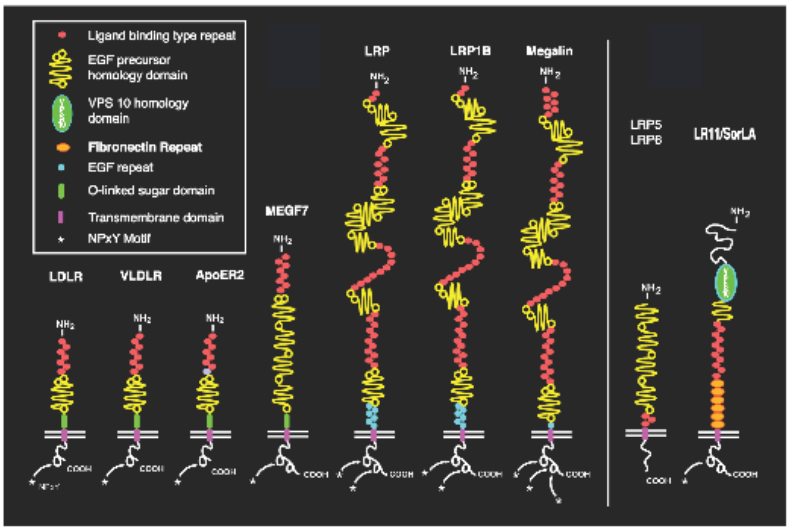

Figure 1 Diagram of the Low-Density Lipoprotein Receptor Gene Family.
This diagram of the LDLR gene family shows the seven core members on the left as well as the three distantly related gene family members on the right. Ligand Binding Repeats- Red; EGF Precursor Homology Domains- Yellow; O-linked Sugar Domain- Green. *Megf7* has an intermediate position within the gene family both in terms of size and structural complexity.

The Extracellular Domain of the LDLR Gene Family

Much of the framework for understanding this gene family involved studies that investigated the founding member of the gene family, *Ldlr*. The amino-terminal motif present in all of the core members of the gene family is the ligand-binding repeat (LR). The LR consists of a unique folded structure held together by three disulfide bonds (Fass et al., 1997; van Driel et al., 1987). The six cysteine residues in the fold form disulfide bonds in a 1 to 3, 2 to 5, and 4 to 6 confirmation. The binding of a calcium ion is also required for proper

folding. The ion is held in place by the six-fold coordination of four residue side chains as well as two backbone interactions (Fass et al., 1997; van Driel et al., 1987).

The 39kDa Receptor Associated Protein (*Rap*) is required for the correct folding and export of most of the members of the LDLR gene family. Rap was initially identified as a protein that bound to Lrp1 on an affinity column (Willnow, 1998). *In vitro* and *in vivo* studies showed that Rap is required for the expression of these gene family members. Rap is especially important in cells that co-express both the LDLR gene family member and its ligand. Rap prevents the premature binding of ligands to the family members by binding to the LRs of the receptors (Willnow, 1998). Rap is released in the cis-golgi and is then recycled to the ER. Overexpression of Rap blocks the function of the receptors by blocking the binding sites for the ligands. Thus, Rap is a chaperone required for the function of not only the Ldlr but also all of the core members of the gene family (Willnow, 1998).

Analysis of the crystal structure of the entire extracellular domain of Ldlr suggests that upon endocytosis and transport to the endosome, the LRs of Ldlr release their bound ligands to bind to the β-propeller domain of the EGF-precursor homology domain. Thus, at the low pH of the endosome, the EGF-precursor homology domain acts as an intramolecular ligand for the LRs of Ldlr (Rudenko et al., 2002). The EGF precursor homology domain consists of six units of four β-strands as well as flanking EGF modules (Jeon et al., 2001). This motif folds into a conformation similar to that seen with a WD40 β-propeller. The YWTD repeat is in the second strand of each fold unit and is required for many of the intramolecular interactions required for folding. The C-terminal EGF module appears to

tightly pack against the β-propeller whereas the N-terminal module looks more loosely packed (Jeon et al., 2001).

Another chaperone, *Boca/Mesd2*, is also required for the expression of the distantly related LDLR gene family members, *Lrp5/6* (Culi & Mann, 2003; Hsieh et al., 2003). Mutants in this protein in either flies or mice have a phenotype similar to a loss of Wnt activity suggesting that Boca/Mesd2 is required for the Wnt-associated receptors Lrp5/6. Boca/Mesd2 bind to Arrow/Lrp5/6 in pulldown assays. Co-expression of Boca/Mesd2 facilitates the transport of Lrp5/6 to the plasma membrane. In contrast to the other members of the LDLR gene family, Rap does not significantly enhance expression of Arrow/Lrp5/6. This suggests that perhaps the function of Boca/Mesd2 is to facilitate the folding of the EGF-precursor homology domain or to prevent the premature binding of ligands (Culi & Mann, 2003; Hsieh et al., 2003). Therefore, there are two known proteins that are required for the folding and export of the LDL receptor gene family members.

Many members of the LDLR gene family undergo N-linked glycosylation. Some members of the LDLR gene family also contain an O-glycosylation motif. *Ldlr*, *Apoer2*, and *Vldlr* all contain an exon that encodes for a serine/threonine rich O-glycosylation motif immediately upstream of the transmembrane domain. The consequence of having a glycosylation site in these receptors is unknown. Alteration of the glycosylation of Ldlr does not appear to affect ligand binding (Davis et al., 1986) but may affect the post-translational processing of the receptor (Yoshimura et al., 1987). One report suggests that glycosylation regulates the γ-secretase dependent cleavage of ApoER2 and Lrp1 (May et al., 2003). The

level of glycosylation is dependent on the tissue that is expressing the receptor and therefore may be a way to regulate the activity of this gene family.

The Cytoplasmic Domain of the LDLR Gene Family

The NPXY motif is an important region within the core members of the LDLR gene family because it is a binding site for several intracellular proteins that regulate cellular signaling as well as the trafficking of the receptor. The first observation concerning the importance of the NPXY motif was the demonstration that the tyrosine in the NPXY motif of LDLR was required for the rapid internalization in response to LDL binding (Davis et al., 1987). The NPXY may not require a direct interaction with the AP-1,2,3 complex, the proteins responsible for most receptor mediated internalization, but instead requires a PTB-containing adapter protein such as Dab2 and ARH (Bonifacino & Traub, 2003). The NPXY motif also serves a signaling role. Lrp1 regulates the PDGF Receptor through its second NPXY motif. Phosphorylation of the tyrosine of this NPXY motif provides a binding site for the intracellular adaptor protein SHC. The bound SHC in turn regulates the activity of the PDGF receptor. The regulation of PDGF Receptor activity by Lrp1 may regulate the progression of atherosclerosis (Boucher et al., 2003; Boucher et al., 2002; Loukinova et al., 2002). Other studies have suggested that the NPXY residues alone are not completely sufficient for signaling. The two or three amino acids upstream of the NPXY motif are also required for adaptor protein recognition (Bonifacino & Traub, 2003).

Along with the NPXY motif, other motifs within the cytoplasmic domains of the gene family members can also regulate receptor-mediated endocytosis. The NPXY motifs of Lrp1

contribute only a minor portion of the endocytic activity of the receptor (Li et al., 2000). Mutational analysis suggests that the YXXΦ motif within the cytoplasmic domain is the endocytic motif in the receptor that contributes to most of the endocytic activity. A dileucine repeat may also contribute to the endocytosis of Lrp1 (Li et al., 2000).

The dileucine repeats in Lrp1 fit into the [DE]XXXL[LI] motif used by many proteins for inducible endocytosis (Bonifacino & Traub, 2003). Endocytosis can also be regulated by ubiquitination. Ubiquitination is usually initiated by the recognition of the substrate by an E3 ubiquitin ligase. Thus, the recognition sequence for ubiquitination is dependent on the E3 ligase that mediates the endocytosis (Bonifacino & Traub, 2003).

PDZ domains are multifunctional binding domains required for many important protein-protein interactions. PDZ motifs recognize four classes of structural motifs on the ligands. Class I ligands contain a X-S/T-X-Φ motif, class II ligands contain a X-Φ-X-Φ motif, and class II ligands contain a X-D/E-X-Φ motif at their carboxy-terminus (Φ represents any hydrophobic amino acid residue). Another class of ligands, that are difficult to predict based on primary structure, has an internal recognition motif that is not at the C-terminus (Hung & Sheng, 2002). PDZ domains also can bind the lipid signaling molecules called inositols (Balla, 2005). Several members of the LDLR gene family contain PDZ-motif binding sites including a potential internal binding site in ApoER2.

Functions of the LDLR Gene Family

The genes of the LDLR gene family serve as both cargo transport proteins as well as signaling proteins. The functions of these proteins range from lipoprotein transport, neural

signaling, membrane receptor signal modulation, etc. and have been reviewed elsewhere (Goldstein, Hobbs & Brown, 2001). This wide variety of functions indicates the importance of this gene family but also complicates the analysis of each member; there is no stereotypical function of any one member of the gene family. There are no common intracellular signaling components that can be used to deduce function. Each member needs to be treated as a novel gene. The members of the gene family will be briefly described to demonstrate the complexity of regulation of these genes.

The Low-Density Lipoprotein Receptor (Ldlr) is the founding member of the LDL Receptor gene family. This gene was initially found through genetic analysis and subsequent biochemical purification (Goldstein et al., 2001). This gene served as a model for surface binding and endocytosis for other receptor systems. Mutations in *Ldlr* results in high plasma cholesterol levels which results in soft-tissue lipid deposits such as atherosclerotic plaques and xanthomas. The disease caused by these mutations, Familial Hypercholesterolemia (FH), normally leads to premature death in the homozygous state (Goldstein et al., 2001).

Endocytosis was found to be modulated through the NPXY motif found in the cytoplasmic domain of the LDL Receptor. In the liver, the intracellular adapter protein ARH binds to the NPXY motif through its PTB domain to facilitate the formation of the complex of the LDL Receptor, ARH, clathrin, and AP-2 (Jones et al., 2003). This complex then induces the internalization of the LDL Receptor as well as its bound cargo (Jones et al., 2003). In other cells, such as fibroblasts, ARH is substituted by another PTB domain-containing protein, Dab2 (Maurer & Cooper, 2006).

The functions of Apoer2 and Vldlr have mainly been analyzed in the brain since the initial discovery that the *Apoer2* and *Vldlr* double knockout has the same phenotype as the *Reelin* and *Dab1* knockout mice, mice that have defects in brain cortical lamination (Trommsdorff et al., 1999). This led to the discovery that ApoER2 and Vldlr are the receptors for Reelin and signal though Dab1 to regulate neuronal positioning during neural development (Trommsdorff et al., 1999).

Apoer2 has also been shown to regulate synaptic plasticity in the mature animal. In wild type mice, Reelin enhances the hippocampal CA1 response to Long-Term Potentiation (LTP) (Weeber et al., 2002). This enhanced LTP appears to occur through an interaction with the NMDA receptors at the post-synaptic terminal (Chen et al., 2005).

Lrp1 is one of the three largest members of the gene family along with *Lrp1b* and *Megalin* (Figure 1). *Lrp1* has multiple functions including an essential function during early embryonic development that leads to early embryonic lethality of knockout embryos (Herz, Clouthier & Hammer, 1992). *Lrp1* has recently been implicated in the pathogenesis of atherosclerotic lesions. Loss of *Lrp1* in the aorta, along with loss of the *Ldlr* and a high fat diet, leads to an increase in the atherosclerotic lesion size in mice (Boucher et al., 2003). The loss of *Lrp1* leads to the upregulation of the PDGF signaling pathway and induces the smooth muscle cells in the vascular wall to proliferate, migrate and disrupt the laminar layers of the aorta (Boucher et al., 2003; Boucher et al., 2002; Loukinova et al., 2002). *Lrp1* has also been implicated in the clearance of chylomicron remnants, the particles responsible for the transport of digested lipids, from the blood stream (Rohlmann et al., 1998).

Lrp1b is very similar in structure to *Lrp1*. Surprisingly, despite the importance of *Lrp1*, the function of *Lrp1b* appears to be redundant. The *Lrp1b* knockout mice appear to be normal upon gross examination (Marschang et al., 2004). This gene may be a tumor suppressor based on the high frequency of *Lrp1b* gene deletion in cancer (Liu et al., 2000). *Lrp1b* may also play a role in regulating the levels of Alzheimer's Precursor Protein, APP, on the cell surface in the brain (Cam & Bu, 2006).

Megalin is another large member of the LDL receptor gene family that is required for multiple functions (Figure 1). *Megalin* is one of the major protein species expressed in the kidney and is required for the transport of multiple proteins and molecules, including Parathyroid Hormone and the Vitamin D Binding Protein. Loss of *Megalin* in the kidney results in a loss of calcium homeostasis through a disruption of vitamin D metabolism (Leheste et al., 2003). *Megalin* also antagonizes the actions of Parathyroid Hormone, PTH, through its internalization (Hilpert et al., 1999).

Recently, it has been demonstrated that *Megalin* can also antagonize BMP signaling through the internalization of BMP4 (Spoelgen et al., 2005). Loss of *Megalin* in the developing brain results in holoprosencephaly. This defect is a result of the hyperactivation of the BMP signaling pathway due to a loss of inhibition by *Megalin* (Spoelgen et al., 2005).

Lrp4/Megf7

Lrp4/Megf7 was originally cloned by Nakayama et al. (Nakayama et al., 1998) This research group was looking for large molecular weight proteins that are expressed in the

brain and contain protein domains that look like EGF repeats. Nine novel genes were found with this search criteria by sequencing the 5' end of brain cDNA clones with large inserts. *Megf7* was the seventh of such clones. Northern blot expression analysis shows that *Megf7* is globally expressed within the rat brain (Nakayama et al., 1998). Since then, several names have been associated with *Megf7*. The standardized LDL receptor gene name for *Megf7* is *Lrp4*. Unfortunately, Tomita et al. called another gene "Lrp4" (accession #Q9Z319)(Tomita et al., 1998). This gene encodes a type II transmembrane protein with EGF repeats and an intracellular protease domain that is expressed mainly in the heart. The topology and domain structure of this gene excludes it from the LDL receptor gene family. Simone-Chazottes also named the gene "LDLR dan" (accession #Q8VI56). Tian et al. independently cloned *Megf7* looking for mRNAs that are localized to the post-synaptic density. They initially called it "Dem26" (Tian et al., 1999) and later called it "synLrp" for synaptic Lrp (Tian et al., 2006). Since then, *Megf7* or *Lrp4* has become the accepted names for this gene.

Structure of Megf7

Megf7 has a unique structure when compared to the other members of the LDLR gene family (Figure 1). The *Megf7* gene consists of 38 exons at position 11p12-p11.2 in humans, on chromosome 2 in mice, and chromosome 15 in cows. The mRNA for *Megf7* is nine kilobases and encodes a protein that contains a signal peptide, eight ligand-binding repeats, four EGF precursor homology domains, a transmembrane domain, and a cytoplasmic tail. The cytoplasmic tail includes one NPXY motif as well as a C-terminal PDZ recognition sequence. There is also one putative YXXL motif as well as two putative [D/E]XXXL[L/I]

motifs, both of which may be involved in endocytosis and endosomal targeting. Duchesne et al. noted that exon prediction programs predict another exon after the first exon and is referred to on Swissprot by reference # O75096 (Duchesne et al., 2006). This putative exon codes for the sequence "AVALGLRAGERTRSGPGSSSPSGGISGGASAGSGLGRGAGLG-RGA". Note the disproportionate number of serines and glycines. This exon is not predicted for all mammalian *Megf7* genes and thus may be an artifact of the exon prediction program.

Several publications looking at the different functions of *Megf7* will be discussed in the next section. Most have been rather descriptive and have very little functional data and do not examine the same topics discussed in the Results section of this thesis. One report (Simon-Chazottes et al., 2006) compliments the data published in our publication (Johnson, Hammer & Herz, 2005) and will be discussed below.

Information on Megf7 Published During this Thesis Work

The transcript for *Megf7* was found in the post-synaptic fraction in neurons (Tian et al., 1999). Tian et al. also found that the expression of *Megf7* is upregulated upon Kainate stimulation, a condition used to examine neuronal excitotoxicity, in neurons of the cerebral cortex. The expression along the dendrites is also apparent with *in situ* hybridization (Figure 2A) (Tian et al., 1999).

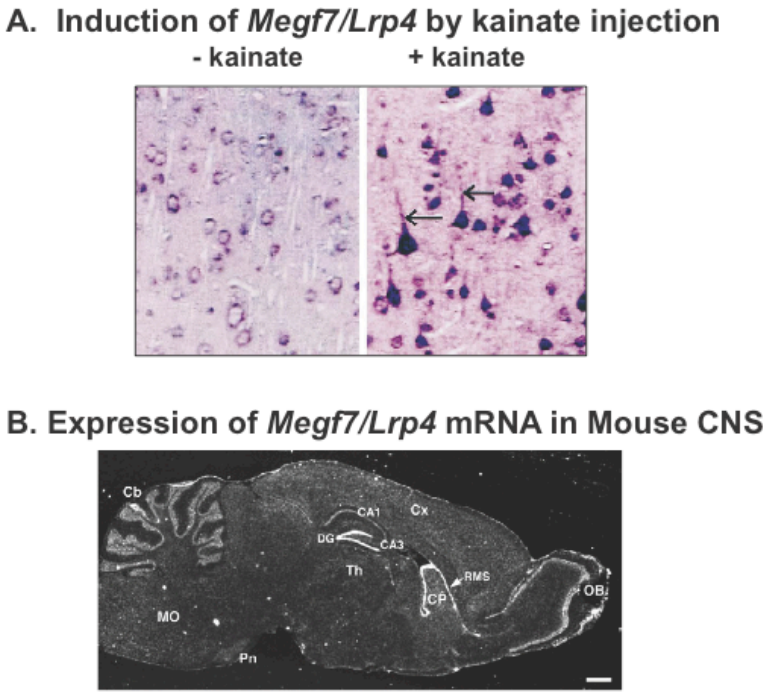

Figure 2 *Megf7* Expression in the CNS.

Tian et al. provided a detailed analysis of *Megf7* within the central nervous system. (A) *Megf7* mRNA is transported along dendrites. Expression of *Megf7* in neurons is upregulated upon kainate stimulation. (B) *Megf7* mRNA is found in the cerebellum (Cb), dentate gyrus (DG), subventricular zone, rostral migratory stream (RMS), and olfactory bulb (OB).

Tian et al. also found that *Megf7* was expressed in several specific regions within the rodent brain. *Megf7* mRNA was localized to the hippocampus, a brain structure that is essential for acquiring memories. Interestingly, the highest hippocampal expression is in the dentate gyrus region whereas the expression in the other hippocampal regions such as the CA1 and CA2 cell layers is much weaker. The transcript is also found in the nerve layer, mitral cell layer, and superficial internal granular layer in the olfactory bulb. Weak expression was seen in the caudate putamen. More interestingly, the subventricular zone and rostral migratory stream next to the caudate putamen had high *Megf7* expression. *Megf7* was

also found in the cerebral cortex, cerebellar granule cell layer, and several brain stem nuclei (Figure 2B) (Tian et al., 2006). *Megf7* is expressed in structures involved in learning and adult neurogenesis.

Using affinity-purified antibodies Tian et al. found that Megf7 is probably localized to post-synaptic densities. Megf7 can also specifically bind to the PDZ domain-containing proteins PSD-95 and SAP97. These interactions probably mediate the association of Megf7 with CAMKII, an important protein involved in synaptic memory. Megf7 can also be phosphorylated on Ser1887 and Ser1900. Phosphorylation subsequently reduces Megf7's affinity for PSD-95 and SAP97. This synaptic biochemical data suggests that Megf7 plays an important role in synaptic memory (Tian et al., 2006).

Megf7/Lrp4 was found to be significantly upregulated in Papillary Thyroid Cancer (Hucz et al., 2006; Jarzab et al., 2005). The functional significance of this upregulation is unknown but it may provide some insight once the molecular mechanism of *Megf7* is elucidated.

Yamaguchi et al. recently demonstrated that *Megf7* may be a specific marker for germ cells progenitors (Yamaguchi et al., 2006). Yamaguchi et al. initially found that *Megf7* was differentially regulated using a germ cell specific differential expression screen. Along with the germ cell expression, they also describe the expression of *Megf7* in the allantoic bud, amnion and forelimbs. *Megf7* expression colocalizes with *Pou5f1*, a marker for germ cells, in the hind gut, the genital ridge, the testes, and the ovaries. *Megf7* is expressed in the DDX4+/TRA98+ spermatogonia in the testes and the DDX4+ immature oocytes in the

ovaries. This suggests that *Megf7* is only expressed in the precursor cell populations but not in the mature spermatocyte or oocyte (Yamaguchi et al., 2006).

Other reports on *Megf7* were published during my thesis. Those results will be referred to at the appropriate time with related data later in this thesis.

Wnt Signaling Pathway

The Wnt signaling pathway is extremely important in many aspects of development and disease. A large body of work has accumulated concerning this central signaling pathway (Logan & Nusse, 2004). This thesis will focus mainly on what is called the canonical pathway, but there are at least two other functions of Wnt components, called the non-canonical pathways, that may contribute to the mechanism of the action of *Megf7*. The Wnt family of genes encodes secreted lipid-modified proteins that are expressed in complex patterns during development and in the mature animal. There are two known classes of receptors for the Wnts, the Frizzled proteins and Lrp5/6. The Frizzled genes encode 7-pass transmembrane proteins that bind to the Wnts and probably provide specificity for each of the different Wnt proteins. Lrp5/6 also bind Wnts but are probably more general in their affinity to each Wnt and are involved in signal transduction (Tamai et al., 2000; Tamai et al., 2004).

In a resting cell, the protein called β-catenin is kept at low levels through tyrosine phosphorylation by GSK3 and CK1 and subsequent degradation by the proteasome. Upon stimulation of the canonical Wnt pathway, GSK3 and CK1 are inhibited and thus β-catenin is

stabilized. The stable β-catenin goes to the nucleus where it can activate Wnt-responsive genes through its interaction with TCF/LEF (Logan & Nusse, 2004). The TOPflash reporter assay that will be used later in this thesis takes advantage of the actions of β-catenin by placing TCF/LEF binding elements in front of a luciferase gene in a reporter plasmid. Therefore, in this assay, the luciferase gene is under the control of the canonical Wnt pathway (Logan & Nusse, 2004).

Lrp5/6 in the Wnt Signaling Pathway

Lrp5 and *Lrp6* are closely related genes that are distantly related to the LDL receptor gene family. Both genes have four EGF-precursor homology domains as well as three ligand-binding repeats immediately upstream of the transmembrane domain. *Lrp5/6* are not considered to be closely related to the core members of the LDLR gene family because they do not contain an NPXY motif in the cytoplasmic region (May et al., 2003). Instead, *Lrp5/6* contain several PPPSP motifs in the cytoplasmic region. The PPPSP motifs are binding sites for Axin. Deletion of the extracellular domain of Lrp5/6 creates a constitutively active form of the receptor that can activate the canonical Wnt signaling pathway. The constitutive activation of the Wnt signaling pathway suggests that Lrp5/6 are the signaling component of the Wnt signaling pathway where the Frizzled proteins may provide a more regulatory role (Tamai et al., 2004).

There are many genes that have been proposed to be regulators of the Wnt signaling pathway (Logan & Nusse, 2004). Three of these genes are *Dkk*, *Kremin*, and *Lrp1*. The DKK genes encode secreted proteins that can bind to the extracellular domain of Lrp5/6 (Bafico et

al., 2001; Brott & Sokol, 2002; Mao et al., 2001). Mao et al. suggest that Dkk1 inhibits the Wnt signaling pathway through its interaction with Kremen, a high affinity receptor for the DKK proteins. The expression of Kremen along with Lrp6 leads to the endocytosis of Lrp6. The binding of the Lrp6 extracellular region to Kremin is dependent on the presence of Dkk1 suggesting that it is required to provide a "bridge" between Lrp6 and Kremen (Mao & Niehrs, 2003; Mao et al., 2002). Another regulator of the Wnt signaling pathway that involves the LDL receptor gene family is *Lrp1*. *Lrp1* has been shown to inhibit the Wnt-dependent reporter gene expression in a commonly used Wnt assay (Zilberberg, Yaniv & Gazit, 2004). This suggests that other members of the LDL receptor gene family other than *Lrp5/6* can regulate the WNT signaling pathway.

Vertebrate Limb Development

The vertebrate limb has three known organizing centers that direct the patterning of the developing limb (Figure 3). The apical ectodermal ridge (AER) is a thin band of pseudostratified epithelium that is located at the dorsal/ventral border of the limb bud before the digits form. The AER provides trophic support for the proximal to distal growth of the developing limb. The factors secreted by the AER are also required for the expression of other genes that are involved in limb development. Another organizing center of the developing limb is called the Zone of Polarizing Activity (ZPA). This region in the posterior mesoderm is characterized by the expression of the morphogen *Shh*. The ZPA is involved in anterior to posterior patterning. The third region of the developing limb that can be

considered an organizing center is the ventral ectoderm. The ectoderm of the developing limb provides dorsal and ventral information through the expression of *Wnt7a* and *En1* respectively. *En1* expressed in the ventral ectoderm inhibits the expression of *Wnt7a*, which in turn specifies tissues to adopt a dorsal fate. The coordination of the gene expression in different regions of the limb bud is required for correct patterning (Capdevila & Izpisua Belmonte, 2001).

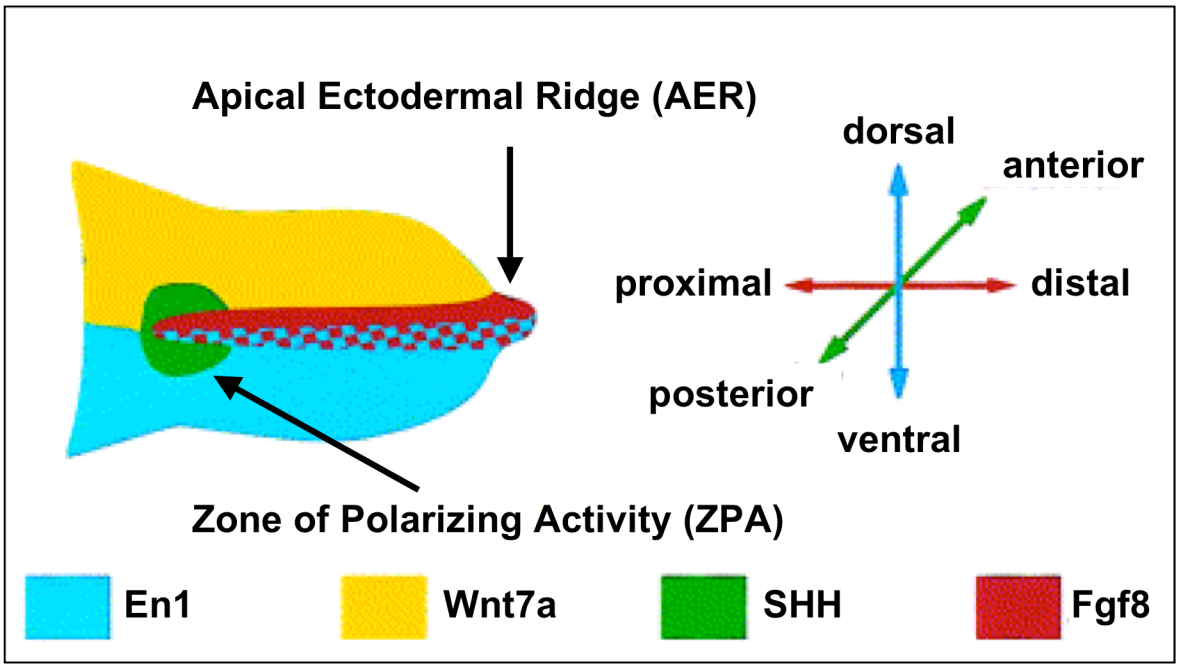

Figure 3 Limb Development

Figure describing the different regions of the developing limbs adapted from Adamska et al. (Adamska, MacDonald & Meisler, 2003). The dorsal ectoderm is characterized by the expression of *Wnt7a* (yellow). *En1* is expressed both in the ventral ectoderm as well as the ventral half of the AER (blue). The AER is marked by *Fgf8* expression (red). The Zone of Polarizing Activity is marked by the expression of *Shh* in the posterior mesoderm (green).

The Wnt Signaling Pathway During Limb Development

As with many aspects of development, the Wnt pathway plays an important role in establishing patterning in the developing limb. Many different Wnts are expressed in different regions within the developing limb. While some Wnts probably have redundant roles, others are essential for establishing the correct patterning of the developing structure. During the initiation of the development of the limb, *Wnt2b* and *8c* are expressed in the lateral plate mesoderm and probably specify where along the body axis the limb should develop (Capdevila & Izpisua Belmonte, 2001). *Wnt7a* is unique in that it is exclusively expressed in the dorsal ectoderm (Parr et al., 1993). This dorsal expression of *Wnt7a* appears to be required for the correct dorsal specification of tissues in the limb (Riddle et al., 1995). Other members of the Wnt family such as *Wnt3, 4, 6, 7b,* and *10a* are expressed throughout the ectoderm of the developing limb (Barrow et al., 2003; Narita et al., 2005; Parr et al., 1993). While some Wnts such as *Wnt5b, 6, 10a*, and *12* are highly expressed in the specialized ectodermal structure called the Apical Ectodermal Ridge (Christiansen et al., 1995; Loganathan et al., 2005; Narita et al., 2005). *Wnt5a* and *Wnt11* have a more general expression pattern in the developing limb (Christiansen et al., 1995; Dealy et al., 1993; Loganathan et al., 2005). The modulation of Wnt activity by *Megf7* in the Results section of this thesis suggests that one or more of these genes may interact with *Megf7* during limb development.

There are many members of the Frizzled gene family that are expressed in the developing limb. The Frizzleds that are expressed in the ectoderm of the developing limb are *Frizzled 1,3, 4, 6,* and 8 (Borello et al., 1999; McQueeney, Soufer & Dealy, 2002; Nohno et

al., 1999; Soshnikova et al., 2003). The Frizzleds expressed in the ectoderm will be relevant to ideas expressed in this thesis because the actions of *Megf7* will primarily affect cells in the ectoderm.

Wnt Activity in the Developing Limbs

There are two Wnt reporter mice that have been developed and one Wnt responsive gene that can be used to detect Wnt activity. The TOPgal mouse was generated by using the promoter used in the TOPFlash reporter assay to control the expression of β-galactosidase in a transgene (DasGupta & Fuchs, 1999). The promoter in this transgene consists of three TCF/LEF binding sites upstream of minimal promoter elements. The TOPgal transgene appears to be expressed in the AER in the developing limb even though extensive analysis of the expression pattern has not been published (Topol et al., 2003). The BAT-gal mouse line is similar to the TOPgal system because the transgene also has a β-galactosidase gene under the influence of TCF/LEF binding sites and minimal promoter (Maretto et al., 2003). The two transgenes differ in the number of TCF/LEF binding sites as well as the choice of the minimal promoter used. The published results show that both mouse lines express β-galactosidase in the AER in a continuous band at the distal edge of the limb (Maretto et al., 2003; Topol et al., 2003). Our results with the BAT-gal mice described below are similar but the expression is not as continuous as what was published.

Axin2/Conductin can also be used as a reporter for canonical Wnt activity. In the limb, *Axin2/Conductin* appears to be expressed in the ventral ectoderm as well as the underlying mesoderm (Soshnikova et al., 2003). Unfortunately, the limb buds used in the

published results appear to be too immature to have an AER. It is possible that the *Axin2/Conductin* expression resolves into the AER once it is formed.

Kidney Development

The mammalian kidney is derived from tubules that branch off of the Wolffian duct. There are three branching events that form the pronephros, mesonephros, and the metanephros (Figure 4)(Perantoni, 2003). The metanephros eventually becomes the functional kidney in mammals. The mesonephros becomes the vas deferens and epididymus in males while in females it is reabsorbed. In females the Wolffian duct becomes the Mullerian duct, which forms the uterus and Fallopian tubes. The pronephros is also reabsorbed soon after its formation in mammals. The development of the metanephric kidney begins with the emergence of the Ureteric Bud (UB) from the Wolffian duct near the cloaca, the rostral structure of the developing digestive tract. The UB is a branching tubule of epithelial cells that induces the condensation of the surrounding mesenchyme at the tip of each branch. Condensed mesenchyme then forms the structures that will eventually become the nephron of the fully functional kidney and the UB forms the ureter and collecting ducts of the kidney (Perantoni, 2003).

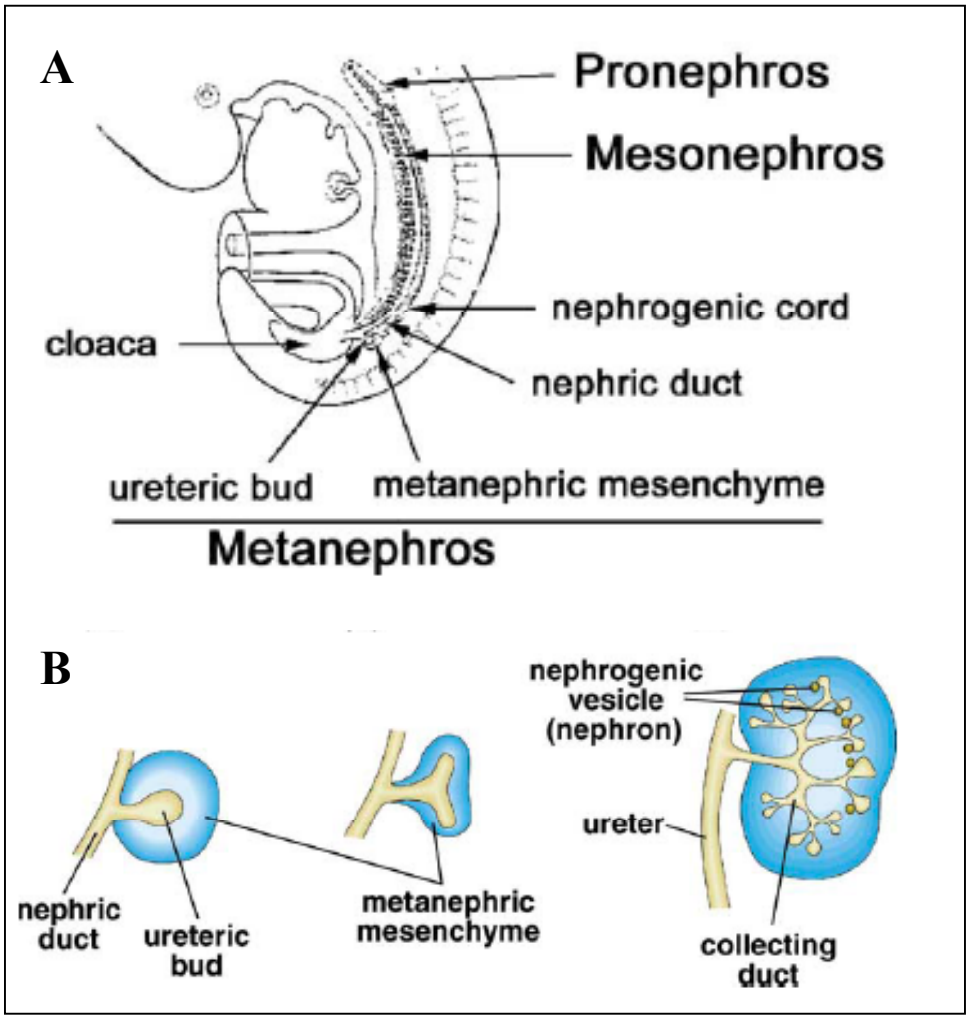

Figure 4 Kidney Development

Description of the different stages of kidney development adapted from a review by Alan Perantoni (Perantoni, 2003). (A) Kidney development is initiated from a structure called the Wolffian duct. The Pronephros, Mesonephros, and Metanephros develops in the mesoderm in a rostral to caudal pattern. (B) The Metanephros begins with the branching of the ureteric bud from the Wolffian duct. The ureteric bud invades the metanephric mesenchyme and branches. The ureteric bud induces the surrounding mesenchyme to condense to form the nephrogenic vesicles.

The coordination of branching and induction in the kidney requires the precise regulation of many genes in many cell types. Three gene families have been found to regulate

such processes: the BMP gene family, the FGF gene family, and the Wnt gene family. All three gene families produce secreted proteins that provide directional cues, induce activities, and provide trophic support to the signal-receiving cells. The functions of Wnts and BMPs will be discussed in more detail to compliment the findings in the results section. Other genes are also important in the regulation of the development of the kidney. *Gdnf*, *WT-1*, *Tgf-β,* and the Pax genes have also been found to be important in regulating nephrogenesis. Schwab et al. provides a large list of genes differentially regulated in the UB and metanephric mesenchyme (Schwab et al., 2006).

Wnts in Kidney Development

Wnt activity appears to be absolutely essential for the correct formation of the kidney. This was first demonstrated using metanephric mesenchyme explant cultures. Previously, it was found that embryonic neural tubes can provide the correct factors to induce tubulogenesis in metanephric mesenchyme (Saxen & Lehtonen, 1987). This was the gold standard for a non-UB tissue that can induce kidney development in the mesenchyme. In order to identify the factor secreted by the neural tube that induces kidney development, investigators looked at the activity of Wnt1. Wnt1 was able to completely induce the formation of nephrons in isolated mesenchyme (Herzlinger et al., 1994). Lithium (Li), a potent inducer of the canonical WNT signaling pathway, was able to induce the initial stages of kidney development in mesenchyme explant cultures. Unfortunately Li, unlike neural tube tissue and Wnt1, was not able to induce the complete formation of patterned nephrons and thus was not a complete inducer of kidney development (Davies & Garrod, 1995). The

difference in activity between Li and Wnt1 suggests that there may be a non-canonical Wnt component involved in tubule patterning.

Several genes involved in Wnt signaling are expressed in the developing kidney. Secreted Frizzled Related Protein 1 (*sFrp1*) is expressed in the interstitial mesenchyme and *sFrp2* is expressed in the condensed mesenchyme. The expression of *sFrp2* appears to be dependent on the expression of *Wnt4* (Lescher, Haenig & Kispert, 1998). *Wnt2b* is expressed in the presumptive stromal cells in the mesenchyme and may be involved in the preparation of the mesenchyme to become competent to be induced by the UB (Lin et al., 2001). *Wnt4* is expressed in the prevesicular mesenchyme, the mesenchyme that will condense to form the tubules of the glomeruli (Stark et al., 1994). *Wnt6* is expressed in the Wolffian duct as well as the UB but is excluded from the tips of the UB. *Wnt6* can induce condensation in mesenchyme explants (Itaranta et al., 2002). *Wnt4* appears to be a negative regulator of *Wnt6* expression (Itaranta et al., 2002). *Wnt7b* is expressed late in kidney development and thus is probably not involved in the initial stages of kidney development. Wnt7b, however can induce the condensation of mesenchyme in explant cultures (Kispert, Vainio & McMahon, 1998; Nguyen et al., 1999). The expression of *Wnt9b* is similar to *Wnt6*, where it is expressed in the Wolffian duct and UB but is excluded from the tips of the UB (Carroll et al., 2005). In contrast to *Wnt6* and *Wnt9b*, *Wnt11* is expressed in the tips of the UB (Kispert et al., 1996). The functions of *Wnt4*, *Wnt9b* and *Wnt11* will be discussed in further detail below.

The expression of *Wnt4* is dependent on *Pax2*, *WT-1*, *Wnt9b* and *Wnt4* itself (Carroll et al., 2005; Sim et al., 2002; Stark et al., 1994; Torban et al., 2006). *Wnt4* induces the expression of *Pax8*, *Wnt4*, and *sFrp2* and inhibits the expression of *Wnt6* (Itaranta et al.,

2002; Lescher et al., 1998; Stark et al., 1994). The *Wnt4* knockout mice die perinatally. The kidney agenesis in these mice appears to be the result of a lack of mesenchymal condensation (Stark et al., 1994).

Wnt9b mutants also die perinatally. Kidney development fails to proceed beyond the initial UB stage with limited associated mesenchyme. *Wnt11*, *Wnt4*, *Gdnf*, *Pax8*, and *Fgf8* are all downregulated in the mutant embryos. *Wnt9b* appears to be involved in mesenchyme condensation but cannot replace the function of *Wnt4* in the mesenchyme. The action of *Wnt9b* appears to involve the canonical Wnt pathway (Carroll et al., 2005).

The phenotype for the *Wnt11* knockout is less severe than the *Wnt4* or *Wnt9b* knockouts. The *Wnt11* mice also die perinatally and the kidneys that are produced have significantly less glomeruli compared to wild type mice. This defect appears to be the result of defective branching. *Wnt11* appears to be reciprocally regulated by *Gdnf* (Majumdar et al., 2003) and may be indirectly regulated by *Bmp4* (Miyazaki et al., 2000). Unlike Wnt4 and Wnt9b, Wnt11 cannot induce mesenchyme condensation in explant cultures (Kispert et al., 1998). Even though *Wnt11* is expressed in a region that would make it a prime candidate for the inducer of condensation of mesenchyme, it is probably involved in the branching of the UB.

BMPs During Kidney Development

The function of BMPs, or related proteins, in the developing kidney is to inhibit the budding and branching of the UB, induce the proliferation, and inhibit the differentiation of the metanephric mesenchymal cells (Hartwig et al., 2005; Miyazaki et al., 2000). *Bmp2,3,4,5*,

and *7* are expressed in the developing kidney (Martinez & Bertram, 2003). The expression patterns of some of the BMPs are overlapping and thus may account for some functional redundancy found in some mutants (Dudley & Robertson, 1997). Of the BMPs expressed in the developing kidney, mutations in *Bmp2,4,5*, and *7* have an effect on kidney development.

Bmp2 is expressed in the prevesicular mesenchyme in the developing kidney (Dudley & Robertson, 1997). The effect of BMP2 on branching is debatable. Analysis of *Bmp2* heterozygotes along with mutants of other modulators of the BMP signaling pathway suggests that BMP2 inhibits the branching of the UB (Hartwig et al., 2005). On the other hand, exogenous BMP2 does not inhibit the branching of kidney explants *in vitro* (Martinez, Mishina & Bertram, 2002).

Bmp4 is expressed in the mesenchyme surrounding the stalk of the UB, the stromal cell population and the mature structures of the kidney (Dudley & Robertson, 1997; Miyazaki et al., 2000). *Bmp4* is also expressed along the Wolffian duct during the initial stages of kidney development. Interestingly, it appears as if *Bmp4* expression is lost in the region of the initial UB budding point suggesting that *Bmp4* regulates where the UB will emerge. *Bmp4* heterozygotes have a broad spectrum of dysplastic and hypoplastic kidney phenotypes. The *Bmp4* deficient kidneys have a pattern of either hydronephrosis or multicystic dysplasia. The branches of the UB in the heterozygotes are shorter compared to wild type mice. Supplementation with BMP4 *in vitro* induces the elongation of the UB but not branching. There are also instances of bifid kidneys in these mutants. Analysis of the *Bmp4* mutant UB at early stages shows that there are occasional ectopic buds at the T-stage UB, which suggests that *Bmp4* inhibits the initiation of branching along the stalk of the UB

(Miyazaki et al., 2000). This can be confirmed *in vitro* where, unlike BMP2, BMP4 can inhibit the branching of kidney explants (Martinez et al., 2002; Raatikainen-Ahokas et al., 2000). Therefore *Bmp4* appears to be a main player in the inhibition of premature branching during nephrogenesis.

Bmp5 may have a similar function as *Bmp4*. *Bmp5* is also expressed in the mesenchyme around the stalk of the UB (Dudley & Robertson, 1997). The natural mutant of *Bmp5*, the short-ear mouse, also has hydroureter and hydronephrosis (Green, 1968; Kingsley, 1994). The mechanism of this phenotype is poorly understood, but it may be similar to that of *Bmp4*.

Bmp7 mutant mouse also has a kidney phenotype. *Bmp7* mutants have small kidneys with a common occurrence of hydroureter. The kidneys that do form in these mutants have a reduction of condensed mesenchyme as indicated by several marker genes. This reduction in condensed mesenchyme results in a significant loss of mature glomeruli. There may also be an effect on branching of the UB (Dudley, Lyons & Robertson, 1995; Luo et al., 1995).

Bmp7 is weakly expressed in the UB and the surrounding metanephric mesenchyme. Expression is upregulated upon condensation of the mesenchyme (Dudley & Robertson, 1997). The function of *Bmp7* appears to be to promote the survival of the mesenchymal cell population. The addition of exogenous BMP7 to explant cultures leads to the production of only a few large glomeruli. There is also an increase in a cell population that appears to be stromal cells with the addition of BMP7. The effect of BMP7 is synergized by the addition of FGF2 (Dudley, Godin & Robertson, 1999).

Other genes that are involved in BMP signaling regulate the developing kidney. *Gremlin1* is a *Bmp2/4* antagonist that is expressed in the metanephric mesenchyme and Wolffian duct. The *Gremlin1* mutant fails to develop kidneys. Analysis of the developmental stages important for kidney development shows that a UB forms in the mutants but it fails to grow past the T-shape. The markers for mesenchyme such as *Gdnf*, *Pax2*, *Bmp2/7* and *Wnt4* fail to be upregulated in the mutants (Michos et al., 2004).

Activin A is also a member of the same gene family as BMPs, the TGF superfamily. Using an *in vitro* culture system, the inhibition of *Activin A* potentiated the ectopic formation of UB in the mesonephric Wolffian duct. Even though *Activin A* does not appear to be involved in the formation of the metanephric kidney, the observations with *Activin A* suggests that a SMAD-dependent mechanism is used during kidney development (Maeshima et al., 2006).

CHAPTER TWO
Materials and Methods

ANIMALS

Megf7$^{EC\ Stop}$ Plasmid Construction

A replacement-type vector was constructed using long and short arms of homology amplified by PCR from ES cell genomic DNA using long-range PCR (Takara Biochemical, Inc., Berkeley, CA) and the following primers: KI3 (5'-CCACCACCTGCAGGGTATA-CTGAGGAGTCCACCGATGGCATAGCTG-3') and KI4 (5'-CCACCACCTGCAGG-CGGCCGCGAATATGATATCATGTCAATACTAGAGACTTACC-3') were used as 5' and 3' primers, respectively, to amplify the long arm. MEJ76 (5'-CCACCACTC-GAGCCTGTGGACCTTCCTATAAGTCAACTTCC-3') and MEJ77 (5'-CCACCACT-CGAGGGTTGACTGCTAACAATCAGAGCAGGCTG-3') were used as 5' and 3' primers, respectively, for the short arm. The short arm was cloned into pJB1 (Gotthardt et al., 2003) at the XhoI site. The long arm was mutated using MEJ143 (5'-CCTAGGTGAAGGA-CTGTAAGTCAGCTATGCCATC-3') and MEJ144 (5'-GATGGCATAGCTGACTT-ACAGTCCTTCACCTAGG-3') to introduce a stop codon into exon 36. The mutated long arm and the bovine growth hormone 3' untranslated region were cloned into the pJB1-short arm containing plasmid using NotI to generate the targeting vector.

Allelic Series Generation

The *Megf7* knockin mice were generated using similar constructs as was used for the *Megf7*$^{EC\ Stop}$ mutant. The same long arm of homology was used, except without the introduced premature stop codon. The mutated cDNA inserts were cloned using an upstream Bst1107I site in the long arm and a BsrGI site in the bovine growth hormone 3' UTR. The oligonucleotide KI5 (5'-GTATACTGCTGATTTTGTTGGTGATCGCGGCTTTG-3') was used as the 5' primer to amplify the cDNA insert for the WT tail knockin (*Megf7*$^{WT\ KI}$), the NPSY→AAAA tail knockin (*Megf7*$^{NPSY\ KI}$), the Alternatively Spliced tail knockin (*Megf7*$^{AS\ KI}$), the PDZ interaction KO tail knockin (*Megf7*$^{PDZ\ KI}$), and the post-transmembrane Myc truncation knockin (*Megf7*$^{Myc\ KI}$). MEJ145 (5'-GTATACTGCTGATTTTGTTGGTGATC-GCGGCTTTGATGCTATACAGGAACTGGCGGCTGAAGAACATCACAATC-3') was used as the 5' primer to amplify the insert for the human LDLR cytoplasmic tail knockin (*Megf7*$^{LDLR\ KI}$). MEJ41 (5'-TGTACATTAGACCTGGCTTTCTGAGGAGAGCTTG-3') was used as the 3' primer to amplify the *Megf7*$^{WT\ KI}$, *Megf7*$^{NPSY\ KI}$, and *Megf7*$^{AS\ KI}$ inserts. MEJ42 (5'-TGTACACTAGG-AGAGCTTGCGTTCGTGTTTCCAGCCTGTG-3') was used as the 3' primer to amplify the *Megf7*$^{PDZ\ KI}$ insert. MEJ380 (5'- GTGTGTTGTAC-ATCAGCTATTCAGATCCTCTTCTGAGATGAGTTTTTGTTCCTTGGATTTCCTGTGT CTGTATAGCATCAAAG-3') was used as the 3' primer to amplify the *Megf7*$^{Myc\ KI}$ insert. MEJ146 (5'-TGTACATCATGCCACATC-GTCCTCCAGGCTGACCATC-3') was used as

the 3' primer to amplify the human *Megf7*$^{LDLR\ KI}$ insert. The NPSY→AAAA tail knockin mutation was introduced as described previously (Johnson et al., 2006).

Megf7 Knockout Generation

The *Megf7* knockout (*Megf7*^{KO}) mouse was generated by replacing the first exon with a neomycin resistance cassette. The long arm of homology upstream of the first exon of *Megf7* was generated by PCR amplification using the primers MEJ23 (5'-GCGGCC-GCCAGGTCATGAAGTGAGTGCTGAGCCACTGGG-3') and MEJ24 (5'-CCACCACC-GCCTCATGGTGCTGCGGCCGCC-3'). The short arm of homology downstream of the first exon of *Megf7* was generated by PCR amplification using the primers MEJ33 (5'-CTCGAGGAGCGGTCTGCAGATCCTGGCGATTCACGG-3') and MEJ35 (5'-CTCGAGGGTTACAGACTCTGCAACTGCTCTACCTCATTG-3'). The long arm and short arm of homology were cloned into pJB1 using the NotI and XhoI restriction sites respectively.

Targeted ES Cell Generation

ES Cell Culture

DMEM (Gibco cat. 12100-046) was reconstituted with 1080 ml of MilliQ H2O and 2.4g of Sodium Bicarbonate. The media was filter-sterilized and put in 500 ml bottles and stored at 4oC.

Complete Media: DMEM, 15% FCS (ES cell qualified), 2mM L-Glutamine (5ml/500ml), 0.1 mM NEAA (5ml/500ml), 0.1 mM β-mercaptoethanol (3.5μl/500ml).

Cells were thawed by taking a vial out of LN_2 and quickly warming at 37°C.

The suspension was transferred to a 15 ml conical and 10 ml of complete media was added dropwise with occasional stirring. The cells were spun at setting 4 on the clinical centrifuge for 1 min. The supernatant was removed and the cells were resuspended in complete media. The cells were seeded in 2 T-75's with 20 ml of media. The ES cells were seeded in one T-25 flask with irradiated STO cells.

The STO cells were split by removing the media and washing with PBS without Mg^{++} or Ca^{++}. The PBS was removed and 1.5 ml of 0.25% Trypsin/EDTA was added and the cells were incubated at 37°C for 5 min. The flask was banged and 10 ml of media was added to the cells to inactivate the trypsin. The cells were triturated to disperse cell clumps and then transferred to a 15 ml conical. The cells were spun at setting 4 on the clinical centrifuge for 1 min. The supernatant was removed and the cells were resuspended in complete media. The cells were split when they reached confluency 1:10. A new vial was used when the passage number reaches ~25.

STO Cell/ES Cell Culture

A 0.1% gelatin PBS solution was added to a T-25 before the STO cells were split. The cells were kept in suspension in a 15 ml conical. The cells were irradiated at 10,000 Rad (~14 min. in the irradiator close to the source, check the calibrated intensity). The gelatin solution was removed from the flask and the cells were transferred to the flask and put in culture at 37°C

with 5% CO2. The cells were allowed to settle for at least 4-6 hr. before ES cell addition. It is important to maintain an excess supply of STO cells in culture to ensure enough cells for splitting the ES cells.

SM-1 ES cells (originally from Bob Hammer) were thawed and seeded to the T-25 with STO cells and 5 ml of media. The ES cells were split by removing the media and washing with PBS without Mg^{++} or Ca^{++}. The PBS was removed and 1.0 ml of 0.25% Trypsin/EDTA was added and the cells were incubated at 37°C for 5 min. The flask was banged and 10 ml of media was added to the cells to inactivate the trypsin. The cells were triturated with the pipette tip perpendicular to the flask wall to disperse cell clumps and then transferred to a 15 ml conical. The cells were spun at setting 4 on the clinical centrifuge for 1 min. The supernatant was removed and the cells were resuspended in complete media and transferred to a new flask with inactivated STO cells. Every passage was a 1:4 split which normally resulted in a passage every two days. Passage ratio was adjusted appropriately if the cells were at less than 90% confluency at the second day. It is very important to keep some STO conditioned media at each media change/passage. At passage, keep all of the media that is in the irradiated STO cell flask. If the STO media is old (>2 days), remove ~3ml of the 5ml and replace with fresh media. The ES cells will need to be fed with fresh media the day after thawing and >2 hours before passage. To do this, remove ~4ml of the 5ml and replace with fresh media.

Electroporation

The targeting vector was linearized with excess restriction enzyme and cleaned with a phenol/chloroform extraction/isopropanol/ethanol precipitation. The DNA was checked for linearization and concentration by running on a gel. Do not use gel-purified DNA because it may contain UV-induced damage. 100 μl (at 1 mg/ml) of the linearized vector was diluted in 1 ml PBS. 2 T-25's of SM-2 cells were trypsinized as before, washed 1X with PBS, and resuspended in 1 ml of PBS. 3/4 of the cells and the DNA were mixed 1:1 and transferred to 2 electroporation chambers. The rest of the cells were transferred to two new T-25s with STO cells for the next electroporation. The electroporator was set at 330 μF, 275 V and low Ohms. The cells were electroporated. The cells were mixed with 60 ml of complete media and transferred to six 100mm plates with inactivated STO cells plus 5ml of conditioned media. Upon electroporation, most of the cells should die and clump up when mixed with the complete media. The clumping shows that the electroporation occurred.

ES Clone Selection and Screening

Day 1: switched media to 190μg/ml G418

Day 2: switched media to 190μg/ml G418

Day 3: switched media to 190μg/ml G418

Day 4: switched media to 190μg/ml G418

Day 5: switched media to 190μg/ml G418 and 2.5 μM of ganciclovir

Day 6: switched media to 190μg/ml G418 and 2.5 μM of ganciclovir

Day 7: switched media to 190μg/ml G418

Day 8: Change media if the media is yellow.

Day 9: switched plain media

Day 12: picked 100 colonies

Day 13: picked 100 colonies

The colonies were picked by replacing the media with PBS. A P-20 pippetman was set at 10 μl. The tip was used to dislodge the colony. The colony was sucked up with the minimum amount of volume and transferred to a 96-well plate with 50ul of 0.25% trypsin/EDTA. Eight colonies were collected. The plate was transferred to 37°C for 5 min. while another eight colonies were picked. 100μl of complete media was added to each well and the cells were triturated. 75 μl of the cells were transferred to a 24-well plate with STO cells. 75 μl of the cells were transferred to a 96-well PCR plate. The PCR plate was spun at 1000rpm for 5 min. The buffer was removed from each well individually and the cells were resuspended in 25μl lysis buffer.

Lysis buffer: 1X soriano buffer, 1.7 μM SDS, 50 μg/ml Proteinase K

The samples were incubated at 37°C for 1h and 94°C for 12 min. The ES cells were screened using an empirically determined protocol that can detect <1fg of plasmid (~1 copy) in the reaction with lysis buffer.

Cell Freezing

The positive clones were passaged from the 24-well well with 200µl of Trypsin/EDTA and transferred to the T-25 when the cells were around 50-70% confluent. If 50-70% confluency was not achieved, the cells were passaged into another 24-well well. When the cells in the flask reached confluency, the cells were trypsonized and resuspended in 1ml media. Half of the cells were frozen down, one quarter was split into a flask with no STO cells for DNA, and one quarter was transferred to a new flask with STO cells for one more passage and then frozen down.

Cell freezing: The ES cells should be resuspended in 1ml/T25 flask. STO cells should be resuspended in 2.5ml/T75 flask. ES freezing media was added 1:1 dropwise with swirling to the cell suspension. The mixture was added to a cryovial and immediately transferred to -80°C in a Styrofoam container. The next day the vials were transferred to LN_2.

ES Freezing Media: 20% DMSO, 40% DMEM, 40% FBS (ES cell certified)

ES Cell Blastocyst Injection

One vial of a positive clone was thawed and transferred to a T25 flask. The cells were grown in complete media plus ESGRO (50µl/500ml media). Two days later there should be enough cells for injection (does not need to be confluent). A 0.1% gelatin PBS solution was added to a T-25 before the ES cell preparation. The ES cells were fed with complete media plus ESGRO around 2hr before trypsonization. The cells were washed 2X with PBS. 2ml of

0.25% Trypsin/EDTA was added to the cells. The cells were digested for 25 minutes in the incubator. 10ml of complete media was added to the cells and resuspended in a 15ml conical tube. The cells were dispersed by slowly triturating (~1ml/2s) 40X with a 1ml serological pipette. Do not press the pipette tip opening against the tube wall. Half of the trituration was done at the bottom half of the tube and half at the top half. The cells were spun in a table-top centrifuge at 1000rpm for 3min. The supernatant was removed and the cells were resuspended in 1ml media. The cells were triturated as above 20X. One quarter of the cells were transferred to a new T25 flask with STO cells for refreezing. The other three quarters of cells were transferred to the T25 coated with gelatin along with 5ml of complete media plus ESGRO. The STO cells were allowed to adhere for 30 minutes in the incubator. The flask was slowly and carefully tilted and the non-adherent cells were transferred to a 15ml conical tube. The conical tube was spun at 1000rpm for 3min. The supernatant was removed and the cells were resuspended in 1ml media. The cells were triturated as above 40X. The cells were given to Liz Lummus for Blastocyst injection.

Genetic Analysis of Mice/ES Cells

Southern Blot Protocol for Knockin Lines

Southern blotting for detecting the 7.4 kb wild-type and the 4.5 kb knockout alleles was performed using standard techniques. The Southern probe was amplified by PCR from mouse genomic DNA using the following primers. MEJ150 (5'-GGCACATATC-CCAGCACACATAGAGGTCAG-3') and MEJ151 (5'-AGTTTGCCCACACTATAA-

GACTCCTCAC-3') and cloned into a plasmid. The digested fragment was labeled with P^{32}-dCTP using the Rediprime II kit (Amersham Pharmacia Biotech). ES cells were cultured without a feeder layer until they were almost confluent. Genomic DNA was isolated from the ES cells using proteinase K digestion and phenol/chloroform extraction. The isolated DNA was digested with EcoRI and SacI, run on agarose gels and blotted onto Hybond-XL (Amersham Pharmacia Biotech). The labeled probe was hybridized to the membrane in Rapid-Hyb Buffer (Amersham Pharmacia Biotech) and washed. Bound radioactivity was detected by phosphoimager.

Genotyping

There are two basic genotyping procedures used for all of the Megf7 mutant mice. Below is a description of each protocol followed by genotype specific information. The Excel template "genotype test" facilitates the calculations and documentation of what is done.

PCR reaction mix #1 (Soriano Method):

1 reaction (25µl total volume) (Add components in the indicated order)

14.7µl water

2.5µl 10X Soriano Buffer

2.5µl dNTPs (10mM)

2.5µl DMSO

1.25µl BSA (1.6mg/ml)

0.2µl 5'primer (100µM)

0.2μl 3'primer (100μM)

0.15μl polymerase (ExTaq 5U/μl)

1μl DNA sample

PCR reaction conditions (SOR protocol in Eric folder)

1. Melting 94°C 2:00

2. Annealing 60°C 2:00

3. Extension 65°C 3:00

4. Melting 94°C 0:30

5. Annealing 60°C 0:30

6. Extension 65°C 2:00

7. Extension 65°C 10:00

8. Storage 4°C ∞

Repeat steps 4-6 for 45 cycles.

The following reactions use the above protocol:

1. *Megf7* wild type #1 (for all Knockin and *Megf7*$^{EC\ Stop}$ mice)

5' primer: MEJ155- 5'-CCCAGCTGGGCCTCTGTGCACATTCCAATG-3'

3' primer: MEJ166- 5'-CCATGGCCTCTGCATTAGTTCTTGCTCTC-3'

Notes: This is the wild type reaction to be run along with the reactions for EC Stop premature extracellular domain truncation (*Megf7*$^{EC\ Stop}$ mouse #Koxxxx), *Megf7* wild type knockin

(*Megf7*$^{WT\ KI}$ mouse #H1xxxx), *Megf7* Alternative Splice knockin (*Megf7*$^{AS\ KI}$ mouse #F7xxxx), *Megf7* NPSY->AAAA knockin (*Megf7*$^{NPSY\ KI}$ mouse #I4xxxx), *Megf7* PDZ domain truncation knockin (*Megf7*$^{PDZ\ KI}$ mouse #1TAxxxx), *Megf7* Cytoplasmic domain truncation knockin (*Megf7*$^{Myc\ KI}$ mouse #TMxxxx), and *Megf7* LDLR cytoplasmic domain knockin (*Megf7*$^{LDLR\ KI}$ mouse #5Cxxxx).

2. *Megf7* KO #1 (for the *Megf7*$^{EC\ Stop}$ allele (mouse #Koxxxx))

5’ primer: MEJ156- 5’-CTCTGAAAGGGATGCCCAGCTGGGCCTCTG-3’

3’ primer: MEJ267- 5’-CGATGGCATAGCTGACTTA-3’

Notes: This reaction should be paired with the above WT #1 reaction for the wild type genotype.

This reaction is based on the difference in hybridization of the last three bases of MEJ267. This slight difference technically requires a wild type sample as a negative control. The wild type band should be barely visible while the mutant band should be strong.

3. *Megf7* Alternative Splice Knockin (*Megf7*$^{AS\ KI}$ allele) (mouse #F7xxxx)

5’ primer: MEJ155- 5’-CCCAGCTGGGCCTCTGTGCACATTCCAATG-3’

3’ primer: MEJ162- 5’-GTCCACCCTGAACTCAAGAGGCAATCAGAAG-3’

Notes: This reaction should be paired with the above WT #1 reaction for the wild type genotype.

This reaction amplifies from upstream of exon 36 to the region in the cytoplasmic domain that is specific to the alternative splice tail sequence.

4. *Megf7* NPSY to AAAA substitution knockin (*Megf7*$^{NPSY\ KI}$ Allele) (mouse #I4xxxx)

5’ primer: MEJ154- 5’-TCTGTGCACATTCCAATGAAGCCGTCCCTG-3’

3’ primer: MEJ159- 5’-CTTCCTGAGTGGAAGTTCGTGCTGCAGCTG-3’

Notes: This reaction should be paired with the above WT #1 reaction for the wild type genotype.

This reaction amplifies from upstream of exon 36 to the region in the cytoplasmic domain that is specific to the alanine substitution.

5. *Megf7* LDLR cytoplasmic domain knockin (*Megf7*$^{LDLR\ KI}$)(mouse #5Cxxxx)

5’ primer: MEJ156- 5’-CTCTGAAAGGGATGCCCAGCTGGGCCTCTG-3’

3’ primer: MEJ165- 5’-TCGTCCTCCAGGCTGACCATCTGTCTTGAG-3’

Notes: This reaction should be paired with the above WT #1 reaction for the wild type genotype.

This reaction amplifies from upstream of exon 36 to the region in the cytoplasmic domain that is specific to the LDLR tail.

6. *Megf7* Wild Type Tail knockin (*Megf7*$^{WT\ KI}$)(mouse #H1xxxx)

5’ primer: MEJ155- 5’-CCCAGCTGGGCCTCTGTGCACATTCCAATG-3’

3’ primer: MEJ161- 5’-GTGTAGCTGTGGTCAGGTCCACCCTCTTTC-3’

Notes: This reaction should be paired with the above WT #1 reaction for the wild type genotype.

This reaction amplifies from upstream of exon 36 to the region in the cytoplasmic domain that is used for the alternative splice knockin. There are other primers available that differentiate between the WT knockin and the other knockin alleles.

7. *Megf7* PDZ domain truncation knockin (*Megf7*$^{PDZ\ KI}$)(mouse #1TAxxxx)

5’ primer: MEJ155- 5’-CCCAGCTGGGCCTCTGTGCACATTCCAATG-3’

3’ primer: MEJ269- 5’-CAGTGTACACTAGGAGAGCTTG-3’

Notes: This reaction should be paired with the above WT #1 reaction for the wild type genotype.

This reaction amplifies from upstream of exon 36 to the border between the end of the cytoplasmic tail and the 3’UTR. This reaction is not as reliable as the WT knockin reaction above, which also works for this allele.

8. *Megf7* cytoplasmic domain truncation knockin (*Megf7*$^{Myc\ KI}$)(mouse #TMxxxx)

5’ primer: MEJ156- 5’-CTCTGAAAGGGATGCCCAGCTGGGCCTCTG-3’

3’ primer: MEJ451- 5’-CTATTCAGATCCTCTTCTGAGATGAGTTTTTGTTC-3’

Notes: This reaction should be paired with the above WT #1 reaction for the wild type genotype.

This reaction amplifies from upstream of exon 36 to the Myc tag at the end of the transmembrane domain.

PCR reaction mix #2:

1 reaction (25µl total volume) (Add components in the indicated order)

16.35µl water

2.5µl 10X Soriano Buffer

2.5µl dNTPs (10mM)

1µl DMSO

1.25µl BSA (1.6mg/ml)

0.1µl 5'primer (100µM)

0.1µl 3'primer (100µM)

0.2µl polymerase (ExTaq 5 U/µl)

1µl DNA sample

PCR reaction conditions (65TAQ protocol in Eric folder)

1. Melting	94°C	1:00
2. Melting	94°C	0:30
3. Annealing	65°C	0:30
4. Extension	72°C	3:00
5. Extension	72°C	10:00
6. Storage	4°C	∞

Repeat steps 2-4 for 45 cycles.

The following reactions use the above protocol:

1. *Megf7* wild type #2 (for the *Megf7* null allele ($Megf7^{KO}$) mouse #Ko2XXXX)

5’ primer: MEJ358- 5’-ACTATATTCACCCGCCGGCTTTTCCACGTG-3’

3’ primer: KOT12- 5’-AGCAGCTTTCAGAAGCACCTCTTCAGGACC-3’

Notes: This is the wild type reaction to be run along with the knockout (*Megf7*^{KO}) reaction.

2. *Megf7* Knockout (for the *Megf7* null allele (*Megf7*^{KO}) mouse #Ko2XXXX)

5’ primer: Neo36- 5’-CAGGACAGCAAGGGGGAGGATTGGGAAGAC -3’

3’ primer: KOT12- 5’-AGCAGCTTTCAGAAGCACCTCTTCAGGACC-3’

Notes: This is the knockout reaction to be run along with the Wild Type #2 reaction. This reaction will not work for the allele that does not have the neomycin resistance cassette.

3. *Megf7* Knockin Integration test (for all Knockin mice)

5’ primer: Neo36- 5’-CAGGACAGCAAGGGGGAGGATTGGGAAGAC -3’

3’ primer: MEJ63- 5’-CTCGAGGGTTCTAACGGACAGCCTTCATTGTGATTC-3’

Notes: This reaction will work with the *Megf7*$^{EC\ Stop}$ allele (mouse #KoXXXX) and all knockin alleles. This reaction will not work if the neomycin resistance cassette has been removed from the allele.

4. *Megf7* Knockout #2 (for the *Megf7* null allele (*Megf7*^{KO}) mouse #Ko2XXXX)

5’ primer: MEJ456- 5’- GGAACTTCGTTGACTCTAGAGGATCCGACC -3’

3’ primer: KOT12- 5’-AGCAGCTTTCAGAAGCACCTCTTCAGGACC-3’

Notes: This is the knockout reaction to be run along with the Wild Type #2 reaction. This reaction will work for the allele with or without the neomycin resistance cassette.

Body Weight Measurements

Starting at P5, the pups were weighed on a digital scale. The pups were placed on a large plastic weighing dish and the weight value was taken when the value settles. (Normally the pups would freeze initially when placed into the dish. This keeps them still long enough for the measurement. Older pups required a little bedding in the dish to keep them distracted long enough for the measurement.)

The pups were weighed daily until weaning. The weaned pups were weighed one last time and the tails were cut for genotyping. (There was not a difference between wt/wt and *Megf7*$^{EC\ Stop}$ /wt pups at weaning and thus it was assumed that there was not a significant difference before that stage. I initially tried to mark the pups with marker on the tails to get weight measurements assigned to each pup during the entire process. Unfortunately, the mothers would remove most of the marker by the next day. Toe punches were not a viable option due to the *Megf7*$^{EC\ Stop}$ / *Megf7*$^{EC\ Stop}$ phenotype. A few wt/wt or *Megf7*$^{EC\ Stop}$ /wt pups died before weaning. The low weights of the pups that died were eliminated from the statistical analysis.)

The weights of the pups from multiple litters of heterozygous X heterozygous matings were averaged for each day. Because each pup was not followed individually, the standard non-paired Student's T-test was used to determine statistical significance. (The bars indicate SEM=SD/square root of n)

Alcian Blue/Alizarin Red Staining

Mice were euthanized with a halothane overdose on the indicated date.

The limbs were removed. Pictures of the limbs were taken using the Nikon digital camera attached to a Leica stereoscope using an over-head light source. The magnification was set at 0.63X. The limbs were cleaned with ethanol and placed on black velvet squares used for transferring yeast colonies.

The mice (or just the limbs) were skinned and as much soft tissue as possible was removed. The skin was removed up to the ankles or wrists and the limbs were placed in PBS to prevent dehydration. (The best way to remove the soft tissue from the autopods: Cut the distal digit foot pad close enough so that the tendon is also cut. Cut along the ventral aspect of the digit to the base of the autopod. Cut along one side of the autopod underneath the tendons including the soft tissue of the digits that were just cut. Continue cutting until all soft tissue is removed from the ventral aspect of the autopod. Pull the dorsal skin of the autopods distally. Use the scissors to aid in the pulling process to make sure that the digits don't break. Pull the skin to the end of each digit and cut the skin as close to the cuticle as possible.)

The skeleton was transferred to a 20ml scintillation vial filled with 95% ethanol and fixed for 5 days. (If the whole skeleton was fixed, the tubes were kept in a horizontal position to allow the skeletons to fix in an elongated position.)

The samples were briefly rinsed with water and then transferred to acetone for two days to remove any fat remaining on the skeleton.

The samples were briefly rinsed with water and then transferred to staining solution and incubated at 37°C for three days.

The samples were briefly rinsed with water and then transferred to 1% KOH for three days or until the skeleton have cleared.

The skeletons were transferred to glycerol/1% KOH solutions around every five days going from 20% to 50% to 80% glycerol/1% KOH for each stage.

After the skeletons have completely cleared, they were transferred to 100% glycerol.

Stain Solution:

1 part 0.3% alcian blue (Sigma #A-5268) in 70% ethanol

1 part 0.1% alizarin red (Sigma #A-5533) in 95% ethanol

1 part glacial acetic acid

17 parts 70% ethanol

The stocks of Alcian Blue and Alizarin Red were dissolved as much as possible by heating the solution to 85°C and grinding the undissolved granules in the tube.

The stocks were passed through a #5 Whatman filter.

Whole Mount *In Situ* Protocol

Probe Preparation (Adapted from Rossant Protocol)

The probe plasmids were linearized with a restriction enzyme that cuts near the 5' end of the insert. (The pCR4 plasmid from the Invitrogen TOPO cloning kit for sequencing is a good vector because it has promoters on both sides of the insert.)

The digest was run on a gel, the linearized band was cut out, and the DNA was purified using the snap-freeze phenol extraction method. RNase-free reagents were used and the DNA was dissolved in nuclease-free water. 1µl of the DNA was run on a gel to estimate the amount of DNA recovered. The DNA was brought up to 1µg/µl.

1µl of probe template was added to 19µl of the following transcription buffer (Make sure the DNA is added last. Some components may precipitate the DNA if not in the final volume.):

5.5µl Water

2µl 10X Transcription Buff.

2µl 10mM ATP

2µl 10mM GTP

2µl 10mM CTP

1.2µl 10mM UTP

0.8µl 10mM digoxigenin-UTP

1µl 250 mM DTT

0.5µl Placental Rnase Inhibitor

2µl T7 RNA Polymerase 100U/ul

Transcription Buffer:

400mM Tris-HCL pH8.0

60mM MgCl2

20 mM Spermidine

100mM NaCl

The reaction was incubated at 37°C for 2h. 1μl of the transcription reaction was run on a 1% gel for 5 min. at the highest voltage in TAE buffer. (The lower band of RNA should be a distinct band and should be approximately 10X as strong as the upper template DNA band.) 2μl of 0.2M EDTA, 2.5μl 4M LiCl and 75μl ethanol were added to stop the reaction and precipitate the RNA.

The RNA was allowed to precipitate at -20°C for 2h. The pellet was redissolved in 22.5 μl of water. 2.5μl 4M LiCl and 75μl ethanol were added and the RNA was reprecipitated at -20°C for 2h. The pellet was dissolved in 200μl of water.

2ul of 1/100 and 1/000 dilutions in 10XSSC was spotted along with RNA standards onto a nylon filter (Hybond-XL).

The membrane was incubated for 30 min. with 10ml freshly made PBS/0.1% Tween-20 with 1% blocking reagent (Roche).

The membrane was blotted with the Anti-dig-AP antibody 1/5000 in TBST with 1% blocking reagent for 30min.

It was then washed 2X for 15min with TBST and equilibrated with NTM for 2min.

The membrane was incubated in the dark with NTM with 4.5 μl NBT and 3.5 μl BCIP.

The reaction was stopped with CMFET.

NTM: 100mM NaCl, 100mM Tris pH9.5, 50mM $MgCl_2$

NBT: 75mg/ml nitroblue tetrazolium salt in 70% DMF

BCIP: 50mg/ml 5-bromo-4-chloro-3-indolyl phosphate, toluidine salt in DMF

Embryo Preparation and Staining

1. Dissect out embryos from the decidua in DEPC-treated PBS at RT. Remove the yolk sac and puncture the brain in E9.5 to E11.5 embryos.

2. Place in 10 ml of 4% paraformaldehyde in PBS at RT. Invert tubes 4X and transfer to ice. Replace fixative with 15ml ice-cold fixative after 5 minutes. Rock at 4°C for 2 hours (for limbs ON for other tissues). Individual embryos were fixed separately in 1.5 ml eppendorph tubes.

3. Wash (invert several times and allow embryos to settle) 3X with 10 ml PBS/0.1% Tween-20 (PBST). Dehydrate with 25%>50%>75%>100% methanol/PBST. Store at -20°C in 100% methanol for up to 2 months. Other investigators use plain PBS or ethanol.

4. Bleach embryos with 4:1 methanol/30% hydrogen Peroxide for 4-6h at RT. You can stop and store at -20°C in 100% methanol.

Rehydrate with 75%>50%>25% methanol/ PBST at 5min/rinse with rocking. Rinse 3X in PBST.

5. Add 10 μg/ml proteinase K (Roche Cat. #3115836) in PBST.

You should add 1.5ml/embryo in 1.5 ml eppendorphs or 15ml in conical tubes to reduce damage to the embryo. Use the same volumes for all procedures to the fixation except rinses. Incubate for the indicated time with rocking at RT.

Age	Prot. K time (min)
E9.5	6-8
E10.5/11.5	8-10

E12.5 10

6. Wash 2X with freshly prepared 2mg/ml glycine in PBST at 5min./wash. Rinse 1X with PBST.

7. Refix the embryos in freshly prepared 0.2%gluteraldehyde/4% paraformaldehyde in PBS at RT for 20 min with rocking.

8. Rinse 2X with PBST.

9. Transfer embryos to 2ml tubes containing 0.5ml hybridization buffer. Allow embryos to fall to bottom of tube. Replace buffer with 1ml of fresh hybridization buffer. Place tubes in paper towel taco in glass hybridization tube. Prehyb >1 hour at 65°C with rotation. Rotate at less than one revolution per minute (any faster and the embryos fall apart)

Hybridization buffer: 50% formamide, 5X SSC hybridization, 50ug/ml tRNA hybridization, 0.05% heparin, 1% SDS.

10. Replace hybridization buffer. Add 10ul of labeled probe. Hybridize ON at 65°C with rocking.

11. Wash 2X with Wash 1 for 30 min. at 65°C with rocking. Wash 1: 50% formamide, 5X SSC, 1% SDS

12. Wash 1X with a 1:1 mix of Wash 1 and 2 for 10min. at 65°C with rocking.

13. Wash 3X with Wash 2 buffer for 5min at RT with rocking. Treat with 100μg/ml Rnase A in Wash 2 for 30 min. at 37°C with rocking. Wash 1X with Wash 2 for 5 min. Wash 2: 0.5M NaCl, 10mM Tris-HCl (pH7.4), 0.1% Tween 20

14. Wash 2X with Wash 3 for 30 min. at 65°C with rocking. Wash 3: 50% formamide, 2X SSC, 0.1% Tween 20

15. Rinse Embryos with TBS/0.1% Tween-20 (TBST) 3X. Transfer embryos to 6-well dish with blocking buffer. Rock in Blocking solution for 1.5h at RT.

Blocking solution: TBST, 10% sheep serum, 2% BSA, 2mM levamisole (0.5mg/ml freshly added)

16. Remove the blocking solution and replace with the antibody solution. Incubate the embryos with the antibody ON at 4°C on the nutator.

Antibody solution: TBST, 1% sheep serum, 2% BSA, 2mM levamisole, anti-dig-AP from Roche at 1:2000

17. Wash 6X in TBST with 2mM fresh levamisole for 1h at RT with rocking. Wash ON in TBST with 2mM fresh levamisole for 1h at 4°C with rocking.

18. Transfer embryos to 12-well dish. Wash 2X with fresh NTMT with 2mM fresh levamisole for 10 min at RT with rocking.

NTMT: 100mM NaCl, 100mM Tris pH9.5, 50mM MgCl2, 0.1% Tween-20

19. Change to Color reagent (4.5µl/ml NBT, 3.5 µl/ml BCIP, and 2mM levamisole in NTMT). Rock for at RT and check every 20min. for signal.

20. Wash 3X with PBS/0.1% Tween-20 and Store at 40C or Wash 3X with TBST

21. Dehydrate with 30%, 50%, 70%, 100%, 100% methanol/TBST. Rehydrate with 70%, 50%, 30% methanol/TBST. Embryos were visualized at this point. The embryos can be further cleared in glycerol.

22. Clear with 1:1 glycerol/CMFET and then 4:1 glycerol/CMFET for 1h each with rocking.

CMFET 100ml: 0.8g NaCl, 0.02g KCl, 0.115g Na2HPO4 anhydrate, 0.02g KH2PO4 anhydrate, 0.02g EDTA, 0.1% Tween-20

Whole Mount In Situ Probes

Several of the probes used in this study were generated in house. The plasmid for the *Megf7* probe was made by TOPO cloning a cDNA insert generated by PCR amplification using the primers MEJ354 (5'-GGCCTGTGCATCAACTCGGGC-TGGCGCTG-3') and MEJ355 (5'-CTGGAAAGCCCCTTCAGTGTTTGTGCAGCCC-3'). The insert for the *Fgf8* template plasmid was generated with: MEJ173 (5'-GAGAGATCT-AGATGGAGACCGATACTTTTGGAAGCAGAGTC-3') and MEJ174 (5'-CCAATTAC-TAGTGCAAACAATATGCACAACTAGAAGGCAGCTCCC-3'). The insert for the *Col2a1* template plasmid was generated with: MEJ33' (5'-CCAATGATGTAGAGAT-GAGGGCCGAGGGCAAC-3') and MEJ331 (5'-GATGTTTTAAAAAATACAG-AGGTGTTTGAC-3'). The insert for the *Lmx1b* template plasmid was generated with: MEJ322 (5'-TGAAGAGTGAGGATGAAGATGGAGACATG-3') and MEJ323 (5'-GGAGGCAAAGTAGGAGCTCTGCATGGAGTAG-3'). The insert for the *Hoxd12* template plasmid was generated with: MEJ328 (5'-TCTACTTTTCCAACCTGA-GAGCCAATGGCAG-3') and MEJ329 (5'-TTGTGTAGGGTTTCCTCTT-CTTGCGGGCCC-3'); The insert for the *Bmp2* template plasmid was generated with:MEJ324 (5'-GTGGCCGGGACCCGCTGTCTTCTAGTGTTG-3') and MEJ325 (5'-GGTGACGTCGAAGCTCTCCCACTGACTTGTG-3'); The insert for the *Gli1* template plasmid was generated with: MEJ326 (5'-GAAACTTTCACCGTGGGGGTAA-ACAGGCCTTC-3') and MEJ327 (5'-CCTTTATTGTCAGGAAACTGTGCTA-TTATTAAAG-3'); The insert for the *Wnt7a* template plasmid was generated with: MEJ314

(5'-GGGCCGAGCCTGCAATAAGACAGCCCCTCAG-3') and MEJ315 (5'-GCGCTGC-AGAAGGGTACTTGTGAAATCAAC-3'). *Shh*, *Msx1*, and *Bmp4* probes were kindly provided by Deepak Srivastava. The probes used for kidney analysis were provided by Dr. Thomas Carrol.

Slicing Stained Embryos

Stained embryos were washed three times in PBS and embedded in 2% agarose. 50-100 μm-serial sections were obtained using a VT1000S vibratome (Leica).

Whole Mount TUNEL Staining

Embryos were prepared and stored in pre-hybridization buffer at -20°C as described in the whole mount in situ methods. Embryos were then thoroughly washed overnight in PBS and equilibrated in 100 ml TUNEL Label mix (Roche Applied Science) at room temperature for 5 min. The TUNEL Label mix was replaced with 95 μl TUNEL Label mix and 5 μl TUNEL Enzyme and incubated at 37°C for 2 h. Embryos were then washed in TBST and labeled using TUNEL AP antibody at 100 μl/embryo and stained as described earlier for the whole mount *in situ* hybridizations.

Mulefoot Gene Analysis

Cow Genomic DNA Sequencing

Wild-type and mulefoot DNA samples (Angus strain) were prepared using standard genomic DNA extraction protocols. The MF sperm sample was obtained from bull 16AN E829 on April 12, 1982. Briefly, approximately 200 mg tissue was digested in 1 ml of SNET buffer (20 mM Tris, pH 8.0, 5 mM EDTA, 1% SDS, 400 mM NaCl) with 200 μg of proteinase K (Roche). Tissues were digested overnight at 55°C with shaking. Five hundred microliters of the digested material was extracted with phenol/chloroform/isoamyl alcohol, precipitated with 500 μl isopropanol, and redissolved in 200 μl TE (10 mM Tris–HCl, 0.1 mM EDTA, pH 7.5). Primers were designed to amplify the bovine exon sequences including approximately 200 bp of flanking intronic sequences. Exons 4, 7, 8, 9, 10, 11, 12, 13, 15, 16, 17, 19, 20, 21, 22, 23, 24, 26, 27, 28, 30, 31, 33, 34, 36, 37, and 38 of the MFD allele were successfully amplified, sequenced, and compared to the reference bovine Megf7 gene sequence in the Ensembl database. No successful PCRs were obtained from the remaining exons.

Mini-Gene Splicing Protocol

Construction of pcAT7-SC12 was essentially as described previously for SC6 (Tong, Nguyen & Lynch, 2005). pcAT7-SC12 is a β-globin minigene expression vector with CD45 exon 4 and introns inserted between exon 1 and exon 2 of the β-globin gene using NdeI and HindIII restriction sites. Wild-type and mulefoot exon 37 and approximately 200 bp of upstream and

downstream flanking sequences were amplified by PCR using primers MEJ415, 5′-GTGTGTCATATGATCCCACACTCTTCTATGTTCTGTTCCAC-3′, and MEJ416, 5′-GTGTGTAAGCTTAGGGCCCCTCAAGCTGGTCCCTCGCAAGCTG-3′. PCR products were digested with NdeI and HindIII and cloned into pcAT7-SC12.

HEK 293 cells were cultured in six-well plates and transfected with the indicated plasmids at 60–80% confluency. Other cell types produced similar results (data not shown). One microgram of plasmid DNA was transfected using Fugene-6 transfection reagent (Roche) and the manufacturer's recommended protocol. At the indicated times total RNA was isolated with RNA STAT-60 (Tel-Test, Inc.) from the cells using the manufacturer's recommended protocol. RT-PCR was performed as described previously. Reactions were separated on 1.5% agarose gels. DNA bands were cut out, isolated from the gel, and cloned into pCR4 using the TOPO Cloning Kit for Sequencing (Invitrogen) and the manufacturer's recommended protocol.

RT-PCR Reaction for Mulefoot RNA Samples

Total RNA was extracted from wild-type and MFD tissue samples as described above. The RT reaction was performed as recommended for the MMLV reverse transcriptase kit (Invitrogen). The RNA was mixed with 500 ng of poly(dT) oligomers (Roche) and nuclease-free water. The mixture was heated to 65°C for 5 min, cooled on ice, and then mixed with 5X First Strand Buffer, dNTPs, recombinant RNase inhibitor, and DTT. MMLV reverse transcriptase was added and reactions were incubated at 37°C for 50 min and then at 70°C for 15 min. RNaseH(2.5 U) was added to the reaction and incubated for 20 min at 37°C. PCR

products were amplified using the following primers: Oligonucleotides MEJ444, 5′-CGCTGAGGAGTCCACCGATGATGTAGCTGG-3′, and MEJ445 5′-GGCCACATT-GCCAAGATCGAACGGGCGAAC-3′, were used to amplify the exon 30 to exon 36 fragment. Oligonucleotides MEJ446, 5′-GGCCTCTGTGCGCATTCCAATGAGGCCGTG-3′, and MEJ448, 5′-AGAAACAAACTCTCAGATGCAAGTCTTCAC-3′, were used to amplify the exon 35 to intron 37 fragment.

Wnt Activity

TOPFlash Wnt Reporter Assay

HEK-293 cells were plated at 400,000 cells/well in 6-well plates and grown to 50–80% confluency in 10% FBS/DMEM. Cells were transfected using the TOP-Flash reporter system (Upstate Cell Signaling Solutions) and the indicated expression plasmids for Wnt1, Lrp6, Megf7, Lrp1 and Vldlr in pCDNA3.1. Transfections were performed with the Fugene 6 reagent (Roche) using the manufacturer's protocol. Cells were lysed two days after transfection and lysates were assayed for firefly and runilla luciferase activities using the Dual Luciferase Reporter Assay System (Promega). Transfections were performed in triplicate. Each transfection was measured in triplicate. Between 3 and 11 independent samples were assayed for each condition.

DKK ELISA

Affinity purified Megf7-Fc (1μg/ml) or anti-human Fc (4μg/ml) antibodies were coated onto Nunc maxisorp 96-well immuno-plates in a 0.1M $NaHCO_3$, 1mM $CaCl_2$, pH 8.2 coating buffer. The plates were covered with plate covers and incubated ON at 4°C. The next day the plates were washed four times in TBS, 0.05% Tween-20. 200μl of blocking buffer (10%FBS, TBS) was added to each well for 30 minutes. Half of the anti-human Fc coated wells were incubated with Megf7-Fc for one hour at RT. The plates were then washed four times and conditioned media containing either Dkk1-AP, Dkk3-AP, or AP were incubated in the wells for 1.5 hours at RT. The amount of bound AP was detected with p-nitrophenyl-phosphate and stopped with 3N NaOH. The plates were read at 405nm.

BAT-gal Staining

Embryos were dissected from timed pregnant females. The extraembryonic tissue was used for genotyping. The embryos were placed in 4% PFA for one hour at 4°C in the dark. The embryos were rinsed in Rinse Buffer (5mM EGTA, 0.01% Deoxycholate, 0.02% NP40, 2mM $MgCl_2$, in PBS) three times for 15 minutes at RT in the dark. The embryos were then transferred to Staining Buffer (Rinse Buffer, 5mM $K_3Fe(CN)_6$, 5mM $K_4Fe(CN)_6$, 1mg/ml X-gal) and incubated in the dark at 37°C. The limbs were stained for ~ one hour. The kidneys were stained initially for 15-30 minutes. The ureteric buds were crudely dissected out to allow for stain perfusion. The kidney staining was allowed to continue for ~ four hours.

Limb β-CATENIN Staining

E10.5-E11.5 embryos were fixed in paraformaldehyde and embedded in O.C.T. Compound (Tissue Tek). 8μm cryosections of the limbs were washed with TBS incubated with glycine. The samples were blocked with 5% goat serum in TBS, incubated for 1 hour with a 1:100 dilution of anti-activated β-catenin antibody (Upstate) in 1% goat serum in TBS. The samples were washed with TBS and a 1:200 dilution of Alexa Fluor 594 goat anti-mouse IgG (Invitrogen) was used to stain the samples. The samples were washed again and mounted with cover slips and Vectashield Mounting Medium + DAPI (Vectashield) and visualized using a Zeiss Axioplan 2 Imaging system.

Yeast Two-Hybrid Screen

The manufacturer's recommended protocol for the Matchmaker system (Clontech) was followed with minor alterations and as described (Gotthardt et al., 2000). The yeast strain EGY48 [p8op Lac-Z] was transformed with the wild-type Megf7/Lrp4 cytoplasmic tail bait plasmid 2-3-4 using the standard LiAc method. Cells were grown on −Ura, −His dropout agar plates to select for transformed colonies. Yeast were then transformed with a mouse brain cDNA library cloned into the pB42 prey plasmid (Gotthardt et al., 2000) using the Yeast Maker 2 system (Clontech) and plated onto −Ura, −His, −Trp dropout agar plates to select for transformed colonies. Colonies were pooled and plated on −Ura, −His, −Trp, −Leu dropout agar plates containing X-gal to select for transformed colonies that expressed prey proteins that interact with the wild-type cytoplasmic domain of mouse Megf7/Lrp4. Positive

clones were replated on −Ura, −His, −Trp, −Leu dropout agar plates containing X-gal to confirm interactions. Prey plasmids from positive clones were isolated as described (Gotthardt et al., 2000), transformed into KC8 bacteria (Clontech), and selected on −Trp dropout agar plates. Plasmids isolated from the bacterial clones were tested for insert by restriction digest and sequencing. Interactions were confirmed by retransforming EGY48 [p8op Lac-Z] with the wild-type Megf7/Lrp4 bait and prey plasmids. Interactions were also confirmed by mating yeast clone EGY48 [p8op Lac-Z] transformed with wild-type Megf7/Lrp4 bait plasmid and yeast clone YM4271 transformed with the prey plasmid. All bait plasmids showed minimal self-activation. Expression of all bait plasmid proteins was confirmed by Western blot using an anti-LexA antibody.

Adult Mouse Tissue RT-PCR

Total RNA from the indicated wild type tissue samples was combined with 1µl of a 45µM mixture of MEJ9 and MEJ10 (Johnson et al., 2006). 48µl of the Titanium One-Step RT-PCR reaction mix (BD Clontech) was added to each RNA/primer mixture. The RT-PCR product was amplified using the manufacturers recommended protocol. The products were resolved on an agarose gel and visualized.

CHAPTER THREE
Results

ANALYSIS OF THE HYPOMORPHIC *MEGF7*$^{EC\ STOP}$ ALLELE

General Description of the *Megf7*$^{EC\ Stop}$ Mutants

Description of the Megf7$^{EC\ Stop}$ *Allele*

The knockout strategy employed for the first *Megf7* mutant is based on the knockin strategy used to generate *Megf7* knockin alleles with specific mutations in the cytoplasmic domain. The *Megf7* premature stop codon knockin allele, subsequently called the *Megf7*$^{EC\ Stop}$ allele, has a mutation that introduces a premature stop codon immediately upstream of the transmembrane domain encoded by the *Megf7* gene (Figure 5A). "EC Stop" refers to the stop codon within the extracellular (EC) region of the *Megf7* gene. The concept behind this mutation was based on the *Apoer2* null mutation, in which a neomycin resistance cassette is placed in the transmembrane sequence of the *Apoer2* gene (Trommsdorff et al., 1999).

The plasmid construct used to generate the *Megf7*$^{EC\ Stop}$ allele contained a 10kb long arm of homology, inserted at the NotI site in pJB1, containing 7 exons of m*Megf7* with the stop codon mutated in the 36th exon. The long arm was followed by the bovine Growth Hormone 3' UTR, the neomycin resistance cassette flanked by loxP and FRT sites, a 1kb short arm of homology containing exon 37 cloned into the XhoI site of pJB1, and two Herpes Simplex Virus Thymidine Kinase genes. Homologous recombination resulted in the deletion

of the downstream portion of exon 36 and the introduction of the premature stop codon (Figure 5B).

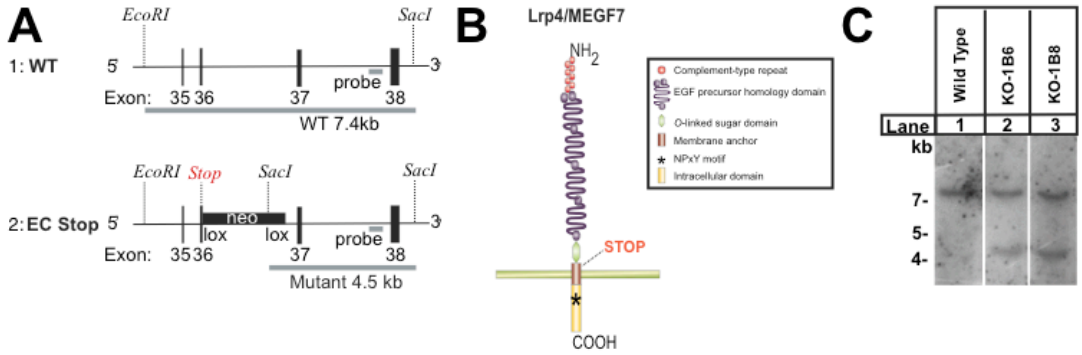

Figure 5 Design of the *Megf7*$^{EC\ Stop}$ Allele.

(A) A premature stop codon was introduced into exon 36 of mouse *Megf7*. Exon 36 encodes the transmembrane domain of *Megf7*. The neomycin Resistance Cassette introduces a SacI restriction site that changes the size of the band in the Southern Blot from 7.4kb in the wild type allele to 4.5kb in the mutant allele. (B) Diagram of the structural organization of MEGF7. The *Megf7*$^{EC\ Stop}$ mutation is downstream of the putative O-Linked Sugar Domain and upstream of the transmembrane domain. (C) Southern blot of the two *Megf7*$^{EC\ Stop}$ ES cell clones used for generation of mice. Both clones have one copy of the mutant band at ~4.5kb.

Electroporation of mouse Embryonic Stem (ES) cells and subsequent selection generated two recombined clones, 1B6 and 1B8, that subsequently generated heterozygous mice. Both lines showed the correct recombination as indicated by Southern blot (Figure 5C). Homozygous mice derived from both cell lines also had a similar phenotype. The 1B6 line was used to generate all of the subsequent data.

RT-PCR Analysis of the Mutant RNA

An RT-PCR reaction was performed to test if the mutant allele generated the expected mRNA products. A primer that primed upstream of the mutation, MEJ342, was used to amplify both wild type and mutant RT products. MEJ342 was combined with either a primer that is homologous to the 3'UTR of wild type *Megf7*, MEJ344, or a primer that is homologous to the BGH 3'UTR, MEJ346, to amplify wild type or mutant RT products respectively. Both the wild type and the mutant RNA samples produced wild type and mutant RT-PCR products respectively that were of the appropriate size and equivalent intensity. The mutant RNA did produce a weak RT-PCR product around the same size as the wild type product (Figure 6). Sequencing of this band revealed that it was an alternative splice product that would have generated a protein that would be similar to the expected mutant protein. This experiment indicates that the $Megf7^{EC\ Stop}$ allele generates a stable form of the expected transcript. Whether or not the transcript is translated into a secreted protein is unknown.

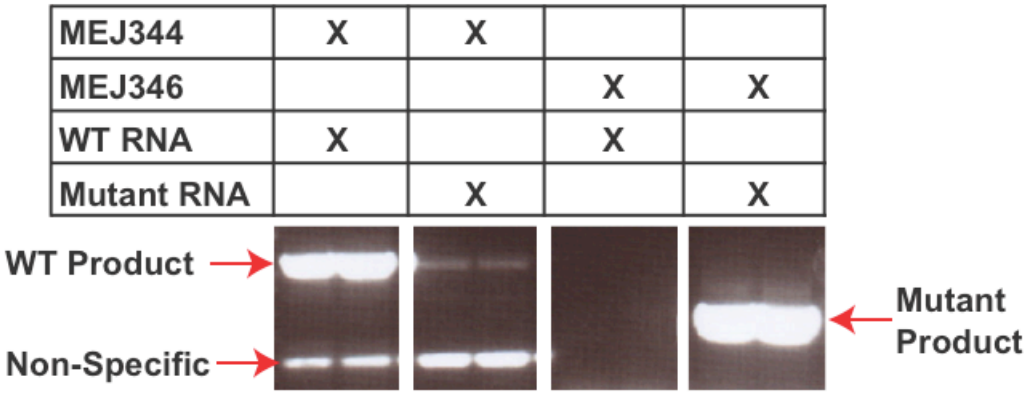

Figure 6 RT-PCR Analysis of the *Megf7*$^{EC\ Stop}$ Transcript.

Brain RNA from wild type and mutant mice were reverse transcribed and amplified in duplicate using primers specific to a region upstream of the *Megf7*$^{EC\ Stop}$ mutation and a region in the 3'UTR. The weak band in the *Megf7*$^{EC\ Stop}$ reaction is an alternatively spiced product that is predicted to have a similar amino acid sequence as the properly spliced mutant product.

Analysis of the Low Body Weight of the Megf7$^{EC\ Stop}$ *Mutants*

The homozygous *Megf7*$^{EC\ Stop}$ mutant pups were easily distinguishable from their litter mates because of their significant size difference at weaning. The pups from multiple litters were weighed to determine how early the weight difference occurs. Starting at the first time point measured, P5, the mutant pups were already significantly smaller than their wild type and heterozygous littermates (Figure 7). The survival rates of the mutants were also examined to see if they have an increased mortality rate. Significantly fewer *Megf7*$^{EC\ Stop}$ homozygous mice survived to P10 than expected based on Mendelian ratios. An examination of the survival rates of embryos *in utero* does not show a significant difference. This suggested that the mutants die perinatally.

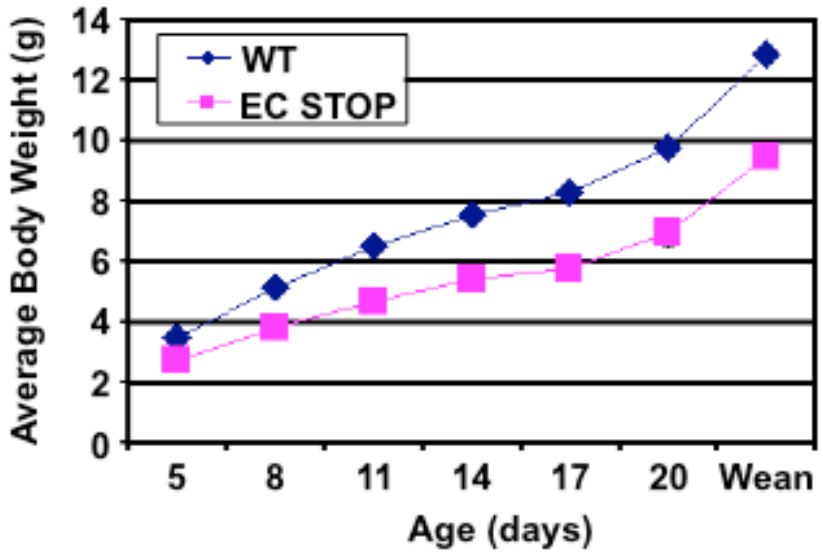

Figure 7 *Megf7*$^{EC\ Stop}$ Mice have Significantly Lower Body Weights.

Pups in four litters were weighed every three days starting at P5. At each time point measured, the *Megf7*$^{EC\ Stop}$ homozygous pups were significantly smaller than either wild type or heterozygous littermates.

The cause of the difference in weight gain and perinatal lethality is unknown. Dr. Robert Hammer observed that mutant pups swallow air and thus have distended stomachs. Whether this is the cause of death and/or the cause of the difference in weight gain is unknown. There may be a neurological defect that may affect the swallowing reflex or there may be an unknown structural defect that allows air to be swallowed.

Regulation of Tooth Development by *Megf7*

I documented the initial incisor defects found in the *Megf7*$^{EC\ Stop}$ mutants. Subsequent work was performed in the lab of Dr. Paul Sharpe, King's College in London, with tissue samples that I provided.

Introduction to Tooth Development

Tooth development begins around E11.5 in the mouse embryo. At this initial stage, the oral epithelium thickens at the sites where each tooth will form. The epithelium then invaginates the underlying condensing mesenchyme to form a cap and then a bell structure. The tip of these structures forms the organizing center for the tooth and is called the enamel knot. The epithelium at the epithelium/mesenchyme border differentiates into the ameloblasts that make the enamel of the tooth. The mesenchymal cells at this border differentiate into odontoblasts that form the dentin (Tucker & Sharpe, 2004).

As with all other processes that are involved in organogenesis, tooth development involves the interaction of many different signaling systems. The initiating signal involved in determining the position of each tooth is unknown for the moment. The expression of *Shh* in the oral epithelium designates the region of tooth formation. In the underlying mesenchyme, the transcription factor *Pax9* is expressed and thus may play a part in the coordination of the *Shh* expression. *Wnt7b* is expressed in a reciprocal pattern to *Shh* and thus designates the non-tooth forming epithelium. The differentiation of molars or incisors is dependent on

Fgf8/9 and *Bmp4* respectively. *Fgf8* and *Bmp4* are mutually antagonistic through a system of positive and negative feed-back loops involving the ligands and the transcription factors that they induce, *Pitx2* and *Islet1* respectively. *Fgf8* induces the expression *Barx1*, *Dlx2*, *Lhx6/7*, and *goosecoid*. These transcription factors are involved in defining the zones of molar formation as well as the formation of the underlying bone. *Bmp4* activates the expression of *Msx1* and *Msx2* to control the region of incisor formation. The interaction of the mentioned signaling pathways as well as other systems controls the precise patterning involved in tooth formation (Tucker & Sharpe, 2004).

Analysis of the Megf7$^{EC\ Stop}$ Tooth Defect

The *Megf7$^{EC\ Stop}$* mutant has an incompletely penetrant oligodontia phenotype. Initially, it was observed that some of the homozygous mutants had defects in the incisors. There were defects in incisor spacing, trajectory, as well as extra incisors (Figure 8A). The lab of Dr. Paul Sharpe at King's College in London has analyzed the effects of the loss of *Megf7* in tooth development in more detail. The defects in molar formation were found to be more frequent and severe than the incisor defect. (Figure 8C). *Megf7$^{EC\ Stop}$* mice often had fusion of the molars as well as dysplastic molar formation (Figure 8B).

A

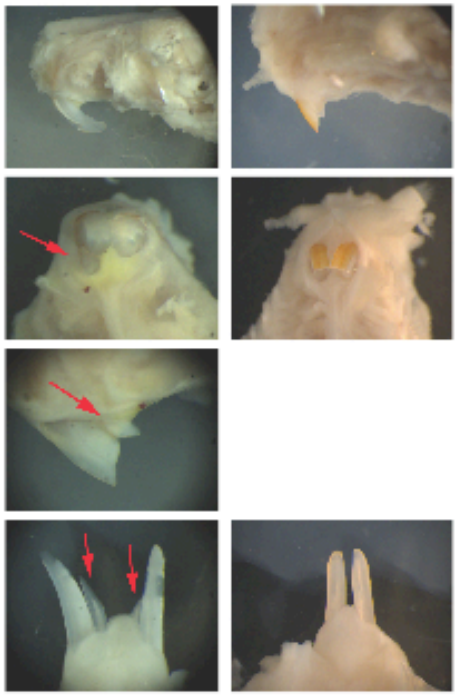

B

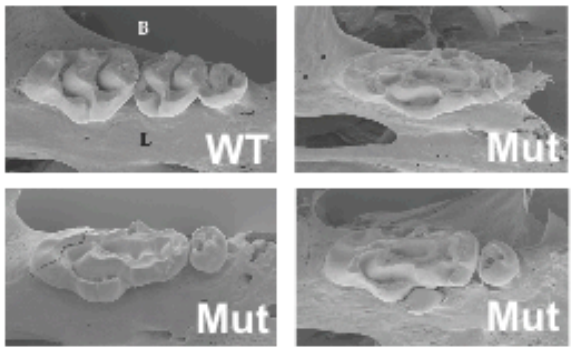

C

Upper Jaw	Mouse #1	Mouse #2	Mouse #3	Mouse #4
Incisor	2 abnormal curved original	2 normal original 1 extra (Left lingual)	2 normal original 1 extra (Right lingual)	2 normal original 1 extra (Left lingual)
right molars	1 big molar (1+2) or (1+2+3)	1 small molar 1 big molar 1 tiny molar	1 big molar (1 + 2) 1 tiny molar 1 extra (Lingual)	1 big molar (1 + 2) 1 tiny molar
left molars	1 big molar (1 + 2) 1 tiny molar	1 small molar 1 big molar 3rd missing	1 big molar (1 + 2) 1 tiny molar	1 big molar (1 + 2) 1 tiny molar 1 extra (Lingual)
Lower Jaw				
Incisor	2 abnormal elongate original 2 small extra	2 normal original	2 normal original	2 normal original
right molars	3 normal original	2 normal original 3rd missing	3 normal original	3 normal original
left molars	1 bit small molar 1 bit big molar 1 tiny molar	2 normal original 3rd missing	3 normal original	3 normal original

Figure 8 Defective Patterning of the Incisors and Molars in the *Megf7*$^{EC\ Stop}$ Mouse.
(Previous Page)(A) A patterning defect in the *Megf7*$^{EC\ Stop}$ mutant leads to a misalignment of the teeth as well as ectopic incisors (arrows). (B) There are three molars that form in wild type mice. In the *Megf7*$^{EC\ Stop}$ mutant, there are fused or ectopic molars present. (C) A table demonstrating the variability of the tooth patterning defect in the *Megf7*$^{EC\ Stop}$ mutants.

The expression of *Megf7* was analyzed to provide clues to the mechanism of its action. Before tooth development begins at E10.5, *Megf7* is broadly expressed in the mesenchyme as well as the oral epithelium. However, at the stage when the oral epithelium thickens over the prospective tooth anlage, E11.5, the expression of *Megf7* goes from a broad expression pattern to be restricted to the thickened epithelium. Later during development, the expression of *Megf7* is concentrated at the enamel knot. At birth *Megf7* is expressed in multiple regions of the developing tooth. This expression data suggests that *Megf7* is involved in the initial patterning of the teeth and establishing tooth boundaries (Figure 9).

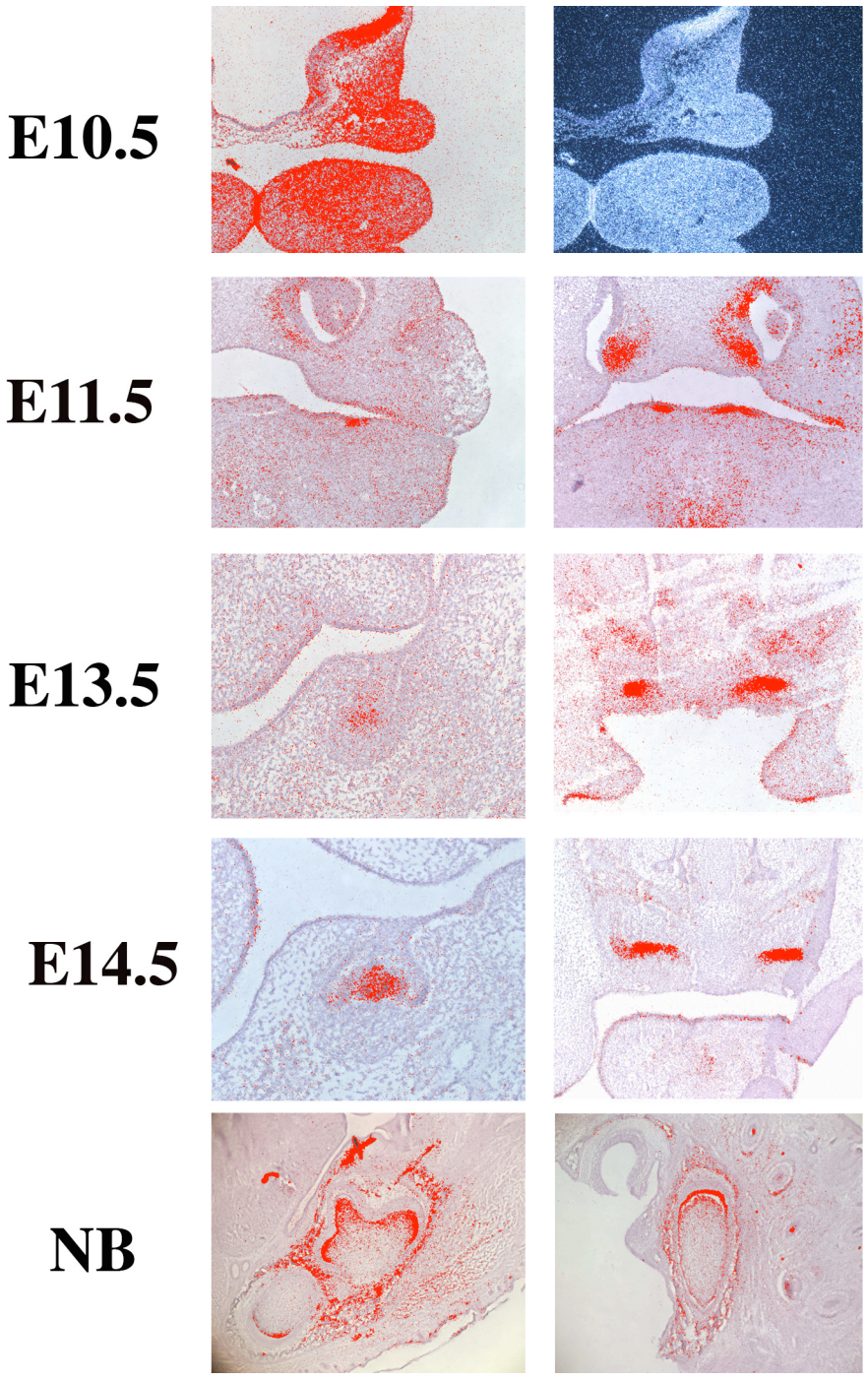

Figure 9 *Megf7* Expression in the Developing Tooth.

The Expression of *Megf7* begins as a diffuse pattern at E10.5. At E11.5 the expression of *Megf7* resolves to the tooth anlage. Expression continues though tooth development in the enamel knot and the early tooth forming cells.

As mentioned above, *Shh* is an early marker for the region in the oral epithelium that will form each tooth. Analysis of the *Megf7*$^{EC\ Stop}$ embryos shows ectopic expression of *Shh* in both the region of the incisors as well as the molars. The expression of *Patched* (Ptc), a *Shh* responsive gene, also shows ectopic *Shh* signaling (Figure 10).

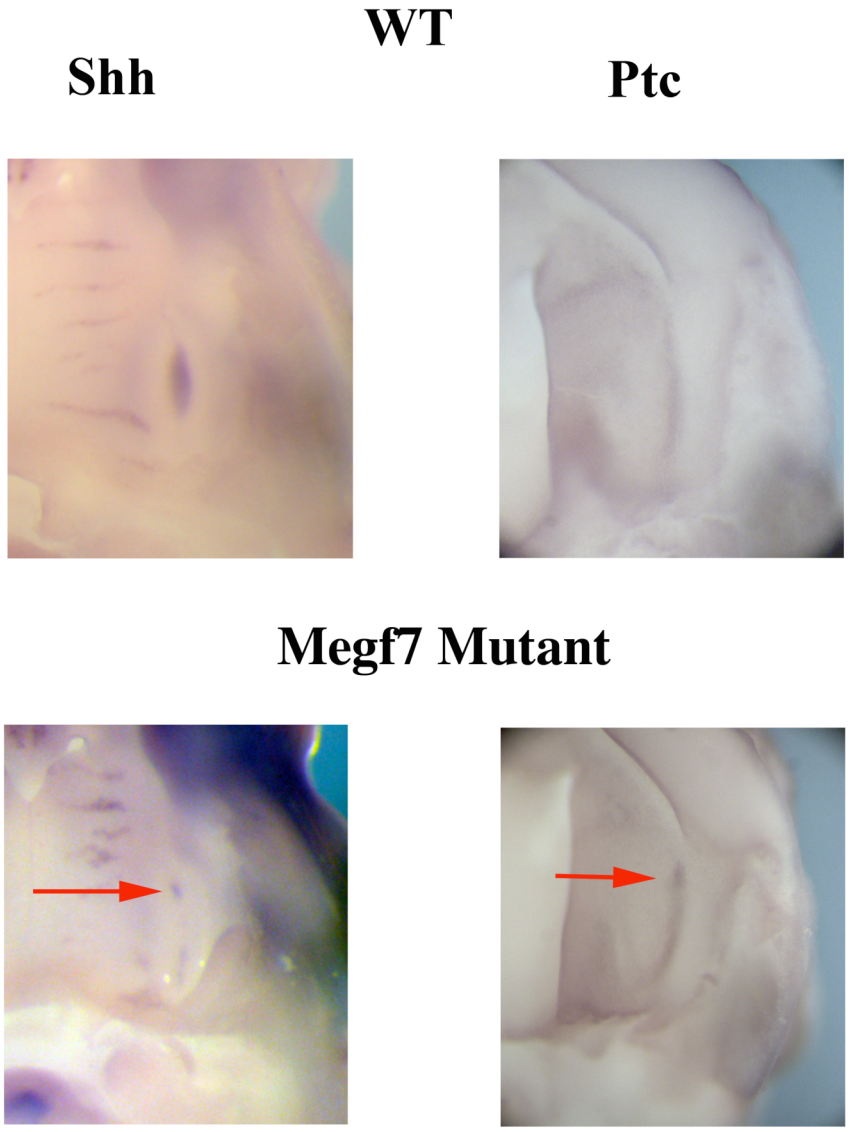

Figure 10 Expression of *Shh* and *Ptc* in the *Megf7*$^{EC\ Stop}$ Mutant.

The expression of *Shh* in the *Megf7*$^{EC\ Stop}$ mutant is weaker compared to wild type expression. There is also ectopic expression of *Shh* as indicated by the arrow. There is also ectopic expression of *Ptc*, a *Shh* responsive gene, in the same region of ectopic *Shh* expression in the *Megf7*$^{EC\ Stop}$ mutant.

The ectopic *Shh* expression, as well as the tooth phenotype, is very similar to the *Ectodin* mutant that was recently reported (Kassai et al., 2005). *Ectodin* is a BMP antagonist that is expressed in the non-enamel knot cells within the developing tooth. Loss of *Ectodin* activity also leads to ectopic *Shh* expression, fused molars, as well as the expected increase in expression of BMP responsive genes (Kassai et al., 2005). This led the Sharpe lab to the hypothesis that *Megf7* may be an inhibitor of the BMP signaling pathway. Analysis of phospho-SMAD levels in the *Megf7* mutants shows that there is an increase in BMP signaling in the developing tooth (Figure 11). This data suggests that *Megf7* may be playing a role in the BMP signaling pathway similar to what is seen with *Megalin*, another member of the LDLR gene family that inhibits BMP signaling in the developing brain through the endocytosis of BMP.

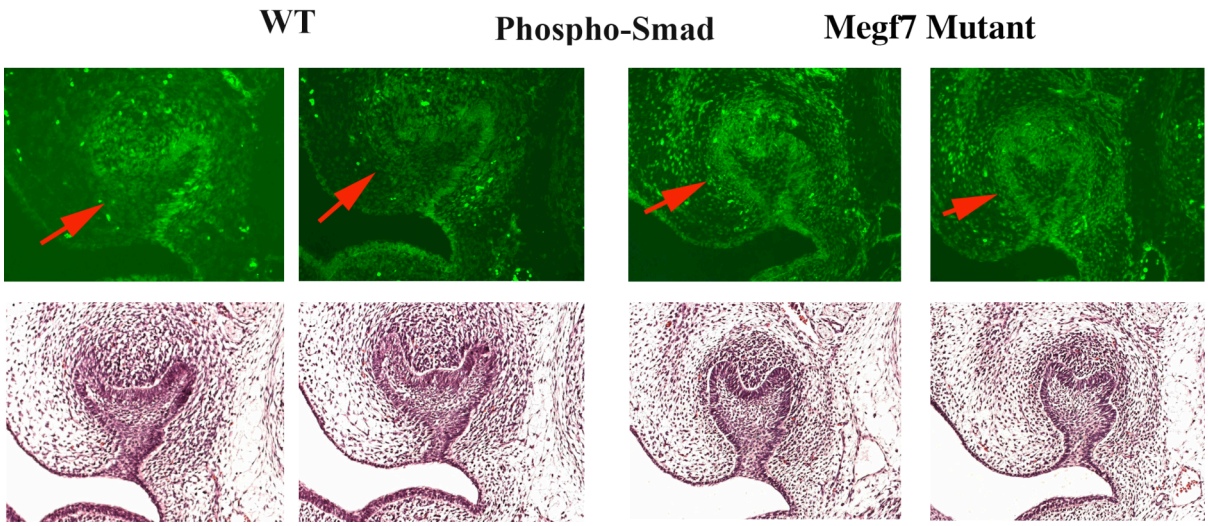

Figure 11 Upregulation of Phospho-SMAD Levels in the *Megf7*$^{EC\ Stop}$ Mutant.
There is an upregulation of phospho-SMAD levels, the downstream effecter of BMPs, in the developing tooth in the *Megf7*$^{EC\ Stop}$ mutant as indicated by the arrow.

Defective Mammary Gland Patterning in the *Megf7*$^{EC\ Stop}$ Mutants

The analysis of the expression pattern of *Megf7* during embryogenesis by Weatherbe et al. prompted us to analyze the patterning of mammary glands in the *Megf7*$^{EC\ Stop}$ mutant mouse. In wild type mice, five mammary placodes are distributed on each side of the mouse. Looking at P10 pups, when the hair is not long enough to cover the nipple skin, it was observed that the *Megf7*$^{EC\ Stop}$ mutants have disrupted patterning of the mammary placodes. There are enlarged regions of nipple skin (Figure 12, arrowheads) as well as ectopic nipples (Figure 12, arrows). The disruption of the patterning of multiple organ systems in *Megf7* mutants suggests again that *Megf7* regulates a common signaling system(s) required for multiple developmental paradigms.

Tooth and mammary gland development shares similar mechanisms that involve the WNT, BMP, and FGF gene families, among others (Mikkola & Millar, 2006). It is likely that *Megf7* regulates one or more of these pathways using a common mechanism.

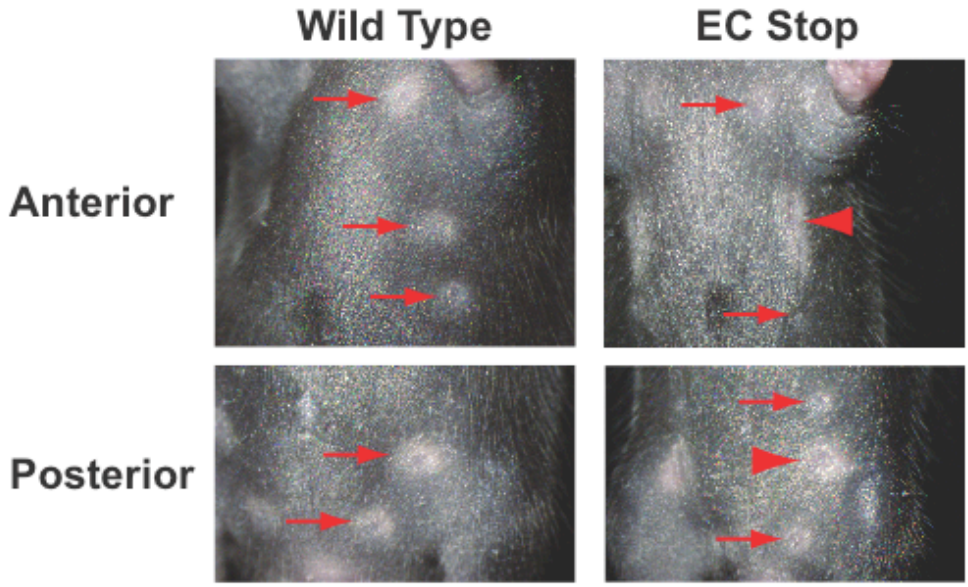

Figure 12 Disruption of Mammary Gland Patterning in the *Megf7*$^{EC\ Stop}$ Mutant.
At 10 days of age, the nipple skin in female mice easily contrasts against the ventral skin. Defective patterning of the mammary gland can be seen in the *Megf7*$^{EC\ Stop}$ mutant pup with ectopic nipple skin as well as enlarged nipple area (arrow heads).

Polysyndactyly in the *Megf7*$^{EC\ Stop}$ Mutants

Initially, we mainly focused on the polysyndactyly ofn the *Megf7*$^{EC\ Stop}$ mutants. Polysyndactyly is a combination of polydactyly, the formation of extra digits, and syndactyly, the fusion of digits. As seen in Figure 13, there is a severe loss of patterning in the autopod of both the hind limbs and fore limbs. This defect occurs with 100% penetrance in all animals examined. There were occasional instances of brachydactyly (one litter) or polydactyly in the heterozygotes (one mouse) that occurred at such a low frequency that it was not reproducible.

Figure 13 Polysyndactyly in the *Megf7*$^{EC\ Stop}$ Mutant.

The *Megf7*$^{EC\ Stop}$ mutants have a polysyndactyly phenotype, which is characterized by the fusion and duplication of digits of the autopod. Defects in limb development occur at 100% frequency in both the fore limbs and hind limbs. The remaining regions of the limbs are largely unaffected.

Alcian Blue and Alizarin Red stain the cartilage and bone respectively. Staining of the bones of the *Megf7*$^{EC\ Stop}$ autopod shows the loss of skeletal patterning (Figure 14). The fusion of digits as well as ectopic bone growths are a consequence of a global loss of autopod patterning and can not be categorized as either preaxial or postaxial as is the case for several autopod deformities.

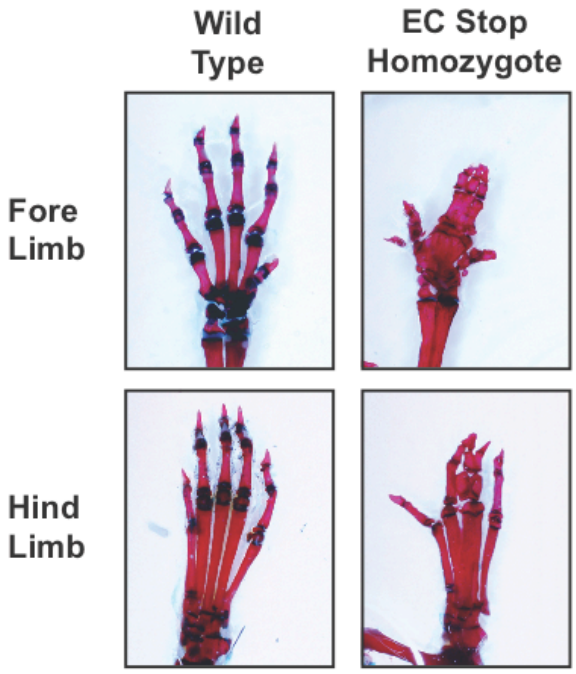

Figure 14 Alizarin Red/Alcian Blue Staining of the *Megf7*$^{EC\ Stop}$ Limbs.

The limbs of wild type and mutant adults were stained with Alizarin red and alcian blue, which stain the bone and cartilage respectively. The staining reveals the ectopic bone growths as well as the fusion of the digits.

Megf7$^{EC\ Stop}$ *Limb Phenotype at E11.5, E12.5, and P0*

Possible explanations for the limb defects in the *Megf7*$^{EC\ Stop}$ mice include an initial loss of patterning early in development, a defect in the condensation of the cartilage from the limb bud mesenchyme, or a defect in the apoptosis of the interdigital mesenchyme. To investigate the etiology of the polysyndactyly phenotype, the different stages of limb development were examined. Staining of the limbs at P0 shows that the defect is already well established. The lack of Alizarin Red staining shows that the deposition of bone is delayed in

the *Megf7*$^{EC\ Stop}$ pups. The Alcian Blue staining also shows the loss of patterning of the cartilage that will eventually be replaced by bone in the adults (Figure 15).

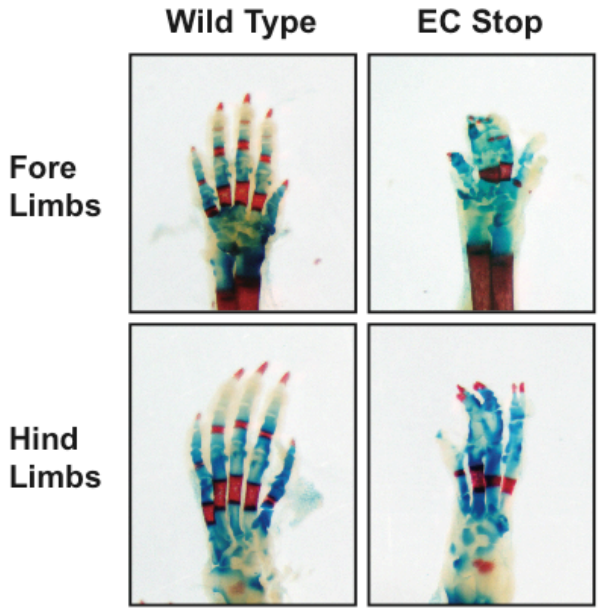

Figure 15 Alizarin Red/Alcian Blue Staining of P0 *Megf7*$^{EC\ Stop}$ Limbs.
At P0, the staining for bone in wild type pups reveal a banded pattern of ossification. This pattern of ossification in the *Megf7*$^{EC\ Stop}$ mutant shows a delay in bone formation. The cartilage staining also shows that the defect of digit patterning is already present at P0.

The limb bud mesenchyme undergoes condensation in the regions in the limb that will form the bones. This condensed mesenchyme differentiates into the chondrocytes that form the cartilage that will eventually be replaced by bone. *Collagen 2A1* is expressed in prehypertropic chondrocytes, and thus marks the pattern of cartilage and bone deposition. At E11.5, the *Col2a1* expression is not significantly different in the mutants as compared to wild type controls. At E12.5 however, *Col2a1* expression shows that the patterning of mesenchymal condensation of the *Megf7*$^{EC\ Stop}$ embryos is already established to form limbs

with polysdyndactyly. In other words, the patterning defect that occurs in the limbs of the *Megf7*$^{EC\ Stop}$ mutants manifests at some time point before E12.5 (Figure 16).

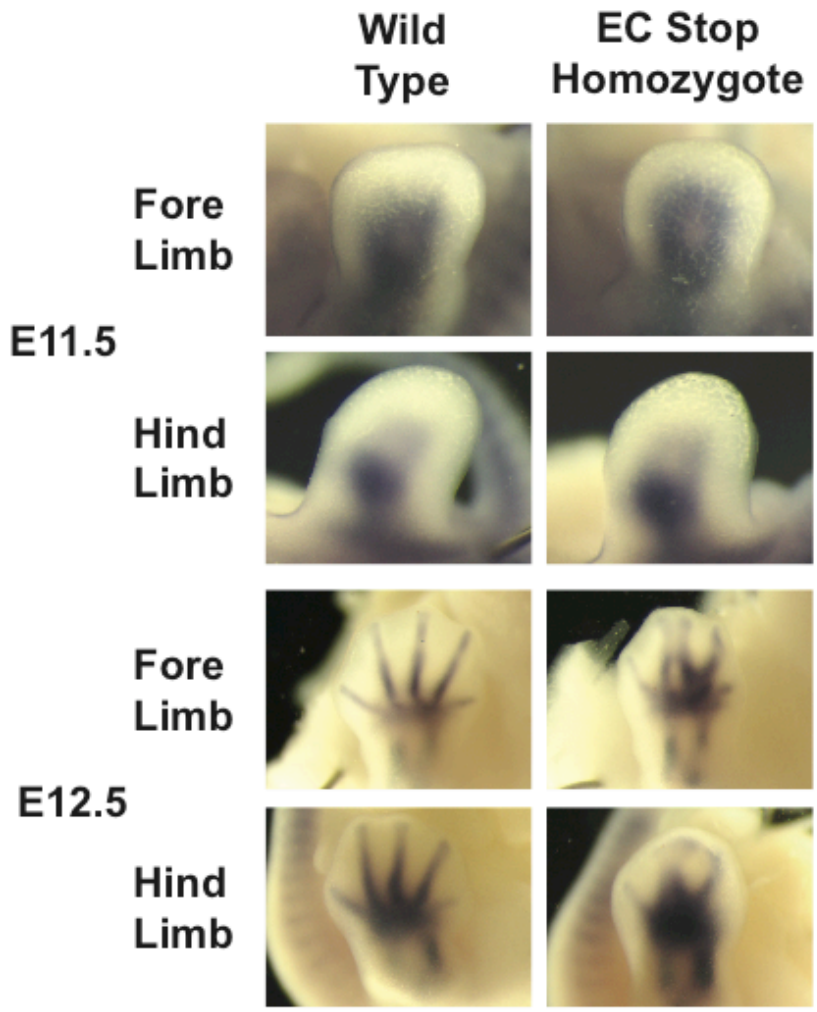

Figure 16 Defective Cartilage Patterning in the *Megf7*$^{EC\ Stop}$ Mutant.

Collagen 2a1, *Col2a1*, expression is a marker for prehypertropic chondrocytes. These chondrocytes will eventually condense and form the cartilage that will later be replaced by bone. At E11.5 the pattern of *Col2a1* expression is similar in both wild type and mutant embryos. At E12.5 the expression of *Col2a1* reveals a disruption of the patterning of the autopod in the *Megf7*$^{EC\ Stop}$ limb. This suggests that the patterning defect in the mutant limbs occurs before E12.5.

Megf7 Expression in the Developing Limb

The expression of *Megf7* during early embryonic development was examined to gain a better understanding of the mechanism of the limb defect in the *Megf7*$^{EC\ Stop}$ mutants. At E9.5 the expression of *Megf7*, as indicated by whole mount *in situ* staining, is expressed in a poorly defined region of the ectoderm of the emerging fore limb bud (Figure 17A). The expression of *Megf7* becomes more pronounced at E10.5 where there is a faint band of expression in the AER (Figure 17B).

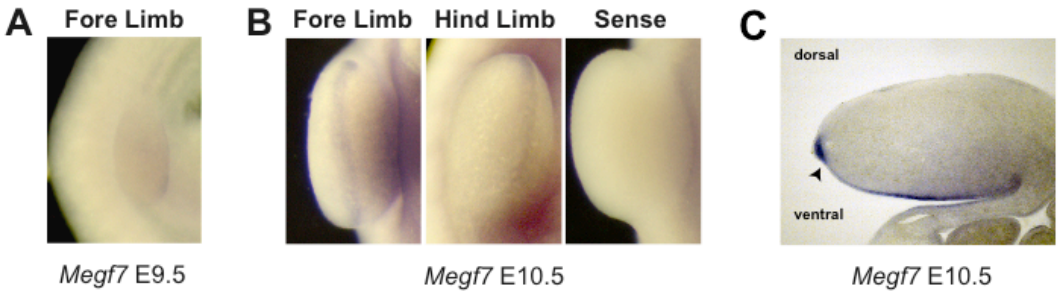

Figure 17 Expression of *Megf7* During Limb Development.
(A) Expression of *Megf7* at E9.5 in the limb is diffuse. (B) At E10.5 the expression of *Megf7* can be seen in the AER. The sense probe shows no signal. (C) Cross-sections through the limbs stained for *Megf7* show that expression is both in the AER as well as the ventral ectoderm.

Serial sections of the limb buds of the stained embryos show that *Megf7* is not only expressed in the AER but is also expressed in the E10.5 limb ventral ectoderm (Figure 17C). This suggests that the signal that is regulated by *Megf7* is received by the cells in the ventral ectoderm and the AER. Subsequent publications show that *Megf7* is also expressed in the interdigital mesenchyme later in the developing limb (Simon-Chazottes et al., 2006). The interdigital expression of *Megf7*as described by Simon-Chazottes et al. probably does not

affect the phenotype of the *Megf7*$^{EC\ Stop}$ mutant because the initial defect found in the mutant is at E10.5 whereas interdigital expression is at E12.5 and thus occurs after the initial defect. The limb expression of *Megf7* was also confirmed by Yamaguchi et al. (Yamaguchi et al., 2006).

Fgf8 Expression Reveals an Expanded AER in the Megf7$^{EC\ Stop}$ *Mutant*

The expression pattern of different marker genes was examined to see if any signals important for limb development are perturbed in the *Megf7*$^{EC\ Stop}$ limb. *Fgf8* expression is a strong marker for the cells in the AER, a discrete ridge of cells on the distal aspect of the developing limb. Examination of *Fgf8* expression in the mutant limbs shows that the *Fgf8* expression is no longer confined to a distinct ridge at the edge of the limb bud but is spread down the lateral aspect of the bud. The expression also appears to be less intense than the expression of *Fgf8* in wild type limbs (Figure 18).

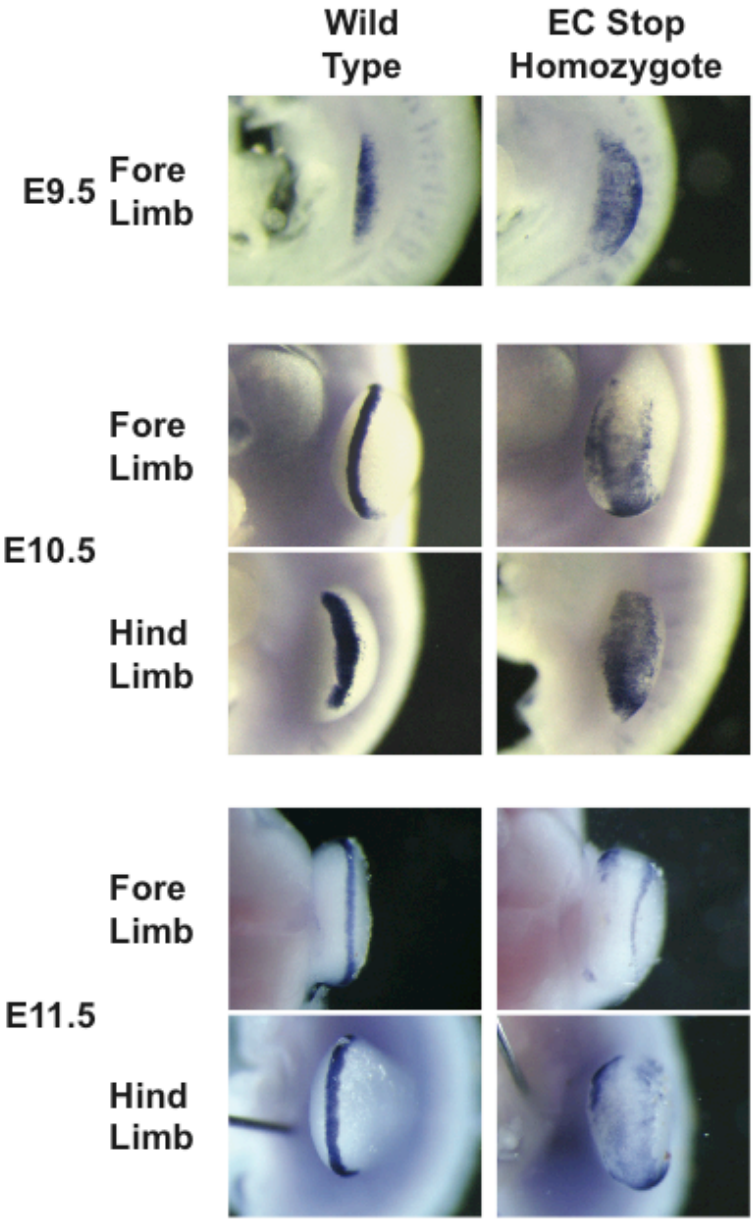

Figure 18 Expression of *Fgf8* in the *Megf7*$^{EC\ Stop}$ Mutant.

Fgf8 is a gene that is used as a marker for the AER. At E9.5 the expression of *Fgf8* is diffuse in wild type fore limbs. Even at E9.5, the expression of *Fgf8* is more diffuse in the *Megf7*$^{EC\ Stop}$ mutant compared to wild type expression. At E10.5 and E11.5 *Fgf8* is expressed in a distinct band at the distal edge of the limb bud in wild type embryos. The expression of *Fgf8* in the *Megf7*$^{EC\ Stop}$ embryos is expanded along both the dorsal and ventral aspects of the limb bud suggesting that the AER is also expanded.

Structure of the Mutant AER

Serial sections also highlight the changes in the AER that occur in the mutant limb. The *Fgf8 in situ* results initially suggested that the cells that were destined to form the AER never aggregate into the band of pseudostratified epithelium found in the wild type AER. Instead, the whole mounts indicated that those cells were still in a single-cell layer of epithelium and yet still retained the ability to express *Fgf8*. Sections through the limbs show that this is not the case. Despite the lower intensity of *Fgf8* expression in the mutants, suggesting that there is a decrease of the number of *Fgf8* expressing cells per area, the AER is still intact and still consists of a pseudostratified epithelium. The boundaries of the AER are expanded down the lateral aspect of the limb. Nomarski optics imaging confirms this phenotype and shows that the cells that express *Fgf8* are also the cells that are morphologically similar to cells in the AER (Figure 19).

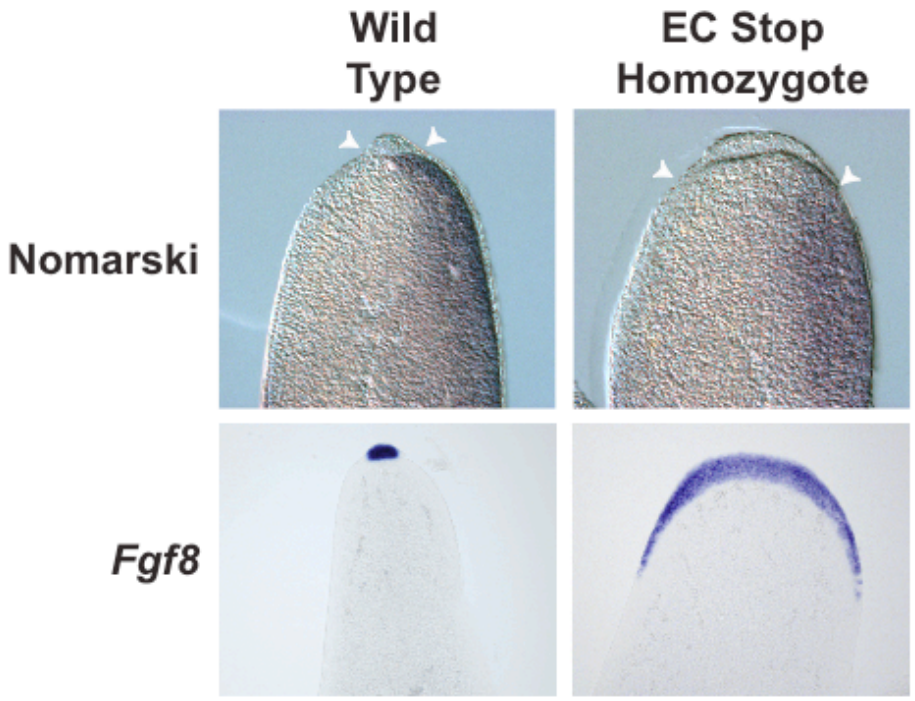

Figure 19 Expansion of the AER in the *Megf7*$^{EC\ Stop}$ Mutants.
Cross sections of the limbs of *Megf7*$^{EC\ Stop}$ mutants were visualized to analyze the structure of the AER. Visualization with Nomarski optics shows that the large AER remains a pseudostratified epithelium. Cross sections through stained limbs show that the cells that are present in the expanded AER still express *Fgf8*.

Decreased Shh Expression in the Developing Megf7$^{EC\ Stop}$ *Limb*

The expansion of the AER is a dramatic structural defect that is probably the cause of the subsequent disruption of patterning that leads to polysyndactyly. During development, different cell populations interact on multiple levels to specify the precise patterning required to achieve the final structure. For example, the Zone of Polarizing Activity (ZPA) is a region of the developing limb that requires signals from the AER for correct patterning to be

established. The disruption of the AER in the *Megf7*$^{EC\ Stop}$ mutant is an example of how the disruption of one region, the AER, affects the development of other regions.

The ZPA is marked by the mesodermal expression of *Shh* in the posterior aspect of the limb. Analysis of the expression of *Shh* in the *Megf7*$^{EC\ Stop}$ mutant shows that the disruption of the structure of the AER results in an overall decrease in the intensity of *Shh* expression. Even though whole mount *in situ* is not a quantitative assay, there is consistently less *Shh* signal in the homozygous mutants compared to litter mate controls. In wild type embryos, the expression of *Shh* is separated into dorsal and ventral compartments by the AER. In the *Megf7*$^{EC\ Stop}$ mutant, the expanded AER leads to a distortion of this dorsal and ventral expression of *Shh* (Figure 20).

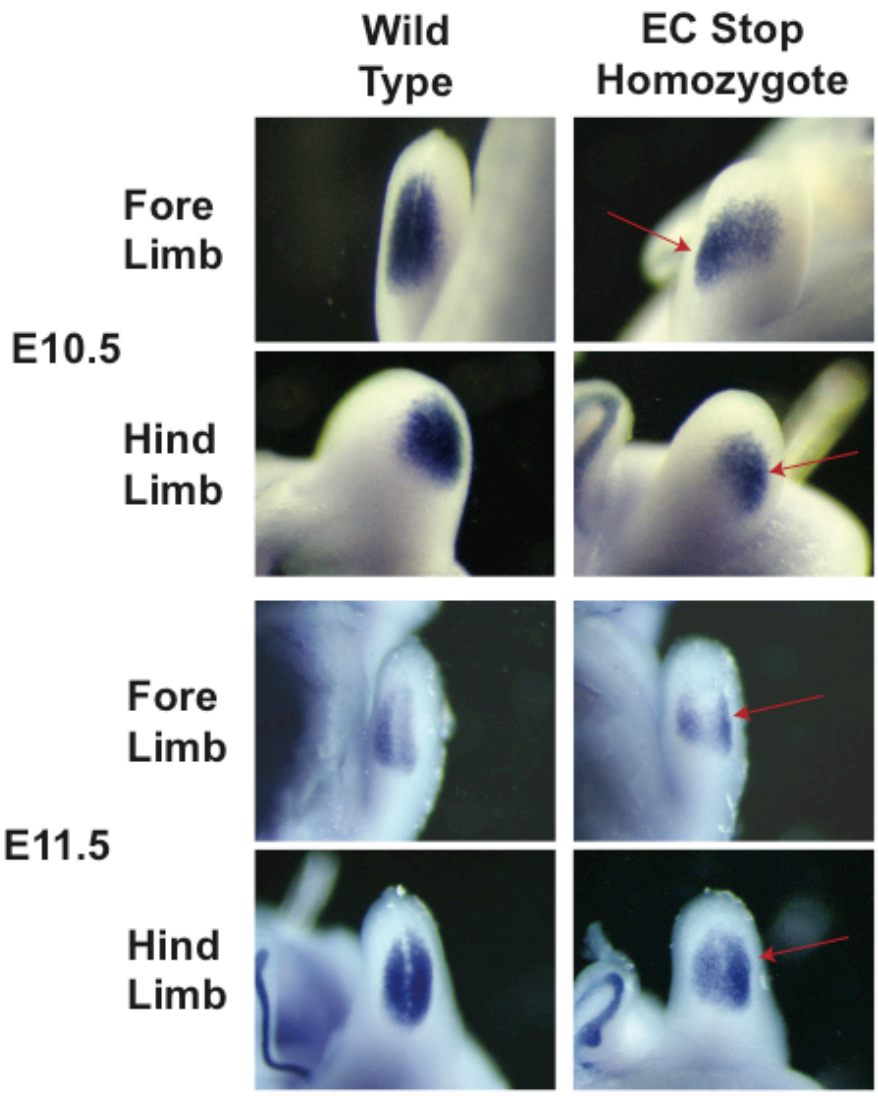

Figure 20 Expression of *Shh* in the *Megf7*$^{EC\ Stop}$ Mutant Limb.

In wild type limbs, *Shh* is expressed in the region called the Zone of Polarizing Activity, ZPA, in the posterior mesoderm. This expression is interrupted at the midline by the AER. In the *Megf7*$^{EC\ Stop}$ mutant limbs, the expression of *Shh* is weak. Also, the separation of the regions of *Shh* expression is distorted due to the expanded AER. Note the higher dorsal *Shh* expression (Arrow).

The function of *Shh* and the ZPA in the developing limb is thought to provide anterior to posterior information to the cells within the developing limb. A weakening of the *Shh* signal may perturb the anterior to posterior patterning for positioning the digits. Expanding the area in which *Shh* is expressed may also change the three-dimensional orientation of the developing structures in the limb and thus may explain the polysyndactyly phenotype of the *Megf7*$^{EC\ Stop}$ mutant.

Disruption of Dorsal Wnt7a Expression in the Megf7$^{EC\ Stop}$ *Mutant*

Wnt7a is expressed exclusively in the dorsal ectoderm. Expression of *Wnt7a* is inhibited by the transcription factor *En1,* which is expressed in the ventral ectoderm. One common defect in several genetic limb deformities is the loss of dorsal-ventral polarity in the developing limb. This loss of polarity leads to the ectopic development of dorsal structures on the ventral aspect of the limb or vice-versa.

The expression of *Wnt7a* in the *Megf7*$^{EC\ Stop}$ mutant was analyzed to examine if the dorsal identity is maintained. As mentioned above, *Wnt7a* is expressed in the dorsal ectoderm and is excluded from the AER. The expression of *Wnt7a* in the mutant embryo is still in the dorsal ectoderm but the expression is displaced proximally by the expanded AER. The loss of *Wnt7a* expression toward the distal aspect of the limb appears to be a downstream effect of the expansion of the AER and thus probably not the cause of the polysyndactyly in the mutant mice (Figure 21).

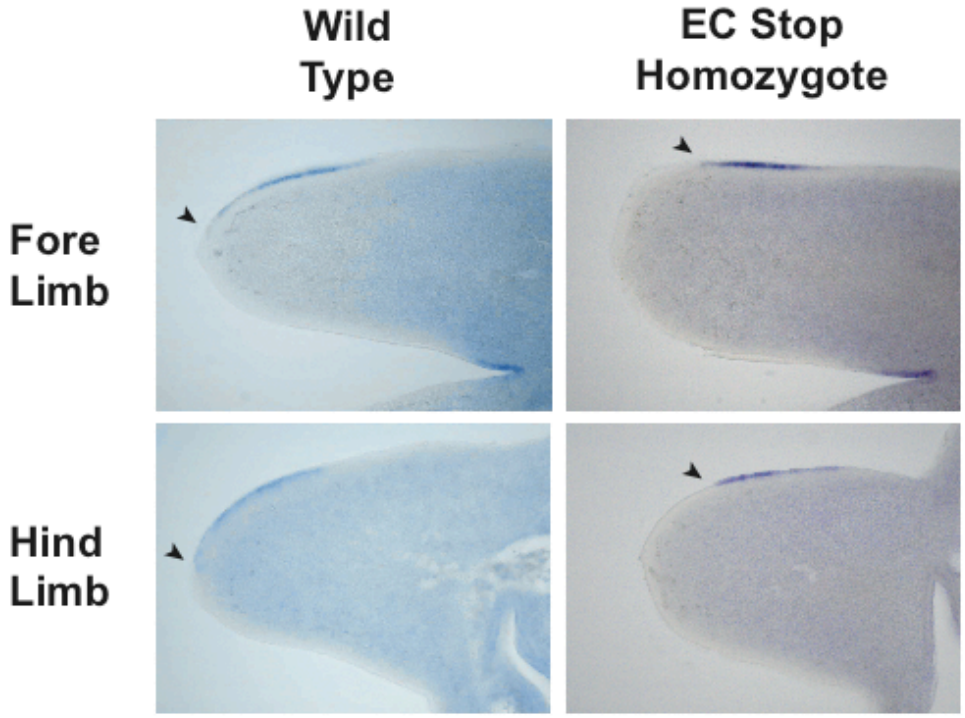

Figure 21 *Wnt7a* Expression in the *Megf7*$^{EC\ Stop}$ Limb.

The expression of *Wnt7a* was analyzed in the *Megf7*$^{EC\ Stop}$ limb bud. In wild type limbs, *Wnt7a* is expressed in the dorsal ectoderm and stops at the dorsal border of the AER (Arrowhead). The expression of *Wnt7a* remains in the dorsal ectoderm in the *Megf7*$^{EC\ Stop}$ mutant. The distal border of expression is more proximal due to the expansion of the AER.

Lmx1b Expression in the Megf7$^{EC\ Stop}$ *Mutant Limb*

Lmx1b expression in the dorsal mesoderm is partially dependent on the signal from *Wnt7a*. Therefore, a perturbation in the expression of *Wnt7a* expression may affect the expression of *Lmx1b*. In the *Megf7*$^{EC\ Stop}$ embryos, the loss of distal *Wnt7a* expression leads to a loss of robust expression of *Lmx1b* in the distal compartment of the developing limb. In wild type limbs, *Lmx1b* expression identifies the dorsal mesoderm with a distinct border between dorsal and ventral mesoderm starting at the midline of the AER to the base of the

limb. This distinct border is no longer present in the mutant limbs (Figure 22). The expression in the mutants is probably disrupted by the increased distance between the *Wnt7a* secreting cells and the target cells near the limb midline.

Lmx1b is a transcription factor that contributes to the dorsal identity of the dorsal mesoderm. Perturbation of the expression of *Lmx1b* in other experimental models leads to the ectopic expression of dorsal or ventral structures. Although there is no ectopic expression of *Lmx1b* in the *Megf7* mutants, the decrease in expression may lead to a loss of the precise patterning required to form a wild type limb.

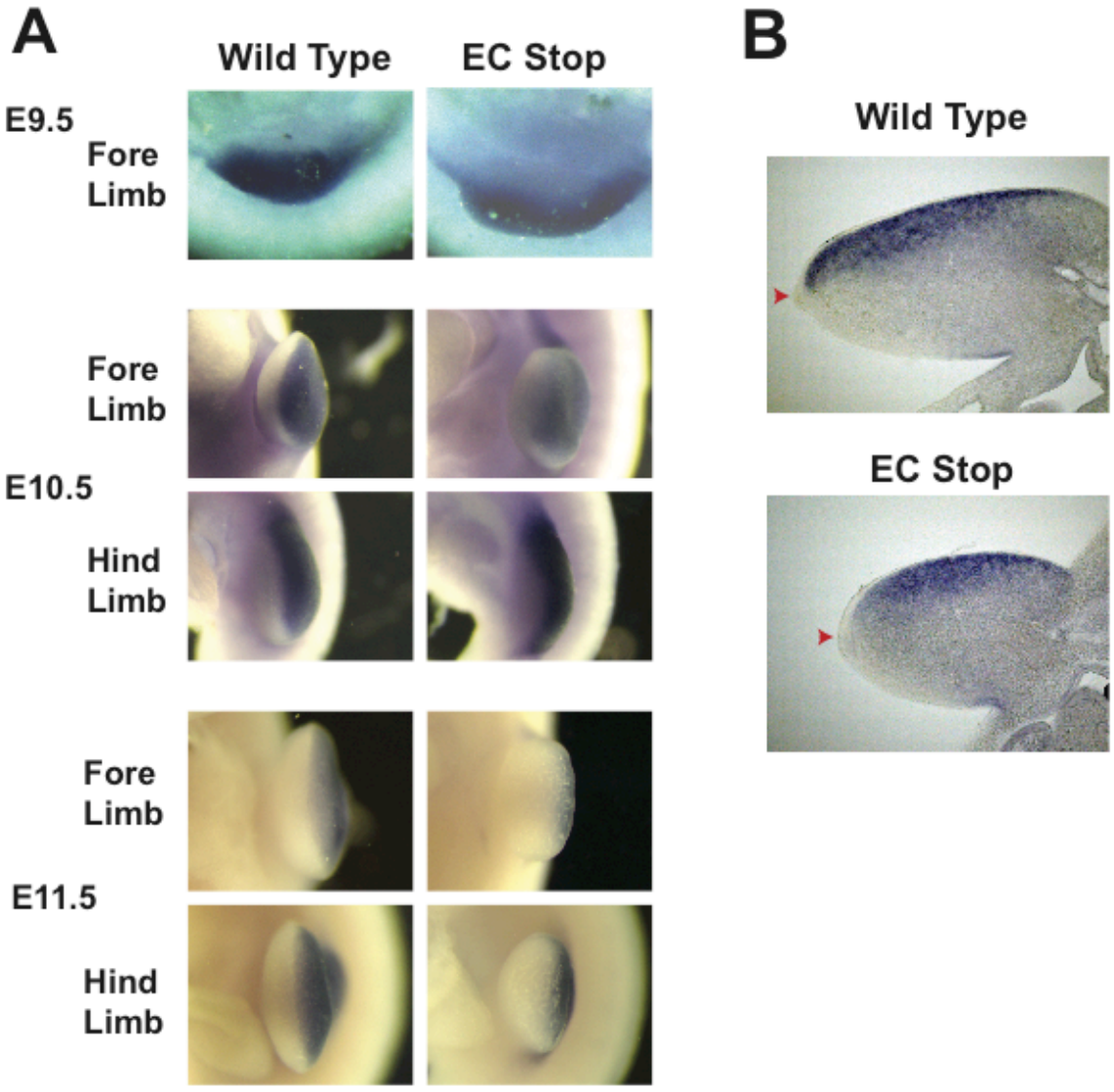

Figure 22 Expression of *Lmx1b* in the *Megf7*$^{EC\ Stop}$ Limb Bud.

Lmx1b is expressed in the dorsal mesoderm in wild type embryo limb buds. (A) Whole mount *in situ* for *Lmx1b* shows that the border between the dorsal expression of *Lmx1b* and the ventral mesoderm in the mutant limbs is less distinct compared to wild type limbs. (B) Cross-sections through stained limbs show that the border of *Lmx1b* expression in the mutant limbs does not reach the midline of the AER (Arrowhead).

As mentioned above, the expression of *Wnt7a* and *Lmx1b* does not suggest that there is a defect in dorso-ventral patterning in the mutant limbs. However, the shape of the limb indicates a ventralization or dorsalization. In wild type limbs, the ventral aspect of the limb is flat while the dorsal aspect is convex. In models where there is a defect in dorso-ventral patterning, the limb buds have a double-convex appearance because both dorsal and ventral aspects of the limb bud have the same shape (Cygan, Johnson & McMahon, 1997; Logan et al., 1997). The *Megf7* mutant limbs appear to have a double-convex shape, which suggests that there is a defect in polarity of the limb bud. An alternative explanation of this structural phenotype is that the expanded mutant AER is providing trophic support to the lateral aspects of the limb and thus induces lateral proliferation of the mesoderm to fill out the sides of the limb. A loss of dorso-ventral polarity of the limb is not evident in cross-sections of adult limbs. Structures that are found on the dorsal aspect of the limb such as tendons, hair, and skin glands are not found on the ventral aspect of the mutant limb. In the same regard, ventral structures such as the foot pads are not found on the dorsal aspect of the limb (Figure 23).

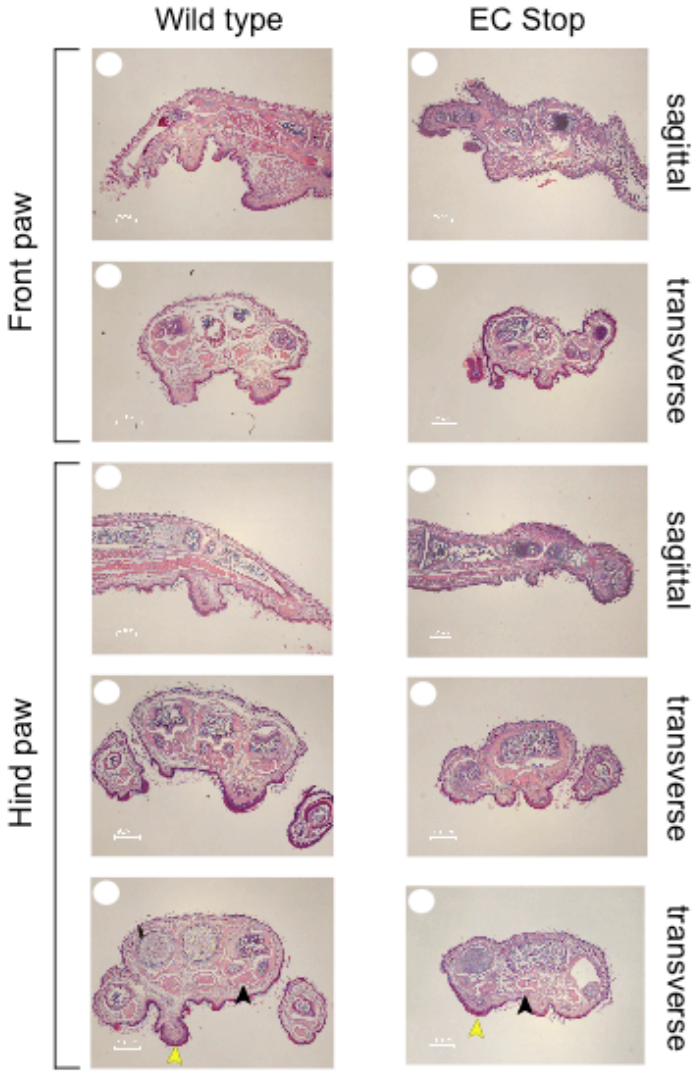

Figure 23 Cross-Sections of the Autopod of Adult *Megf7*$^{EC\ Stop}$ Mice.

Cross-sections through the limbs of the *Megf7*$^{EC\ Stop}$ mice do not indicate that there is a defect in dorsal/ventral patterning. There are no ectopic dorsal foot pads (yellow arrowheads), dorsal tendons (black arrowheads), or ventral hair/glands.

Disruption of the Zones of BMP Signaling in the Megf7$^{EC\ Stop}$ Mutant

As in all developmental processes, the precise coordination of signals is required for patterning of the developing organ. The limb is no exception. BMP expression in the limb is also changed by the expansion of the AER in the *Megf7* mutants. *Bmp4* and *Bmp7* are expressed in the AER as well as the mesoderm beneath the AER. As can be expected, the expansion of the AER in the mutant limbs leads to the expansion of the expression domain of the two BMPs.

As mentioned above, *Bmp4* is expressed in the AER as well as the underlying mesoderm in wild type embryos. The expression of the mesodermal *Bmp4* is limited in the lateral aspects of the limb. The enlarged mutant AER displaces the expression of *Bmp4* ectopically along the lateral aspect of the limb (Figure 24).

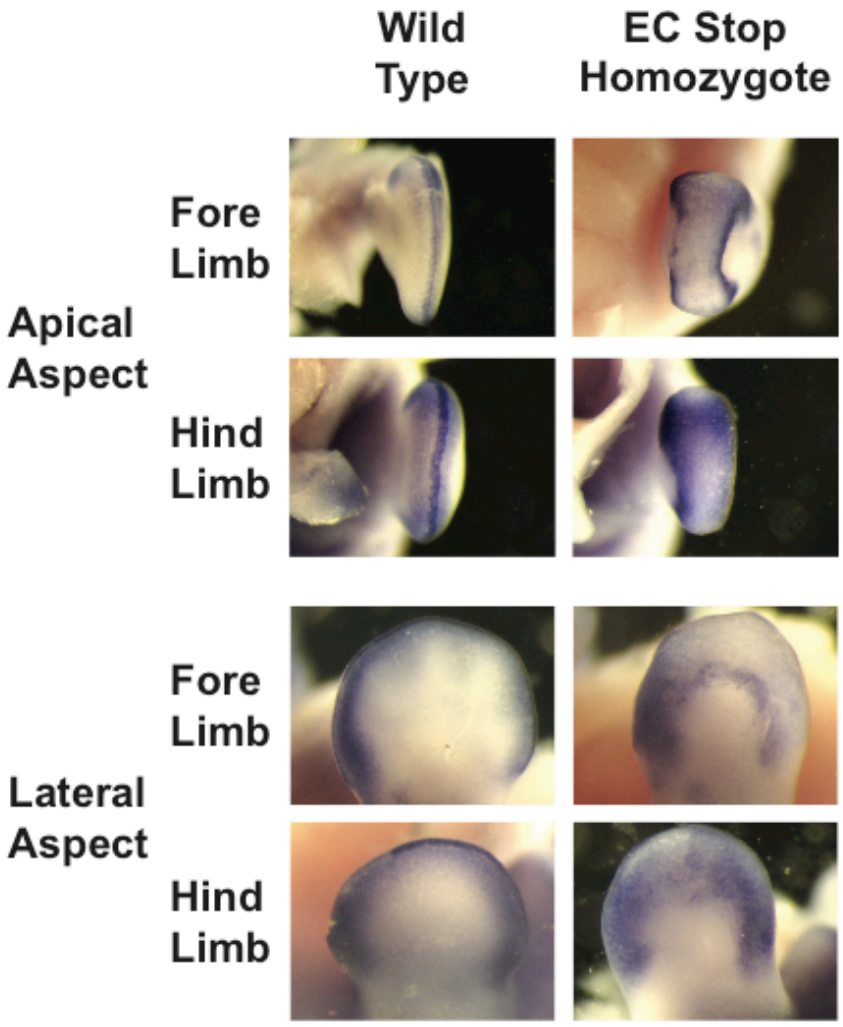

Figure 24 Expression of *Bmp4* in the *Megf7*$^{EC\ Stop}$ Limb.

In wild type mice, *Bmp4* is expressed in the AER as well as in the underlying mesoderm. As expected, the expression of *Bmp4* in the *Megf7*$^{EC\ Stop}$ mutant is expanded along both the dorsal and ventral aspects of the limb bud along with the AER.

Downstream genes of the BMP signaling pathway are *Msx1* and *Msx2*. Both genes are responsive to changes in BMP expression. As seen with *Bmp4,* the expression of *Msx1* is also expressed in the AER and the underlying mesoderm. With the expansion of the zone of BMP signaling in the *Megf7* mutant, there is a concomitant expansion of the zone of MSX

expression. In the *Megf7* mutants there is an expansion of *Msx1* along the lateral aspect of the developing mutant limb (Figure 25).

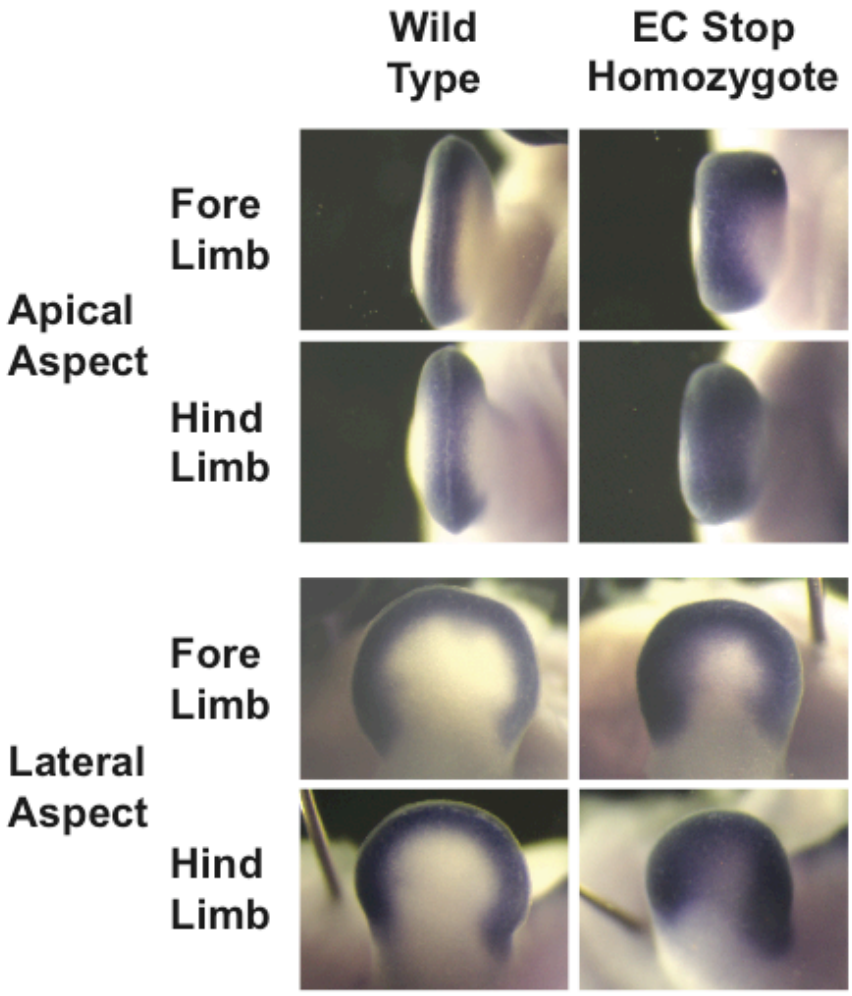

Figure 25 Expression of *Msx1* in the *Megf7*$^{EC\ Stop}$ Mutant.

Along with *Bmp4*, the expression of *Msx1* is also in the AER and the underlying mesoderm. The expansion of the AER in the *Megf7*$^{EC\ Stop}$ mutants leads to the expansion of the zone of *Msx1* expression.

Bmp2 is also expressed in the developing limb. The expression of *Bmp2* is different from *Bmp4* or *Bmp7*. *Bmp2* is mainly expressed in the interdigital mesenchyme when it

begins to condense to form cartilage. Thus, *Bmp2* is a good marker for the developing interdigital mesenchyme and the boundaries of the future digits.

As expected, the pattern of expression of *Bmp2* is disrupted in the *Megf7*$^{EC\ Stop}$ limb. The intensity of staining for the *Bmp2* message is also less than wild type staining. *Bmp2* is one of the signals that induces the interdigital mesenchyme to undergo apoptosis and thus is required for the separation of the digits. It is unclear if a loss of precise *Bmp2* patterning is the downstream factor contributing to the disorganization of the autopod. There may be other genes that may be more important for providing the spatial information for the division of the digits and in turn provide information for the expression of *Bmp2* (Figure 26).

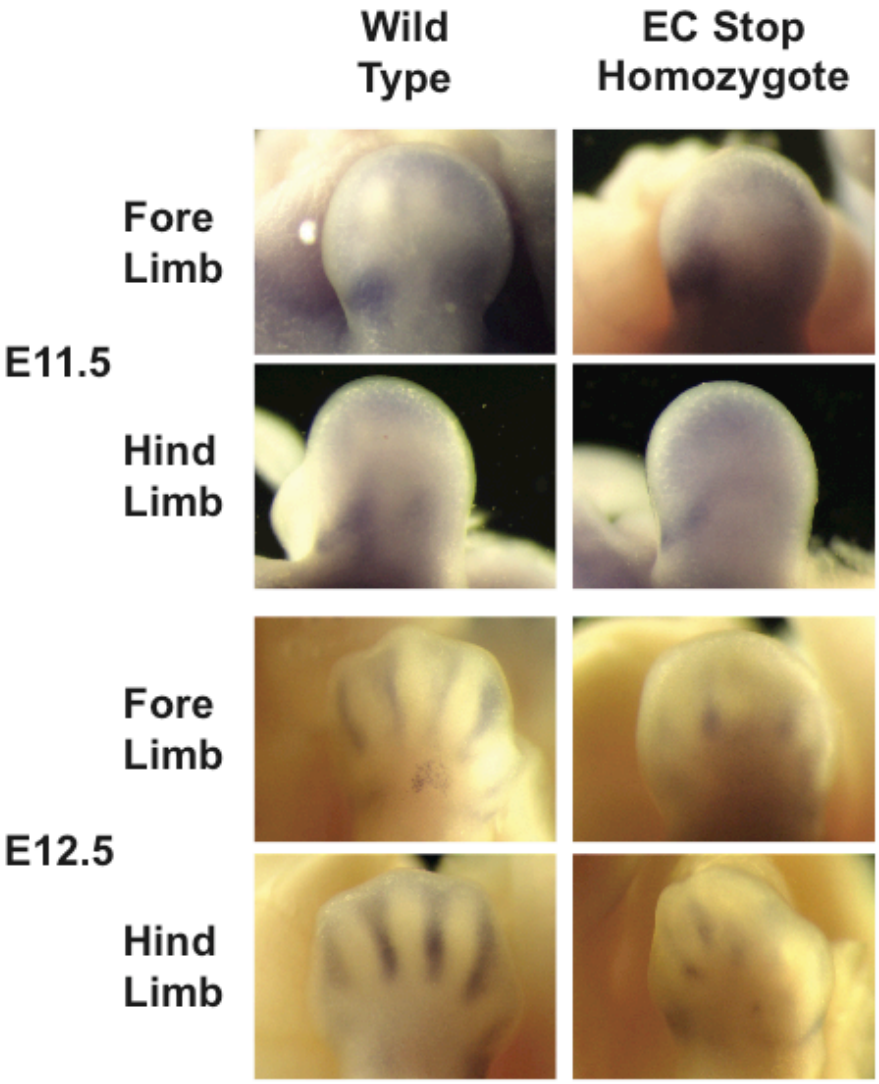

Figure 26 Expression of *Bmp2* in the *Megf7*$^{EC\ Stop}$ Mutants.

Bmp2 is expressed in the interdigital mesenchyme in wild type embryos. At E11.5 the pattern of *Bmp2* expression in the *Megf7*$^{EC\ Stop}$ limb buds is similar to wild type expression. At E12.5 the pattern of *Bmp2* expression is severely disrupted and weakened. This demonstrates that the patterning defects caused by a mutation in *Megf7* leads to a loss of patterning required for digit formation.

As mentioned above, BMPs have a role in regulating the pattern of apoptosis in the developing limb. Attempts at detecting interdigital apoptosis were unsuccessful. Although,

detecting apoptosis in the ectoderm was possible. Apoptosis normally occurs in the AER in the wild type limb. In the expanded AER of the *Megf7*$^{EC\ Stop}$ mutant, the pattern of apoptosis is spread over the area of the AER. It is unclear if the overall amount of apoptosis is affected in the mutant limbs. There is definitely a loss of the distinct pattern of apoptosis found in wild type limbs. It is unknown whether this is simply a consequence of the structural defect associated with the expanded AER or the change in BMP expression (Figure 27).

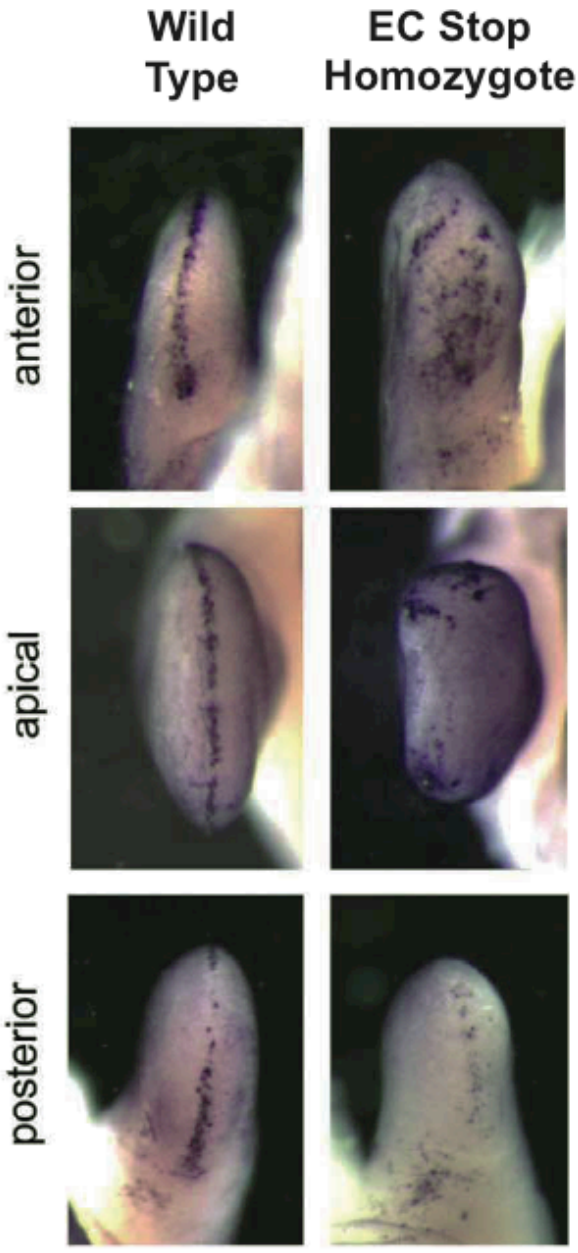

Figure 27 Apoptosis in the *Megf7*$^{EC\ Stop}$ Limb.

Cells within the developing limb were stained for TUNEL labeling, purple stain, to measure the pattern of apoptosis. Apoptotic cells are normally found within the AER. In mutant limbs, the pattern of apoptosis is disrupted along with the enlarged AER.

Unaffected Gene Expression in the Megf7$^{EC\ Stop}$ Mutant

Not all genes were severely affected in the *Megf7$^{EC\ Stop}$* homozygous embryos. *Hoxd12* is a member of the homeobox transcription factors, a group of genes that establishes the body pattern in almost all metazoans. *Hoxd12* is expressed in the handplate of the limb with a bias towards the posterior edge. The expression of *Hoxd12* is similar between wild type and mutant embryos. There are slight differences between wild type and mutant limbs, but they are probably a secondary result of the structural changes associated with the loss of patterning in the mutants (Figure 28).

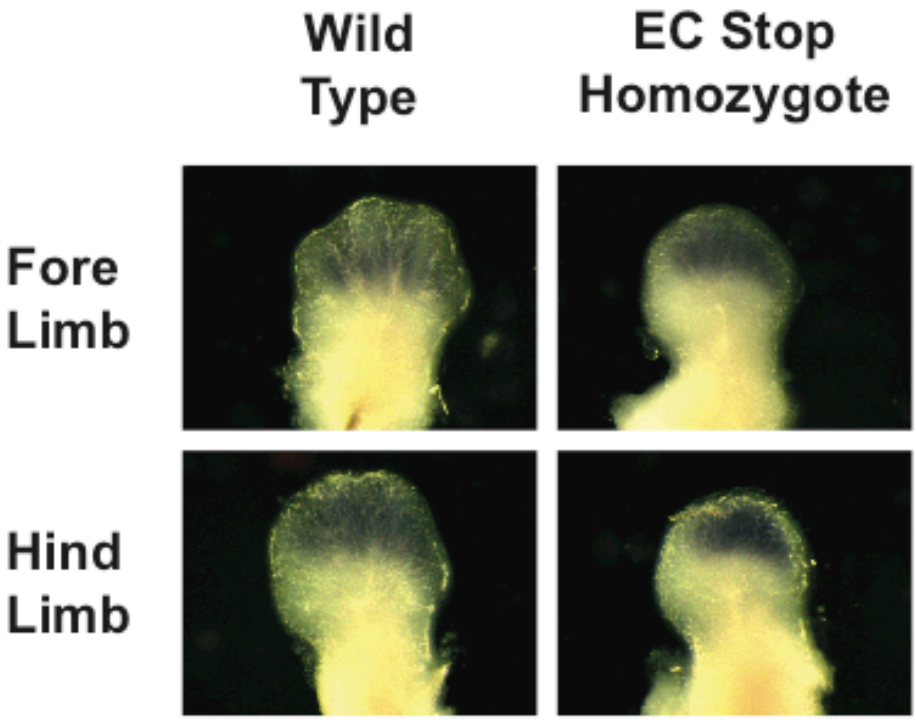

Figure 28 Expression of *Hoxd12* in the *Megf7$^{EC\ Stop}$* Limb.
In wild type limb buds, *Hoxd12* is expressed in the autopod with a bias towards the posterior side. This pattern is retained in the *Megf7$^{EC\ Stop}$* mutant. The differences in expression appear to be secondary to the structural changes caused by the mutation.

Gli1 is a gene that is regulated by the *Shh* pathway both at the transcriptional and post-translational level. At E12.5 the *Gli1* expression is localized to the distal end of the zeugopod and the phalanges and thus have a banded pattern in the limb. There is still a banded pattern of *Gli1* expression in the mutant limbs. The signal is weaker and is distorted based on the structural defects associated with the phenotype. The expression of *Gli1* does not appear to be involved in the etiology of the phenotype because like Hoxd12, the disruption of *Gli1* expression occurs after the initial patterning defect of the mutant (Figure 29).

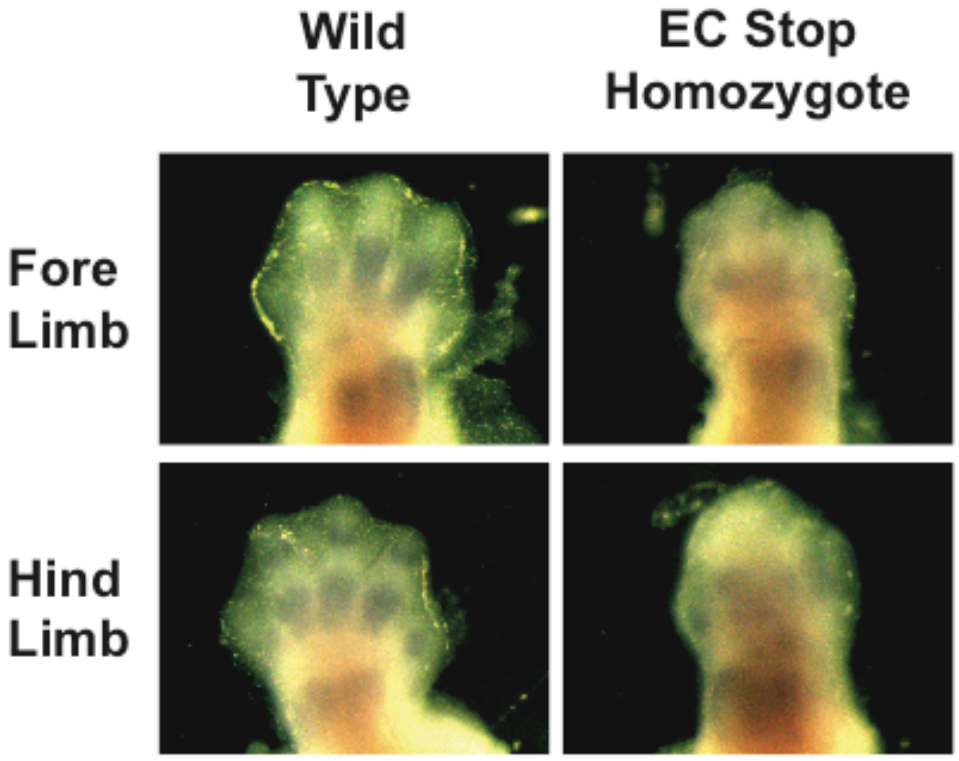

Figure 29 Expression of *Gli1* in the *Megf7*$^{EC\ Stop}$ Limb.

In wild type limb buds, *Gli1* is expressed in the autopod both in the wrist and the phalanges. This pattern is retained in the *Megf7*$^{EC\ Stop}$ mutant. The differences in expression appear to be secondary to the structural changes caused by the mutation.

Disruption of Wnt Signaling in *Megf7* Mutant Limbs

Comparison of the Megf7$^{EC\ Stop}$ *Phenotype and other Models of Wnt Modulation*

Megf7 is required to establish patterning in the developing limb by regulating the size of the AER. To gain insight into the molecular mechanism of *Megf7*, we referred to other experimental models that induce an ectopic AER. There are nine animal models that we

could find that demonstrate ectopic growth of the AER. Six of these models involve activation of the Wnt signaling pathway. The remaining three models involve the activation or inhibition of the BMP pathway. At the time of this investigation I focused mainly on a possible Wnt model based on the hypothesis that *Megf7* shares homologous regions with *Lrp5/6* and thus may contain Wnt binding regions.

All of the animal models involving the Wnt pathway could be considered as models of a loss of inhibition of the Wnt signaling pathway. The first animal model found was a hypomorph of the *Dkk1* gene, the *doubleridge* mouse. This mouse has a phenotype that is very similar to the *Megf7* mutant phenotype (Adamska et al., 2003; MacDonald, Adamska & Meisler, 2004). *Dkk1* is an inhibitor of the Wnt signaling pathway and thus the hypomorph has a hyperactivated Wnt signal in the limbs.

Overexpression of *Wnt3a*, *Wnt10a*, *Lef1* and *β-catenin* all induce ectopic AER development suggesting that the activation of the canonical Wnt signaling pathway regulates the size and position of the AER (Kengaku et al., 1998; Narita et al., 2005; Soshnikova et al., 2003). Also, treatment of the developing limbs with LiCl, a potent activator of the canonical signaling pathway, also increases the size of the AER (McQueeney et al., 2002).

Inhibition of the Canonical Wnt Signaling Pathway by Megf7

The similarity of the phenotypes observed with the activation of the canonical Wnt signaling pathway and the phenotype of the $Megf7^{EC\ Stop}$ mutant suggests that Wnt signaling may be involved in the activity of *Megf7*. This leads us to the hypothesis that MEGF7 is an inhibitor of the Wnt signaling pathway. As mentioned in the introduction, *Lrp1* has already

been shown to be an inhibitor of the Wnt signaling pathway in the *in vitro* TOPFlash assay (Zilberberg et al., 2004).

Just as in the Zilberberg report, the TOPFlash assay was used to test the hypothesis of *Megf7* as a Wnt inhibitor. As in the Zilberberg assay, h*Wnt1* was used to activate the canonical Wnt signaling pathway. m*Lrp6* was also transfected into the cells to increase the signaling through WNT1 and the Frizzleds on the cell surface. When Megf7 was expressed along with Wnt1 and Lrp6, there was a significant decrease in the Luciferase signal compared to Wnt1 and Lrp6 alone. The co-expression of Lrp1 further decreased the signal in this assay. Megf7 also inhibited this reporter assay in a dose-dependent manner (Figure 30). Complete inhibition of the Luciferase signal was not possible because there was a limit on the amount of plasmid that can be tranfected before the TOPFlash signal was non-specifically reduced.

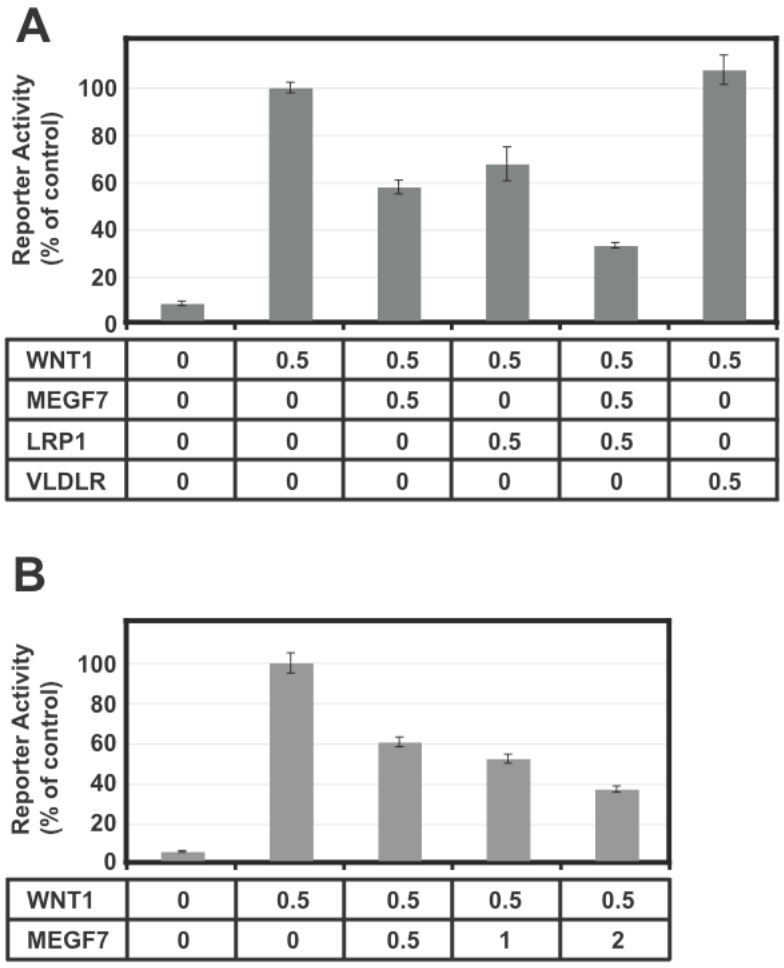

Figure 30 Megf7 Inhibits the Wnt Signaling Pathway in the TOPflash Assay.

The TOPflash assay is a reporter systems that measures the β-catenin dependent expression of a luciferase gene. Upon activation of the canonical Wnt pathway by Wnt1, β-catenin is stabilized and induces the expression of Wnt responsive genes. In this assay, HEK293 cells are transfected with plasmids to induce the expression of Wnt1 and Lrp6 to activate the Wnt signaling pathway. (A) Expression of Megf7 or Lrp1 inhibits the TOPflash signal. Vldlr, the negative control, does not inhibit the TOPflash signal. (B) Megf7 inhibits the TOPflash signal in a dose-dependent manner.

BAT-gal Transgene Expression in the Megf7 Mutant

The activity of the Wnt signaling pathway was further examined to see if there was a loss of inhibition in the *Megf7* mutant limbs. We first used the BAT-gal transgene to examine the *in vivo* Wnt activity in these mutant mice. The BAT-gal transgene has a β-galactosidase gene under the control of TCF/LEF binding sites and a *siamois* minimal promoter (Maretto et al., 2003). The activity of the BAT-gal transgene is responsive to the activity of the canonical Wnt signaling pathway as indicated by previously published data (Maretto et al., 2003).

The activity of the BAT-gal transgene was examined in the *Megf7* knockout limbs (the knockout will be described later). Staining for β-galactosidase shows an activation of the Wnt signal in cells within the AER in wild type limbs. In the knockout, the staining is seen within the expanded AER. It is difficult to say if there is an increase in the amount of staining in the limbs because the dimensions of the wild type and knockout limbs are not comparable. (Figure 31)

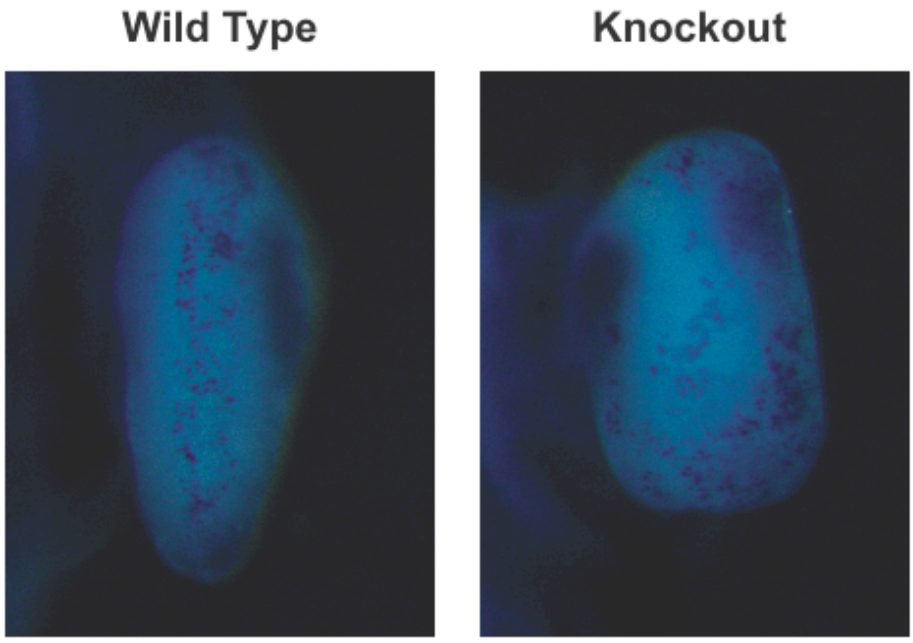

Figure 31 BAT-gal Expression in the *Megf7* Mutant Limb.

E11.5 embryos carrying the BAT-gal transgene were stained for β-galactosidase. In wild type limbs the staining is restricted mainly to the region around the AER. The staining in the knockout is spread over the expanded AER.

Stabilization of β-Catenin in the Ectoderm of Megf7 Mutant Limb Buds

The analysis of the Wnt signaling pathway in the *Megf7*$^{EC\ Stop}$ mutant is complicated by the fact that the region of the limb that responds to canonical Wnt signals, the AER, is expanded. It is difficult to differentiate between an increase in Wnt signaling and the expansion of the zone of Wnt responsive cells. The former possibility suggests a direct biochemical pathway whereas the later possibility can be the result of the modulation of multiple possible signaling pathways. The BAT-gal transgenic mouse did not help to differentiate between those two possibilities. The analysis of the activity of the Wnt signaling pathway using a more direct method would be needed to examine the two possibilities. The

stabilization of the intracellular β-catenin is the downstream consequence of the activation of the canonical Wnt signaling pathway. Therefore, we hypothesized that the loss of *Megf7* activity in the limbs would lead to the increased stabilization of β-catenin.

The limbs from both wild type and knockout embryos were sectioned and stained for activated β-catenin by Christian Tennert in our lab. The mesoderm of both the wild type and knockout limbs stained with equal intensity. This is not surprising considering *Megf7* is only expressed in the ectoderm of the developing limb and would not affect the mesoderm. The β-catenin levels in the mesoderm can thus serve as an internal control for equal staining of each slice. The ectoderm, on the other hand, has stronger staining for β-catenin in the mutant limbs when compared to wild type limbs (Figure 32). The stabilization of β-catenin in the ectoderm of mutant mice suggests that the Wnt signaling pathway is hyperactivated in the ectoderm of the mutant embryos.

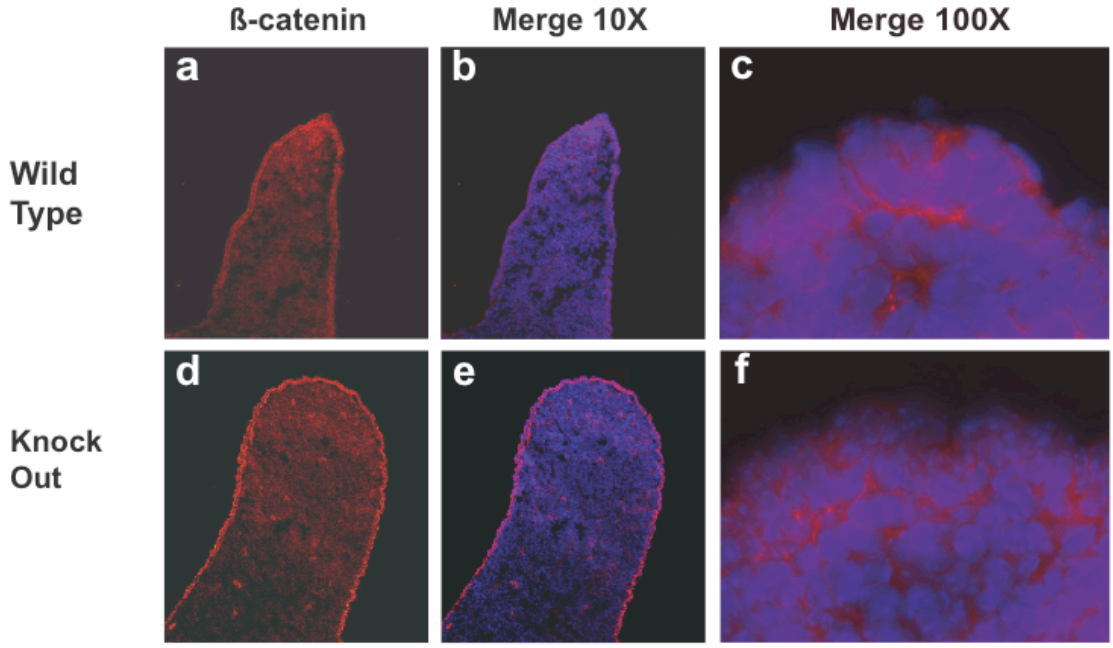

Figure 32 Stabilization of β-catenin in the Ectoderm of the *Megf7*^{KO} limb.

Sagital sections of E10.5 wild type and *Megf7*^{KO} embryo limb buds were stained for β-catenin (red) and DAPI (blue). Notice that the β-catenin signal in the ectoderm at 10X magnification is more intense compared to the wild type sample. The knockout limbs are characteristically broader due to the expanded AER. At 100X magnification, the β-catenin can be seen in the nucleus of the ectodermal cells.

DKK Proteins Do Not Bind to Megf7

There are many possible mechanisms that *Megf7* could use to inhibit the Wnt signaling pathway. One possible mechanism of action of Megf7 would be to interact with an already established inhibitor of the Wnt signaling pathway, such as Dkk1, and facilitate its action. To test this hypothesis, the binding of Megf7 to Dkk1 and Dkk3 was tested in an ELISA assay. In this assay, the ectodomain of Megf7 fused to the human IgG Fc was used to coat ELISA plates. Alkaline Phosphatase conjugated proteins were then allowed to bind to

the Megf7 fusion protein bound to the ELISA plate. The plates were washed and a colorimetric reagent was added to detect the bound Alkaline Phosphatase (AP) conjugate.

A positive control protein, Anti-IgG-AP, was used to detect the amount of Megf7-Fc that was bound to the wells. The detection of AP activity on the coated plates suggested that Megf7-Fc efficiently bound to the plates. The mock condition, with no Megf7-Fc bound to the plates, shows that the signal detected with the anti-IgG-AP was specific. These controls show that Megf7-Fc are bound to the ELISA plate and the binding of an AP-conjugated protein can be detected in this assay using an AP fusion binding partner. Incubation of Dkk1-AP or Dkk3-AP or AP alone does not show any specific binding to Megf7. Therefore, it is unlikely that Megf7 binds to either Dkk1 or Dkk3 and in turn inhibits the WNT signaling pathway (Figure 33).

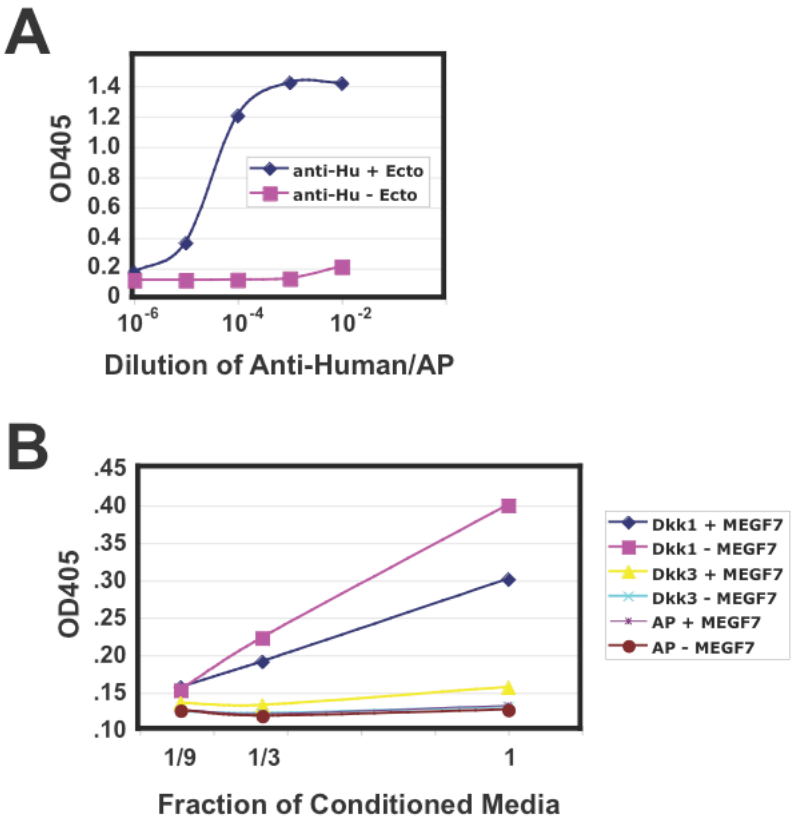

Figure 33 Megf7 does not Bind to Dkk1 or Dkk3.

An ELISA-based assay was used to determine if Megf7 can bind to members of the Dkk gene family. The extracellular domain of Megf7, fused to human Fc, was either bound to an ELISA plate directly or indirectly through pre-bound anti-human IgG antibodies. Binding was measured with the detection of alkaline phosphatase fusion proteins. (A) Megf7 was efficiently detected in this assay. Megf7 was bound to the ELISA plates and detected with an anti-human IgG antibody-AP fusion protein. The antibody specifically detected the Megf7 protein bound to the plates. (B) Both Dkk1 and Dkk3 do not bind to Megf7. Conditioned media containing either Dkk1-AP, Dkk3-AP, or AP alone was incubated in Megf7-coated ELISA plates. None of the proteins specifically bound to the ELISA plates as indicated by AP activity.

CHAPTER FOUR
Results

FUNCTIONAL MOTIFS WITHIN THE CYTOPLASMIC DOMAIN OF MEGF7

Megf7 Knockin Alleles

The cytoplasmic domains of the members of the LDLR gene family all contain motifs that are required for their function. The LDLR gene family members interact with multiple intracellular proteins through functional motifs, most notably through their NPXY motif. Other non-NPXY motifs within the cytoplasmic domain have proven to be important for function such as exon 19 of ApoER2, the PPPXP motifs in Lrp5/6, the YXXL motif in Lrp1, etc. Along these lines, an allelic series in mice was generated with specific mutations within the cytoplasmic domain of *Megf7*. This strategy, which has proven to be quite useful for the analysis of the *ApoER2* gene, was used to determine which regions within the cytoplasmic domain of Megf7 are important for function.

The construction of the knockin alleles is similar to that of the $Megf7^{EC\ Stop}$ allele described in Chapter 2 except that there is not a premature stop codon upstream of the transmembrane domain. In these alleles, a cDNA insert is cloned in frame with exon 36 of *Megf7* using a silently mutated Bst1107I restriction site within the long arm of homology of the knockin construct. The 3' end of the insert was cloned into the bovine growth hormone 3'UTR using a BsrGI restriction site. The resulting allele, after recombination in embryonic stem cells, is expected to constitutively express the specifically engineered mutation in the cytoplasmic domain. Six mutants were generated using this strategy. A wild type cytoplasmic

domain mutant (*Megf7*$^{WT\ KI}$) was generated to serve as a control for any unforeseen complications of the disruption of the *Megf7* locus using the *Megf7* knockin construct. A NPSY→AAAA mutant (*Megf7*$^{NPSY\ KI}$) was generated to eliminate any protein interactions with the one NPXY motif of *Megf7*.

As described with the yeast two-hybrid data, Megf7 can bind to PDZ domain-containing proteins through a consensus PDZ binding motif (Johnson et al., 2006; Tian et al., 2006). A mutant allele was generated that removes the five carboxy-terminal amino acids of Megf7. This mutant allele (*Megf7*$^{PDZ\ KI}$) eliminates any interactions with proteins that can bind to Megf7 through their PDZ domains.

Two alleles were generated that replace the entire cytoplasmic domain. The first allele was engineered to replaces the entire cytoplasmic domain of *Megf7* with the human LDL Receptor cytoplasmic domain (*Megf7*$^{LDLR\ KI}$). This mutant is expected to retain endocytic activity but will remove all other functional motifs within the cytoplasmic domain of Megf7. The other allele eliminates the entire cytoplasmic domain of *Megf7* and replaces it with a Myc epitope. This allele (*Megf7*$^{Myc\ KI}$) will remove every activity of the Megf7 cytoplasmic domain but still remain attached to the plasma membrane.

The last allele (*Megf7*$^{AS\ KI}$) contains an alternatively spliced form of the cytoplasmic domain of *Megf7*. Before the generation of these knockin alleles, an RT-PCR screen was performed on a collection of adult tissue RNA samples to identify tissues that express *Megf7* (Figure 34). The RT-PCR reaction results suggest that *Megf7* is expressed in almost every adult tissue. Interestingly, there was a higher molecular weight PCR product that was amplified in the thyroid, heart, stomach and muscle. This PCR product had an extra exon

spliced between exon 37 and 38. The insertion event leads to a frame shift in relation to exon 38 and adds 13 or 14 missense amino acids followed by a premature stop codon. The function of this alternatively spliced form is unknown. It might be part of a mechanism of tissue specific down-regulation similar to the mechanism seen with chloride channels during development (Lueck et al., 2006). Independent of the function of this alternatively spliced form, the expected protein product eliminates the carboxy-terminal two-thirds of the cytoplasmic domain and yet retains the NPXY motif and the putative YXXL motif.

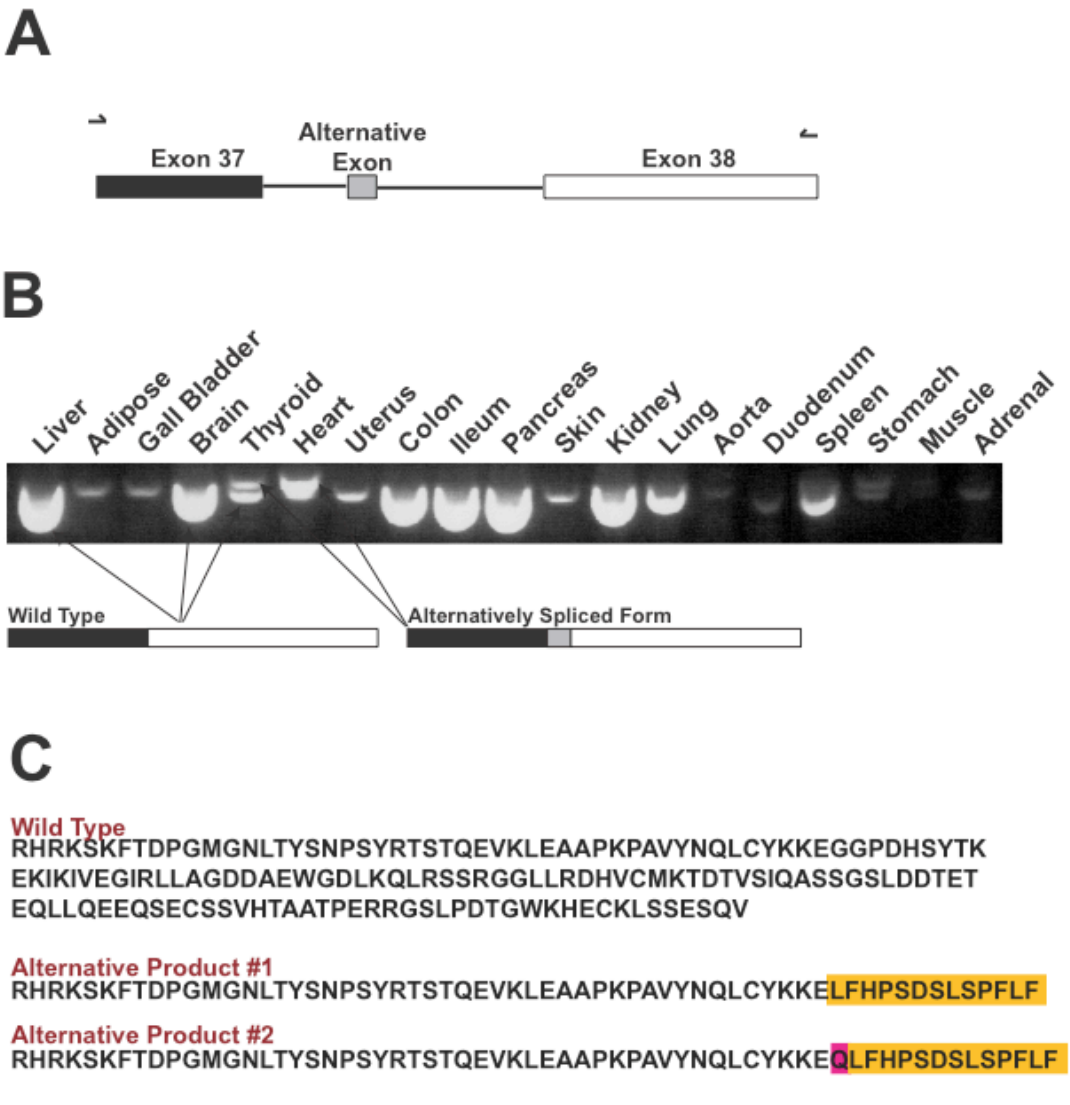

Figure 34 RT-PCR Analysis of *Megf7* Expression in Adult Tissues.

(A) Diagram of the PCR product. Primers complimentary to the 5' end of exon 37 and the 3' end of exon 38 were used to amplify a region of *Megf7* mRNA. (B) The *Megf7* mRNA from different wild type mouse tissues was reverse transcribed and amplified using primers corresponding to the beginning and end of the coding sequence of the cytoplasmic domain. RNA from the liver, brain, colon, ileum, pancreas, kidney, lung, and spleen produced significant amounts of PCR product. The thyroid, heart, and stomach RNA produced an alternatively spliced RT-PCR product. (C) Representations of the expected protein products of the alternative splice forms. Non-sense amino acids are highlighted.

Barring an unpredicted corrective mechanism, the knockin alleles should exclusively express the predicted mutant transcript. First, exon 36, the exon in which the mutant cDNA sequence is cloned, encodes the transmembrane domain. Any splicing mechanism that splices around the mutant exon 36/cDNA sequence, would exclude the sequence required for the transmembrane domain and thus would not be incorporated into the plasma membrane. Second, an RT-PCR reaction was performed using the knockin RNA with the same technique used for figure 6. The results for the knockin alleles were identical to the results for the *Megf7*$^{EC\ Stop}$ allele in which the majority of the mutant transcript contained the expected sequence (data not shown). Any alternatively spliced transcripts that contained the wild type exon 37 and 38 also contained intronic sequence that would produce a protein product that does not contain a transmembrane domain and thus would not be anchored to the plasma membrane.

The embryonic stem cells were confirmed for correct recombination using the same probe described for the *Megf7*$^{EC\ Stop}$ mutant. All correctly recombined alleles were used to generate the different knockin mouse lines. Genotyping was performed using a primer in the upstream region of *Megf7* and a downstream primer that was specific to the cDNA insert for each particular allele.

The Limb Phenotype of the Knockin Alleles Suggests that there are Multiple Motifs Present within the Cytoplasmic Domain that are Required for Endocytosis

Both homozygous and compound heterozygous (knockin allele paired with the knockout allele) mice were generated to analyze the function of different regions of the cytoplasmic domain of Megf7. The compound heterozygous mice should have a stronger phenotype compared to homozygous mice due to a reduction of gene dosage. A wild type phenotype was observed for the *Megf7*$^{WT\ KI}$, *Megf7*$^{AS\ KI}$, *Megf7*$^{PDZ\ KI}$, and *Megf7*$^{NPSY\ KI}$ mice both in the homozygous and compound heterozygous state. As expected, the *Megf7*$^{EC\ Stop}$ allele compound heterozygous mouse also had polysyndactyly and yet the single *Megf7*$^{EC\ Stop}$ allele was able to rescue the perinatal lethality found in the null mice. The *Megf7*$^{LDLR\ KI}$ mouse had a wild type phenotype in the homozygous state while the compound heterozygous mouse had a very mild polysyndactyly phenotype. The example given in figure 36 for the *Megf7*$^{LDLR\ KI}$ allele is an extreme case of polydactyly in the compound heterozygous state. Most of the *Megf7*$^{LDLR\ KI}$ mice did not have a detectable limb defect. The mice that had a defect had mild soft tissue syndactyly in the hind limbs. The fore limbs of the *Megf7*$^{LDLR\ KI}$ mice were never affected. This difference between fore limbs and hind limbs suggests that the development of the hind limbs is slightly more sensitive to a loss of *Megf7* activity than the fore limbs (Figures 35-37).

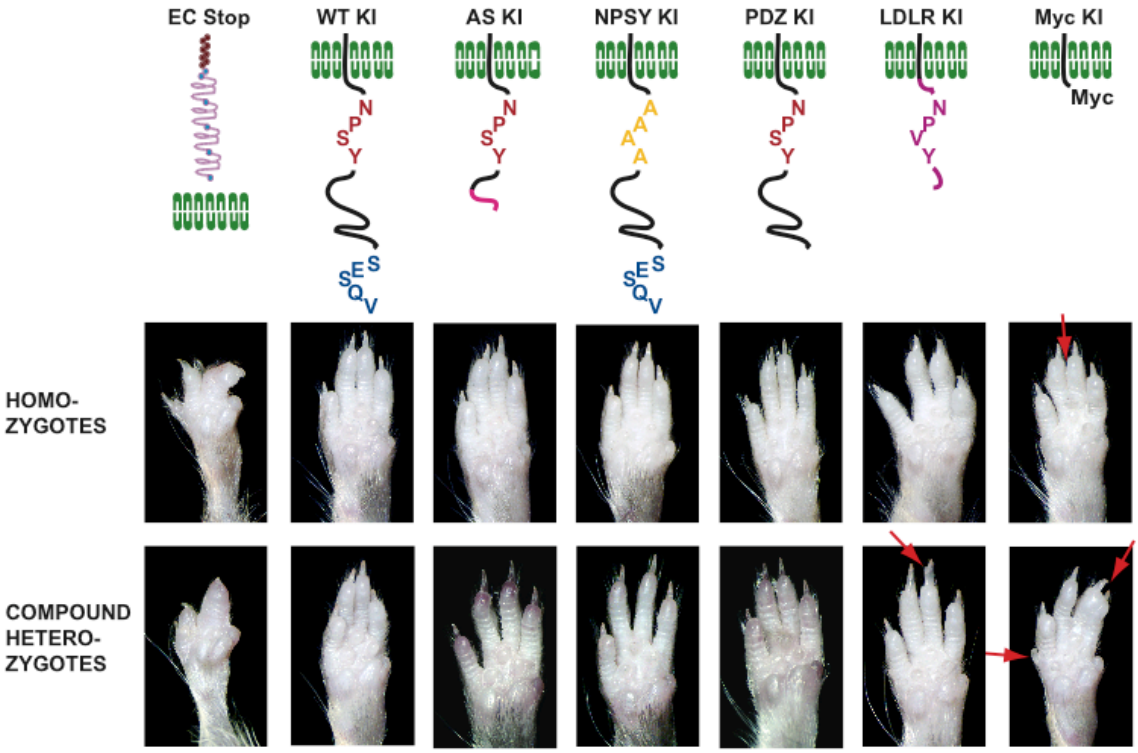

Figure 35 Whole Fore Limbs of the Allelic Series.

Representative pictures of the fore limbs of adult mice that are either homozygous or compound heterozygous (knockin allele paired with the *Megf7*^{KO} allele). (Top) Diagrams representing the predicted protein product from each allele. (Bottom) The ventral aspect of the fore limbs show defects in patterning in the *Megf7*$^{EC\ Stop}$ mutants, *Megf7*$^{LDLR\ KI}$ compound heterozygote, and the *Megf7*$^{Myc\ KI}$ mutants. Arrows indicate defects in patterning.

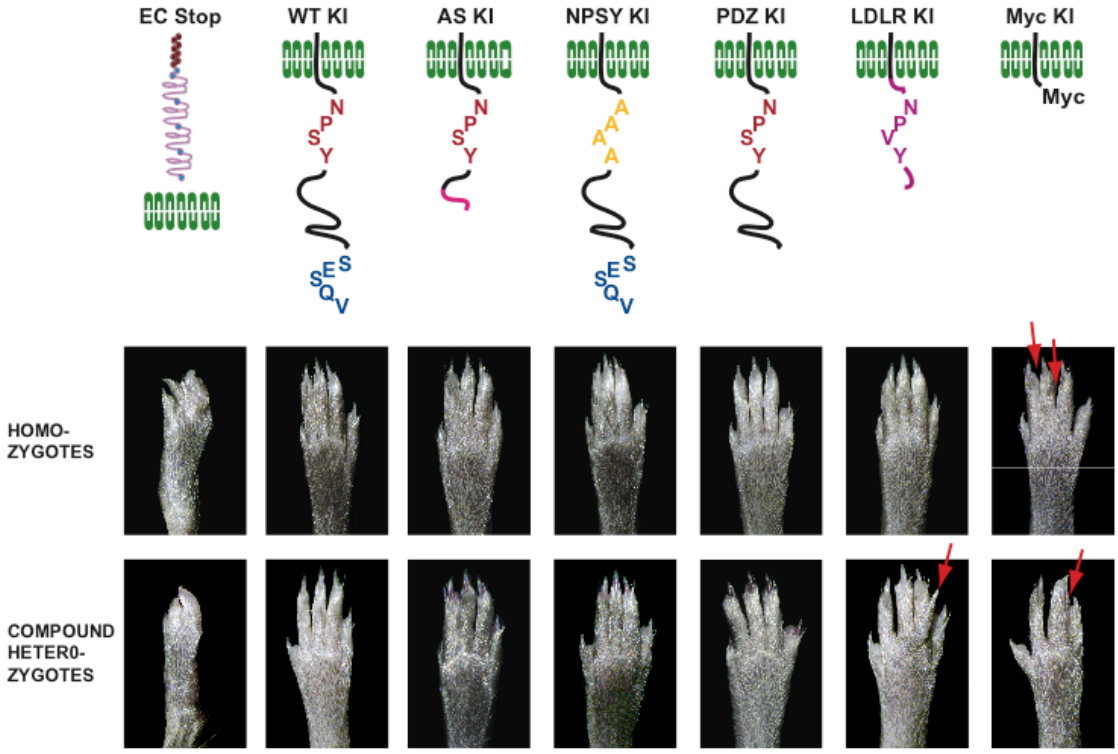

Figure 36 Whole Hind Limbs of the Allelic Series.

Representative pictures of the hind limbs of adult mice that are either homozygous or compound heterozygous (knockin allele paired with the *Megf7*^{KO} allele). (Top) Diagrams representing the predicted protein product from each allele. (Bottom) The dorsal aspect of the hind limbs show defects in patterning in the *Megf7*$^{EC\ Stop}$ mutants, *Megf7*$^{LDLR\ KI}$ compound heterozygote, and the *Megf7*$^{Myc\ KI}$ mutants. Arrows indicate defects in patterning.

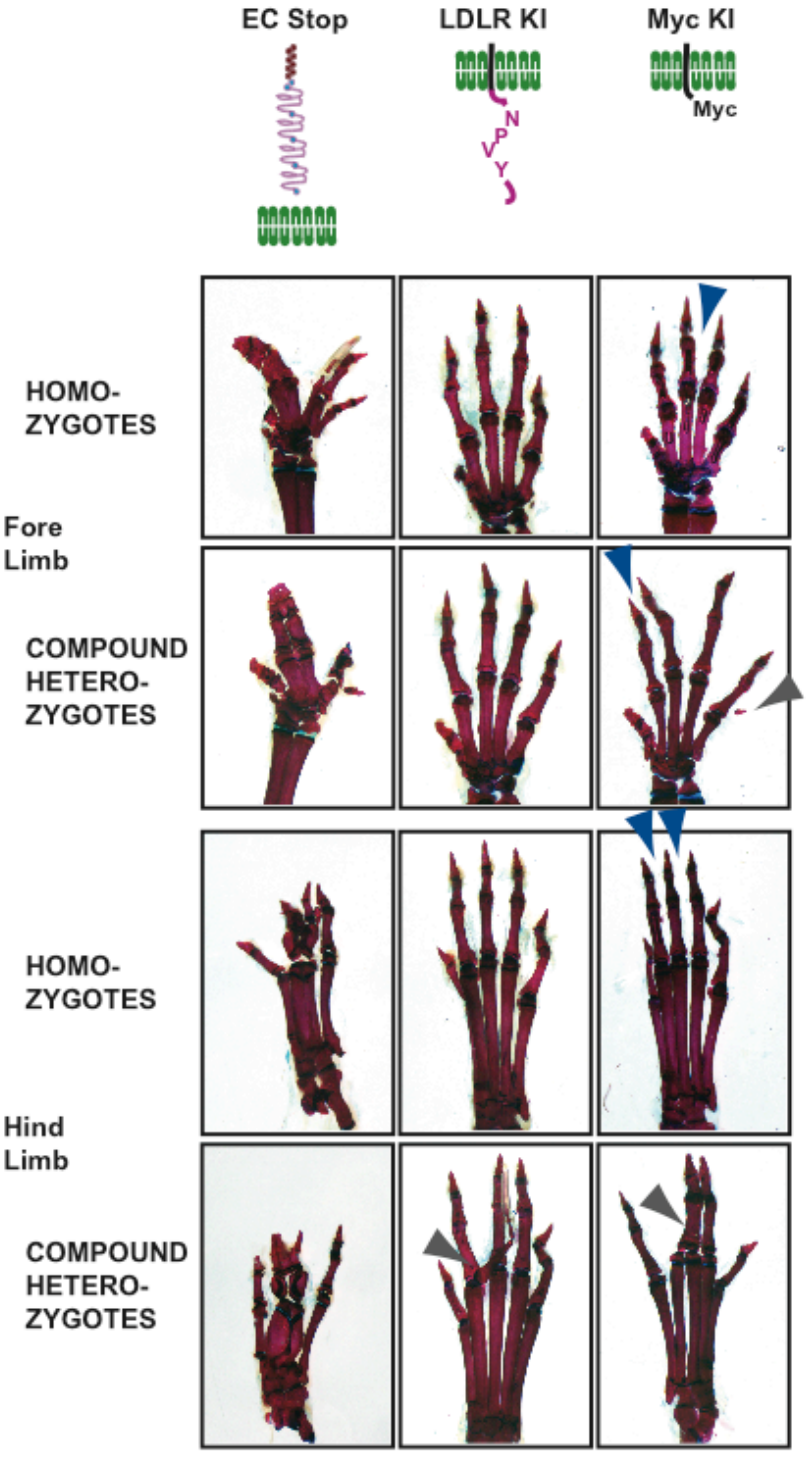
EC Stop
LDLR KI
Myc KI
N
P
V
Y
Myc
HOMO-
ZYGOTES
Fore
Limb
COMPOUND
HETERO-
ZYGOTES
HOMO-
ZYGOTES
Hind
Limb
COMPOUND
HETERO-
ZYGOTES

Figure 37 Alizarin Red/Alcian Blue Staining of the Allelic Series Mutants.
(previous page) The limbs of the different allelic series mutants were stained with alizarin red and alcian blue to examine bone and cartilage structure respectively. Grey arrowheads indicate ectopic bone or bony fusion. Blue arrowheads indicate regions of soft-tissue fusion.

As expected, the *Megf7*$^{Myc\ KI}$ allele had the most extreme phenotype compared to all of the other knockin alleles. The homozygous *Megf7*$^{Myc\ KI}$ mice have infrequent soft tissue syndactyly of the forelimbs and a more frequent incidence of soft tissue syndactyly in the hind limbs. The homozygous *Megf7*$^{Myc\ KI}$ phenotype suggests that this allele removes an activity that is required for full *Megf7* function that is partially replaced in the *Megf7*$^{LDLR\ KI}$ allele. The compound heterozygous *Megf7*$^{Myc\ KI}$ mice had a more extreme phenotype with polysyndactyly in both the fore limbs and hind limbs. Again, the phenotype of the *Megf7*$^{Myc\ KI}$ allele is not as extreme as the *Megf7*$^{EC\ Stop}$ allele suggesting that retaining the protein in the plasma membrane is sufficient to rescue some activity (Figure 35-37).

The ability of the *Megf7*$^{LDLR\ KI}$ allele, the allele that replaces the *Megf7* cytoplasmic region with a peptide sequence that is only known to have endocytic activity, to rescue almost all of the activity of *Megf7* suggests that the function of *Megf7* involves endocytosis, at least in the limbs and teeth. Currently, the only observed function of the cytoplasmic domain of the LDL receptor is to induce endocytosis. Simply providing endocytic activity, through the LDLR cytoplasmic domain, to *Megf7* is sufficient to rescue most of the activity suggesting that the function of the cytoplasmic domain is to regulate endocytosis. The slight hypomorphic phenotype of the *Megf7*$^{LDLR\ KI}$ allele may be due to an accessory activity of the *Megf7* cytoplasmic domain that is not provided by the LDLR cytoplasmic domain.

Yeast Two-Hybrid

A Yeast Two-Hybrid screen was used to identify candidate proteins that bind to the cytoplasmic domain of Megf7. This strategy has been used successfully for other members of the LDLR gene family. The identified binding proteins may give an indication of the biochemical mechanism of action of Megf7, as was seen with ApoER2 and Dab1.

The complete cytoplasmic domain of *Megf7* was cloned into the pLexA vector as described in the Materials and Methods. This construct was then screened using a prey plasmid library constructed from mouse brain cDNA. 92 prey plasmids that indicated a positive interaction were isolated from yeast clones. 40 of these clones produced in-frame cDNA inserts. Nine unique sequences were obtained from the screen that reproduced the positive interaction when retransformed into yeast.

The yeast two-hybrid positive clones were then tested with truncation and alanine substitution mutants of the tail of Megf7. The truncation mutants were generated by serially deleting approximately 15 amino acids from the C-terminus of the tail of Megf7. There were also two mutants that removed the C-terminal valine or the complete PDZ-binding consensus motif.

PDZ Domain-Containing Proteins that Interact with Megf7

The positive clones can be put into three categories based on where they bind within the cytoplasmic domain of Megf7. The largest category of positively interacting proteins is the PDZ-containing hits. These proteins, ARIP2, LIN-7, PSD-95, SERBIN, and Synectin, all

contain a PDZ domain that can bind to the consensus motif mentioned above. Three of these genes, PSD-95, Synectin, and ARIP-2, have already been demonstrated to interact with other members of the LDL Receptor gene family. ARIP-2 appears to be an alternatively spliced version of the OMP-25 gene found previously in this lab (Gotthardt et al., 2000). LIN-7 and SERBIN are novel LDL Receptor gene family member interacting proteins. These PDZ-containing proteins are all potentially involved in targeting receptors to specific subcellular compartments (Borg et al., 2000; Johnson et al., 2006; Matsuzaki et al., 2002; Naccache, Hasson & Horowitz, 2006; Simske et al., 1996; Tian et al., 2006). (Figure 38)

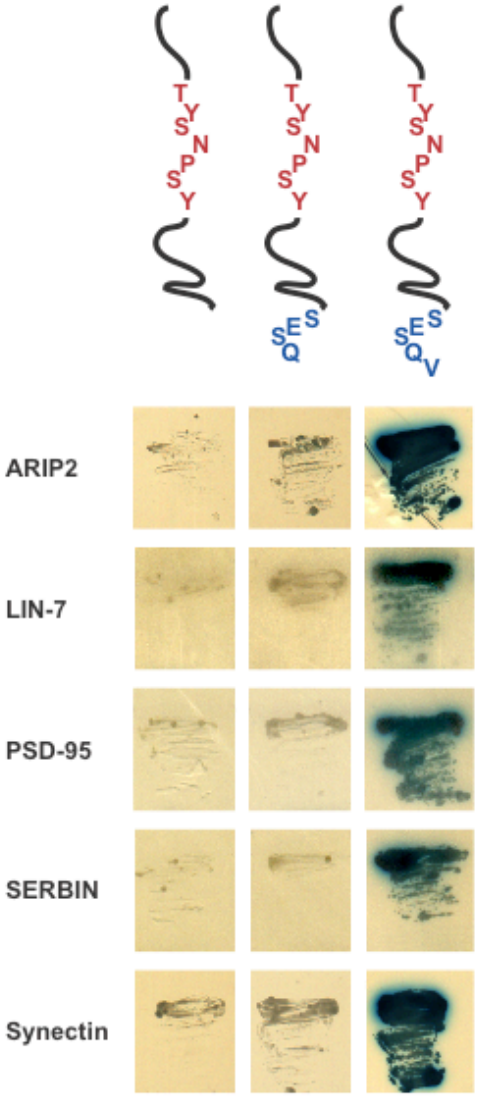

Figure 38 PDZ Domain Proteins that Bind to Megf7.

Five proteins that contain PDZ domains were found to interact with Megf7 in the yeast two-hybrid assay. (Top) Diagram of the Megf7 cytoplasmic tails fused to LexA. These proteins were tested against Megf7 LexA constructs with a cDNA insert with the last five amino acids removed, a cDNA insert with a terminal valine truncation, or a full-length cDNA insert. (Bottom) Yeast transfected with the LexA-Megf7 construct were mated with yeast transfected with the PDZ-containing cDNA. The yeast were then grown on selective agar plates. Growth and blue pigment production indicate a positive interaction.

PTB Domain-Containing Proteins Interact with MEGF7

PTB domains have been found to interact with the NPXY motif containing proteins such as the LDLR gene family members (Bonifacino & Traub, 2003). CAPON is the only PTB-containing protein found in the yeast-two-hybrid screen using Megf7 as the bait (Figure 39A). This gene was also previously found to interact with the large members of the gene family, Lrp1 and Megalin (Gotthardt et al., 2000). CAPON regulates nNOS activity at synaptic terminals by competing with PSD-95. The carboxy-terminal portion of CAPON interferes with the unique PDZ-PDZ interaction between nNOS and PSD-95 (Jaffrey et al., 1998). The interaction between members of the LDL receptor gene family and CAPON suggests a regulatory role controlling the levels of nitric oxide in neurons.

Interestingly, Dab1 failed to interact with the cytoplasmic domain of Megf7 (Figure 39B). Dab1 can bind to most of the NPXY motifs found in the intracellular tails of the members of the LDL receptor gene family (Gotthardt et al., 2000). The unique sequence preceding the NPXY motif may determine the specificity seen with Dab1 for Megf7, Lrp1, and Megalin.

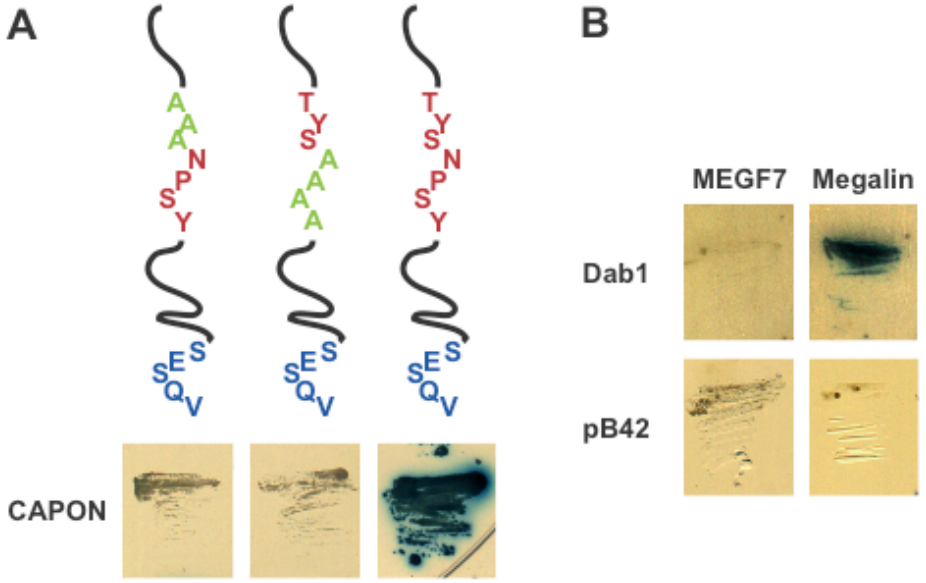

Figure 39 PTB Domain Proteins that Bind to Megf7.

One protein that contains a PTB domain, CAPON, was found to interact with Megf7 in the yeast two-hybrid assay. (A, Top) Diagram of the Megf7 cytoplasmic tails fused to LexA. CAPON was tested against LexA-Megf7 constructs with a cDNA insert with the three amino acids upstream of the NPXY motif substituted to alanines, a cDNA insert with the NPXY motif substituted to alanines, or a full-length cDNA insert. (A, Bottom) Yeast transfected with the LexA-Megf7 construct were mated with yeast transfected with the CAPON expression construct. The yeast were then grown on selective agar plates. Growth and blue pigment production indicate a positive interaction. (B) Megf7 does not interact with Dab1. Yeast cells expressing the Megf7 construct fail to show a positive interaction with Dab1 while another member of the LDLR gene family, Megalin, is able to show an interaction.

Nuclear Proteins that Interact with Megf7

Three cDNA sequences were retrieved from the yeast two-hybrid screen that did not make much sense because all three were proteins that typically reside within the nucleus. Thus, it is questionable whether nuclear proteins would interact with the cytoplasmic domain of a transmembrane protein thought to be found at the plasma membrane.

The first nuclear protein found in the screen is called *Polycomb 2 homolog* (mPC2), also called *Chromobox protein homolog 4* or *E3 SUMO-protein ligase CBX4* (gi: O55187). This protein has a putative chromatin organization modifier domain. mPC2 is found in the nucleus bound to the multiprotein polycomb complex and can inhibit the expression of genes in Gal4 expression studies. The gene is located on chromosome 11 near the loci for tail short (Ts) and rabo torcido (Rbt) mouse mutations. mPC2 is also the E3 ligase responsible for the sumoylation of CtBP (Alkema et al., 1997; Kagey, Melhuish & Wotton, 2003).

A second potential Megf7 interacting protein is listed as *SMAD-interacting zinc finger protein 2* (gi: AAH17627.1) in the genbank database. There are no published reports of the function of this protein. This protein is also called zinc finger, CCHC domain containing protein 18 (Zcchc18).

The third gene that interacts with Megf7 is called *Exosome component 9* or *Polymyositis/scleroderma autoantigen 1* (gi: BAB27749.1). The sera of patients with polymyositis/scleroderma is autoreactive to this protein (Bliskovski et al., 2000). This protein contains two RNase PH domains that are a part of a CAG2123 domain. This protein appears to be involved in the processing of rRNA.

All three nuclear proteins appear to interact with the amino-terminal portion of the cytoplasmic domain as indicated by the truncation LexA mutants (Figure 40A). Testing interactions with other members of the gene family shows that Lrp1 can interact with mPC2 and PSA1 (Figure 40B).

As mentioned before, it is unlikely that an integral membrane protein on the plasma membrane could interact with a nuclear protein. It is possible though, that Megf7 may release

the cytoplasmic domain through intramembrane cleavage just like many transmembrane receptors such as Notch and SREBP. Actually, other members of the gene family, ApoER2 and Lrp1, also undergo intramembrane cleavage (May et al., 2003). Megf7 can release its cytoplasmic domain from the plasma membrane as indicated by a reporter gene assay (data not shown). Whether Megf7 actually releases the cytoplasmic domain and interacts with the mentioned nuclear proteins *in vivo* is unknown.

An alternative explanation is that Megf7 retains these proteins at the plasma membrane and prevents their nuclear import. This model would suggest that the affinity of Megf7 for these nuclear proteins changes in response to a cellular signal.

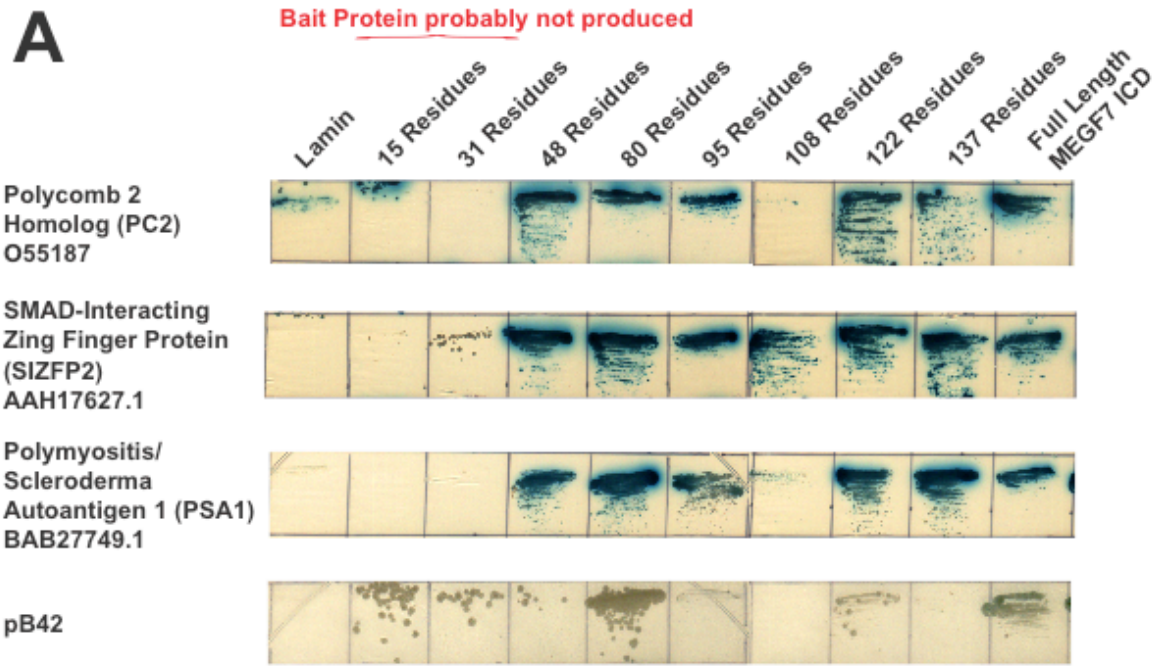
A
Bait Protein probably not produced
Lamin
15 Residues
31 Residues
48 Residues
80 Residues
95 Residues
108 Residues
122 Residues
137 Residues
Full Length MEGF7 ICD
Polycomb 2 Homolog (PC2) O55187
SMAD-Interacting Zing Finger Protein (SIZFP2) AAH17627.1
Polymyositis/ Scleroderma Autoantigen 1 (PSA1) BAB27749.1
pB42

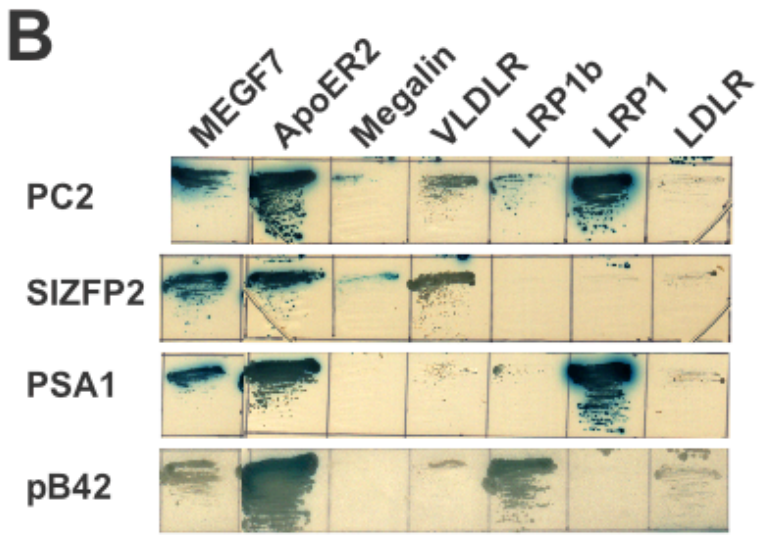
B
MEGF7
ApoER2
Megalin
VLDLR
LRP1b
LRP1
LDLR
PC2
SIZFP2
PSA1
pB42

Figure 40 Nuclear Proteins that Bind to Megf7

(previous page) Three proteins were found to interact with Megf7 that do not contain either PDZ or PTB domains. These proteins are largely found in the nucleus. (A) These proteins were tested against serial C-terminal truncations of the cytoplasmic domain of Megf7 using the yeast mating assay. pB42 and Lamin are fusion constructs used as a negative controls. All three proteins interact with a region of Megf7 that is within the upstream 48 amino acid residues of the cytoplasmic domain. (B) The interacting proteins were tested against the other members of the LDLR gene family. Lrp1 interacts with mPC2 and PSA1.

CHAPTER FIVE
Results

MULEFOOT DISEASE AND MEGF7

Introduction to Mulefoot Disease

The observation that a mutation in the *Megf7* gene leads to polysyndactyly in the mouse leads to the hypothesis that mutations in *Megf7* may also cause limb deformities in other species. Polydactyly and syndactyly occurs at a relatively high rate in the human population. The causes of these deformities are mostly attributed to a handful of known genetic disorders (Goodman, 2002; Wilkie et al., 2002). Therefore, mutations in *Megf7* may be overshadowed by more common causes of limb dysgenesis. However, there are cases of limb deformities in other species in which the etiology is unknown. MuleFoot Disease (MFD), a form of bovine syndactyly, was the best candidate for a syndrome of unknown etiology that could be caused by mutations in *Megf7*.

MFD is a deformity that affects a wide variety of commercially valuable bovine breeds (Drogemuller & Distl, 2006). This defect is characterized by the fusion of the hoof, which is normally separated into two digits. This defect is variable and can occur in one to all of the limbs with more proximal structures in the limb being affected to variable degrees (Figure 41) (Duchesne et al., 2006). Currently, the only diagnostic tools for the identification of carriers is through diagnostic breeding or microsatellite analysis (Charlier et al., 1996) because the location of the mutation responsible for MFD has remained elusive. Charlier et

al. showed through identity-by-decent mapping that the MFD locus was located in a peri-telomeric region on chromosome 15 in the bovine genome. Since then, the location has been refined to a 6.3 cM region around the markers RM004, BM848, and BMS820 (Drogemuller & Distl, 2006).

Figure 41 Mulefoot Disease.
Examples of mulefoot disease (MFD) in two breeds of cattle. The affected hooves in MFD animals are fused.

The region that contains the MFD locus is syntenic with a region on human chromosome 11 (11p12-p11.2) that also contains the *Megf7* gene (Figure 42). Based on our previous findings that mutations in *Megf7* can cause limb deformities in mice, it was possible that the causative mutation of MFD could be in the *Megf7* locus.

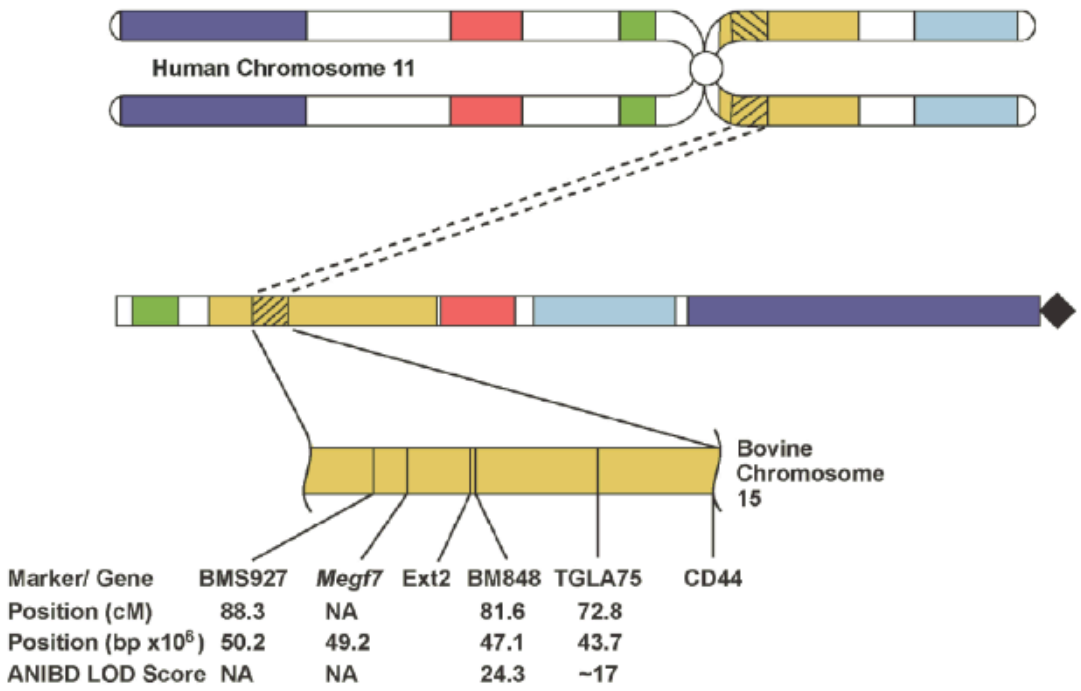

Figure 42 Location of *Megf7* Relative to the MFD Locus.

Comparative schematic of human chromosome 11 and bovine chromosome 15 from data collected from the NCBI (http://www.ncbi.nih.gov), Ensembl (http://www.ensembl.org), and USDA MARC (http://www.marc.usda.gov) databases and from Charlier et al. and Gautier et al. Bovine *Megf7/Lrp4* is separated by 2.1 Mb from BM848, the marker linked to MFD with the highest LOD score (24.3). TGLA75 and BM848 are markers shown by Charlier at al. to be linked to MFD.

Discovery of a Splice Junction Mutation in *Megf7* in MFD Samples

To test the hypothesis that a mutation in *Megf7* may be the causative allele of MFD, the peri-exonic region of exons 4, 7, 8, 9, 10, 11, 12, 13, 15, 16, 17, 19, 20, 21, 22, 23, 24, 26, 27, 28, 30, 31, 33, 34, 36, 37, and 38 were amplified from a confirmed mulefoot skin sample. The DNA was isolated, sequenced, and compared to the online record for the sequence of the

wild type bovine *Megf7* (ENSEMBL). The comparison of the coding sequences did not provide any difference between the data base sequence and the sequence obtained from the MFD sample. However, there was a single point mutation in the region immediately downstream of exon 37. Subsequent sequencing of another MFD sperm sample also revealed the same mutation (Figure 43). The indicated G to A mutation destroys the recognition site for the U1 RNA. The U1 snRNP recognizes this sequence to initiate splicing at each exon-intron boundary (Brow, 2002).

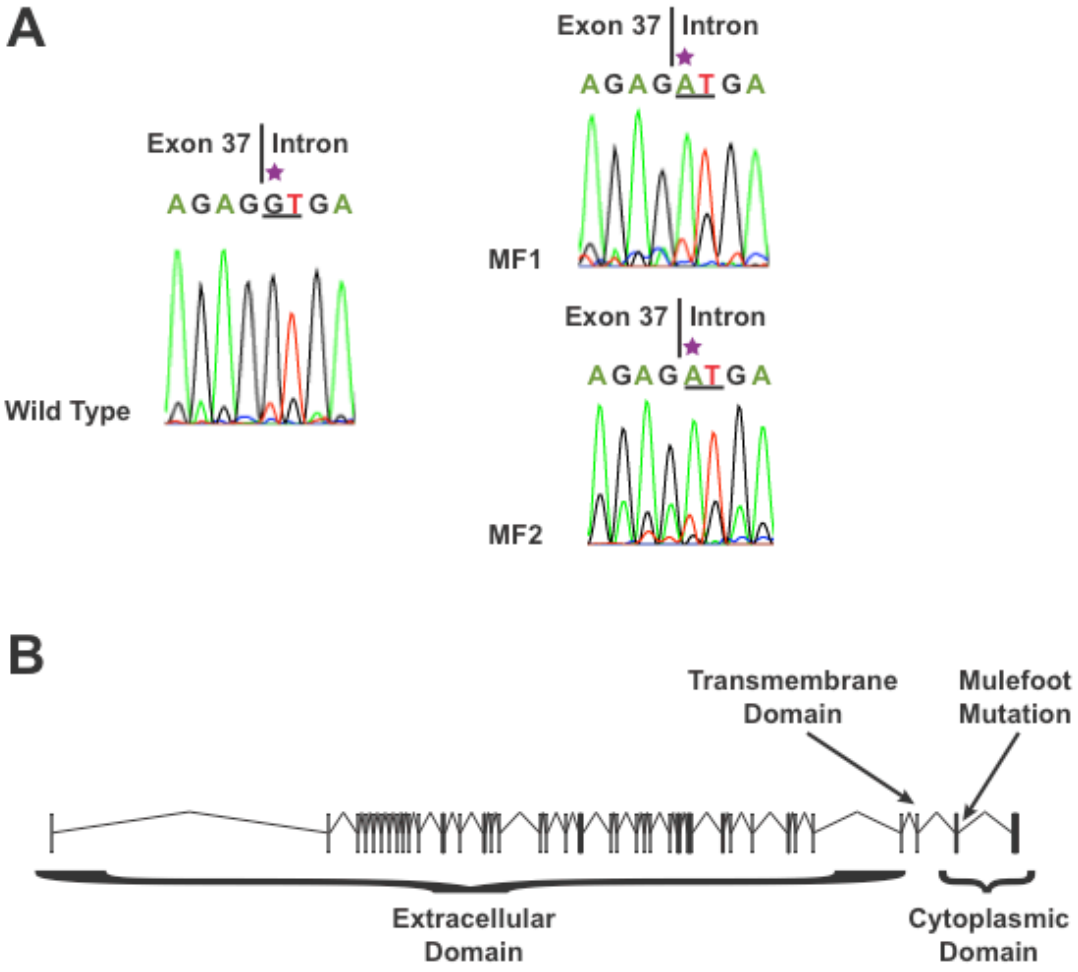

Figure 43 A G-to-A MFD Mutation Disrupts the 5' Splice Site of Intron 37 of *Megf7* in Angus cattle.

(A) The sequence of the 3′ exon/intron border of bovine exon 37. In wild type (left) the first base of intron 37 is G. In the mulefoot samples (right) this highly conserved G is mutated to A. The purple star indicates the mutated base. The underlined nucleotides are the intronic bases that bind to U1 RNA. (B) Graphic representation of the bovine *Megf7/Lrp4* sequence. Vertical lines represent exons. The first 35 exons encode the extracellular domain. Exon 36 encodes the transmembrane domain. Exons 37 and 38 encode the cytoplasmic domain of *Megf7/Lrp4*. The mulefoot mutation occurs at the first base of intron 37.

Analysis of Altered Splicing in Megf7 Mutant Transcripts

Testing the hypothesis of the altered splicing of the MFD transcript was complicated by the limited resources that were available. Until recently, sperm had been considered to be devoid of RNA and the amount that is recoverable is not enough for analysis. Therefore, the sperm samples could not be used for gene expression analysis. The other samples that were obtained were freeze-thawed multiple times and thus the RNA from either sample would be limiting. Despite this barrier, RT-PCR reactions were performed to amplify the different *Megf7* transcripts that are produced in both wild type and mutant tissue samples.

Two primer sets were successfully used to amplify regions within the b*Megf7* transcript. The primers were designed to specifically detect spliced or partially spliced transcripts (Figure 44A). Amplification of a region of the transcript that includes a large intron would allow us to differentiate between spliced and unspliced transcript by the product size. The control reactions, lanes 1 and 3, used primers within exon 30 and exon 36. Amplification using these primers leads to the amplification of the region of *Megf7* mRNA that should not be affected by the MFD mutation and thus should serve as a control RT-PCR reaction for the detection of the total amount of *Megf7* mRNA that has been spliced up to exon 36. The amount of PCR product using these primers is approximately equivalent suggesting that the amount of *Megf7* RNA used in each reaction is roughly comparable (Figure 44B).

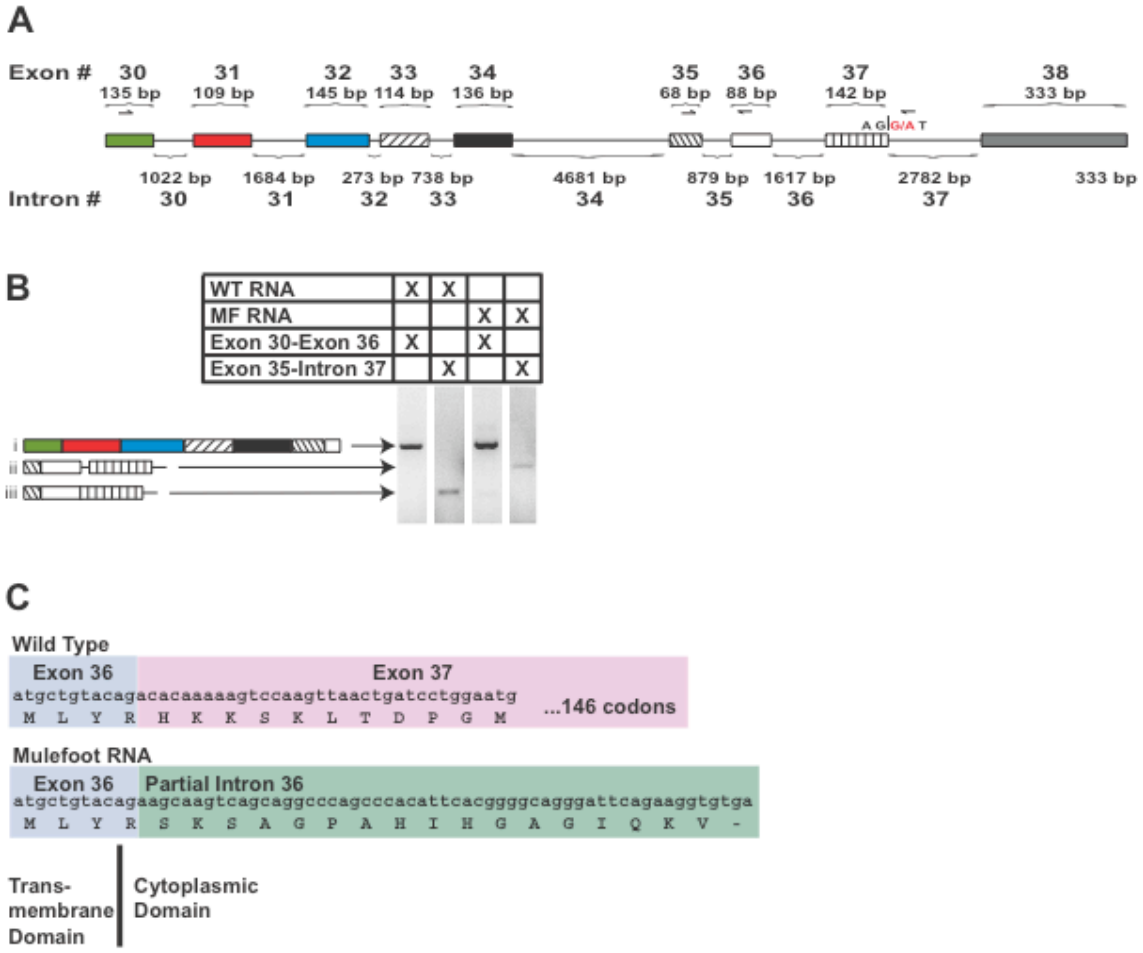

Figure 44 RT-PCR Analysis of Wild Type and MFD RNA.

(A) Structure of the *Megf7/Lrp4* gene ranging from exon 30 to 38. The location of the splice site mutation is shown in red. Forward primers in exons 30 and 35 and reverse primers in exon 36 and intron 37 are indicated by arrows. (B) Normal and equivalent RT-PCR products including exon 30–36 sequences are obtained from wild type and MFD mRNA, while a longer product, indicating incomplete splicing of the MFD sample, is obtained when exon 35 and intron 37 primers are used. (C) Incomplete splicing of intron 36 in MFD *Megf7/Lrp4* mRNA was confirmed by sequencing. Partial inclusion of intron 36 is predicted to replace the wild-type cytoplasmic domain of Megf7 with 17 mis-sense amino acids followed by a premature stop codon.

The test reactions, lanes 2 and 4, used primers that were located within exon 35 and intron 37. The amplification product would differentiate partially spliced species that have

removed intron 35 versus unspliced species or contaminating DNA that would contain intron 35. The wild type sample produced a RT-PCR product that excluded all of intron 36 as well as intron 35 (lane 2). This shows that splicing occurred efficiently with the amplified products. On the other hand, in the MFD sample, lane 4, the RT-PCR product was slightly larger. Cloning and sequencing of this product showed that a portion of intron 36 was still retained in the transcript (Figure 44B).

The inclusion of part of the intron suggests that the definition of the intron/exon boundary is disrupted with the MFD mutation. Loss of the 5' splice site recognition sequence in the MFD transcript probably makes the splicing machinery search for an alternative splice site in the region. The MFD leads to the loss of exon definition on both sides of exon 37. This intronic sequence that is included in the mutant transcript is predicted to introduce non-sense amino acids following exon 36 which would lead to a truncation of the protein product shortly after the transmembrane domain (Figure 44C). The loss of the cytoplasmic domain of the protein product would eliminate any sequence motifs that may be required for the normal signaling performed by Megf7 during limb development. This loss of signaling would essentially eliminate most of the function of *Megf7* similar to what is seen with the $Megf7^{Myc\ KI}$ mouse allele.

In Vitro Analysis of the MFD Splicing Defect

The analysis of the MFD tissue samples was not thorough due to the limitations imposed by the quality and number of the samples. An *in vitro* assay was used to confirm the

hypothesis that the MFD mutation actually affects splicing. A mini-gene assay was used to test the effect of the mutation on splicing in a heterologous cell culture system.

For the *in vitro* splicing assay, two mini-gene expression constructs were generated. Both constructs contained bovine *Megf7* exon 37 flanked by approximately 200 bases of bovine intronic sequence. The bovine sequence insert was cloned between the first and second exons of the mini-gene construct. The only difference between the two plasmids was at the position immediately downstream of exon 37 with an Adenosine mutation in the MFD construct or the Guanosine residue for the wild type construct (Figure 45A).

The plasmids were transfected into multiple cell lines and the transcribed RNA was isolated at different time points. Primers at both ends of the mini-gene were used to amplify the resulting product from each construct. The wild type construct produced the expected spliced product with all of the introns efficiently spliced out (lanes 4-6). The other RT-PCR products represent transcripts that retained one of the introns and thus were probably splicing intermediates. On the other hand, the MFD construct produced a product in which both of the introns flanking the inserted exon 37 were still retained. None of the splicing products seen with the wild type reaction were produced with the MFD construct (Figure 45B). In conclusion, the MFD mutation significantly alters the recognition of the 5'splice site of the exon 37/intron 37 boundary.

A

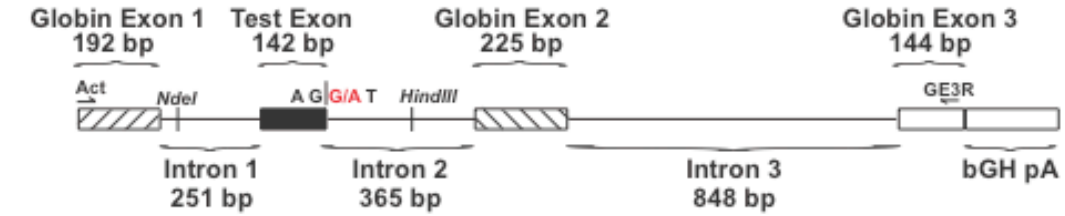

B

Days Post-Transfection	2	3	4	2	3	4	2	2
pcAT7-WT				X	X	X		
pcAT7-MF	X	X	X					
pcAT7-SC12							X	

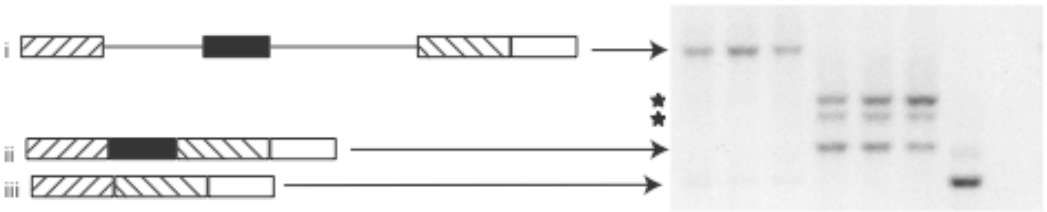

C

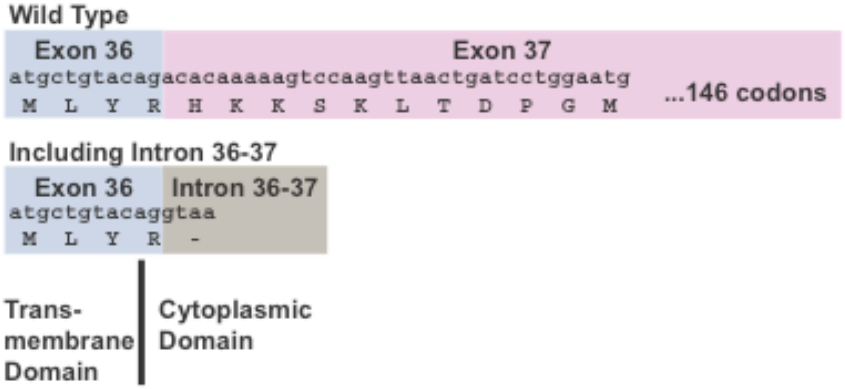

Figure 45 Minigene Splicing Analysis of the MFD Mutation.

(previous page) (A) Diagram of the primary unspliced product of the minigene. Bovine exon 37 and 200 bp of flanking intronic sequence was cloned between the first and the second exon of the β-globin minigene using the restriction enzymes NdeI and HindIII. The only difference between the wild-type and mulefoot minigene constructs is the G-to-A mulefoot mutation (red) at the first residue of intron 37. (B) Both exon 37 and flanking introns fail to splice in the mulefoot minigene RNA. Transcripts from the transfected minigene constructs were reverse-transcribed and amplified by PCR using the indicated Act and Ge3R primers. The regions of the minigene that generated the observed products are indicated on the left and these splice products were verified by sequencing. (Lanes 1–3) Mulefoot sequence (MF), (lanes 4–6) wild-type sequence (WT), (lane 7) parental pcAT7-SC12 plasmid, (lane 8) untransfected cells. (C) Expected MFD-MEGF7/LRP4 translation product. Wild-type sequence is shown at the top, MFD sequence (including intron 36) below.

As shown with the RT-PCR reaction of the mulefoot samples, the inclusion of intron 36 introduces missense sequence to the *Megf7* transcript and leads to the premature truncation after the transmembrane domain. This premature truncation eliminates all of the putative signaling motifs found within the cytoplasmic domain of Megf7. As seen with the $Megf7^{EC\ Stop}$ mouse, the expression of the extracellular domain is sufficient for partial *Megf7* function. The different severities of the limb phenotype of the two mutant mice may explain the variable phenotype found in the mulefoot cows.

CHAPTER SIX
Results

THE FUNCTION OF MEGF7 DURING KIDNEY DEVELOPMENT

Generation of the *Megf7*^{KO} Allele

There is a strong possibility that the *Megf7*$^{EC\ Stop}$ allele described in Chapter 3 may have some residual *Megf7* activity or may create a gene product that may have a new function. It is possible that the RNA product of the *Megf7*$^{EC\ Stop}$ allele is stable, efficiently translated, and the protein product is secreted. Indeed, the RT-PCR reaction described in Figure 6 suggests that the transcript from this allele is present. The stop codon upstream of the encoded transmembrane domain would stop translation of the protein before it can be anchored to the membrane and thus the expected protein product would be a secreted form of the extracellular domain that is not membrane bound. If part of the function of *Megf7* is to bind extracellular proteins, a secreted version may retain a portion of the wild type activity.

Another *Megf7* knockout allele was generated in mice to confirm the observations of the function of Megf7 found in the *Megf7*$^{EC\ Stop}$ mouse as well to uncover other possible roles *Megf7* may have in other tissues. This allele will be termed the knockout allele (*Megf7*^{KO}) because it probably eliminates all activity of *Megf7*. The construct used to generate the knockout allele eliminates the first exon of *Megf7* and thus prevents the use of the initiating methionine as well as eliminating the signal peptide required for entry into the endoplasmic reticulum. The construction of the *Megf7*^{KO} allele is described in Chapter 2 and Figure 46.

The removal of the neomycin resistance cassette by Flp mediated recombination does not affect the observed phenotype of the *Megf7*^{KO} homozygous mouse described below (data not shown). This suggests that the *Megf7*^{KO} phenotype is not a consequence of the disruption of the expression of genes near the *Megf7* locus caused by the proximity of the neomycin resistance cassette promoter. Homologous recombination replaces the first *Megf7* exon as well as some intronic sequence with the neomycin resistance cassette (Figure 46). This allele is not expected to produce a functional protein product because the first exon encodes the initiating methionine as well as the signal peptide required for the protein product to enter the endoplasmic reticulum. Therefore, even if some unexpected splicing mechanism leads to the production of a stable transcript, the protein product would never reach the plasma membrane and thus would be non-functional.

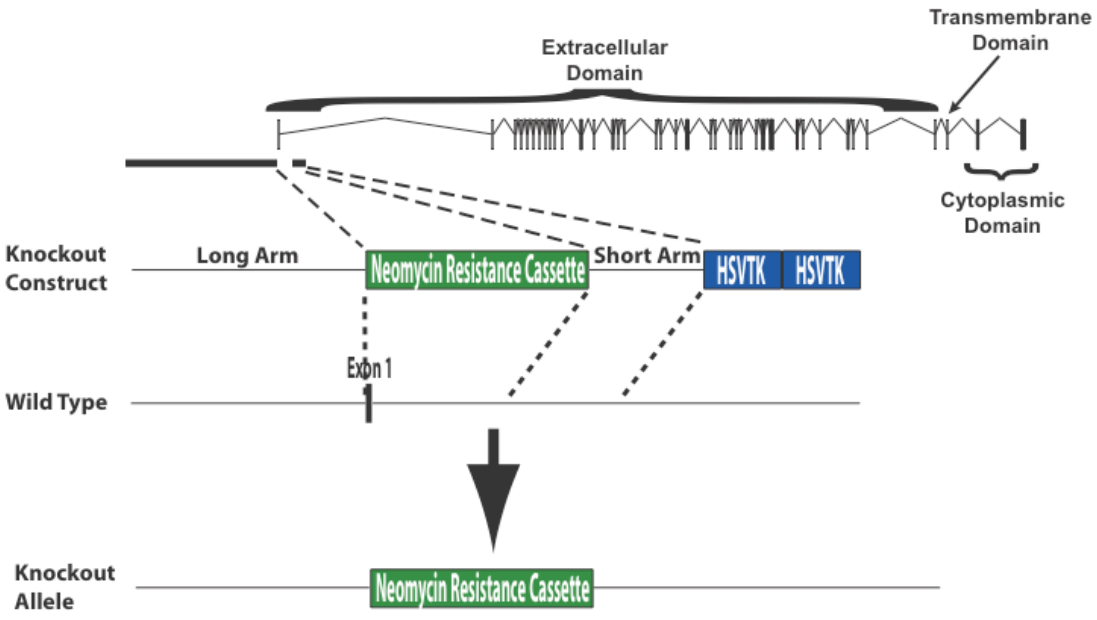

Figure 46 Diagram of the *Megf7*^{KO} Allele.

The knockout construct consists of a long arm of homology, a neomycin resistance cassette flanked by LoxP and FRT sequences, a short arm of homology, and two HSVTK genes. The long arm is homologous to 8kb of genomic sequence upstream of the first exon of *Megf7*. The short arm is homologous to 0.9kb of intron sequence downstream of the first exon of *Megf7*. Homologous recombination results in the replacement of the first exon with a neomycin resistance cassette.

General Description of the Megf7^{KO} *Phenotype*

The phenotype of the mice that are homozygous for the *Megf7*^{KO} allele is more severe than the phenotype of the *Megf7*$^{EC\ Stop}$ allele. In addition to the limb defects seen in the *Megf7*$^{EC\ Stop}$ mutant, the homozygous knockouts also have lung, heart, kidney, and neuromuscular junction defects.

Recently, a *Megf7* null mouse allele was generated through a forward genetic screen. The investigators showed that these mice failed to form neuromuscular junctions

(Weatherbee, Anderson & Niswander, 2006). This thesis will not focus on the neuromuscular junction defects.

Before birth, the frequency of homozygous embryos from a heterozygous X heterozygous cross is close to the expected Mendelian ratio suggesting that there is not an early lethality phenotype. However, no homozygous pups were found alive after birth suggesting that the pups were still-born. Cesarean sections of E18.5 fetuses from a heterozygous X heterozygous cross show that the pups indeed are not able to live outside of the womb. The pups do not move which suggests that there may be some neurological defect that causes paralysis. Whether or not this paralysis is a more severe phenotype of the post-natal lethality found in the *Megf7*$^{EC\ Stop}$ mutants is unknown. Consistent with the paralysis hypothesis, the pups do not take the initial breath after being removed from the uterus. Also, the *Megf7*^{KO} pups removed by cesarean section adopt a distinct posture with the limbs in an extended position, which is reminiscent of what is seen in mice with neuromuscular junction defects (DeChiara et al., 1996). This fetal posture was also observed by Weatherbee at al. and was explained by the paralysis caused by the failure of the embryos to form neuromuscular junctions (Weatherbee et al., 2006).

Upon gross examination, the knockout embryos obtained through cesarean-section had defects of the heart and/or lungs. Gross examination shows that both organs in the homozygous *Megf7*^{KO} pup are significantly smaller than the organs of the littermate pups. Both organs appear to be hypovascular based on the lack of red pigmentation and visible blood vessels. The phenotype seen in the cross-sections of the lung suggests that the architecture of the lung is disrupted. Alcian Blue staining of the bronchi was performed to

see if the patterning of the cartilage rings is disrupted in the *Megf7* knockouts. Compared to the wild type pups, the pattern of cartilage deposition of the bronchi of the *Megf7* knockouts appears to be normal.

As in the *Megf7*$^{EC\ Stop}$ mutant, the *Megf7*^{KO} mutant also has polysyndactyly. Alcian Blue and Alizarin Red staining of the developing limbs of the newborn pups shows that there is a similar degree of a loss of autopod patterning as in the *Megf7*$^{EC\ Stop}$ mutant (Figure 47). The *Megf7*^{KO} homozygotes have a disrupted pattern of calcium deposition as well as a loss of patterning of the cartilage condensation (Figure 48).

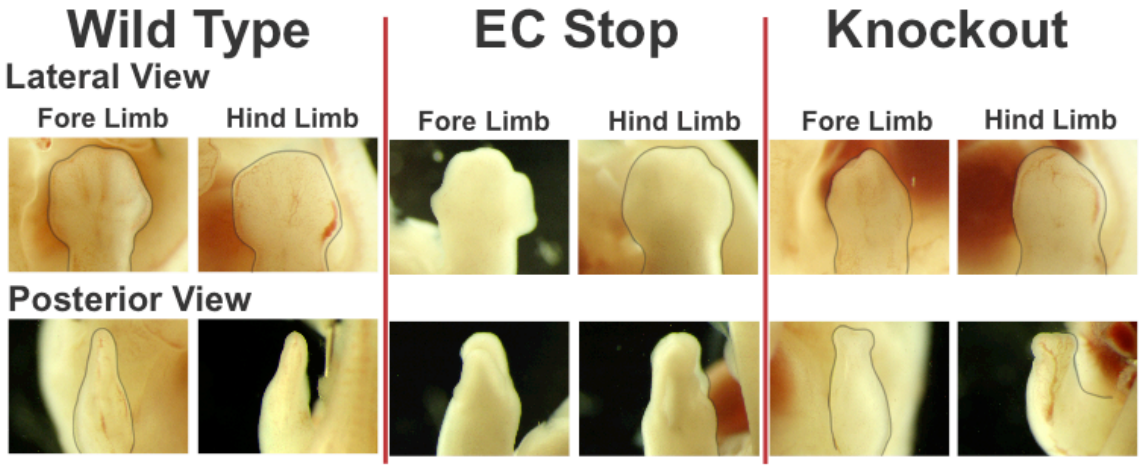

Figure 47 Defective Limb Development in *Megf7*^{KO} Embryos.

Hand plates of E12.5 (left) wild type, (middle) *Megf7*$^{EC\ Stop}$ mutants, or (right) *Megf7* knockout embryos. The border of the hand plate was outlined to highlight structural defects. The defect of limb patterning previously described for the *Megf7*$^{EC\ Stop}$ mutant is similar to the phenotype of the *Megf7*^{KO} mutant.

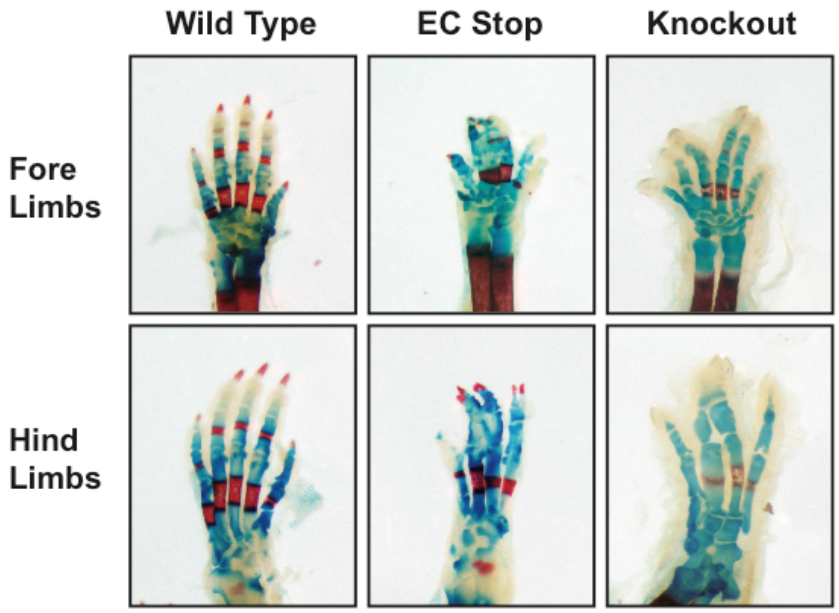

Figure 48 Polysyndactyly in *Megf7* Mutant Mice.

Alizarin red and alcian blue staining of P0 (left) wild type, (middle) *Megf7*$^{EC\ Stop}$ mutants, or (right) *Megf7* knockout mice. The disruption of patterning found in the *Megf7*^{KO} mutant is similar to the defect described previously for the *Megf7*$^{EC\ Stop}$ mutant.

Fgf8 staining of the developing E11.5 limbs was performed to confirm that the same AER defect occurs in the *Megf7*^{KO} mutant as described in Chapter 3 for the *Megf7*$^{EC\ Stop}$ allele. Whole mount *in situ* shows that the expansion of the AER is approximately equivalent to the expansion seen in the *Megf7*$^{EC\ Stop}$ embryos (Figure 49).

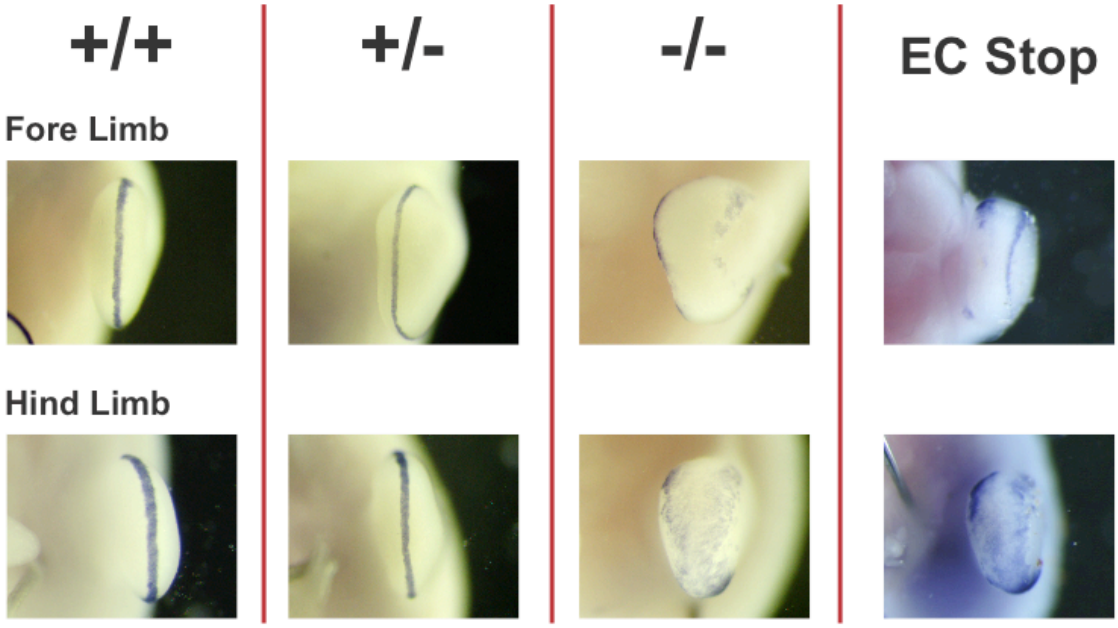

Figure 49 Expansion of the AER in *Megf7*^{KO} Embryos.

Fgf8 expression was detected using wholemount *in situ* hybridization on wild type, heterozygous *Megf7*^{KO}, homozygous *Megf7*^{KO}, and homozygous *Megf7*$^{EC\ Stop}$ embryos. The Apical Ectodermal Ridge (AER) of wild type and heterozygous embryos consists of a distinct band of *Fgf8*-expressing cells at the distal edge of developing limb. There is an equivalent degree of expansion of the AER in the *Megf7* knockout and *Megf7*$^{EC\ Stop}$ embryos.

Kidney Agenesis in the Megf7 Knockout

In contrast to the *Megf7*$^{EC\ Stop}$ mutant, which to date have not exhibited any kidney defects, the knockout has a kidney agenesis phenotype. Of the knockout pups that were found *in utero* at E18.5 or pups that were still-born from Heterozygous X Heterozygous matings, 51% of the pups had no kidneys, 22% had one kidney, and 27% had both kidneys. Therefore 62% of all potential kidneys fail to develop in the *Megf7*^{KO} mutant. As shown in figure (Figure 50) kidneys fail to develop while the remaining urogenital system remains intact.

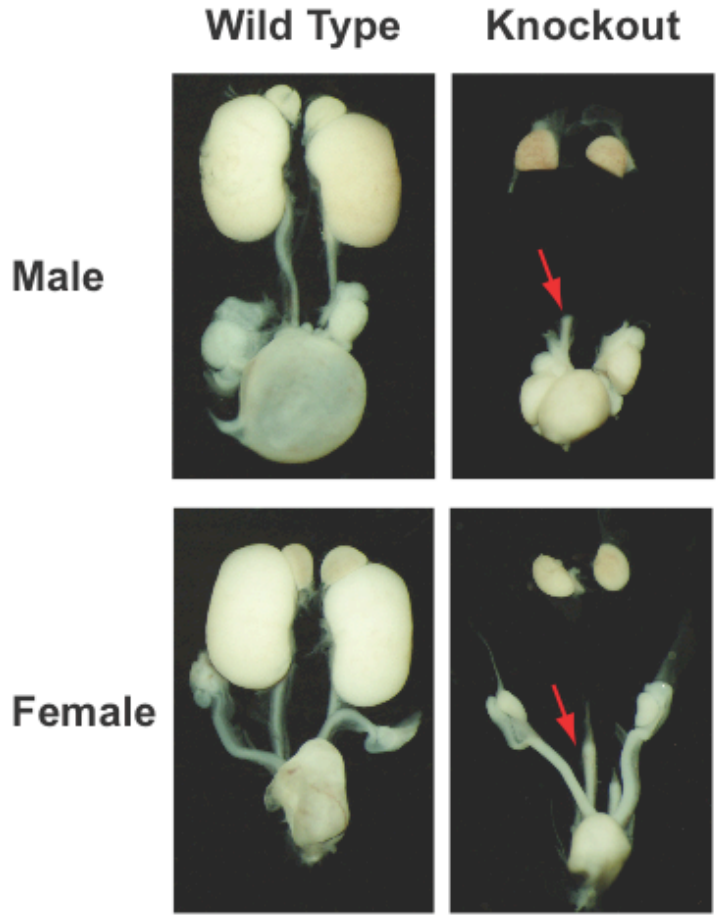

Figure 50 Kidney Agenesis in the *Megf7*^{KO} Mutant.

62% of kidneys fail to form in both male and female *Megf7*^{KO} mice. The remaining urogenital system and adrenal glands appear grossly normal. A fraction of the *Megf7*^{KO} embryos that do not form kidneys have a truncated ureter (arrows).

As seen in Figure 50, a rudimentary ureter was found in many of the knockout embryos that did not form a kidney. This suggests that primary branching of the ureteric bud occurs but subsequent secondary branching and mesenchyme condensation fails to occur in those instances.

As mentioned above, kidneys form 38% of the time in the *Megf7*^{KO} homozygote. H&E staining of the *Megf7*^{KO} kidneys shows that there are no gross morphological defects in these kidneys (Figure 51). The number of glomeruli and collecting ducts appears to be roughly equivalent between wild type and *Megf7*^{KO} kidneys. No grossly abnormal kidneys were found in the knockouts suggesting that kidney development progresses normally once it passes a certain stage. Perhaps any functions of *Megf7* later during kidney development are compensated by another gene.

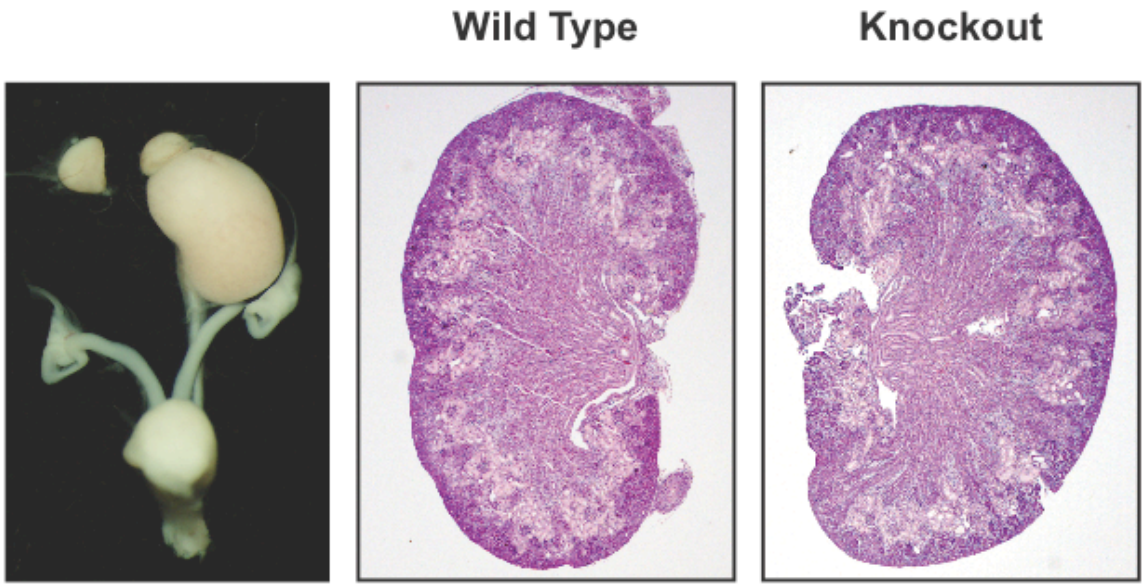

Figure 51 Normal Appearance of the *Megf7*^{KO} Kidney.

(left) Urogenital system of a *Megf7* knockout mouse containing one kidney. (middle) Wild type and (right) knockout kidney cross-sections. The kidneys that form in the *Megf7* knockout appear to be normal with comparable amounts of collecting ducts, ascending and descending tubules, and glomeruli. The presence of normal kidneys without *Megf7* suggests that *Megf7* regulates an initial step in kidney formation.

Megf7 Expression in the Developing Kidney

The expression of *Megf7* was analyzed to provide clues for its function during kidney development. *Megf7* is initially expressed in the region of the Wolffian duct that branches to form the ureteric bud. Note that *Megf7* expression is limited to the region of ureteric bud branching and not in the remaining Wolffian duct. This expression patternsuggests that *Megf7* plays a role in the initiation and positioning of branching during kidney development. At E11.5, when the ureteric bud is at the T-stage, *Megf7* is expressed in the ureteric bud as well as the prevesicular mesenchyme. Subsequent stages of development show the expression of *Megf7* in the distal branches of the ureter as well as the prevesicular mesenchyme (Figure 52). It is unclear why *Megf7* is expressed during the later stages of kidney development because loss of *Megf7* activity does not appear to affect the formation of glomeruli, tubules and collecting ducts once kidney development has passed a certain developmental hurdle.

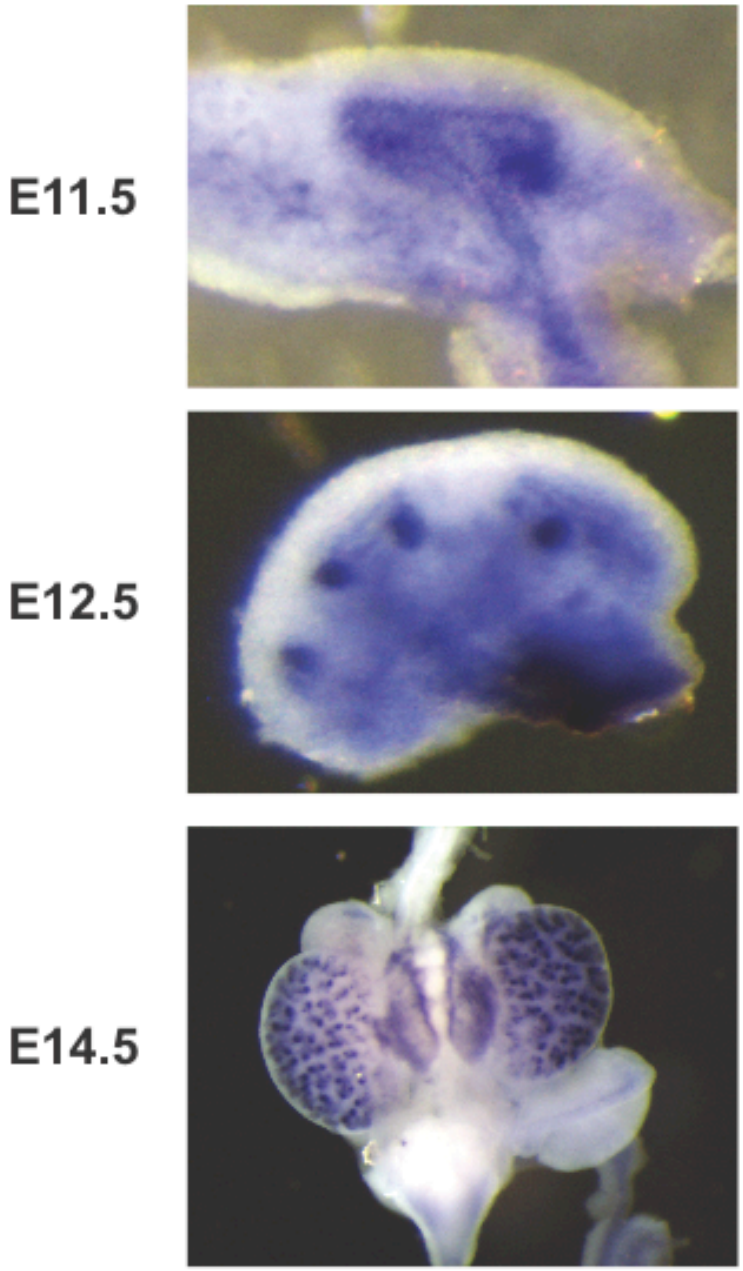

Figure 52 Expression of *Megf7* in the Developing Kidney.

(previous page) Expression of *Megf7* in E11.5 (top), E12.5 (middle), and E14.5 (bottom) kidneys. *Megf7* is expressed both in the ureteric bud and the prevesicular mesenchyme at E11.5. The ureteric bud and prevesicular mesenchyme expression continues through E14.5.

Gene Expression During Kidney Development in the Megf7^{KO} *Embryo*

Wnt9b is expressed in the Wolffian duct as well as the ureteric bud but is excluded from the distal tips of the ureteric bud. *Wnt9b* appears to interact with many of the genes involved in kidney development (Carroll et al., 2005). The *Megf7^{KO}* embryo does not appear to have a defect in *Wnt9b* expression. *Wnt9b* is expressed in the ureteric bud during the early stages of kidney development and is present at the point of primary branching as well as at the T-stage of ureteric bud development. However, a portion of the E11.5 *Megf7^{KO}* embryos have a UB that is only at the stalk stage. This defect appears at a frequency that is roughly equivalent to the frequency of kidney agenesis. At E12.5, when there are no apparent kidney structures remaining, the expression of *Wnt9b* follows a rudimentary ureteric bud and the signal quickly diminishes (Figure 53). The *Wnt9b* expression suggests that the ureteric bud grows past the initial primary branching but fails to progress to the T-stage in the cases when the kidneys fail to form.

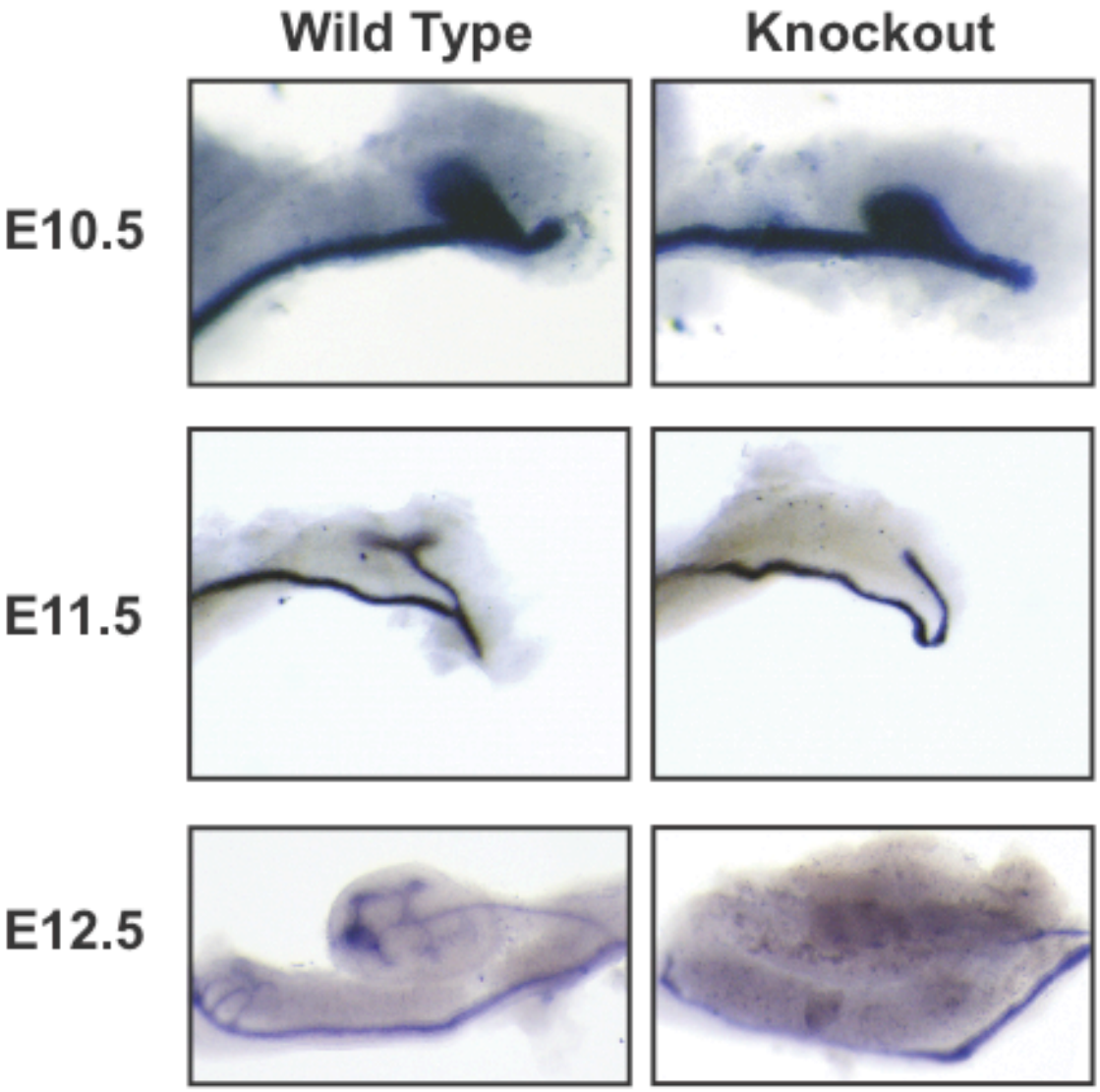

Figure 53 Expression of *Wnt9b* in the *Megf7*^{KO} Embryo.

Expression of *Wnt9b* in E10.5 (top), E11.5 (middle), and E12.5 (bottom) kidneys. The expression of *Wnt9b* is maintained in the ureteric bud of the *Megf7*^{KO} embryo. At E11.5, there is an obvious defect in UB growth and branching in knockout embryos that results in the failure to form a kidney at E12.5.

The *Wnt9b* data suggest that the mutant ureteric bud emerges from the Wolffian duct but fails to efficiently branch and/or participate in the positive feedback signals with the

mesenchyme. The ureteric bud was stained at different time points to differentiate between a delay in the emergence of the ureteric bud from the Wolffian duct and a defect in branching and elongation. The BAT-gal mouse transgene was used to easily mark the ureteric bud during development with a relatively simple staining technique.

At E10.5 the ureteric bud is just beginning to emerge from the Wolffian duct. There is no apparent difference in the size of the ureteric bud at that stage between wild type and knockout embryos. This suggests that the timing of ureteric bud formation is not altered in the *Megf7*^{KO} embryo. At E11.5 the ureteric bud should be at the T-stage with two well-developed branches. In the knockout, the growth of the ureteric bud is retarded. Some buds fail to achieve the T-stage and remain a single branch off of the Wolffian duct while other ureteric buds get to the secondary branching stage but growth is clearly inhibited (Figure 54).

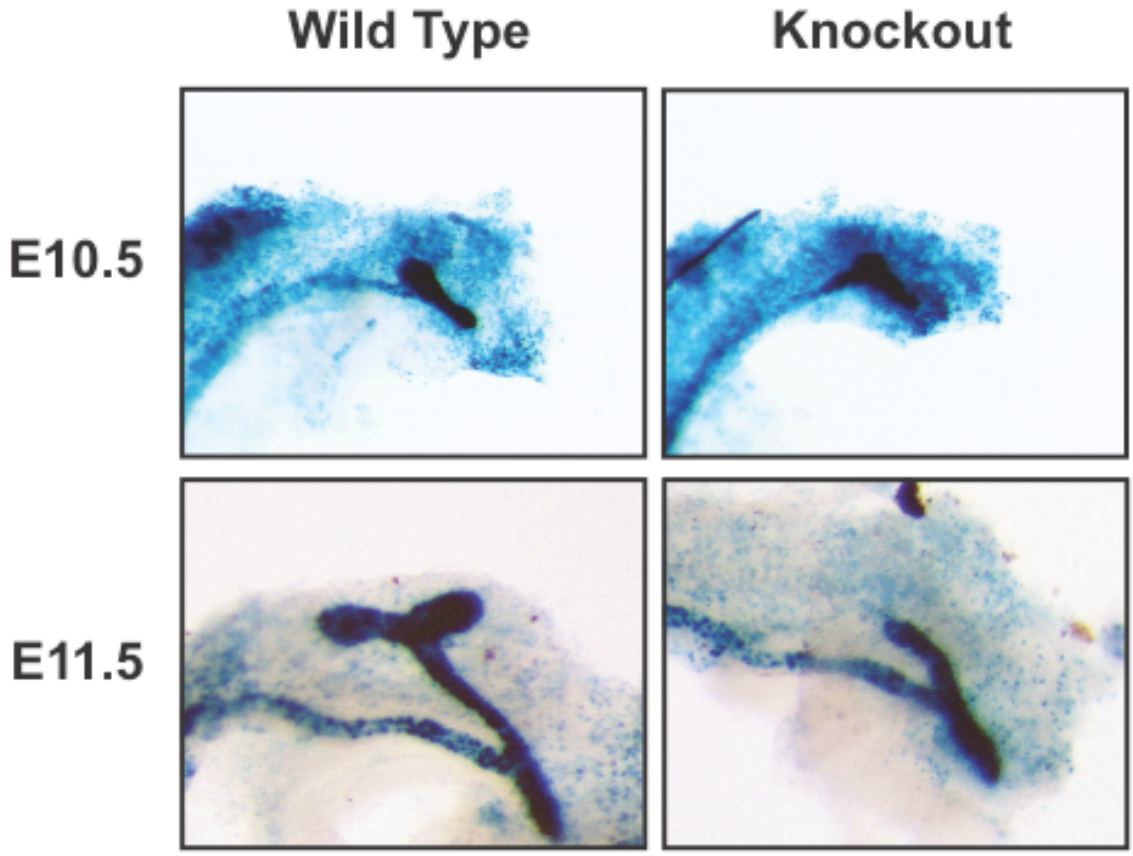

Figure 54 Retarded Ureteric Bud Growth and Branching in the *Megf7*^{KO} embryo.

The BAT-gal transgene was used to mark the ureteric bud during development. Expression of the BAT-gal β-galactosidase in E10.5 (top) and E11.5 (bottom) kidneys. The primary branching of the ureteric bud occurs at the correct developmental stage in the *Megf7*^{KO} embryo. At E11.5 the UB in wild type embryos have undergone secondary branching. By E11.5, the growth of the UB of knockout embryos has slowed significantly and often fails to undergo secondary branching.

The loss of UB growth in the *Megf7*^{KO} embryo suggests that the UB fails to receive signals from the metanephric mesenchyme. One gene that is responsive to a signal from the mesenchyme is *c-Ret*. *C-Ret* expression is upregulated in wild type ureteric buds in response to *Gdnf*, the ligand for *c-Ret*. At E10.5 the expression of *c-Ret* is upregulated at the point

where the ureteric bud emerges from the Wolffian duct. In the *Megf7*^{KO} embryos, however, *c-Ret* expression is not upregulated. The same loss of *c-Ret* expression can be seen more clearly at E11.5. At E12.5 the UB has failed to induce kidney formation and leads to a loss of the *c-Ret* expression signal (Figure 55).

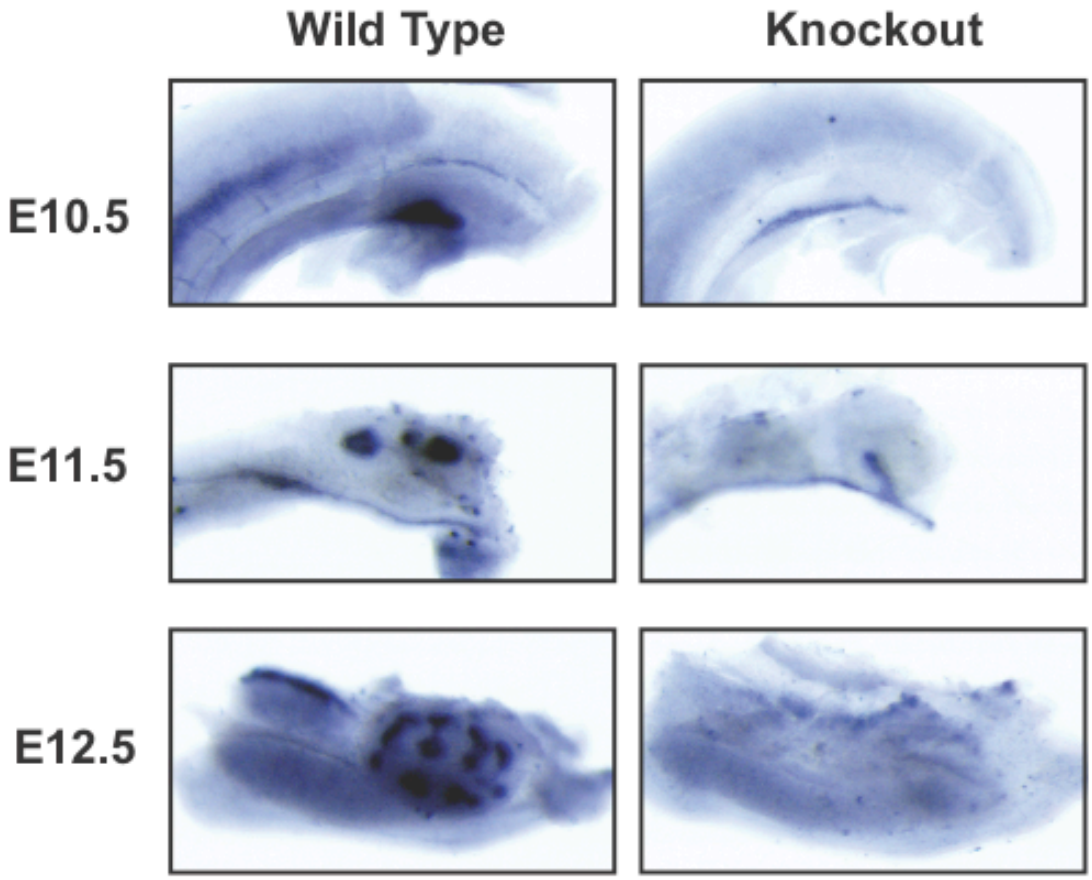

Figure 55 Expression of *c-Ret* in the *Megf7*^{KO} embryo.

Expression of *c-Ret* in E10.5 (top), E11.5 (middle), and E12.5 (bottom) kidneys. *c-Ret* is expressed in the ureteric bud at basal levels in the *Megf7*^{KO} embryo. The *Megf7*^{KO} UB fails to upregulate *c-Ret* expression at the tips of the UB as seen in the wild type embryos at E11.5. This suggests that *Megf7* is required for gene activation at the tip of the UB.

Wnt11 is a gene that is expressed in the distal tips of the ureteric bud. Previously, it had been suggested that *Wnt11* and *Gdnf* interact in a positive feedback loop during kidney development (Majumdar et al., 2003). Therefore, *Wnt11* also acts as a reporter gene for the reception of the *Gdnf* signal in the ureteric bud as well as an indicator of the health of the ureteric bud. As mentioned, the signal for *Wnt11* is present at the distal portion of the developing ureteric bud starting at the point of primary branching on the Wolffian duct. Even though the UB does not reach the T-stage, *Wnt11* is still expressed in the tip of the ureteric bud in the *Megf7* knockout during the initial stages of development. Only later during development, when the ureteric bud is lost, do we see a loss of the *Wnt11* signal (Figure 56). The expression of *Wnt11* and the loss of expression of *c-Ret* in the UB suggests that the *Wnt11-Gdnf-Ret* positive feedback loop is interrupted in the $Megf7^{KO}$ embryo.

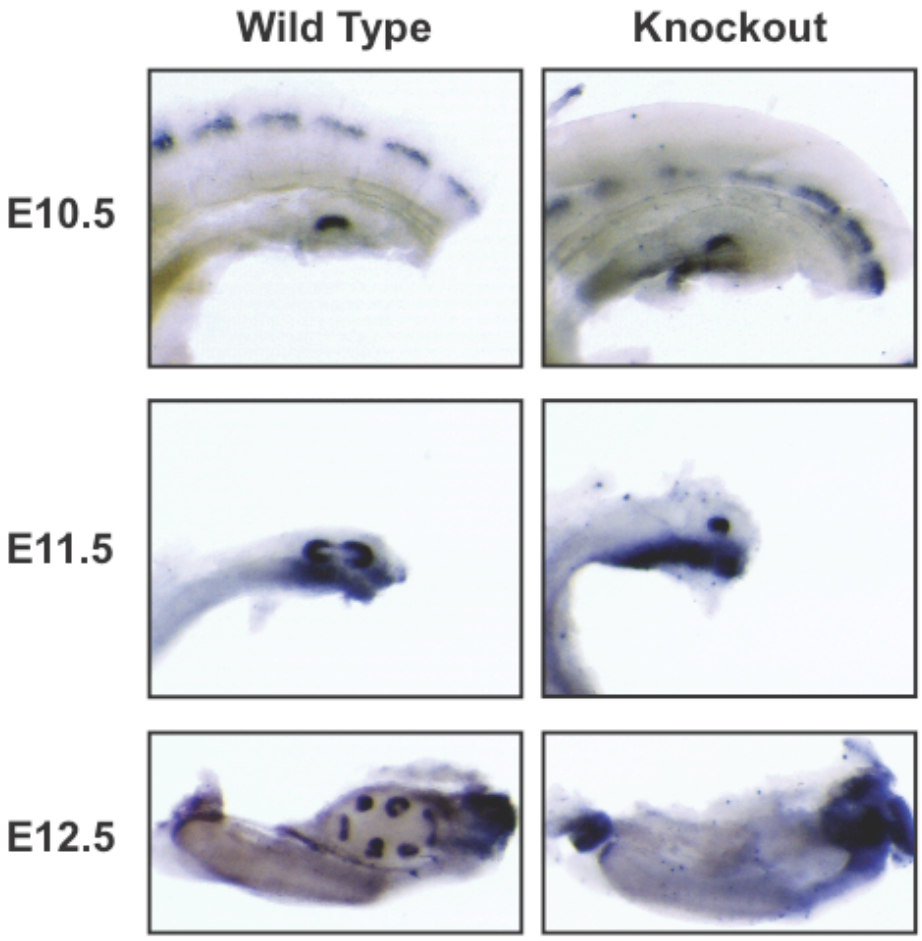

Figure 56 Expression of *Wnt11* in the *Megf7*^{KO} embryo.

Expression of *Wnt11* in E10.5 (top), E11.5 (middle), and E12.5 (bottom) kidneys. *Wnt11* is expressed at the tips of the ureteric bud of both wild type and *Megf7*^{KO} embryos. At E12.5 the expression of *Wnt11* is lost in the UB that fails to form a kidney in the *Megf7*^{KO} embryo.

The defect of retarded ureteric bud growth found in the *Megf7*^{KO} embryos suggests that the ureteric bud depends on the function of *Megf7* to regulate the signal generated by the surrounding mesenchyme. Precise biochemical and cellular characterization of the function of Megf7 should provide some insight into which signals during kidney development are being affected in the *Megf7* knockout embryo.

During the initial stages of kidney development, the ureteric bud emerges from the Wolffian duct and sends signals to the surrounding mesenchyme. These signals in turn induce the expression of a subset of genes in the mesenchyme required for survival and differentiation. *Pax8* is a gene that is induced in the mesenchyme by the ureteric bud. Therefore, *Pax8* is a reporter of the ability of the ureteric bud to send signals to the surrounding mesenchyme or for the mesenchyme to receive such signals. Initially there is very little *Pax8* expression in both wild type and $Megf7^{KO}$ E10.5 embryos. Later during development, the expression of *Pax8* is upregulated in the mesenchyme surrounding the ureteric bud in the wild type embryos. In the $Megf7^{KO}$ embryo, the expression of *Pax8* is barely visible (Figure 57). This suggests that *Megf7* is either responsible for the mesenchyme's reception of the ureteric bud signal, the ureteric bud is not competent to produce a signal to induce the expression of *Pax8* in the surrounding mesenchyme, or the ureteric bud bud growth is not sufficient to reach the mesenchyme and thus participate in cell-cell communication.

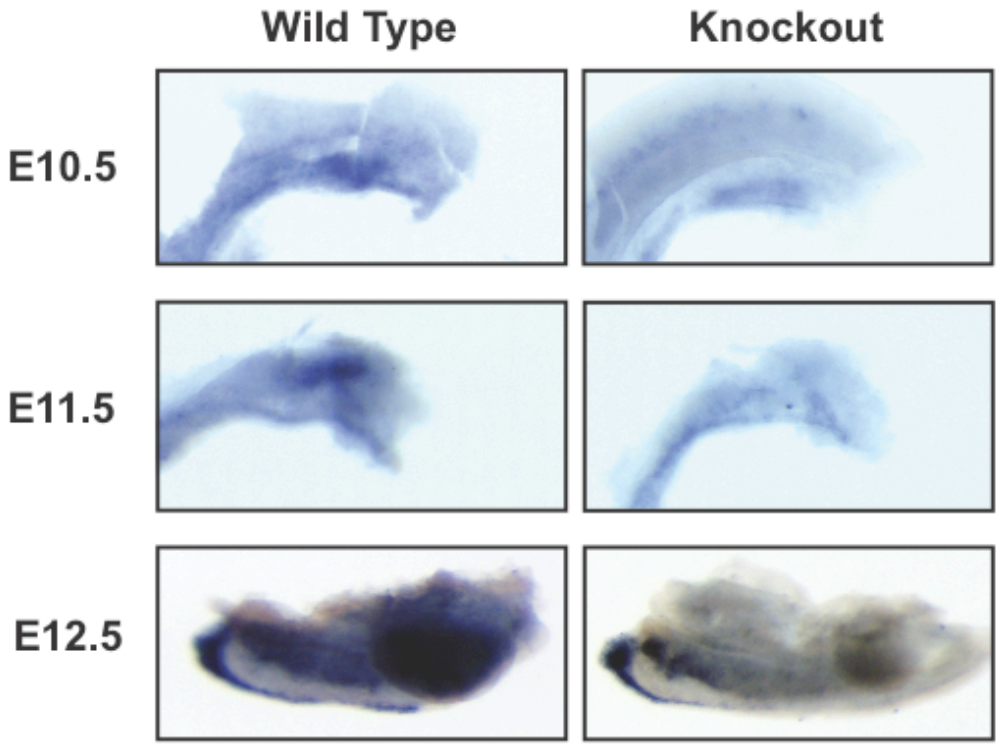

Figure 57 Expression of *Pax8* in the *Megf7*^{KO} embryo.

Expression of *Pax8* in E10.5 (top), E11.5 (middle), and E12.5 (bottom) kidneys. *Pax8* is expressed mainly in the metanephric mesenchyme. Expression appears normal at E10.5 in the knockout. At E11.5 the ureteric bud fails to achieve secondary branching and induce the expression of Pax8 in the metanephric mesenchyme. At E12.5 the expression of Pax8 is absent due to the failure to form a kidney in the *Megf7*^{KO} embryo.

Pax2 is a gene that is expressed both in the UB and in the metanephric mesenchyme and thus allows us to examine the UB and the mesenchyme simultaneously. At E10.5 the expression of *Pax2* appears to be equivalent in both the wild type and knockout embryos. However, the E11.5 embryos reveal that the UB fails to reach the active metanephric mesenchyme. The loss of interaction between the UB and mesenchyme can be seen in the lower expression level of *Pax2* in the mesenchyme of the *Megf7*^{KO} embryo compared to the

wild type embryos. A remnant of the UB remains at E12.5, but the mesenchyme is no longer active where only a faint patch of mesenchyme expression is present (Figure 58).

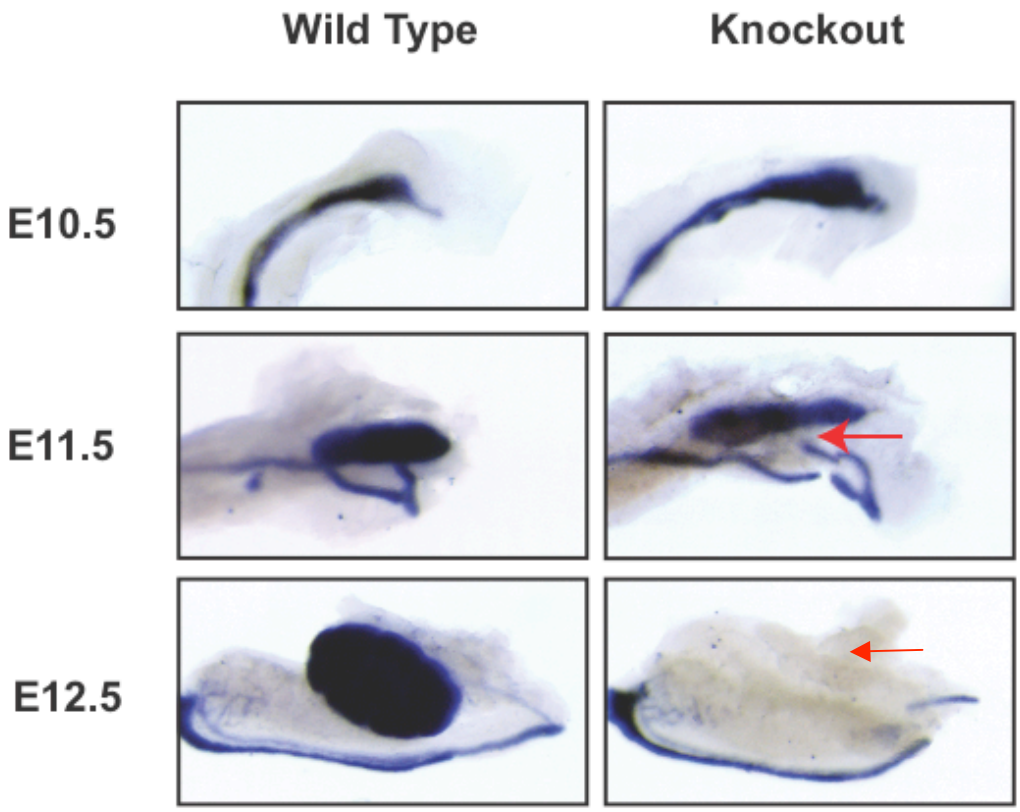

Figure 58 Expression of *Pax2* in the *Megf7*^{KO} Embryo.

Expression of *Pax2* in E10.5 (top), E11.5 (middle), and E12.5 (bottom) kidneys. *Pax2* is expressed in both UB and the metanephric mesenchyme. Expression appears normal at E10.5 in the knockout. At E11.5 the ureteric bud fails to reach the zone of *Pax2* expression in the mesenchyme in the knockout embryo (Arrow). The expression of *Pax2* is not upregulated by the UB at E11.5 and expression is almost completely eliminated at E12.5 in the mesenchyme of the knockout embryo.

Gdnf is a factor secreted by the mesenchyme that supports the growth of the ureteric bud. At the same time, the expression of *Gdnf* is maintained through the stimulation of the mesenchyme by the ureteric bud (Majumdar et al., 2003). Therefore, loss of a signal from the

ureteric bud leads to the loss of *Gdnf* expression. A possible explanation for a defect in the growth of the ureteric bud may be that the surrounding mesenchyme fails to provide trophic support. In wild type embryos the expression of *Gdnf* is present in the mesenchyme at the initial stage of ureteric bud branching to the completion of nephrogenesis. During the initial stages of development, *Gdnf* appears to be normal in the *Megf7* knockout embryos. Later during development, at E12.5, the expression of *Gdnf* is lost in the mesenchyme where the ureteric bud fails to develop past the T-stage (Figure 59). Therefore, it is unlikely that there is a defect in *Gdnf* secretion and mesenchymal trophic support in the *Megf7* mutants. Instead the loss of the ureteric bud leads to the loss of the surrounding mesenchyme and thus a loss of *Gdnf* expression.

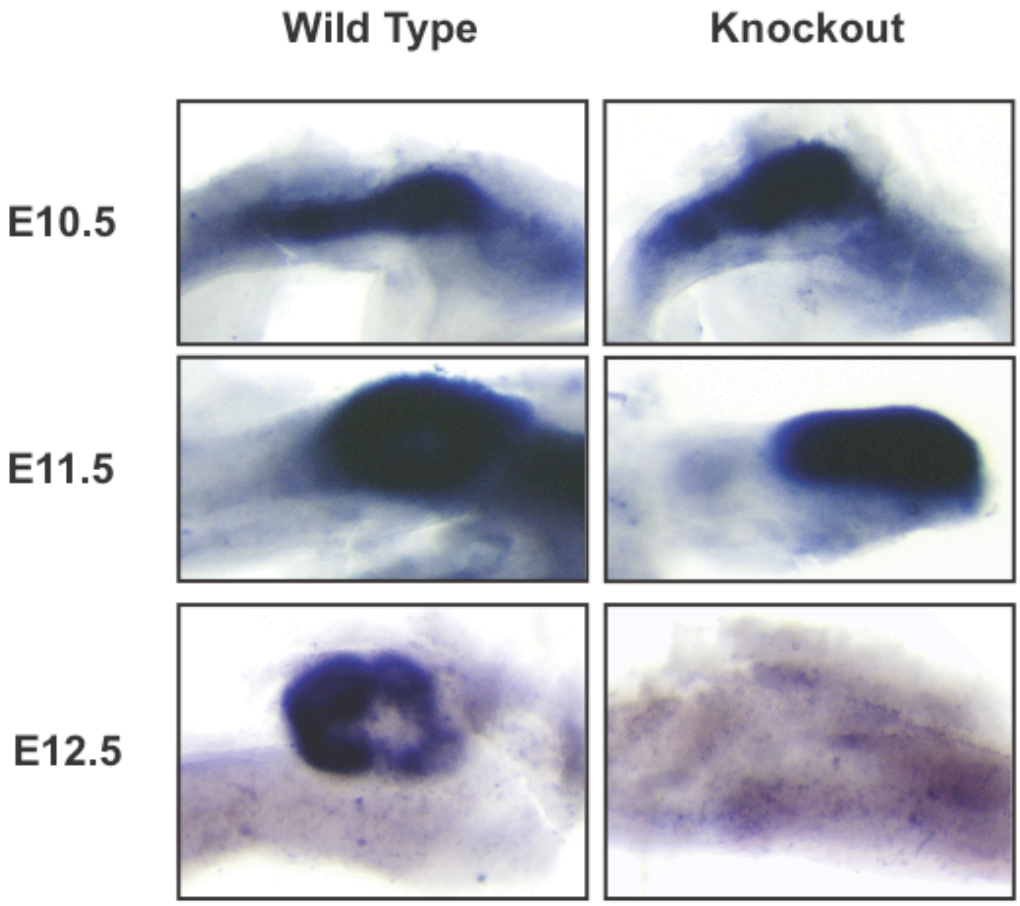

Figure 59 Expression of *Gdnf* in the *Megf7*^{KO} Embryo.

Expression of *Gdnf* in E10.5 (top), E11.5 (middle), and E12.5 (bottom) kidneys. The expression of *Gdnf* is maintained in the metanephric mesenchyme of the *Megf7*^{KO} embryo up to E11.5. *Gdnf* expression is lost at E12.5 when the UB fails to provide sufficient inductive stimuli to form a kidney. *Gdnf* remains active at E12.5 if the UB completes secondary branching and reaches the mesenchyme.

The exact mechanism of the kidney defect in the *Megf7*^{KO} embryo is currently unknown. There appears to be a defect in the growth and branching of the UB. It is unclear whether there is a defect in the reception of a signal from the mesenchyme or simply a defect in proliferation. One possibility discussed with Dr. Thomas Carrol is that the cells in the

Megf7^{KO} UB prematurely differentiate and thus reduce the pool of cells that are able to proliferate and contribute to UB growth. Perhaps a resolution of the mechanism of Megf7's action will improve the understanding of its function in the mature kidney.

CHAPTER SEVEN
Discussion

CLUES FOR THE FUNCTION OF MEGF7

Megf7 in Limb Development

At this point it is indisputable that *Megf7* is involved in limb development. There are 14 total animal models in which mutations in *Megf7* lead to polysyndactyly or syndactyly, five of which were developed or discovered in this lab (Figure 60). There are four knockout or knockin mice that were developed in this lab: the premature stop codon knockin designated as the $Megf7^{EC\ Stop}$ mutant in Chapter 3, the *Megf7* knockout described in Chapter 6, the *Megf7* Myc KI cytoplasmic domain truncation ($Megf7^{Myc\ KI}$), and the $Megf7^{LDLR\ KI}$ mutant discussed in Chapter 4. There are also two spontaneous *Megf7* mutants that were described by Simone-Chazottes et al. We found that a mutation in *Megf7* causes mulefoot disease in cows. There are also five other reported mutations in bovine *Megf7* that are responsible for mulefoot disease in the homozygous state (Drogemuller et al., 2007; Duchesne et al., 2006).

Murine and Bovine *Megf7* mutations with limb defects

Mutation	**Comments**	**Species**	**Organs Affected**	**Publication**
Megf7$^{EC\ Stop}$	Premature stop codon	Mouse	L, T, MG	Johnson, 2005
Megf7^{KO}	1st codon deletion, Eric Johnson	Mouse	L, T, MG, NM	
Megf7$^{Myc\ KI}$	Cytoplasmic region deletion, Eric Johnson	Mouse	L	
Megf7$^{LDLR\ KI}$	LDLR cytoplasmic region knockin, Eric Johnson	Mouse	L	
Megf7^{dan}	Viral integration, low expression	Mouse	L	Simone-Chazottes, 2006
Megf7^{mdig}	Spontaneous mutant, low expression	Mouse	L	Simone-Chazottes, 2006
Megf7^{mte}	ENU mutant, null allele	Mouse	L, T, MG, NM	Weatherbe, 2006
Megf7^{mitt}	ENU mutant, null allele	Mouse	L, T, MG, NM	Weatherbe, 2006
Megf7^{Spl}	MFD allele, results in a mRNA splicing defect	Bovine	L	Johnson, 2006
Megf7$^{G\rightarrow C}$	MFD allele	Bovine	L	Duchesne, 2006
Megf7^{G81S}	MFD allele	Bovine	L	Drogemuller, 2007
Megf7^{G907R}	MFD allele	Bovine	L	Drogemuller, 2007
Megf7^{G1199S}	MFD allele	Bovine	L	Drogemuller, 2007
Megf7^{P1647L}	MFD allele	Bovine	L	Drogemuller, 2007

Figure 60 List of Known *Megf7* Mutations

(Previous Page) A table listing all known *Megf7* mutations with a brief desciption, species, organ systems affected, and reference (if available). L, Limbs; T, Teeth; MG, Mammary Glands; NM, NeuroMuscular Junctions; MFD, MuleFoot Disease

One of the mouse mutants described in Simone-Chazottes et al. was produced through a random integration event using a defective Maloney retrovirus (*digitation anormale*- *dan*). The other mutant that they found was a naturally occurring mutant found in the Jackson Laboratory mouse colony (malformed digits- *mdig*). They found that the two mutations were allelic suggesting that both mutations affect the same gene. The retroviral insertion mutant, dan, had an integration site within the first intron of *Megf7*. The naturally occurring mutant, mdig, has a mutation in the 5' splice junction of exon 15. Both alleles lead to the decreased expression of *Megf7* in these mice (Simon-Chazottes et al., 2006). Therefore, these mice confirm the phenotype that was found in the *Megf7* mutants described in Chapter 3. The decreased expression but not the complete elimination of expression found in both mutants probably explains why the phenotype is not as extreme as the $Megf7^{KO}$ mutant described in Chapter 6.

The mulefoot mutation described by Duschennes et al. was found using the opposite approach used by this lab. They found the mutation by refining the position of the locus to a 3.5Mb region through comparative mapping whereas we started with the hypothesis that mutations in *Megf7* should cause syndactyly phenotypes in one or more animal models. In their cattle, a CpG doublet is mutated to ApT in exon 33. This mutation changes a glycine to a cysteine within the EGF repeat of the bovine *Megf7* gene. This mutation may result in disrupted folding by altering the disulfide pairing within the EGF fold. This would result in

the impaired function of Megf7 but may not completely abolish activity. Again, the mulefoot phenotype is probably similar to the *Megf7*$^{EC\ Stop}$ phenotype because partial *Megf7* function is still retained.

New Mulefoot Disease Mutation Reports

As mentioned in the description of the mulefoot alleles, there are a total of six published mutations that are associated with mulefoot disease in cows. The first two have been described in Chapter 2: the exon 37 splicing mutation found by this lab and the NG1621-1622KC mutation found by Duchesne et al.(Duchesne et al., 2006). The other four are mutations found by the Eggen lab (Drogemuller et al., 2007).

The G81S mutation found by Drogemuller et al. is in the second ligand binding repeat of *Megf7*. The G907R mutation is within the YWTD domain of the second EGF precursor homology domain. The G1199S mutation is within the third EGF precursor homology domain and is also in the YWTD domain. The P1647L mutation is in the fourth EGF precursor homology domain in the downstream EGF repeat (Drogemuller et al., 2007). The functional consequence of these mutations is unknown although it appears as if these mutations would affect the folding of the extracellular domain or would have decreased affinity for the relevant ligands and thus would be classified as class 2 or class 3 mutations, meaning the mutations affect the folding, trafficking of the receptor to the plasma membrane, or binding of the ligand (Goldstein et al., 2001).

The mulefoot mutation that we found was predicted to result in the exclusion of exon 37 from the final spliced transcript. We expected that the loss of the exon/intron boundary would eliminate exon definition for exon 37 and thus would not be recognized by the splicing machinery and spliced out of the mature mRNA. The empirical evidence suggests otherwise. The results from the mini-gene assay as well as the RT-PCR reaction from the mulefoot sample shows that exon 37 as well as portions of the flanking intronic sequence are still retained in the final spliced transcript.

The splicing results from our lab could be explained by the observed phenomenon in the report by Ibrahim el et al. They found that there are specific regions within exons that bind to SR proteins that lead to the absolute inclusion of that particular exon is not excluded from the final spliced product. This is perhaps an evolutionary mechanism that ensures that a particular exon is not in any mRNA products. This is probably the case for exons in which their inclusion is absolutely required for the gene products function. Exon 37 is also essential for the function of Megf7. Exclusion of exon 37 would result in the elimination of all of the elements within the cytoplasmic domain of Megf7. The results from the allelic series of *Megf7* show that elimination of the cytoplasmic domain of Megf7 in mice leads to a limb phenotype that phenocopies the mulefoot phenotype.

Design of the Megf7$^{EC\ Stop}$ Allele

The design of the *Megf7$^{EC\ Stop}$* allele was based on the *Apoer2* and *Lrp1b* knockout vectors (Marschang et al., 2004; Trommsdorff et al., 1999). The *Apoer2* knockout vector had the same basic conformation of components and thus served as a model for a successful

knockout strategy. The *Apoer2* knockout vector had a long arm of homology that contained the exons immediately upstream of the transmembrane domain. The neomycin resistance cassette replaced exon 17 and 18, which code for the transmembrane domain of *Apoer2* (Trommsdorff et al., 1999). In the case of the *Apoer2* null allele, there is no stable transcript nor a detectable protein product (Beffert et al., 2006). Thus, the lack of a gene product indicates that the *ApoER2* knockout allele is a true null allele and the strategy used to make the *Apoer2* knockout allele is a viable strategy to generate a null allele. The *Lrp1b* knockout construct also eliminates the exon that encodes the transmembrane domain (Marschang et al., 2004). Although, recently unpublished results suggest that the allele generated in the Herz lab is not a true null allele.

There are some differences between the $Megf7^{EC\ Stop}$ allele and the *Apoer2* and *Lrp1b* knockout alleles that may have some functional significance. First, a premature stop codon was inserted into the $Megf7^{EC\ Stop}$ allele whereas the *Apoer2* and *Lrp1b* allele do not have a stop codon within the normal coding sequence. The stop codon in the $Megf7^{EC\ Stop}$ allele ensures that translation stops before any non-*Megf7* sequence is encountered. Therefore, no missense amino acids, encoded by a transcript that includes intronic sequence or has a frame shift due to incorrect splicing, are incorporated into the protein product. A lack of a stop codon may also destabilize the transcript of the *Apoer2* and *Lrp1b* knockout alleles. The machinery of Nonsense Mediated Decay may recognize the *Apoer2* transcript and target it for degradation. Second, the $Megf7^{EC\ Stop}$ allele contains the bovine Growth Hormone 3'UTR downstream of the stop codon. This may serve to stabilize the transcript. The *Apoer2* allele may be less stable because it does not have a 3'UTR. There is a 3'UTR in the neomycin

resistance cassette, but it is probably in the opposite orientation to affect RNA processing. Third, there may be some unknown splicing phenomenon that may serve to destabilize the *Apoer2* transcript whereas the *Megf7*$^{EC\ Stop}$ transcript should not have any splicing issues. The RT-PCR data using mutant RNA suggests that the transcript is stable (Figure 6). This leaves the possibility that a protein product is made and thus may contribute to the hypomorphic phenotype.

There is no predictable way, based on current knowledge, that the *Megf7*$^{EC\ Stop}$ allele could produce the wild type transcript through alternative splicing. The mutated allele removes a portion of exon 36, which corresponds to the transmembrane domain of Megf7. Any alternatively spliced product would still be missing most, if not all, of the transmembrane domain and thus the minor protein product of the transcript would be functionally equivalent to the predicted product of the mutant allele.

Evidence for Signaling Pathway Modulation

We began with mutational analysis to understand the biochemical mechanism of action for Megf7. Characterization of the *Megf7* mutant phenotypes can now be used to find analogous experimental models to generated hypotheses about the function of *Megf7*. Unfortunately, the generation of hypotheses is complicated by the promiscuity of the LDL receptor gene family. As mentioned above, the LDL receptor gene family has been found to interact with Wnts, BMPs, SHH, PDGF, as well as other signaling and non-signaling molecules. This does not facilitate the biochemical analysis of the gene family considering all of the possibilities of ligands. Wnts and BMPs will be discussed below as possible

interacting proteins of Megf7. The evidence, however, is not overwhelming and does not eliminate other gene products as possible interacting molecules. Alternatively, *Megf7* may interact with multiple proteins and signaling pathways and thus may have multiple functions that contribute to the correct patterning of the limbs, teeth, kidneys, etc.

In the limb, the Wnt signaling pathway appears to be regulated directly or indirectly by *Megf7*. As mentioned above, the phenotype of the *Megf7* mutant limb is similar to other animal models where there is a loss of inhibition of the Wnt signaling pathway. The loss of DKK1, the activation of β-catenin, and the overexpression of Wnt activating proteins in the mouse limb produces an expanded AER. This suggests that the boundaries of the AER or the proliferation of the AER cells is regulated by the Wnt signaling pathway.

Perhaps the expression pattern of *Megf7* can give some insight into which signaling pathway is being regulated. *Megf7* is expressed in the AER as well as the ventral ectoderm of the limb bud. Interestingly, *Megf7* is expressed in the same region of the limb that provides the cells that form the AER.

Results from the Joyner lab suggests that there are distinct borders present during the formation of the AER that regulate the migration of ectodermal cells (Kimmel et al., 2000). Cells do not appear to cross the dorsal border of the AER. Early during AER formation, there is a dorsal/ventral border within the AER that disappears at later stages. Cells within the ventral ectoderm can migrate in and out of the AER before the final formation of the mature structure. After the formation of the ventral border, cells remain within the AER until the structure disappears with the formation of the hand plate (Kimmel et al., 2000). It is interesting to note that *Megf7* is expressed in the same cells that migrate from the ventral

ectoderm into the AER. Perhaps *Megf7* regulates the formation of the dorsal and or the dorsal/ventral boundary of the AER. Or perhaps, *Megf7* limits how many cells migrate into the AER.

A conditional allele of *Megf7* and the inducible Msx2-Cre used by Kimmel et al. could be used to investigate the hypothesis that *Megf7* deficient cells in the ventral ectoderm migrate at a higher rate into the AER (Kimmel et al., 2000). A conditional allele can be used to remove *Megf7* in the AER but keep the activity in the ventral ectoderm intact. First, this experiment would test if *Megf7* acts on the cells in the AER or in the ectoderm. Second, if *Megf7* regulates the rate of migration of ventral ectoderm cells into the AER, a loss of *Megf7* in the AER should not affect the formation of the AER and thus the *Megf7* deficient AER should be similar to a wild type AER. If, on the other hand, *Megf7* does not control the migration of the ventral ectoderm cells into the AER, the conditional allele deletion of *Megf7* would still produce an enlarged AER.

A technique used by Kimmel et al. can be used to test the possibility that *Megf7* regulates the dorsal border of the AER (Kimmel et al., 2000). In their report, Kimmel et al. used a non-replication competent virus to express *LacZ* in progenitor cells and then map the fate of the progeny. This virus can also be used to examine the fate of cells at the ventral border of the AER in the *Megf7* mutant embryos. The data from Kimmel et al. suggests that the cells in the ventral portion of the AER continuously migrate in and out of the ventral ectoderm. If cells are retained in the AER in the *Megf7* mutant limb bud, and thus fewer cells migrate into the ventral ectoderm, there should be a semi-quantitative decrease in the number of AER-derived progeny that are labeled with *LacZ.* This experiment may also be used to

measure the rate of proliferation of cells within the different regions of the limb bud. If the progenitor cells within the AER are infected with the virus at the same time between wild type and mutant limbs, the number of times a cell multiplies can be measured by the number of progenitor cells present at the time of harvest.

The activity of Megf7 can also be analyzed using the same techniques used for the *Fringe* genes. In one example, the expression of Raddical Fringe and Lunatic Fringe induce ectopic AER, indicating that these genes regulate the patterning of the AER (Laufer et al., 1997). In the same way, the ectopic expression of Megf7 in knockout embryos can be used to test the hypothesis that Megf7 regulates the borders of the AER. The partial viral expression of Megf7 should reduce the size of the AER in the regions of Megf7 expression. If, on the other hand, Megf7 regulates the number of cells in the AER through proliferation or migration, the viral expression of Megf7 in the AER should not significantly affect the size of the AER because the effect would be independent of the location of Megf7 expression.

The hypothesis that *Megf7* is an inhibitor of the Wnt signaling pathway may be confirmed by replacing *Megf7* activity with an alternative inhibitor of the Wnt signaling pathway. This hypothesis can be tested by generating a transgenic mouse line that overexpresses the Wnt inhibitor Dkk1 in the limb bud. Expression of *Dkk1* can be directed to the limb bud with a *En1* or *Msx2* promoter similar to what was done previously be Kimmel et al. (Kimmel et al., 2000). The overexpression of a Wnt inhibitor in the limb will compensate for the loss of *Megf7* and thus will at least partially correct the limb defect of the *Megf7* knockout.

Shh Expression in the Megf7 Mutant Limb

As mentioned in Chapter 3, there is weak expression of *Shh* in the *Megf7*$^{EC\ Stop}$ mutant limb. There is also consistently more transcript in the dorsal streak of *Shh* expression in the mutant whereas the streaks of *Shh* expression in wild type embryos are equivalent in both dorsal and ventral streaks (Figure 20). This is reminiscent of the expression pattern seen when ectopic *Shh* expression is induced by FGF4 (Yang & Niswander, 1995). In this experimental model, an FGF4 soaked bead is placed in the proximal posterior region of the limb bud. Two patches of *Shh* are induced on either side of the bead with the dorsal patch of expression being consistently stronger than the ventral patch.

The unequal expression of *Shh* in the dorsal and ventral streaks in the FGF4 bead experiment by Yang et al. suggests that there is a component that is not present in the proximal region of the limb that is required for the equal expression of *Shh* in the dorsal and ventral streaks (Yang & Niswander, 1995). This factor that maintains *Shh* expression is presumably secreted from the AER and does not diffuse sufficiently to reach the proximal region of the limb bud. The unequal expression of *Shh* between the dorsal and ventral streaks in the *Megf7*$^{EC\ Stop}$ mutant suggests that the same factor that affects *Shh* expression in the FGF4 bead experiment is not being produced efficiently by the AER in the *Megf7*$^{EC\ Stop}$ mutant limbs. This may be a consequence of the disrupted structure of the AER or may be the result of the down-regulation of the expression of a factor that is normally expressed in the AER. Several things can be done to investigate the loss of unequal expression of *Shh* in the *Megf7* mutant limb buds. One hypothesis to test is that the loss of *Megf7* directly reduces the expression of *Shh* in the underlying mesoderm. This hypothesis can be tested by

expressing *Megf7* with a viral expression system in *Megf7* knockout embryos. If *Megf7* directly regulates the expression of Shh, the expression of Shh beneath the cells that express Megf7 should be upregulated.

If the viral expression of *Megf7* induces *Shh* expression in the $Megf7^{KO}$ embryo, this activity can be used in an assay to understand *Megf7*'s mechanism of action. For instance, if *Megf7* inhibits the Wnt signaling pathway, incubation of a bead soaked with a secretable inhibitor of the Wnt signaling pathway such as Dkk1 or a secreted Frizzled should induce the expression of *Shh*. If Shh expression goes up with the incubation of a Wnt inhibitor, it would suggest that the Wnt signaling pathway is directly involved in the activity of *Megf7*. The same experiment can be performed with other proteins that modulate other signaling pathways such as the BMP, TGF, FGF pathways, etc.

Regulation of Signaling Pathways

If Megf7 interacts with Wnt signaling components, it would have to regulate a Wnt signal coming from specific regions within the developing limb. Unfortunately, like most of the signaling pathways involved in organogenesis, there are many Wnts expressed in different regions of the limb. To complicate matters, some of these Wnt proteins signal through the canonical signaling pathway whereas the others appear to signal through unknown non-canonical signaling pathways. As mentioned in the Introduction, *Wnt2b* and *8c* are expressed in the early mesoderm. *Wnt3,5a*, and *6* are expressed in the ectoderm. *Wnt5b, 10a,* and *12* appear to be expressed specifically in the AER. *Wnt5a, 10b*, and *11* are expressed in the mesoderm. *Wnt7a* is expressed exclusively in the dorsal ectoderm. This

leaves *Wnt2, 8a, 8b, 9a, 9b,* and *16* that have yet to be characterized. *Wnt 1, 3a, 4,* and *7b* may also be expressed in the limb but all reported expression studies indicate otherwise. The sheer number of Wnts that are expressed in the limb does not provide a clear unifying hypothesis of action for *Megf7* and leads to many unanswered questions. If *Megf7* regulates a Wnt signal, does it regulate a Wnt that signals through the canonical or non-canonical signaling pathway? Does *Megf7* regulate a paracrine or autocrine Wnt signal from the mesoderm or the ectoderm respectively? Does *Megf7* regulate boundary formation, cell proliferation, and/or cell migration within the AER? All of these questions are difficult to answer with the limb as a model organ system due to its complexity.

The fly is a simpler system that can be used to answer some of the questions asked above. *Drosophila* species also have a *Megf7* ortholog. The *Drosophila* system is also well-characterized for many aspects of development. There are also many well-characterized mutant stocks that can be used to facitliate the analysis of epistasis. The wing imaginal disc is very similar to the developing vertebrate limb bud in terms of gene expression and genetic interactions (Laufer et al., 1997; Wolpert, 1998). The *Drosophila* system is much simpler. For instance, there are 7 *Drosophila* Wnt genes whereas there are 19 mammalian Wnt genes (http://www.stanford.edu/~rnusse/Wntwindow.html). Fewer genes will simplify the analysis when taking a candidate gene approach. Unfortunately, there is no known mutant fly strain for *Megf7*. There is a P-element upstream of *Megf7*. The P-element can be used to remove the upstream portion of *Megf7* using P-element excision. The P-element is too far from *Megf7* to make the process of specific P-element excision efficient. Currently, there is no downstream P-element that can be used for recombinase-mediated excision. But, a new strain

of P-element flies may be generated that may be useful for the generation of a *Megf7* deficient fly stock.

There is also a chance that the *Megf7* deficient *Drosophila* strains will be paralyzed because they fail to form neuromuscular junctions. If that is the case, a conditional allele or hypomorphic allele will need to be generated. A hypomorphic allele can be generated with a mutant screen for flies that have wing defects. The screen is complicated by the fact that it would be difficult to predict the phenotype of a *Megf7* deficient fly. A conditional *Megf7* allele can be made, but this would require the generation of a complicated recombination procedure that is more difficult than simple P-element excision or mutant screens.

The Drosophila system provides a more efficient paradigm to analyze the interaction between *Megf7* and other genes. The *Megf7* mutants can be bred to other available fly strains to produce double mutants and detect changes in the severity of the phenotype. *Megf7* can also be selectively deleted or over-expressed using heat-shock techniques to detect an interaction between expressing and non-expressing cells.

The LDL receptor gene family member *Megalin* has been shown to inhibit the BMP signaling pathway through the endocytosis of BMPs (Spoelgen et al., 2005). This raises the possibility that *Megf7* may also have a similar function. Unfortunately, the evidence pointing to BMP regulation in the limb is not clear. The Birchmeier lab places the BMP signaling pathway above the Wnt signaling pathway in the formation of the AER. The epistasis experiments that brought them to this conclusion used a conditional allele of BMPRIA to eliminate BMP signaling in the ectoderm. In this experiment, the expansion of the AER induced by the activation of the Wnt signaling pathway was reduced to no AER with the

BMPRIA mutant (Soshnikova et al., 2003). This suggests that the BMP pathway may be upstream of the Wnt pathway but it does not eliminate the possibility that the BMP pathway is required for the AER maintenance that is independent of the Wnt effect. The Birchmeier results conflict with other reports of the loss of BMP signaling in the AER. In these reports, the loss of BMP4 or the ectopic expression of the BMP inhibitor Noggin leads to the expansion of the AER (Pizette & Niswander, 1999; Selever et al., 2004). These results suggest that a loss of BMP signaling in the limb leads to an expansion of the AER whereas the Birchmeier results show that a loss of BMP signaling leads to the loss of the AER. Again, the developing limb is a very complex model that is difficult to interpret in regards to what regulates the formation of the AER.

If there is an interaction between the Wnt pathway and the BMP pathway in the limb, *Wnt5a* is the most likely candidate for the relevant Wnt gene. *Wnt5a* is the only known Wnt that is expressed in the same pattern as some of the BMPs in the limb. *Wnt5a* is expressed in the distal region of the limb in the mesoderm as well as the ectoderm and AER. *Megf7* may either interact with the BMPs that are expressed in the distal aspect of the limb that in turn regulate the expression of *Wnt5a*. Or, *Megf7* may regulate the response of the AER to *Wnt5a* that is induced by the expression of the BMPs. Interestingly, the *Wnt5a* mutant has limb defects that appear to be independent of the AER. The AER is intact in these mutants even though the borders of the AER appear to be less distinct than wild type AERs (Yamaguchi et al., 1999).

Wnt5a is a clear example of how difficult it is to unravel mechanism from phenotype. In developmental biology, with all of the interacting gene families with multiple family

members, there is rarely a clear answer. I found that *Wnt5a* may act as an inhibitor of the canonical Wnt signaling pathway. This suggests the possible model that Megf7 may interact with Wnt5a to activate a non-canonical Wnt pathway that in turn inhibits the canonical pathway (Topol et al., 2003). Therefore, *Megf7* can be either an inhibitor or an activator of the Wnt pathway and still have the same effect in the limbs. The downstream result is dependent on which Wnt protein interacts with Megf7. Experimentally, this is a problem because it would require testing an interaction between Megf7 and all 19 Wnt genes. This does not even include the possible interaction with Wnt-interacting genes such as the DKKs or Wise.

Megf7 in Kidney Development

In contrast to the observations in the limb, the kidney phenotype of the $Megf7^{KO}$ homozygote does not appear to involve the Wnt signaling pathway. First, we could not find any Wnt signaling mutant phenotypes that were similar to the observed phenotype of the *Megf7* knockout. Second, unpublished observations from Dr. Thomas Carrol suggest that constitutive activation of β-catenin in the developing kidney does not compromise the initial stages of ureteric bud growth. Therefore it is unlikely that Wnt signals are involved in the signaling modulation of *Megf7* in the developing kidney. On the other hand, as mentioned above, if *Megf7* activates a non-canonical Wnt pathway, then the loss of *Megf7* in the knockout may not be predictable. For instance, a double Wnt gene knockout has a similar phenotype as the *Megf7* kidney agenesis phenotype. These are unpublished results from Dr. Thomas Carrol with an N=1, but may provide a clue about the function of *Megf7*.

The phenotypic analysis of kidney development in the *Megf7*^{KO} mouse suggests that BMPs may be involved. First, the phenotype of the *Megf7*^{KO} mouse is very similar to that of the *Gremlin1* knockout (Michos et al., 2004). So in this case, the loss of *Megf7* appears to be similar to a loss of an inhibitor of the BMP signaling pathway. Also, previous reports have suggested that hyperactivation of the BMP pathway leads to an inhibition of ureteric bud growth and branching (Miyazaki et al., 2000; Raatikainen-Ahokas et al., 2000).

It is difficult to interpret the partial penetrance of the kidney agenesis found in both the *Megf7* null embryos produced by me and the Niswander lab (Weatherbee et al., 2006). Also, the *Megf7* expression in the kidney after ureteric bud branching suggests that it has a function in late kidney development and yet the *Megf7* knockout kidneys form normally once the T-stage of the ureteric bud is reached. One explanation is that another gene is compensating for the loss of *Megf7* in the knockout embryos. One strong possibility is for a gene that compensates for the loss of *Megf7* is another LDLR gene family member, *Megalin*. This gene is also expressed in the kidney during development, although the detailed analysis of expression is not available for the early stages of kidney development (Yamagata et al., 2001). The expression of *Megalin* is not the same as *Megf7* where *Megalin* appears to be mainly expressed in the tubules and not in the prevesicular mesenchyme (Figure 61). Megalin may partially compensate for the loss of *Megf7* in the knockout embryos. If *Megf7* inhibits the BMP pathway, as proposed from the phenotype observations, it is possible that *Megalin* may also serve as an BMP inhibitor as it does in the developing brain (Spoelgen et al., 2005).

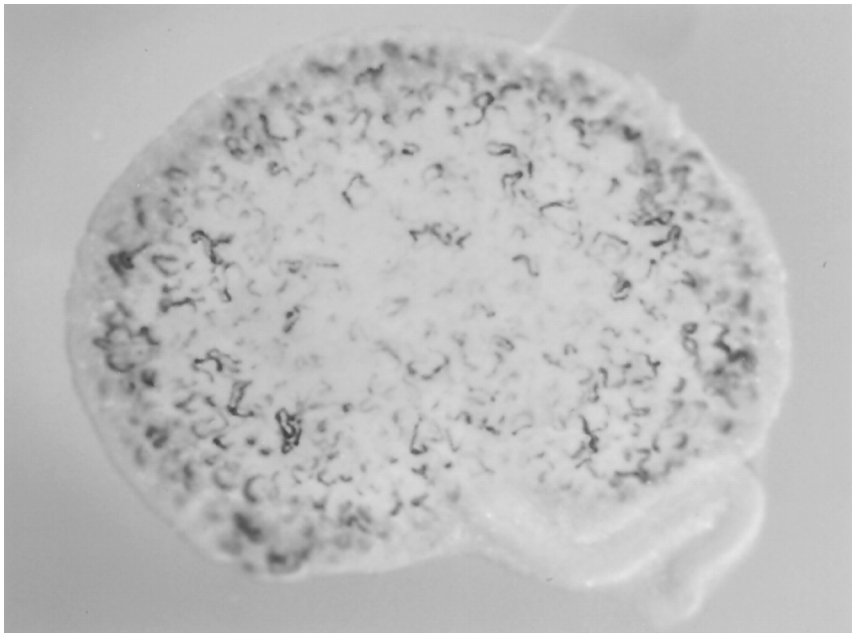

Figure 61 *Megalin* Expression in the Developing Kidney
Wholemount *in situ* analysis for *Megalin* expression in an E15.5 kidney. Taken from Yamagata et al. 2001.

A double knockout of *Megf7* and *Megalin* can be made to see if *Megalin* compensates for the loss of *Megf7* in the knockout kidney. We should be able to observe kidney development in the double knockout because *Megalin* knockouts are viable past E12.5 (Willnow et al., 1996). A conditional allele is also available in case *Megalin* synergizes with *Megf7* in the development of an organ that is required for earlier viability (Spoelgen et al., 2005). If *Megalin* compensates for the loss of *Megf7*, the double knockout should have a higher rate of kidney agenesis than the single *Megf7* knockout.

We hypothesize that *Megf7* inhibits the BMP signaling pathway based on the similarity of the *Megf7* knockout phenotype to other BMP mutant phenotypes. If *Megf7* is an inhibitor of the BMP pathway, the *Megf7* knockout should have increased BMP signaling in the developing kidney. This is similar to what is seen in the *Megf7* knockout limb. The only

difference being the limb has an increase in Wnt signaling and the kidney has an increase in BMP signaling. The activity of the BMP pathway can be tested by staining tissue sections with anti-phosphoSMAD antibodies. Phosphorylated SMAD is the main downstream signaling component of the BMP, and other TGF, signaling pathway. We would predict that there would be an increase in nuclear phosphorylated SMAD in the nuclei of the cells in the developing *Megf7* knockout kidney.

Another way to test the hypothesis of BMP inhibition by *Megf7* is to replace *Megf7*'s activity with another BMP inhibitor. Proteins such as Gremlin1, which have been shown to be inhibitors of the BMP pathway, can be ectopically expressed using multiple methods. One way to express an ectopic inhibitor is to make a transgenic mouse line that expresses the inhibitor under the control of a kidney-specific promoter. The BMP inhibitor can also be placed in the developing kidney by surgically inserting inhibitor expressing cells or inhibitor soaked beads into the region of kidney development. The experiments using cells or beads would be facilitated by performing the experiment using *in vitro* explant cultures. Replacing the BMP inhibitor into the kidney of a *Megf7* knockout embryo should increase the frequency of kidney formation if the function of *Megf7* is to inhibit the BMP pathway.

Functional Regions within Megf7

There is very limited information concerning the ligands of Megf7. Expression of the extracellular domain of Megf7 shows that Rap can bind but Mesd2 cannot bind to Megf7 (Figure 62). It is also assumed that Megf7 can bind to ApoE just like all other members of

the LDL receptor gene family. Otherwise, the identity of the other Megf7 ligands is unknown.

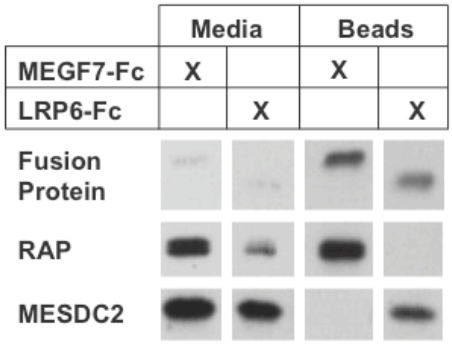

Figure 62 Binding of Megf7 to Rap and Mesd2

Fc fusion proteins of either Megf7 or Lrp6 were co-expressed with Rap and Mesd2 (lanes 1,2). Rap remains bound to Megf7-Fc (lane 3) whereas Mesd2 remains bound to Lrp6-Fc (lane 4).

So far, all *in vitro* evidence indicates that Megf7 interacts with the Wnt signaling pathway, which suggests that Megf7 may bind to Wnt proteins. This idea is supported by the fact that all of the LDLR gene family members that can modulate the Wnt signaling pathway, Megf7, Lrp1 and Lrp5/6, have four consecutive EGF-precursor homology domains. This suggests that perhaps all of these genes are derived from exon duplication and rearrangement of an ancestral "Lrp" gene that had a Wnt binding capacity within the common four EGF-precursor homology domains (Figure 63). Further binding studies using candidate and screening methods will be needed to identify the ligands for Megf7.

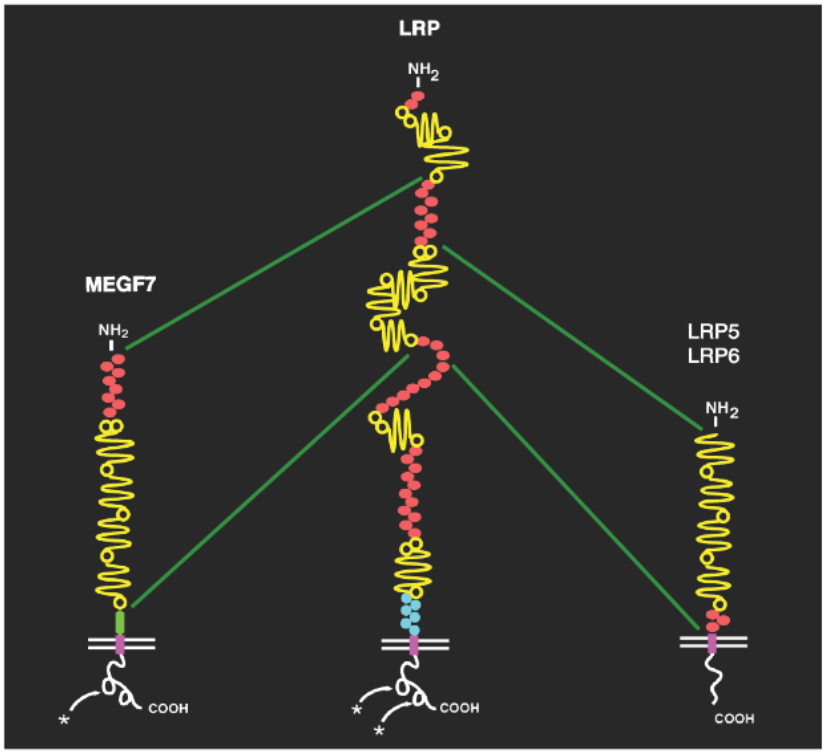

Figure 63 Common Putative Wnt binding Domains

All of the genes in the LDLR gene that can modulate the Wnt signaling pathway contain four consecutive EGF precursor homology domains. These domains may contain a binding site for a Wnt modulating protein.

Megf7 Ligands

A binding assay can be developed if Megf7 is a receptor for a Wnt modulating protein such as the Wnt proteins themselves or secreted modulators such as Wise and Dkk1. As proposed by Dr. Joseph Goldstein, a chimeric receptor can be used to create a binding assay using well-established protocols. A Lrp6/Megf7 chimera can be generated in which the extracellular region of Megf7 is fused to the transmembrane and intracellular region of Lrp6. This chimeric protein can then be used in the TOPflash Wnt reporter assay as described in Chapter 2. If a protein binds to the extracellular region of the Megf7/Lrp6 chimera, it will

activate the canonical Wnt pathway and produce a positive signal. Conditioned media containing the protein of interest can be added to cell expressing the chimeric protein and binding can be assayed with luciferase expression. This assay may also work with proteins that are not involved in the Wnt signaling pathway. This approach eliminates the need to understand the signaling properties of *Megf7* before performing *in vitro* binding assays.

We currently have several proteins that are candidates as binding partners of Megf7 including the Wnts, BMPs, RSpondins, Wise, and Gremlin1. These candidates are based on the interpretation of the available phenotypic data. Binding assays are currently being performed to try to isolate which of these proteins are involved in the function of Megf7. Various methods are being employed using full-length Megf7 as well as Megf7 fused to the Fc region of Human IgG. The IgG fusion can be used to precipitate bound proteins using protein A or protein G. Other assays can also be used to detect binding to Megf7. Surface plasmon resonance can be used to detect the binding of candidate proteins. One shortfall of this assay is that relatively large quantities of purified Megf7 protein is required to perform the assay.

A blind approach can also be used to identify Megf7 ligands. An affinity column can be made using purified Megf7. I already attempted to generate purified full-length extracellular region of Megf7. The expression level of the different systems that I used (stable HEK293 cells and bacculovirus expression) was relatively low and did not provide enough protein to make an affinity column. Two different approached can be used to generate more protein. One approach would involve the expression of portions of the extracellular region of Megf7 using the bacculovirus system. One problem with what I did

was that the insect cells had difficulty expressing a 200kD protein in large quantities. A 6xHis tag purification protocol may be more efficient than the human Fc/ protein A protocol used previously. Another approach would involve expressing a membrane bound form of Megf7 with a carboxy-teminal 6XHis tag using the bacculovirus system. The purification of His tagged proteins is much easier if the protein is expressed in cells rather than the media.

Megf7 and Endocytosis

The evidence from the different knockin mice that I generated suggests that Megf7 has endocytic activity (Figure 64). Most of the specific mutations introduced into the cypolasmic region of *Megf7*, $Megf7^{NPSY\ KI}$, $Megf7^{AS\ KI}$, $Megf7^{PDZ\ KI}$, $Megf7^{WT\ KI}$, failed to generate mice with limb defects. As far as we can tell there are no gross defects in these mutants in both the homozygous or compound heterozygous state. The $Megf7^{Myc\ KI}$ mutant has syndactyly in the homozygous state and more severe polysyndactyly in the compound heterozygotes. The limb defects in the $Megf7^{Myc\ KI}$ mutant was expected because this mutant eliminates all putative intracellular signaling motifs of *Megf7*. Only when you replace the cytoplasmic tail with the LDL Receptor cytoplasmic tail, the only known function of which is to mediate endocytosis, is the function of *Megf7* recovered. Therefore, it is likely that the function of Megf7 is to endocytose a secreted protein.

Phenotypic strength of the allelic series of *Lrp4/Megf7* mutants

	WT KI	AS KI	PDZ KI	NPSY KI	LDLR KI	Myc KI	EC Stop	KO
Limb	-	-	-	-	+	++	+++	+++
Kidney	-	-	-	-	-	-	-	+
Neuromuscular Junction	-	-	-	-	-	-	+	++
Teeth	-	-	-	-	-	-	+	+?
Mammary Gland	-	-	-	-	-	-	+	+?

Figure 64 Organ Defects in *Megf7* Knockin Mutants

Summary of the severity of all of the developmental defects found in the *Megf7* mutant mice. Severity ranges from normal (-) to mild (+) to extreme (+++).

Again, a chimeric Megf7 protein can be used to analyze endocytic activity. A LDL Receptor/Megf7 chimera can be generated by fusing the extrecellular region of the LDL Receptor to the cytoplasmic region of Megf7. This cloning reaction can be facilitated with the pLDLR17-NarI plasmid that has a NarI site mutated into the LDLR cDNA between the transmembrane region and the cytoplasmic region. Well-established endocytosis assays used for the LDLR can then be performed using the chimeric protein. It would suggest that Megf7 has endoctyic activity if internalization is observed with the chimeric protein. The chimeric protein also eliminates the need to know the identity of the ligands for Megf7.

A GFP linked form of Megf7 can also be used to observe endocytosis. In this experiment, the ligand for Megf7 would need to be known. Upon application of the ligand to cells expressing the GFP fusion protein, the GFP signal should move from the plasma

membrane to intracellular vesicles. The fusion protein would be a carboxy-teminal fusion. This would block the putative PDZ consensus motif of Megf7. Therefore, any contribution toward endocytosis by this motif would be lost. An alternative approach to this assay would be to use fluorescently labeled ligand. Again, the identity of the ligand would need to be known.

Another tool to analyze the endocytic function of Megf7 is the TOPflash assay. This assay is one of the few assays that has been used to detect Megf7 activity. There are multiple putative endocytic motifs within he cytoplasmic region of Megf7. As described in the Introduction, there are two EXXXLL motifs, one NPXY motif, and one YXXL motif that can be used by Megf7 to induce endocytosis. All of these motifs can be mutated in the cDNA of Megf7 and tested in the TOPflash. A decrease of activity in one of these mutants would suggest a role in endocytosis. It is likely, however, that these motifs may be redundant. This redundancy would require the mutagenesis of combinations of the motifs to lead to complete loss of activity.

Megf7 May Provide a Signaling Bias

The differences in the phenotypes seen between the hypomorphic *Megf7*$^{EC\ Stop}$ mutant and the *Megf7*^{KO} allele suggests that the *Megf7*$^{EC\ Stop}$ allele produces a partially functional protein product. The residual activity in the *Megf7*$^{EC\ Stop}$ allele may be sufficient to satisfy the needs of the developing kidney, heart, lungs, nervous system or any other unknown organ system that is differentially affected between the *Megf7*^{KO} and *Megf7*$^{EC\ Stop}$ mutant.

The ability of the *Megf7*$^{EC\ Stop}$ protein product to rescue the kidney and neuromuscular defects seen in the *Megf7*^{KO} embryo suggests that *Megf7* provides a bias in cell fate relative to the surrounding cells. In these instances, only a slight amount of *Megf7* activity is sufficient to provide patterning information in the kidney and the neuromuscular junction. This bias may be similar to several developmental examples where initial patterning occurs at random. Slight variations in the protein concentration or activity may lead to a polarization due to the subsequent actions of feed-forward and feed-back mechanisms. Thus, a slight bias leads to the initial patterning step.

One example of this type of mechanism of bias formation can be seen in the differentiation of the R3/R4 photoreceptors in the drosophila eye. In this system, the two cells initially express equivalent amounts of Notch and Delta. Delta is the ligand for Notch and Notch activation in turn inhibits the expression of Delta. A slight difference in Frizzled activity, which activates the expression of Delta, is found in the cell that is closest to the equator of the eye. This slight difference creates a bias of signaling for one photoreceptor cell over another and initiates the system of feed-back and feed-forward signaling. This bias ultimately results in the complete activation of Notch, inhibition of Delta, and activation of R4 specific genes in the R4 photoreceptor cell (Strutt & Strutt, 1999).

A similar mechanism may be in place using *Megf7*. *Megf7* may play a role in establishing a bias of one cell population over another. The bias is then amplified by other feed-forward mechanisms to establish the final tissue patterning. Therefore, only a little *Megf7* activity may be required to tip the scales in favor of the appropriate signal. In the case of the developing limbs, more *Megf7* activity may be needed compared to the kidneys, lungs,

heart, nervous system, etc. Conversely, *Megf7* may have a completely different role in the limbs whereas the other tissues may require the gene for establishing a bias between cells.

Common Patterning Mechanisms by Megf7

So far, the regulation of limb, tooth, and kidney development by *Megf7* has been analyzed extensively in this thesis. The function of *Megf7* in mammary gland development has been analyzed superficially in this lab and the function of *Megf7* in neuromuscular junction development has been analyzed extensively by another lab. Even though these organ systems are very different, there are some common mechanisms used during their development. For instance, many of the same gene families involved in patterning such as Wnt, BMP, FGF, SHH, Notch, etc. play a role in the development of these organs. There may be a common patterning mechanism involved in all of these developmental systems that is regulated by *Megf7*.

One clue may come from the expression pattern of *Megf7* itself. In the cases where the expression of *Megf7* expression has been extensively analyzed (the limb, tooth, kidney, and neuromuscular junction) there is a diffuse or weak generalized expression during early development that resolves to a more distinct pattern later during development. This suggests that the expression of *Megf7* is resolved to a particular region of developing tissue through a positive feedback mechanism. The expression of *Megf7* then provides the positional information for the development of the AER, the tooth anlage, the ureteric bud, or the neuromuscular junction (Figure 65).

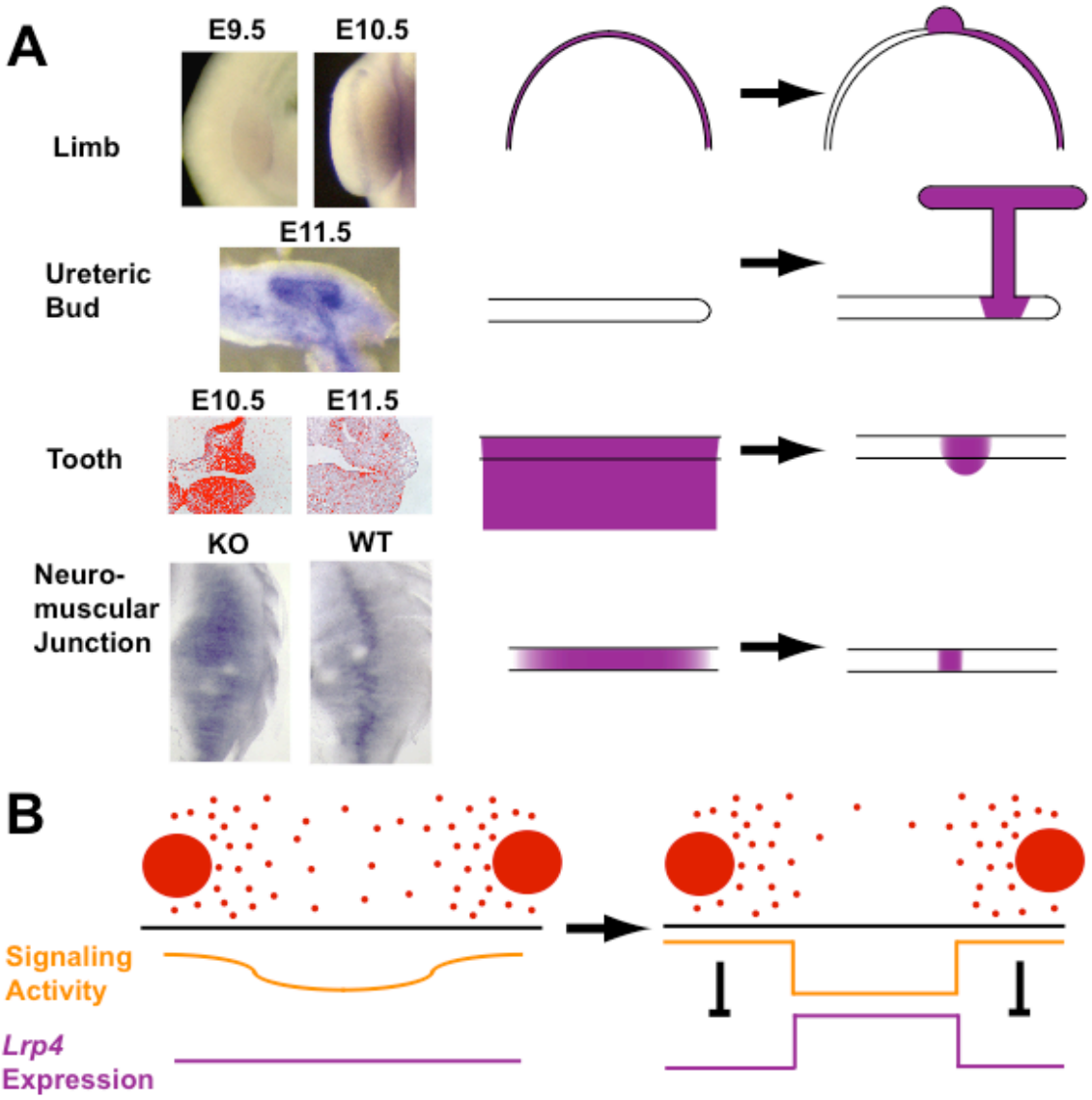
A
E9.5
E10.5
Limb
E11.5
Ureteric Bud
E10.5
E11.5
Tooth
KO
WT
Neuro-muscular Junction
B
Signaling Activity
Lrp4 Expression

Figure 65 Model of the Mechanism of Patterning by *Megf7*

(previous page)(A, left) Expression of *Megf7* in the limb, ureteric bud, tooth anlage, and diaphragm showing the diffuse pattern of expression early during development and a more restricted pattern later during development. (A, right) Diagram of the patterning of *Megf7* expression as development progresses. (B) Proposed model of *Megf7* regulation. Sources of morphogens (red) will produce a morphogen gradient along which there is a spectrum of morphogen intracellular signaling activity (yellow). At early stages, the expression of *Megf7* is low and diffuse. Later during development, the endocytosis of morphogens by Megf7 eliminates morphogen signaling distal to the morphogen source but does not significantly affect signaling proximal to the morphogen source. The high morphogen signaling proximal to the source in turn inhibits the expression of *Megf7*.

The data from the *Megf7*$^{LDLR\ KI}$ mice showing that the LDL receptor cytoplasmic tail can almost completely replace the function of the Megf7 cytoplasmic tail suggests that Megf7 may serve as an endocytic inhibitor of signaling molecules. Therefore, it is possible that the function of *Megf7* is to "sharpen" morphogen gradients. As diagramed in Figure 65B, Megf7 may reduce the total amount of morphogen that is present in the extracellular compartment at an early developmental stage. This could then reduce the morphogen below the effective concentration required to activate the intracellular signaling pathway. If the signaling pathway activated by the morphogen in turn inhibits *Megf7* expression, a feed back mechanism will resolve expression to a particular distance from the morphogen source and thus provide positional information for *Megf7* expression.

This mechanism of morphogen gradient regulation may be a way for the developing organism to create more patterning information using the same morphogens in different organs. *Megf7* may regulate the amount of morphogen that is exposed to each cell and can also regulate the distance that a particular morphogen can travel by reducing the diffusion

rate or half-life. Loss of *Megf7* may result in a higher basal morphogen signal that may result in the failure to form a structure, in the case of the ureteric bud, or may reduce the definition of borders, in the case of the AER and the neuromuscular junction.

The modulation of a gradient of signaling activity can be observed with several experimental models. In all experimental models, there is a source of a morphogen such as a Wnt or a BMP. The experiments can be done in the presence or absence of *Megf7*. The distance that the morphogen can travel can be measured through the downstream signaling pathway.

One way to examine the effect that *Megf7* has on morphogen gradients is to introduce an external source of morphogen such as a protein soaked bead or transplanted cells that express the morphogen. The morphogen can also be expressed with a viral expression construct. A reporter transgenic mouse strain, such as the BATgal mouse, can be used to measure the distance the morphogen travels. If *Megf7* sharpens the Wnt singaling gradient, the distance that the morphogen travels, as detected by β-galactosidase expression, should be less in the wild type embryos compared to the knockout embryos. If a *Megf7* deficient Drosophila stock is available, this experiment can be performed using the conditional deletion or expression of a morphogen and detect the distance that the morphogen travels. The Drosophila system appears to be better characterized for this analysis. The same test for regulation of the morphogen gradient can be done with other morphogens. The main limitation of this assay is that you would need to know the identity of the morphogen that is regulated by *Megf7*.

Functional Motifs Present within the Cytoplasmic Domain of Megf7

The function of the different regions within the cytoplasmic domain has been difficult to unravel. There are five putative regulatory elements within the cytoplasmic domain of Megf7: the PDZ consensus binding sequence, the NPXY motif, the YXXL motif, and the two [DE]XXXL[LI] motifs. The deletion of the cytoplasmic domain in the *Megf7*$^{Myc\ KI}$ allele suggests that the cytoplasmic domain probably has some endocytic function because the *Megf7*$^{LDLR\ KI}$ allele, which was designed to replace endocytic activity to the *Megf7* cytoplasmic region, is able to provide the activity to recover the wild type phenotype. The proteins and interaction sites that regulate this function, and any unknown function, are unknown at the moment.

The majority of the functional evidence has focused on the PDZ domain consensus binding sequence at the carboxy-terminus of the cytoplasmic domain of Megf7. We published that several proteins can bind through their PDZ domains to the tail of Megf7 in a yeast two-hybrid assay (Johnson et al., 2006). Others have also reported that PSD-95, a PDZ protein involved in organizing the post-synaptic compartment in neurons, can bind to Megf7 in a phosphorylation-dependent manner (Tian et al., 2006). It is currently unknown if the other proteins that bind to Megf7 through their PDZ domains actually interact *in vivo*. At least in terms of limb development, the interaction with PDZ proteins is not required as indicated by the phenotype of the *Megf7*$^{PDZ\ KI}$ mice. Also, PDZ domains are known for being very promiscuous in binding assays, especially sensitive assays like the yeast two-hybrid assay.

Currently, there is no known function for the NPXY, YXXL, or [DE]XXXL[LI] motifs present within the cytoplasmic domain of Megf7. The *Megf7*$^{NPSY\ KI}$ mouse allele eliminates the NPXY motif and yet its phenotype appears normal. Also, the *Megf7*$^{AS\ KI}$ mouse has a wild type phenotype and yet this allele removes the two [DE]XXXL[LI] motifs present in the cytoplasmic domain. The YXXL motif is the only motif present that has not been mutated in *Megf7 in vivo*.

I would not expect a mutant *Megf7* allele that removes the YXXL motif to have an abnormal phenotype. The absence of an abnormal phenotype in the *Megf7*$^{NPSY\ KI}$ and the *Megf7*$^{AS\ KI}$ mice suggests that there may be functional redundancy with the different endocytic motifs. The loss of one endocytic motif may not significantly affect the function of Megf7 if cells use multiple motifs for endocytosis. Although, there may be a cell type that only uses one motif for the endocytosis of Megf7. The different knockin alleles may have an abnormal phenotype in that particular organ. But, currently there is not an organ system that would fit those criteria.

There may be other putative functional regions within the cytoplasmic domain of Megf7. There are regions that may be regulated by phosphorylation or ubiquitination. It is difficult to determine if there are regions that may be post-translationally modified. For instance, the ubiquitination or sumoylation of the cytoplasmic tail is dependent on a particular E3-ubiquitin ligase. Determining the motif recognized by a ligase without any empirical data is nearly impossible. Indeed, there are many serines, threonines, and lysines present in the tail of Megf7 that are subject to post-translational modification.

Discovering Megf7 Mutants in Humans

The abundance of natural and experimentally produced mutants in *Megf7* suggests that there may be humans with *Megf7* mutations. With the initial discovery of the phenotype of the $Megf7^{EC\ Stop}$ mutant, we went to clinicians in the Dallas area to see if we could find human mutants. Unfortunately, we asked the clinicians if they had patients that were similar to the $Megf7^{EC\ Stop}$ phenotype, with severe polysyndactyly. They were not able to find patients with such extreme polysyndactyly with unknown etiology.

Since then, we have found that other hypomorphic mutations in *Megf7* have a less severe phenotype such as polydactyly and syndactyly. It may be worth re-examining human patients to see if milder forms of autopod defects may be associated with mutations in *Megf7*. Cases of oligodontia may also account for some of the human *Megf7* mutations. The phenotype of the *Megf7* null allele also suggests that there may be cases of stillborn infants with mutations in the gene.

Recently, we were informed through a personal communication from Bernd Wollnik that human *Megf7* mutations have been found. Analysis of these patients may provide more insight into the function of *Megf7*. They may provide clues about the function of *Megf7* in the adult organism. Considering the close association of the LDLR gene family and the susceptibility to neurodegeneration, it would be interesting to see if these human mutants are more susceptible to the development of Alzheimer's Disease.

This work has opened new fields of investigation in several important aspects of biology. *Megf7* may prove to be a major regulator both during development but also during homeostasis and disease in the adult.

BIBLIOGRAPHY

ADAMSKA, M., MACDONALD, B. T. & MEISLER, M. H. (2003). Doubleridge, a mouse mutant with defective compaction of the apical ectodermal ridge and normal dorsal-ventral patterning of the limb. *Dev Biol* **255,** 350-62.

ALKEMA, M. J., JACOBS, J., VONCKEN, J. W., JENKINS, N. A., COPELAND, N. G., SATIJN, D. P., OTTE, A. P., BERNS, A. & VAN LOHUIZEN, M. (1997). MPc2, a new murine homolog of the Drosophila polycomb protein is a member of the mouse polycomb transcriptional repressor complex. *J Mol Biol* **273,** 993-1003.

BAFICO, A., LIU, G., YANIV, A., GAZIT, A. & AARONSON, S. A. (2001). Novel mechanism of Wnt signalling inhibition mediated by Dickkopf-1 interaction with LRP6/Arrow. *Nat Cell Biol* **3,** 683-6.

BALLA, T. (2005). Inositol-lipid binding motifs: signal integrators through protein-lipid and protein-protein interactions. *J Cell Sci* **118,** 2093-104.

BARROW, J. R., THOMAS, K. R., BOUSSADIA-ZAHUI, O., MOORE, R., KEMLER, R., CAPECCHI, M. R. & MCMAHON, A. P. (2003). Ectodermal Wnt3/beta-catenin signaling is required for the establishment and maintenance of the apical ectodermal ridge. *Genes Dev* **17,** 394-409.

BEFFERT, U., DURUDAS, A., WEEBER, E. J., STOLT, P. C., GIEHL, K. M., SWEATT, J. D., HAMMER, R. E. & HERZ, J. (2006). Functional dissection of Reelin signaling by site-directed disruption of Disabled-1 adaptor binding to apolipoprotein E receptor 2: distinct roles in development and synaptic plasticity. *J Neurosci* **26,** 2041-52.

BLISKOVSKI, V., LIDDELL, R., RAMSAY, E. S., MILLER, M. J. & MOCK, B. A. (2000). Structure and localization of mouse Pmscl1 and Pmscl2 genes. *Genomics* **64,** 106-10.

BONIFACINO, J. S. & TRAUB, L. M. (2003). Signals for sorting of transmembrane proteins to endosomes and lysosomes. *Annu Rev Biochem* **72,** 395-447.

BORELLO, U., BUFFA, V., SONNINO, C., MELCHIONNA, R., VIVARELLI, E. & COSSU, G. (1999). Differential expression of the Wnt putative receptors Frizzled during mouse somitogenesis. *Mech Dev* **89,** 173-7.

BORG, J. P., MARCHETTO, S., LE BIVIC, A., OLLENDORFF, V., JAULIN-BASTARD, F., SAITO, H., FOURNIER, E., ADELAIDE, J., MARGOLIS, B. & BIRNBAUM, D. (2000).

ERBIN: a basolateral PDZ protein that interacts with the mammalian ERBB2/HER2 receptor. *Nat Cell Biol* **2,** 407-14.

BOUCHER, P., GOTTHARDT, M., LI, W. P., ANDERSON, R. G. & HERZ, J. (2003). LRP: role in vascular wall integrity and protection from atherosclerosis. *Science* **300,** 329-32.

BOUCHER, P., LIU, P., GOTTHARDT, M., HIESBERGER, T., ANDERSON, R. G. & HERZ, J. (2002). Platelet-derived growth factor mediates tyrosine phosphorylation of the cytoplasmic domain of the low Density lipoprotein receptor-related protein in caveolae. *J Biol Chem* **277,** 15507-13.

BROTT, B. K. & SOKOL, S. Y. (2002). Regulation of Wnt/LRP signaling by distinct domains of Dickkopf proteins. *Mol Cell Biol* **22,** 6100-10.

BROW, D. A. (2002). Allosteric cascade of spliceosome activation. *Annu Rev Genet* **36,** 333-60.

CAM, J. A. & BU, G. (2006). Modulation of beta-amyloid precursor protein trafficking and processing by the low density lipoprotein receptor family. *Mol Neurodegener* **1,** 8.

CAPDEVILA, J. & IZPISUA BELMONTE, J. C. (2001). Patterning mechanisms controlling vertebrate limb development. *Annu Rev Cell Dev Biol* **17,** 87-132.

CARROLL, T. J., PARK, J. S., HAYASHI, S., MAJUMDAR, A. & MCMAHON, A. P. (2005). Wnt9b plays a central role in the regulation of mesenchymal to epithelial transitions underlying organogenesis of the mammalian urogenital system. *Dev Cell* **9,** 283-92.

CHARLIER, C., FARNIR, F., BERZI, P., VANMANSHOVEN, P., BROUWERS, B., VROMANS, H. & GEORGES, M. (1996). Identity-by-descent mapping of recessive traits in livestock: application to map the bovine syndactyly locus to chromosome 15. *Genome Res* **6,** 580-9.

CHEN, Y., BEFFERT, U., ERTUNC, M., TANG, T. S., KAVALALI, E. T., BEZPROZVANNY, I. & HERZ, J. (2005). Reelin modulates NMDA receptor activity in cortical neurons. *J Neurosci* **25,** 8209-16.

CHRISTIANSEN, J. H., DENNIS, C. L., WICKING, C. A., MONKLEY, S. J., WILKINSON, D. G. & WAINWRIGHT, B. J. (1995). Murine Wnt-11 and Wnt-12 have temporally and spatially restricted expression patterns during embryonic development. *Mech Dev* **51,** 341-50.

CULI, J. & MANN, R. S. (2003). Boca, an endoplasmic reticulum protein required for wingless signaling and trafficking of LDL receptor family members in Drosophila. *Cell* **112,** 343-54.

CYGAN, J. A., JOHNSON, R. L. & MCMAHON, A. P. (1997). Novel regulatory interactions revealed by studies of murine limb pattern in Wnt-7a and En-1 mutants. *Development* **124,** 5021-32.

DASGUPTA, R. & FUCHS, E. (1999). Multiple roles for activated LEF/TCF transcription complexes during hair follicle development and differentiation. *Development* **126,** 4557-68.

DAVIES, J. A. & GARROD, D. R. (1995). Induction of early stages of kidney tubule differentiation by lithium ions. *Dev Biol* **167,** 50-60.

DAVIS, C. G., ELHAMMER, A., RUSSELL, D. W., SCHNEIDER, W. J., KORNFELD, S., BROWN, M. S. & GOLDSTEIN, J. L. (1986). Deletion of clustered O-linked carbohydrates does not impair function of low density lipoprotein receptor in transfected fibroblasts. *J Biol Chem* **261,** 2828-38.

DAVIS, C. G., VAN DRIEL, I. R., RUSSELL, D. W., BROWN, M. S. & GOLDSTEIN, J. L. (1987). The low density lipoprotein receptor. Identification of amino acids in cytoplasmic domain required for rapid endocytosis. *J Biol Chem* **262,** 4075-82.

DEALY, C. N., ROTH, A., FERRARI, D., BROWN, A. M. & KOSHER, R. A. (1993). Wnt-5a and Wnt-7a are expressed in the developing chick limb bud in a manner suggesting roles in pattern formation along the proximodistal and dorsoventral axes. *Mech Dev* **43,** 175-86.

DECHIARA, T. M., BOWEN, D. C., VALENZUELA, D. M., SIMMONS, M. V., POUEYMIROU, W. T., THOMAS, S., KINETZ, E., COMPTON, D. L., ROJAS, E., PARK, J. S., SMITH, C., DISTEFANO, P. S., GLASS, D. J., BURDEN, S. J. & YANCOPOULOS, G. D. (1996). The receptor tyrosine kinase MuSK is required for neuromuscular junction formation in vivo. *Cell* **85,** 501-12.

DROGEMULLER, C. & DISTL, O. (2006). Genetic analysis of syndactyly in German Holstein cattle. *Vet J* **171,** 120-5.

DROGEMULLER, C., LEEB, T., HARLIZIUS, B., TAMMEN, I., DISTL, O., HOLTERSHINKEN, M., GENTILE, A., DUCHESNE, A. & EGGEN, A. (2007). Congenital syndactyly in cattle: four novel mutations in the low density lipoprotein receptor-related protein 4 gene (LRP4). *BMC Genet* **8,** 5.

DUCHESNE, A., GAUTIER, M., CHADI, S., GROHS, C., FLORIOT, S., GALLARD, Y., CASTE, G., DUCOS, A. & EGGEN, A. (2006). Identification of a doublet missense

substitution in the bovine LRP4 gene as a candidate causal mutation for syndactyly in Holstein cattle. *Genomics*.

DUDLEY, A. T., GODIN, R. E. & ROBERTSON, E. J. (1999). Interaction between FGF and BMP signaling pathways regulates development of metanephric mesenchyme. *Genes Dev* **13,** 1601-13.

DUDLEY, A. T., LYONS, K. M. & ROBERTSON, E. J. (1995). A requirement for bone morphogenetic protein-7 during development of the mammalian kidney and eye. *Genes Dev* **9,** 2795-807.

DUDLEY, A. T. & ROBERTSON, E. J. (1997). Overlapping expression domains of bone morphogenetic protein family members potentially account for limited tissue defects in BMP7 deficient embryos. *Dev Dyn* **208,** 349-62.

FASS, D., BLACKLOW, S., KIM, P. S. & BERGER, J. M. (1997). Molecular basis of familial hypercholesterolaemia from structure of LDL receptor module. *Nature* **388,** 691-3.

GOLDSTEIN, J. L., HOBBS, H. H. & BROWN, M. S. (2001). Familial hypercholesterolemia. In *Eds.) Metabolic and Molecular Bases of Inherited Disease* (ed. C. R. B. Scriver, A.L. Sly, W.S. Valle, D. Childs B. Kinzler, K.W. Vogelstein, B.), pp. 2863–2913. McGraw–Hill, New York.

GOODMAN, F. R. (2002). Limb malformations and the human HOX genes. *Am J Med Genet* **112,** 256-65.

GOTTHARDT, M., HAMMER, R. E., HUBNER, N., MONTI, J., WITT, C. C., MCNABB, M., RICHARDSON, J. A., GRANZIER, H., LABEIT, S. & HERZ, J. (2003). Conditional expression of mutant M-line titins results in cardiomyopathy with altered sarcomere structure. *J Biol Chem* **278,** 6059-65.

GOTTHARDT, M., TROMMSDORFF, M., NEVITT, M. F., SHELTON, J., RICHARDSON, J. A., STOCKINGER, W., NIMPF, J. & HERZ, J. (2000). Interactions of the low density lipoprotein receptor gene family with cytosolic adaptor and scaffold proteins suggest diverse biological functions in cellular communication and signal transduction. *J Biol Chem* **275,** 25616-24.

GREEN, M. C. (1968). Mechanism of the pleiotropic effects of the short-ear mutant gene in the mouse. *J Exp Zool* **167,** 129-50.

HARTWIG, S., HU, M. C., CELLA, C., PISCIONE, T., FILMUS, J. & ROSENBLUM, N. D. (2005). Glypican-3 modulates inhibitory Bmp2-Smad signaling to control renal development in vivo. *Mech Dev* **122,** 928-38.

HERZ, J., CLOUTHIER, D. E. & HAMMER, R. E. (1992). LDL receptor-related protein internalizes and degrades uPA-PAI-1 complexes and is essential for embryo implantation. *Cell* **71,** 411-21.

HERZLINGER, D., QIAO, J., COHEN, D., RAMAKRISHNA, N. & BROWN, A. M. (1994). Induction of kidney epithelial morphogenesis by cells expressing Wnt-1. *Dev Biol* **166,** 815-8.

HILPERT, J., NYKJAER, A., JACOBSEN, C., WALLUKAT, G., NIELSEN, R., MOESTRUP, S. K., HALLER, H., LUFT, F. C., CHRISTENSEN, E. I. & WILLNOW, T. E. (1999). Megalin antagonizes activation of the parathyroid hormone receptor. *J Biol Chem* **274,** 5620-5.

HSIEH, J. C., LEE, L., ZHANG, L., WEFER, S., BROWN, K., DEROSSI, C., WINES, M. E., ROSENQUIST, T. & HOLDENER, B. C. (2003). Mesd encodes an LRP5/6 chaperone essential for specification of mouse embryonic polarity. *Cell* **112,** 355-67.

HUCZ, J., KOWALSKA, M., JARZAB, M. & WIENCH, M. (2006). [Gene expression of metalloproteinase 11, claudin 1 and selected adhesion related genes in papillary thyroid cancer.]. *Endokrynol Pol* **57,** 18-25.

HUNG, A. Y. & SHENG, M. (2002). PDZ domains: structural modules for protein complex assembly. *J Biol Chem* **277,** 5699-702.

ITARANTA, P., LIN, Y., PERASAARI, J., ROEL, G., DESTREE, O. & VAINIO, S. (2002). Wnt-6 is expressed in the ureter bud and induces kidney tubule development in vitro. *Genesis* **32,** 259-68.

JAFFREY, S. R., SNOWMAN, A. M., ELIASSON, M. J., COHEN, N. A. & SNYDER, S. H. (1998). CAPON: a protein associated with neuronal nitric oxide synthase that regulates its interactions with PSD95. *Neuron* **20,** 115-24.

JARZAB, B., WIENCH, M., FUJAREWICZ, K., SIMEK, K., JARZAB, M., OCZKO-WOJCIECHOWSKA, M., WLOCH, J., CZARNIECKA, A., CHMIELIK, E., LANGE, D., PAWLACZEK, A., SZPAK, S., GUBALA, E. & SWIERNIAK, A. (2005). Gene expression profile of papillary thyroid cancer: sources of variability and diagnostic implications. *Cancer Res* **65,** 1587-97.

JEON, H., MENG, W., TAKAGI, J., ECK, M. J., SPRINGER, T. A. & BLACKLOW, S. C. (2001). Implications for familial hypercholesterolemia from the structure of the LDL receptor YWTD-EGF domain pair. *Nat Struct Biol* **8,** 499-504.

JOHNSON, E. B., HAMMER, R. E. & HERZ, J. (2005). Abnormal development of the apical ectodermal ridge and polysyndactyly in Megf7-deficient mice. *Hum Mol Genet* **14,** 3523-38.

JOHNSON, E. B., STEFFEN, D. J., LYNCH, K. W. & HERZ, J. (2006). Defective splicing of Megf7/Lrp4, a regulator of distal limb development, in autosomal recessive mulefoot disease. *Genomics* **88,** 600-9.

JONES, C., HAMMER, R. E., LI, W. P., COHEN, J. C., HOBBS, H. H. & HERZ, J. (2003). Normal sorting but defective endocytosis of the low density lipoprotein receptor in mice with autosomal recessive hypercholesterolemia. *J Biol Chem* **278,** 29024-30.

KAGEY, M. H., MELHUISH, T. A. & WOTTON, D. (2003). The polycomb protein Pc2 is a SUMO E3. *Cell* **113,** 127-37.

KASSAI, Y., MUNNE, P., HOTTA, Y., PENTTILA, E., KAVANAGH, K., OHBAYASHI, N., TAKADA, S., THESLEFF, I., JERNVALL, J. & ITOH, N. (2005). Regulation of mammalian tooth cusp patterning by ectodin. *Science* **309,** 2067-70.

KENGAKU, M., CAPDEVILA, J., RODRIGUEZ-ESTEBAN, C., DE LA PENA, J., JOHNSON, R. L., BELMONTE, J. C. & TABIN, C. J. (1998). Distinct WNT pathways regulating AER formation and dorsoventral polarity in the chick limb bud. *Science* **280,** 1274-7.

KIMMEL, R. A., TURNBULL, D. H., BLANQUET, V., WURST, W., LOOMIS, C. A. & JOYNER, A. L. (2000). Two lineage boundaries coordinate vertebrate apical ectodermal ridge formation. *Genes Dev* **14,** 1377-89.

KINGSLEY, D. M. (1994). What do BMPs do in mammals? Clues from the mouse short-ear mutation. *Trends Genet* **10,** 16-21.

KISPERT, A., VAINIO, S. & MCMAHON, A. P. (1998). Wnt-4 is a mesenchymal signal for epithelial transformation of metanephric mesenchyme in the developing kidney. *Development* **125,** 4225-34.

KISPERT, A., VAINIO, S., SHEN, L., ROWITCH, D. H. & MCMAHON, A. P. (1996). Proteoglycans are required for maintenance of Wnt-11 expression in the ureter tips. *Development* **122,** 3627-37.

LAUFER, E., DAHN, R., OROZCO, O. E., YEO, C. Y., PISENTI, J., HENRIQUE, D., ABBOTT, U. K., FALLON, J. F. & TABIN, C. (1997). Expression of Radical fringe in limb-bud ectoderm regulates apical ectodermal ridge formation. *Nature* **386,** 366-73.

LEHESTE, J. R., MELSEN, F., WELLNER, M., JANSEN, P., SCHLICHTING, U., RENNER-MULLER, I., ANDREASSEN, T. T., WOLF, E., BACHMANN, S., NYKJAER, A. & WILLNOW, T. E. (2003). Hypocalcemia and osteopathy in mice with kidney-specific megalin gene defect. *Faseb J* **17,** 247-9.

LESCHER, B., HAENIG, B. & KISPERT, A. (1998). sFRP-2 is a target of the Wnt-4 signaling pathway in the developing metanephric kidney. *Dev Dyn* **213,** 440-51.

LI, Y., MARZOLO, M. P., VAN KERKHOF, P., STROUS, G. J. & BU, G. (2000). The YXXL motif, but not the two NPXY motifs, serves as the dominant endocytosis signal for low density lipoprotein receptor-related protein. *J Biol Chem* **275,** 17187-94.

LIN, Y., LIU, A., ZHANG, S., RUUSUNEN, T., KREIDBERG, J. A., PELTOKETO, H., DRUMMOND, I. & VAINIO, S. (2001). Induction of ureter branching as a response to Wnt-2b signaling during early kidney organogenesis. *Dev Dyn* **222,** 26-39.

LIU, C. X., MUSCO, S., LISITSINA, N. M., YAKLICHKIN, S. Y. & LISITSYN, N. A. (2000). Genomic organization of a new candidate tumor suppressor gene, LRP1B. *Genomics* **69,** 271-4.

LOGAN, C., HORNBRUCH, A., CAMPBELL, I. & LUMSDEN, A. (1997). The role of Engrailed in establishing the dorsoventral axis of the chick limb. *Development* **124,** 2317-24.

LOGAN, C. Y. & NUSSE, R. (2004). The Wnt signaling pathway in development and disease. *Annu Rev Cell Dev Biol* **20,** 781-810.

LOGANATHAN, P. G., NIMMAGADDA, S., HUANG, R., SCAAL, M. & CHRIST, B. (2005). Comparative analysis of the expression patterns of Wnts during chick limb development. *Histochem Cell Biol* **123,** 195-201.

LOUKINOVA, E., RANGANATHAN, S., KUZNETSOV, S., GORLATOVA, N., MIGLIORINI, M. M., LOUKINOV, D., ULERY, P. G., MIKHAILENKO, I., LAWRENCE, D. A. & STRICKLAND, D. K. (2002). Platelet-derived growth factor (PDGF)-induced tyrosine phosphorylation of the low density lipoprotein receptor-related protein (LRP). Evidence for integrated co-receptor function betwenn LRP and the PDGF. *J Biol Chem* **277,** 15499-506.

LUECK, J. D., LUNGU, C., MANKODI, A., OSBORNE, R., WELLE, S., DIRKSEN, R. T. & THORNTON, C. A. (2006). Chloride channelopathy in myotonic dystrophy resulting from loss of post-transcriptional regulation for CLCN1. *Am J Physiol Cell Physiol*.

LUO, G., HOFMANN, C., BRONCKERS, A. L., SOHOCKI, M., BRADLEY, A. & KARSENTY, G. (1995). BMP-7 is an inducer of nephrogenesis, and is also required for eye development and skeletal patterning. *Genes Dev* **9,** 2808-20.

MACDONALD, B. T., ADAMSKA, M. & MEISLER, M. H. (2004). Hypomorphic expression of Dkk1 in the doubleridge mouse: dose dependence and compensatory interactions with Lrp6. *Development* **131,** 2543-52.

MAESHIMA, A., VAUGHN, D. A., CHOI, Y. & NIGAM, S. K. (2006). Activin A is an endogenous inhibitor of ureteric bud outgrowth from the Wolffian duct. *Dev Biol*.

MAJUMDAR, A., VAINIO, S., KISPERT, A., MCMAHON, J. & MCMAHON, A. P. (2003). Wnt11 and Ret/Gdnf pathways cooperate in regulating ureteric branching during metanephric kidney development. *Development* **130,** 3175-85.

MAO, B. & NIEHRS, C. (2003). Kremen2 modulates Dickkopf2 activity during Wnt/LRP6 signaling. *Gene* **302,** 179-83.

MAO, B., WU, W., DAVIDSON, G., MARHOLD, J., LI, M., MECHLER, B. M., DELIUS, H., HOPPE, D., STANNEK, P., WALTER, C., GLINKA, A. & NIEHRS, C. (2002). Kremen proteins are Dickkopf receptors that regulate Wnt/beta-catenin signalling. *Nature* **417,** 664-7.

MAO, B., WU, W., LI, Y., HOPPE, D., STANNEK, P., GLINKA, A. & NIEHRS, C. (2001). LDL-receptor-related protein 6 is a receptor for Dickkopf proteins. *Nature* **411,** 321-5.

MARETTO, S., CORDENONSI, M., DUPONT, S., BRAGHETTA, P., BROCCOLI, V., HASSAN, A. B., VOLPIN, D., BRESSAN, G. M. & PICCOLO, S. (2003). Mapping Wnt/beta-catenin signaling during mouse development and in colorectal tumors. *Proc Natl Acad Sci U S A* **100,** 3299-304.

MARSCHANG, P., BRICH, J., WEEBER, E. J., SWEATT, J. D., SHELTON, J. M., RICHARDSON, J. A., HAMMER, R. E. & HERZ, J. (2004). Normal development and fertility of knockout mice lacking the tumor suppressor gene LRP1b suggest functional compensation by LRP1. *Mol Cell Biol* **24,** 3782-93.

MARTINEZ, G. & BERTRAM, J. F. (2003). Organisation of bone morphogenetic proteins in renal development. *Nephron Exp Nephrol* **93,** e18-22.

MARTINEZ, G., MISHINA, Y. & BERTRAM, J. F. (2002). BMPs and BMP receptors in mouse metanephric development: in vivo and in vitro studies. *Int J Dev Biol* **46,** 525-33.

MATSUZAKI, T., HANAI, S., KISHI, H., LIU, Z., BAO, Y., KIKUCHI, A., TSUCHIDA, K. & SUGINO, H. (2002). Regulation of endocytosis of activin type II receptors by a novel PDZ protein through Ral/Ral-binding protein 1-dependent pathway. *J Biol Chem* **277,** 19008-18.

MAURER, M. E. & COOPER, J. A. (2006). The adaptor protein Dab2 sorts LDL receptors into coated pits independently of AP-2 and ARH. *J Cell Sci* **119,** 4235-46.

MAY, P., BOCK, H. H., NIMPF, J. & HERZ, J. (2003). Differential glycosylation regulates processing of lipoprotein receptors by gamma-secretase. *J Biol Chem* **278,** 37386-92.

MCQUEENEY, K., SOUFER, R. & DEALY, C. N. (2002). Beta-catenin-dependent Wnt signaling in apical ectodermal ridge induction and FGF8 expression in normal and limbless mutant chick limbs. *Dev Growth Differ* **44,** 315-25.

MICHOS, O., PANMAN, L., VINTERSTEN, K., BEIER, K., ZELLER, R. & ZUNIGA, A. (2004). Gremlin-mediated BMP antagonism induces the epithelial-mesenchymal feedback signaling controlling metanephric kidney and limb organogenesis. *Development* **131,** 3401-10.

MIKKOLA, M. L. & MILLAR, S. E. (2006). The Mammary Bud as a Skin Appendage: Unique and Shared Aspects of Development. *J Mammary Gland Biol Neoplasia*.

MIYAZAKI, Y., OSHIMA, K., FOGO, A., HOGAN, B. L. & ICHIKAWA, I. (2000). Bone morphogenetic protein 4 regulates the budding site and elongation of the mouse ureter. *J Clin Invest* **105,** 863-73.

NACCACHE, S. N., HASSON, T. & HOROWITZ, A. (2006). Binding of internalized receptors to the PDZ domain of GIPC/synectin recruits myosin VI to endocytic vesicles. *Proc Natl Acad Sci U S A* **103,** 12735-40.

NAKAYAMA, M., NAKAJIMA, D., NAGASE, T., NOMURA, N., SEKI, N. & OHARA, O. (1998). Identification of high-molecular-weight proteins with multiple EGF-like motifs by motif-trap screening. *Genomics* **51,** 27-34.

NARITA, T., SASAOKA, S., UDAGAWA, K., OHYAMA, T., WADA, N., NISHIMATSU, S., TAKADA, S. & NOHNO, T. (2005). Wnt10a is involved in AER formation during chick limb development. *Dev Dyn* **233,** 282-7.

NGUYEN, H. T., THOMSON, A. A., KOGAN, B. A., BASKIN, L. S. & CUNHA, G. R. (1999). Expression of the Wnt gene family during late nephrogenesis and complete ureteral obstruction. *Lab Invest* **79,** 647-58.

NOHNO, T., KAWAKAMI, Y., WADA, N., KOMAGUCHI, C. & NISHIMATSU, S. (1999). Differential expression of the frizzled family involved in Wnt signaling during chick limb development. *Cell Mol Biol (Noisy-le-grand)* **45,** 653-9.

PARR, B. A., SHEA, M. J., VASSILEVA, G. & MCMAHON, A. P. (1993). Mouse Wnt genes exhibit discrete domains of expression in the early embryonic CNS and limb buds. *Development* **119,** 247-61.

PERANTONI, A. O. (2003). Renal development: perspectives on a Wnt-dependent process. *Semin Cell Dev Biol* **14,** 201-8.

PIZETTE, S. & NISWANDER, L. (1999). BMPs negatively regulate structure and function of the limb apical ectodermal ridge. *Development* **126,** 883-94.

RAATIKAINEN-AHOKAS, A., HYTONEN, M., TENHUNEN, A., SAINIO, K. & SARIOLA, H. (2000). BMP-4 affects the differentiation of metanephric mesenchyme and reveals an early anterior-posterior axis of the embryonic kidney. *Dev Dyn* **217,** 146-58.

RIDDLE, R. D., ENSINI, M., NELSON, C., TSUCHIDA, T., JESSELL, T. M. & TABIN, C. (1995). Induction of the LIM homeobox gene Lmx1 by WNT7a establishes dorsoventral pattern in the vertebrate limb. *Cell* **83,** 631-40.

ROHLMANN, A., GOTTHARDT, M., HAMMER, R. E. & HERZ, J. (1998). Inducible inactivation of hepatic LRP gene by cre-mediated recombination confirms role of LRP in clearance of chylomicron remnants. *J Clin Invest* **101,** 689-95.

RUDENKO, G., HENRY, L., HENDERSON, K., ICHTCHENKO, K., BROWN, M. S., GOLDSTEIN, J. L. & DEISENHOFER, J. (2002). Structure of the LDL receptor extracellular domain at endosomal pH. *Science* **298,** 2353-8.

SAXEN, L. & LEHTONEN, E. (1987). Embryonic kidney in organ culture. *Differentiation* **36,** 2-11.

SCHWAB, K., HARTMAN, H. A., LIANG, H. C., ARONOW, B. J., PATTERSON, L. T. & POTTER, S. S. (2006). Comprehensive microarray analysis of Hoxa11/Hoxd11 mutant kidney development. *Dev Biol* **293,** 540-54.

SELEVER, J., LIU, W., LU, M. F., BEHRINGER, R. R. & MARTIN, J. F. (2004). Bmp4 in limb bud mesoderm regulates digit pattern by controlling AER development. *Dev Biol* **276,** 268-79.

SIM, E. U., SMITH, A., SZILAGI, E., RAE, F., IOANNOU, P., LINDSAY, M. H. & LITTLE, M. H. (2002). Wnt-4 regulation by the Wilms' tumour suppressor gene, WT1. *Oncogene* **21,** 2948-60.

SIMON-CHAZOTTES, D., TUTOIS, S., KUEHN, M., EVANS, M., BOURGADE, F., COOK, S., DAVISSON, M. T. & GUENET, J. L. (2006). Mutations in the gene encoding the low-density lipoprotein receptor LRP4 cause abnormal limb development in the mouse. *Genomics*.

SIMSKE, J. S., KAECH, S. M., HARP, S. A. & KIM, S. K. (1996). LET-23 receptor localization by the cell junction protein LIN-7 during C. elegans vulval induction. *Cell* **85,** 195-204.

SOSHNIKOVA, N., ZECHNER, D., HUELSKEN, J., MISHINA, Y., BEHRINGER, R. R., TAKETO, M. M., CRENSHAW, E. B., 3RD & BIRCHMEIER, W. (2003). Genetic interaction between Wnt/beta-catenin and BMP receptor signaling during formation of the AER and the dorsal-ventral axis in the limb. *Genes Dev* **17,** 1963-8.

SPOELGEN, R., HAMMES, A., ANZENBERGER, U., ZECHNER, D., ANDERSEN, O. M., JERCHOW, B. & WILLNOW, T. E. (2005). LRP2/megalin is required for patterning of the ventral telencephalon. *Development* **132,** 405-14.

STARK, K., VAINIO, S., VASSILEVA, G. & MCMAHON, A. P. (1994). Epithelial transformation of metanephric mesenchyme in the developing kidney regulated by Wnt-4. *Nature* **372,** 679-83.

STRUTT, H. & STRUTT, D. (1999). Polarity determination in the Drosophila eye. *Curr Opin Genet Dev* **9,** 442-6.

TAMAI, K., SEMENOV, M., KATO, Y., SPOKONY, R., LIU, C., KATSUYAMA, Y., HESS, F., SAINT-JEANNET, J. P. & HE, X. (2000). LDL-receptor-related proteins in Wnt signal transduction. *Nature* **407,** 530-5.

TAMAI, K., ZENG, X., LIU, C., ZHANG, X., HARADA, Y., CHANG, Z. & HE, X. (2004). A mechanism for Wnt coreceptor activation. *Mol Cell* **13,** 149-56.

TIAN, Q. B., NAKAYAMA, K., OKANO, A. & SUZUKI, T. (1999). Identification of mRNAs localizing in the postsynaptic region. *Brain Res Mol Brain Res* **72,** 147-57.

TIAN, Q. B., SUZUKI, T., YAMAUCHI, T., SAKAGAMI, H., YOSHIMURA, Y., MIYAZAWA, S., NAKAYAMA, K., SAITOH, F., ZHANG, J. P., LU, Y., KONDO, H. & ENDO, S. (2006). Interaction of LDL receptor-related protein 4 (LRP4) with postsynaptic scaffold proteins via its C-terminal PDZ domain-binding motif, and its regulation by Ca/calmodulin-dependent protein kinase II. *Eur J Neurosci* **23,** 2864-76.

TOMITA, Y., KIM, D. H., MAGOORI, K., FUJINO, T. & YAMAMOTO, T. T. (1998). A novel low-density lipoprotein receptor-related protein with type II membrane protein-like structure is abundant in heart. *J Biochem (Tokyo)* **124,** 784-9.

TONG, A., NGUYEN, J. & LYNCH, K. W. (2005). Differential expression of CD45 isoforms is controlled by the combined activity of basal and inducible splicing-regulatory elements in each of the variable exons. *J Biol Chem* **280,** 38297-304.

TOPOL, L., JIANG, X., CHOI, H., GARRETT-BEAL, L., CAROLAN, P. J. & YANG, Y. (2003). Wnt-5a inhibits the canonical Wnt pathway by promoting GSK-3-independent beta-catenin degradation. *J Cell Biol* **162,** 899-908.

TORBAN, E., DZIARMAGA, A., IGLESIAS, D., CHU, L. L., VASSILIEVA, T., LITTLE, M., ECCLES, M., DISCENZA, M., PELLETIER, J. & GOODYER, P. (2006). PAX2 activates WNT4 expression during mammalian kidney development. *J Biol Chem* **281,** 12705-12.

TROMMSDORFF, M., GOTTHARDT, M., HIESBERGER, T., SHELTON, J., STOCKINGER, W., NIMPF, J., HAMMER, R. E., RICHARDSON, J. A. & HERZ, J. (1999). Reeler/Disabled-like disruption of neuronal migration in knockout mice lacking the VLDL receptor and ApoE receptor 2. *Cell* **97,** 689-701.

TUCKER, A. & SHARPE, P. (2004). The cutting-edge of mammalian development; how the embryo makes teeth. *Nat Rev Genet* **5,** 499-508.

VAN DRIEL, I. R., GOLDSTEIN, J. L., SUDHOF, T. C. & BROWN, M. S. (1987). First cysteine-rich repeat in ligand-binding domain of low density lipoprotein receptor binds Ca2+ and monoclonal antibodies, but not lipoproteins. *J Biol Chem* **262,** 17443-9.

WEATHERBEE, S. D., ANDERSON, K. V. & NISWANDER, L. A. (2006). LDL-receptor-related protein 4 is crucial for formation of the neuromuscular junction. *Development* **133,** 4993-5000.

WEEBER, E. J., BEFFERT, U., JONES, C., CHRISTIAN, J. M., FORSTER, E., SWEATT, J. D. & HERZ, J. (2002). Reelin and ApoE receptors cooperate to enhance hippocampal synaptic plasticity and learning. *J Biol Chem* **277,** 39944-52.

WILKIE, A. O., PATEY, S. J., KAN, S. H., VAN DEN OUWELAND, A. M. & HAMEL, B. C. (2002). FGFs, their receptors, and human limb malformations: clinical and molecular correlations. *Am J Med Genet* **112,** 266-78.

WILLNOW, T. E. (1998). Receptor-associated protein (RAP): a specialized chaperone for endocytic receptors. *Biol Chem* **379,** 1025-31.

WILLNOW, T. E., HILPERT, J., ARMSTRONG, S. A., ROHLMANN, A., HAMMER, R. E., BURNS, D. K. & HERZ, J. (1996). Defective forebrain development in mice lacking gp330/megalin. *Proc Natl Acad Sci U S A* **93,** 8460-4.

WOLPERT, L. (1998). Pattern formation in epithelial development: the vertebrate limb and feather bud spacing. *Philos Trans R Soc Lond B Biol Sci* **353,** 871-5.

YAMAGATA, M., KIMOTO, A., MICHIGAMI, T., NAKAYAMA, M. & OZONO, K. (2001). Hydroxylases involved in vitamin D metabolism are differentially expressed in murine embryonic kidney: application of whole mount in situ hybridization. *Endocrinology* **142,** 3223-30.

YAMAGUCHI, T. P., BRADLEY, A., MCMAHON, A. P. & JONES, S. (1999). A Wnt5a pathway underlies outgrowth of multiple structures in the vertebrate embryo. *Development* **126,** 1211-23.

YAMAGUCHI, Y. L., TANAKA, S. S., KASA, M., YASUDA, K., TAM, P. P. & MATSUI, Y. (2006). Expression of low density lipoprotein receptor-related protein 4 (Lrp4) gene in the mouse germ cells. *Gene Expr Patterns* **6,** 607-12.

YANG, Y. & NISWANDER, L. (1995). Interaction between the signaling molecules WNT7a and SHH during vertebrate limb development: dorsal signals regulate anteroposterior patterning. *Cell* **80,** 939-47.

YOSHIMURA, A., YOSHIDA, T., SEGUCHI, T., WAKI, M., ONO, M. & KUWANO, M. (1987). Low binding capacity and altered O-linked glycosylation of low density lipoprotein receptor in a monensin-resistant mutant of Chinese hamster ovary cells. *J Biol Chem* **262,** 13299-308.

ZILBERBERG, A., YANIV, A. & GAZIT, A. (2004). The low density lipoprotein receptor-1, LRP1, interacts with the human frizzled-1 (HFz1) and down-regulates the canonical Wnt signaling pathway. *J Biol Chem* **279,** 17535-42.

VITAE

Eric Boyd Johnson was born in Santa Monica, California on March 10, 1976, the son of Wesley and Elizabeth Johnson. After graduating from Van Nuys High School Math/Science magnet program in 1994, he entered the University of California San Diego. In 1998 he graduated with a Bachelor of Science in Molecular Biology with an optional minor in Chemistry. Eric's first exposure to scientific research was in the laboratory of Robert Sah, M.D., Sc.D. at UCSD studying the integrative repair of cartilage. During his last year of undergraduate studies, Eric was awarded a summer internship at Neurocrine Biosciences Inc. He remained an employee of Neurocrine after his graduation from UCSD where he studied the effectiveness of the Altered Peptide Ligand technology both in mice and humans under the supervision of Paul Conlon, Ph.D. Eric moved to Dallas in the summer of 2001 to study at the University of Texas Southwestern Medical Center and subsequently joined the lab of Joachim Herz to study the function of *Megf7*. During his studies he was awarded "Honorable Mention" in the 2005 Graduate Student Organization Poster Competition, "Best of Show" in the 2007 Integrative Biology Poster Competition, and a GSO travel scholarship. Eric also had the honor of being the representative for the Integrative Biology program for the 2007 UT Southwestern Nominata Award. Eric was awarded a PhD. in Integrative Biology in 2007.

Pre-Graduate School Publications:

Simpson, P.B., M.S. Mistry, W. Yang, E.B. Johnson, D.A. Schwarz, F.M. Lio, R.A. Maki, and D.G. Alleva. Diabetes-Associated Locus, Idd4, is Responsible for the Over-Expression IL-12p40 Defect in the Non-Obese Diabetic (NOD) Mouse. J. Immunology 171(7):3333-7 (2003)

Alleva, D.G., Gaur, A., Jin, L., Wegmann, D., Gottlieb, P.A., Pahuja, A., Johnson, E.B., Motheral, T., Putnam, A., Crowe, P.D., Ling, N., Boehme, S.A. and Conlon, P.J. Immunological Characterization and Therapeutic Activity of an Altered-Peptide Ligand, NBI-6024, Based on an Immunodominant Type 1 Diabetes Autoantigen, Insulin B(9-23) Diabetes. 51(7):2126-34. (2002)

Alleva, D.G., Johnson, E.B., Lio, F.M., Boehme, S.A., Conlon, P.J., Crowe, P.D. Regulation of murine macrophage proinflammatory and anti-inflammatory cytokines by ligands for peroxisome proliferator-activated receptor-gamma: counter-regulatory activity by IFN-gamma. Journal of Leukocyte Biology 71(4):677-85. (2002)

Kappos, L. et al. Induction of a non-encephalitogenic type 2 T helper-cell autoimmune response in multiple sclerosis after administration of an altered peptide ligand in a placebo controlled, randomized phase II trial. Nature Medicine 6(10), 1176-1182.

Alleva, D.A., Johnson, E.J., Wilson, J., Beller, D.I., and Conlon, P.J. SJL and NOD macrophages are uniquely characterized by genetically programmed elevated expression of the IL-12(p40)

gene, suggesting a conserved pathway for the induction of organ-specific autoimmunity. Journal of Leukocyte Biology 69(3), 440-448 (2001)

Permanent Address: 20661 Dumont St.

Woodland Hills, CA, 91364